UNIVERSITY OF CAMPINAS

SCHOOL OF CHEMICAL ENGINEERING

Pedro Yoritomo Souza Nakasu

EVALUATION OF SUGARCANE BAGASSE PRETREATMENT PROCESS WITH PROTIC IONIC LIQUIDS FOR CELLULOSIC ETHANOL PRODUCTION

AVALIAÇÃO DO PROCESSO DE PRÉ-TRATAMENTO DO BAGAÇO DA CANA-DE-AÇÚCAR COM LÍQUIDOS IÔNICOS PRÓTICOS PARA A PRODUÇÃO DE ETANOL CELULÓSICO

Campinas

2019

PEDRO YORITOMO SOUZA NAKASU

EVALUATION OF SUGARCANE BAGASSE PRETREATMENT PROCESS WITH PROTIC IONIC LIQUIDS FOR CELLULOSIC ETHANOL PRODUCTION

AVALIAÇÃO DO PROCESSO DE PRÉ-TRATAMENTO DO BAGAÇO DA CANA-DE-AÇÚCAR COM LÍQUIDOS IÔNICOS PRÓTICOS PARA A PRODUÇÃO DE ETANOL CELULÓSICO
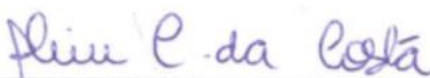
<div style="margin-left:50%">

Tese apresentada à Faculdade de Engenharia Química da Universidade Estadual de Campinas como parte dos requisitos exigidos para a obtenção parcial para obtenção do título de Doutor em Engenharia Química

PhD thesis presented to the Faculty of Chemical Engineering of State University of Campinas in partial fulfillment of the requirements for the degree of Doctor in Chemical Engineering

</div>

SUPERVISOR: Dr. ALINE CARVALHO DA COSTA

CO-SUPERVISOR: Dr. SARITA CÂNDIDA RABELO

ESTE EXEMPLAR CORRESPONDE À VERSÃO FINAL DA TESE DEFENDIDA PELO ALUNO PEDRO YORITOMO SOUZA NAKASU E ORIENTADA PELA PROF.A DR.A ALINE

_____

CARVALHO DA COSTA

<center>

CAMPINAS

OCTOBER 2019

</center>

Nakasu, Pedro Yoritomo Souza, 1989-

N145e   Evaluation of sugarcane bagasse pretreatment process with protic ionic liquids for cellulosic ethanol production / Pedro Yoritomo Souza Nakasu. – Campinas, SP : [s.n.], 2019.

Orientador: Aline Carvalho da Costa.
Coorientador: Sarita Cândida Rabelo.
Tese (doutorado) – Universidade Estadual de Campinas, Faculdade de Engenharia Química.

1. Líquidos iônicos. 2. Pré-tratamento. 3. Hidrólise enzimática. 4. Etanol 2G. 5. Fermentação. I. Costa, Aline Carvalho da, 1970-. II. Rabelo, Sarita Cândida. III. Universidade Estadual de Campinas. Faculdade de Engenharia Química. IV. Título.

Folha de Aprovação da Defesa de Tese de Doutorado defendida por Pedro Yoritomo Souza Nakasu aprovada em 31 de outubro de 2019 pela banca examinadora constituída pelos seguintes doutores:

Profa. Dra. Aline Carvalho da Costa - (Orientador)

FEQ / UNICAMP

Dra. Simone Coelho Nakanishi

CTBE / CNPEM

Dra. Lívia Beatriz Brenelli de Paiva

CNPEM / CTBE

Profa. Dra. Camila Alves de Rezende

IQ / UNICAMP

Dr. Rafael Ramos de Andrade

Universidade Federal de São Paulo

ATA da Defesa com as respectivas assinaturas dos membros encontra-se no SIGA/Sistema de Fluxo de Dissertação/Tese e na Secretaria do Programa da Unidade.

To my Sun that enlightened me and guided me
In this world until his last rays,
my father Licurgo Nakasu.

To my Moon that still lights my path
Even in the darkest nights,
my mother Julita Nakasu.

To my three jewels which I lovely keep
In my chest wherever I go,
my sisters Sarah and Airana and my niece Sayumi.

And to the cosmic force that unites everything
— by the force of love —
In this complex thing called universe, God.

ACKNOWLEDGEMENTS

FEQ / UNICAMP for the infra-structure to pursue my research;

CAPES, the portal for electronic journals, which allows quick and efficient access to scientific knowledge;

Google and Wikipedia as additions to the previous item;

to everyone who somehow contributed to my progress as a student and as a human being.

"[...] Rastro de flor e de estrela,
nuvem e mar.
Meu destino é mais longe e meu passo mais rápido:
a sombra é que vai devagar."

\- Cecília Meireles.

ABSTRACT

Using by-products from the agricultural sector to establish a biorefinery is a promising alternative in our society's transition to a biobased economy. Sugarcane bagasse is a lignocellulosic biomass that stands out in the Brazilian scenario due to its production volume and can be converted into second generation ethanol (E2G) in three main steps, pretreatment, enzymatic hydrolysis. and fermentation. In this work, we evaluated the pretreatment process with protic ionic liquids (LIPs) — which can be up to 40 times cheaper than the more commonly known aprotic ionic liquids — for the production of E2G. In the initial stage of the project, 12 LIPs were produced and evaluated in a screening, in which monoethanolammonium acetate, [MEA][OAc], was chosen for the subsequent stages of the studies because due to its great potential as a pretreatment agent. [MEA][OAc] pretreatment has undergone an optimization of operating parameters considering time, temperature, solids loading, water content and anti-solvent type as factors of the experimental design. Such variables were evaluated to ensure maximum carbohydrate conversion and pulp delignification. A study of the acid-base ratio (ABR) of [MEA][OAc] showed that low ABR values provided an almost quantitative yield of cellulose/hemicellulose within 72 h of enzymatic hydrolysis with up to 84% delignification, standing out as one of the best pretreatments available for sugarcane bagasse. The ABR was successfully measured before and after the experiments by NMR-H[1] spectroscopy, a pioneering achievement of this work. Thereafter, [MEA][OAc] recycle was assessed over 6 pretreatment cycles. It was observed that the decrease in LIP performance is strongly correlated to its decomposition into an acetamide. This problem was solved by using an excess base mixture, ABR 0.5, which was recycled over 3 cycles and showed that PIL performance was still considerably high with low acetamide formation. Then, quantitative relationships were established between the amount of washing water and its temperature, with the enzymatic saccharification and alcoholic fermentation yields with *S. passalidarum*, a yeast capable of metabolizing xylose and glucose. Among the partial wash samples (from 13 to 66 g water /g biomass), the wash performed at the highest temperature, 80 °C, and the highest solvent: biomass ratio considered, 66: 1, provided the highest hydrolysis yields. 81% and 64% for cellulose and hemicellulose, respectively, and for fermentation with 85% of the theoretical ethanol yield; while the complete wash (625 g water/ g biomass) yielded 98% and 85% yield of cellulose and hemicellulose, respectively, and 87% of the theoretical yield of ethanol. Although *S. cerevisiae* did not consume xylose, the fermentation of the complete wash sample had the highest ethanol yield, 1.41 g ·/L·h with approximately the same theoretical ethanol yield, 87%. Mass balances for the complete E2G production process (via *S. passalidarum*) showed that up to 228 and 300 L of ethanol per tonne of bagasse can be produced with 66 and 625 tonnes of wash water / tonne of bagasse respectively. with the first yield superior to the best pretreatments found in the literature, ie alkaline hydrogen peroxide and sodium hydroxide.

Keywords: ionic liquids, pretreatment, enzymatic hydrolysis, 2G ethanol, fermentation.

RESUMO

O uso de subprodutos do setor agrícola para o estabelecimento de uma biorrefinaria é uma alternativa promissora na transição da nossa sociedade para uma economia biobaseada. O bagaço da cana-de-açúcar é uma biomassa lignocelulósica que se destaca no cenário brasileiro devido ao seu volume de produção e pode vir a se transformado em etanol de segunda geração (E2G) por meio de três etapas, pré-tramento, hidrólise enzimática e fermentação. Neste trabalho, foi avaliado o processo de pré-tratamento com líquidos iônicos próticos (LIPs) — que podem chegar a ser até 40 vezes mais baratos que os líquidos iônicos apróticos, mais comumente conhecidos — para a produção de E2G. No estágio inicial do projeto, 12 LIPs foram produzidos e avaliados em um screening, no qual o acetato de monoetanolamônio, [MEA][OAc], foi escolhido para as etapas subsequentes dos estudos por apresentar grande potencial como agente de pré-tratamento. O pré-tratamento com este LIP passou por uma otimização de parâmetros operacionais considerando o tempo, temperatura, carga de sólidos, teor de água e tipo de anti-solvente como fatores do planejamento estatístico. As variáveis foram avaliadas para garantir a máxima conversão de carboidratos e deslignificação das polpas. Um estudo da razão ácido-base (RAB) do [MEA][OAc] mostrou que baixos valores de RAB (excesso de base) proporcionavam um rendimento quase quantitativo de celulose/hemicelulose em 72 h de hidrólise enzimática com até 84% de deslignificação, destacando-se como um dos melhores pré-tratamentos existentes para o bagaço de cana-de-açúcar. A RAB foi medida com sucesso antes e após os experimentos por espectroscopia de NMR-H[1], um feito pioneiro deste trabalho. Em seguida, o reciclo do [MEA][OAc] foi avaliado ao longo de 6 ciclos de pré-tratamento. Foi observado que a diminuição no desempenho do LIP está fortemente correlacionada à sua decomposição em uma acetamida. Esse problema foi contornado com o uso de uma mistura com excesso da base, RAB 0,5, cujo reciclo, ao longo de 3 ciclos, mostrou que o desempenho do PIL ainda era consideravelmente alto, com baixa formação de acetamida. Em seguida, estabeleceram-se relações quantitativas entre a quantidade de água de lavagem das polpas e sua temperatura, com os rendimentos em sacarificação enzimática e fermentação alcoólica com *S. passalidarum*, uma levedura capaz de metabolizar xilose e glicose. Entre as amostras com lavagem parcial (de 13 a 66 g água/g biomassa), a lavagem realizada em temperatura mais alta, 80°C, e com a maior relação solvente:biomassa considerada, 66:1, proporcionou os maiores rendimentos na hidrólise enzimática, 81% e 64% para a celulose e hemicelulose, respectivamente, e na fermentação com 85% do rendimento teórico de etanol; enquanto que a lavagem completa (625 g água/g biomassa) obteve 98% e 85% de rendimento de celulose e hemicelulose, respectivamente, e 87% do rendimento teórico de etanol. Apesar de *S. cerevisiae* não consumir xilose, a fermentação da amostra de lavagem completa apresentou a maior produtividade de etanol, 1.41 ·/L·h com aproximadamente o mesmo rendimento teórico de etanol, 87%. Os balanços de massa para o processo completo de produção de E2G (via *S. passalidarum*) mostraram que até 228 e 300 L de etanol por tonelada de bagaço podem ser produzidos com 66 e 625 toneladas de água de lavagem/tonelada de bagaço, respectivamente, com o primeiro rendimento superior aos melhores pré-tratamentos encontrados no literatura, ou seja, peróxido de hidrogênio alcalino e hidróxido de sódio.

Palavras-chave: líquidos iônicos, pré-tratamento, hidrólise enzimática, etanol 2G, fermentação.

LIST OF FIGURES

LIST OF TABLES

LIST OF ABBREVIATIONS, INITIALS AND ACRONYMS

1G – First generation

2G – Second generation

ABR – Acid-base ratio

AFEX – Ammonia fiber expansion

ANOVA – Analysis of variance

APIL – Aprotic ionic liquid

ATR – Atenuated total reflection

C5 – Pentose

C6 – Hexose

C9 – phenylpropanic units

[Ch][OAc] – Cholinium acetate

DCM – Direct conversion by the microorganism

DI – Deionized

DM – dry mass

DMSO – Dimethyl sulfoxide

DTG – Thermogravimetric derivative

E2G – Second generation ethanol

[EMIM][OAc] – 1-ethyl-3-methyl imidazolium acetate

[EMIM][DEP] – 1-ethyl-3-methyl-imidazolium diethyl phosphate

EtOH – Ethanol

FA – Ferulic acid

FPU – Filter paper unit

FTIR – Fourier transform infrared

G – Guayacyl

GHG – Greenhouse gases

GPC – Gel permeation chromatography

H – p-coumaryl

HSQC – Heteronuclear single quantum coeherence

HPLC – High performance liquid chromatography

HR – High resolution

IL – Ionic liquids

IUPAC – International Union of Pure and Applied Chemistry

LPG – Liquefied petroleum gas

MEA – Monoethanolamine
[MEA][OAc] - Monoethanolammonium acetate

MESP – Minimum ethanol selling price

M_n – Number average molecular weight

M_w – Weight average molecular weight

NAD – Nicotinamide adenine dinucleotide

NMR – Nuclear magnetic resonance

NREL – National Renewable Energy Laboratory

PCA – p-coumaric acid

PCB – p-benzoic acid

PD – polydispersity

PIL – Protic ionic liquid

PMO – Polysaccharide mono-oxygenases

Q_p – Ethanol volumetric productivity

RPM – Rotations per minute

S – Syringyl

SD – Standard deviation

SSF – Simultaneous saccharification and fermentation

[TEA][HSO$_4$] – Triethyl ammonium hydrogen sulfate

TG – thermogravimetric

XPS – X-ray photoelectron spectroscopy

$Y_{P/S}$ – Product yield coefficient

$Y_{X/S}$ – Cell mass yield coefficient

TABLE OF CONTENTS

Chapter 1

Introduction

Second-generation (2G) ethanol is a biofuel that can potentially replace fossil fuels and curb increasing green-house gases emissions (VOHRA *et al.*, 2014). Currently, the Brazilian market presents ethanol as biofuel for light vehicles, which can be either mixed as an additive in gasoline to increase octane in the form of anhydrous ethanol, or directly used in its hydrated form by flex-fuel engines. The consumption of hydrated ethanol has been increasing (NOVACANA.COM, 2019), which, together with the global demand (ZAFALON, 2016), offers a positive outlook for sugar and ethanol plants to expand their production.

Such expansion implies a boost in productivity of ethanol and can be rationalized in two ways. The first, focused on agriculture, aims to introduce new varieties of sugarcane and transgenic species. The second, focused on the industrial area, aims to develop technologies for the whole use of sugarcane biomass in the production of 2G ethanol or other renewable products, adding value to the sugarcane chain (RABELO, 2010, *apud* BONOMI, 2006).

Due to the compact structure of lignocellulosic biomass, a pretreatment is required to reduce its natural recalcitrance. Pretreatment with ionic liquids (ILs) have been studied in the past years and shown promising results (COSTA LOPES *et al.*, 2013). One of the main advantages of using ILs is their capacity to be tailored to their application, and so, by choosing a suitable cation/anion combination, it is possible to increase the selectivity of pretreatment (GREAVES and DRUMMOND, 2008).

Lignin is one of the main components of lignocellulosic biomass and its presence hinders enzyme accessibility (RAHIKAINEN *et al.*, 2013). An ideal pretreatment selectively removes/solubilizes the lignin and preserves the carbohydrates — cellulose and hemicelluloses — in the remaining pulp, which may then be further converted into sugar monomers by enzyme cocktails. The price of the IL also needs to be taken into account during IL design. Aprotic ILs have demonstrated promising results in terms of biomass fractionation, but their high cost poses a significant economic hurdle on process development (BRANDT *et al.*, 2017a).

Protic ionic liquids (PILs) have been recently studied for biomass fractionation and have shown promising features, especially in terms of lignin solubilisation (BRANDT *et al.*, 2013; ROCHA *et al.*, 2017). PILs such as triethylammonium hydrogen sulfate, [TEA][HSO$_4$], are potential pretreatment agents to selectively solubilize lignin and hemicelluloses and generate cellulose-rich pulps (GEORGE *et al.*, 2014). Most studies, however, were performed at small scale in vials or glass tubes, suitable for introductory studies, but lacking information on following scale up. In this work, we aimed to evaluate the performance of a protic ionic liquid, monoethanolammonium acetate, [MEA][OAc], by testing several conditions in bench scale reactors (0.5 L) without milling or sieving of the raw biomass, in order to mimic a larger-scale process.

Pretreatment severity is a parameter mainly affected by temperature and residence time; higher severity usually implies higher biomass fractionation at the cost of lower selectivity (CHUM *et al.*, 1990). Pretreatment with PILs such as [MEA][OAc], however, may provide high delignification selectivity whilst effectively fractionating biomass components even under high severities (BRANDT *et al.*, 2013). Pretreatment parameters that are directly linked to mass transfer properties, such as solids loading and water content, may also be considered in process optimization. The influence of water content is not as easily predictable. Early studies that evaluated the impact of water in ionic liquid pretreatment systems claimed ILs required a hygroscopic medium for a high performance (COSTA LOPES *et al.*, 2013), but this has been shown not to be true for PILs, which are water-compatible (BRANDT *et al.*, 2011). Although it had not been much discussed, the acid-base ratio, ABR, in the PIL synthesis is also an important parameter. Depending on the ABR, excess acidity or basicity may enhance the selectivity of some chemical reactions that occur during pretreatment.

An anti-solvent is added to the pretreatment mixture after the reaction to facilitate the separation of the pulp from the IL. By changing the polarity/structure of the anti-solvent, lignin extraction may be improved and possibly increase enzyme accessibility and lignin recovery (ESPINOZA-ACOSTA *et al.*, 2014). Additionally, chemical interactions between the anti-solvent and lignin may affect lignin structure upon its precipitation. Enzyme loading also plays an important role in the economics of cellulosic ethanol production and should thus be carefully optimized (KLEIN-MARCUSCHAMER *et al.*, 2010). However, there is a lack of such studies in the

literature. To integrate and add value to sugarcane biorefinery, a structural characterization of the recovered lignins needs to be performed so that possible future applications may be identified (GRAGLIA, KANNA and ESPOSITO, 2015). Therefore, in this study we also aimed to analyze the structure of the lignins obtained in the PIL pretreatment.

1. Scope

In this scenario, the scope of this work was to evaluate the pretreatment process of sugarcane bagasse with the protic ionic liquid monoethanolammonium acetate, [MEA][OAc], which can selectively extract the lignin from the bagasse. A graphic summary of the project is shown in Fig. 1.1. The specific goals were:

1. Synthesis and characterization of PILs. Although monoethanolammonium acetate, [MEA][OAc], has shown to be effective on lignin extraction from bagasse, a screening was also performed to guarantee the best anion/cation combination in terms of pretreatment efficiency;

2. Optimization of the pretreatment process by means of factorial designs followed by single-variable experiments, if necessary. Evaluated factors were solid:liquid ratio, temperature, pretreatment time, water content and type of anti-solvent.

3. Structural analysis of lignins recovered with different anti-solvents;

4. Optimization of the enzyme loading (cellulases and hemicellulases) used in the enzymatic hydrolysis of the pretreated materials;

5. Study of the impact of acid-base ratio on pretreatment performance;

6. PIL recovery and recycling with evaluation of efficiency over the cycles and strategies to overcome possible bottlenecks;

7. Quantification of wash water usage on pretreatment and its impact on enzymatic hydrolysis and alcoholic fermentation, as well as calculation of mass balances.
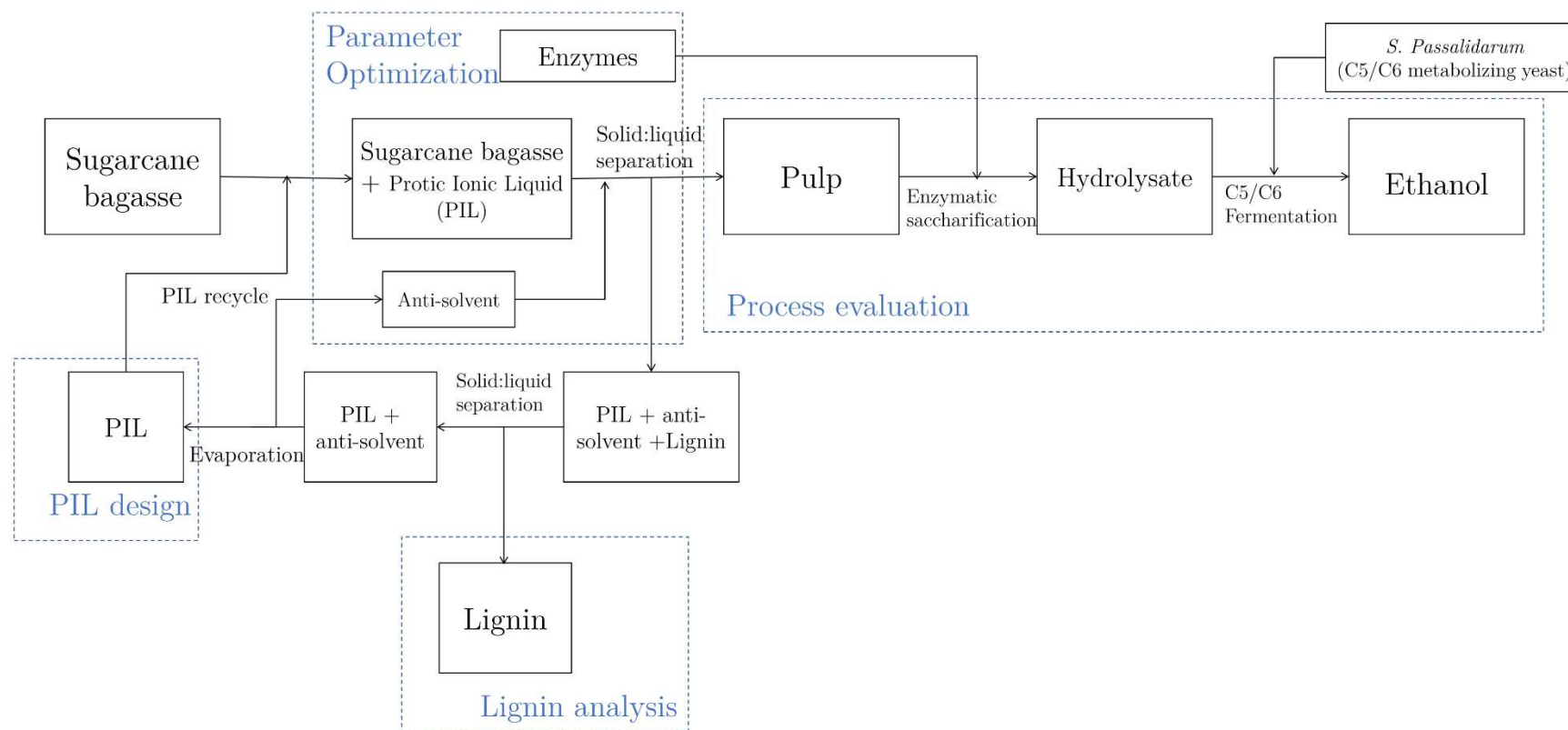
Fig. 1.1 — Graphical abstract of this PhD project. The dotted blue boxes are the key aspects that were studied.

Chapter 2

2. Literature review

2.1. Transition to a biobased economy

The imbalances caused by anthropic action demand a transition to a new era in which humanity becomes more aware of its role in the natural cycles of the planet. Consumption of products from non-renewable raw materials, i.e. fossil resources, culminates in the pollution of the biosphere and amplification of the greenhouse effect; thus, transition to a biobased economy is inexorable. The most recent verification of such progress was the ratification of the Paris Agreement by China, one of the most polluting countries in the world, at COP21 in September 2016 (GLOBO, 2016).

While an economy based on fossil fuels utilizes fractions obtained from the distillation of petroleum such as ethylene, LPG (liquefied petroleum gas) and naphtha, etc., for the production of consumer goods, a biobased economy uses parts from various forms of biomass. In the case of lignocellulosic biomass, one can imagine biomass processing in the same way as an oil refinery, with an integrated biorefinery, which consists of a process plant that extracts carbohydrates, oils, lignin and other biomass materials, converting them into fuels, high-value chemical inputs and other materials with minimal waste generation (KAMM *et al.*, 2007).

In the transportation sector, the transition takes place by replacing fossil fuels with biofuels, especially second-generation ones derived from lignocellulosic (non-edible biomass) materials, which can increase the productivity of first-generation biofuel crops. Additionally, they present the following advantages: reduce the level of subsidies, increase the mitigation of greenhouse gases (GHGs) released into the atmosphere; reduce deforestation and allow a better use of resources, such as low fertility soils, and increase income opportunities, especially in the agricultural sector (ZUURBIER and VAN DE VOOREN, 2008). The IEA (International Energy Agency) predicts that by 2050 there will be a substantial increase in the production of biofuels (Fig. 2.1); together they will account for about 27% of total fuels and avoid around 2.1 Gt of carbon dioxide emissions per year.
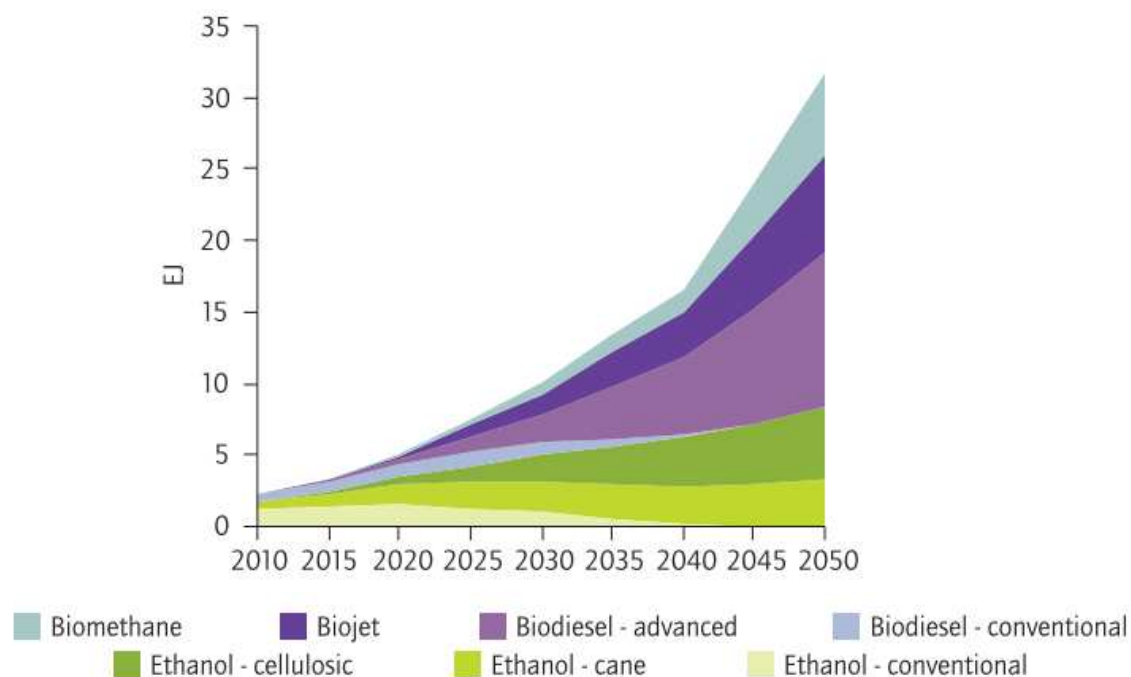
Fig. 2.1 — Estimates of increased demand for biofuels by 2050 (TANAKA, 2011).

2.2. Ethanol from sugarcane

Brazil has an intimate history with sugarcane, which was introduced in the country by the Portuguese in the first century of occupation (1600). Mainly used for sugar production, ethanol production as fuel dates back to 1920 after the industrial revolution. Since its dawn, such production would be strongly linked to the oil commercial balance in the country and worldwide. The Proálcool (National Alcohol Program), introduced in the mid-1970s due to an international oil crisis, was the first major short-medium term project to insert ethanol as a fuel; attention to ethanol in the following decades decreased due to lack of government support and low oil prices. In 2003, the insertion of flex fuel engines contributed to ethanol's popularization and consumption. Although there have not been many subsidy policies for alcohol production, fixing the percentage of anhydrous ethanol added to ordinary gasoline — which rose from 4.5% in 1977 to 27% in Dilma Rousseff's government — still ensures a base production.

At the top of the ethanol production ranking, just below the US (Fig. 2.2), Brazil achieved a total production of around 28.48 billion litres of ethanol by 2015 (UNICA, 2015). Such expressive commodity's participation in the market is the bet for the transition to a biobased economy, especially when considering the side products from the first generation ethanol (E1G) production — straw and bagasse — whose carbohydrates can be converted by

chemical and biochemical processes into second generation ethanol (E2G), which, in turn, can increase ethanol productivity by up to 50% (MILANEZ *et al.*, 2015).
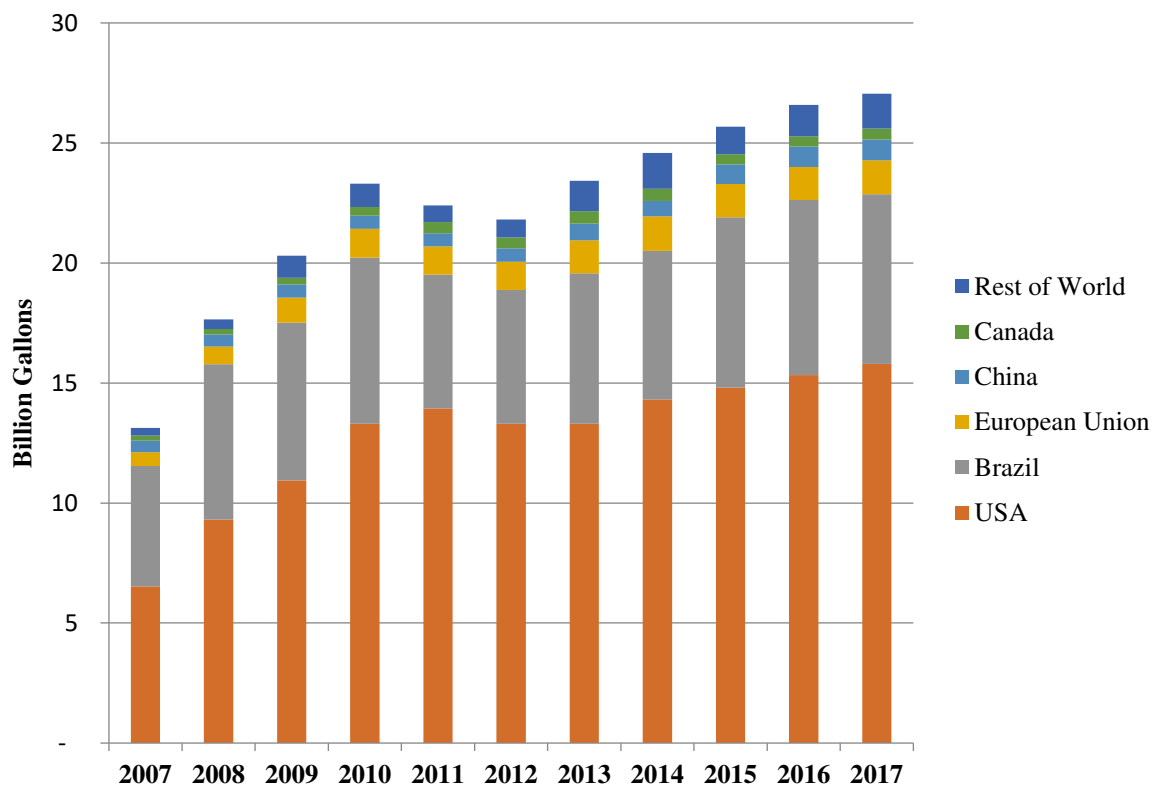
Fig. 2.2 — Global ethanol production by country/region and year (RENEWABLE-FUELS-ASSOCIATION, 2016).

Sugarcane ethanol is considered environmentally friendly because it has a high energy content and its combustion emits less pollutants than fossil hydrocarbons. If we think in terms of the ratio between the energy contained in a given volume of ethanol by the fossil energy needed to produce it in the form of fertilizers, pesticides, fuels, etc. (Fig. 2.3), we find this value reaches from 8.2 to 10; which places it high amongst other biomasses, such as corn used as substrate in the USA, or beet, in Europe (GOLDEMBERG, 2008).
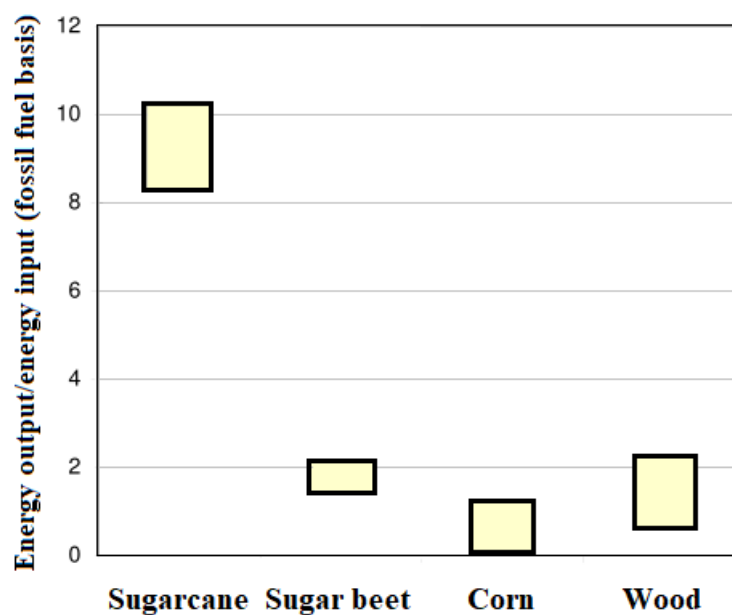
Fig. 2.3 — Energy balance of alcohol production from different types of feedstocks (GOLDEMBERG, 2008).

A massive production of E1G/sugar implies an equally high production of sugarcane bagasse, in fact, about 634 million tons of sugarcane were ground in the 2014/2015 harvest (UNICA, 2015). Bagasse and straw from sugarcane is one of the main lignocellulosic feedstocks produced in the country and it is currently burned in boilers for heat and electricity generation, called cogeneration, but it has recently drawn attention towards E2G production. Bagasse as raw material for E2G has a number of advantages: it is already processed from mills; it is readily available; it is cheap; and it is ready for on-site use, thus avoiding extra expenses due to transportation (SOCCOL *et al.*, 2010).

The biochemical platform of sugarcane biorefinery aims to ferment sugars extracted from biomass. After proper conditioning of the raw material, conversion technologies involve: i) conversion of biomass into sugars or substrate molecule for fermentation; ii) bioconversion of these biomass intermediates using biocatalysts; iii) product processing to generate value-added products, such as ethanol, butanol, heat and /or electricity (PENG, REN, and SUN, 2011).

Specifically, in E2G production from sugarcane bagasse, step i) corresponds to the enzymatic saccharification (or hydrolysis) and it is necessary to depolymerize cellulose into glucose monomers and, also, hemicelluloses into pentoses monomers (mainly xylose) and

hexoses (in smaller amounts), which then will be the carbon sources for fermenting microorganisms in step ii) in the alcoholic fermentation. The recalcitrant nature of raw bagasse does not make it susceptible to direct hydrolysis. Several pretreatment methods have been developed aiming to remove the recalcitrant barriers and increase the biomass digestibility by changing its composition and physical structure (HENDRIKS and ZEEMAN, 2009).

2.3. Lignocellulosic biomass and its recalcitrance

Lignocellulosic biomass refers to the dry mass of the plant, also it is called lignocellulose. When compared to fossil fuels, lignocellulosic biomass is more abundant and homogeneously distributed on the planet, which makes it inexpensive and susceptible to technological bioconversion. However, lignocellulosic biomass is responsible for the mechanical support and must be recalcitrant to guarantee plants' survivability. Biomass recalcitrance, therefore, refers to the physical, chemical and morphological characteristics of lignocellulosic biomass — the presence of lignin, cellulose and hemicelluloses and their crosslinks (Fig. 2.4) — which constitute physical barriers that protect cellulose from degradation by microorganisms or enzymes (SUN and CHENG, 2002).

Plants natural features that are responsible for biomass recalcitrance are, from a macrostructural perspective (HIMMEL *et al.*, 2007): (i) the epidermal tissue of the plant body, particularly the cuticular and epicuticular waxes; (ii) the arrangement and density of vascular bundles; (iii) the relative amount of sclerenchyma (thick wall); (iv) the degree of lignification; (v) the structural heterogeneity and complexity of the components of the cell wall, such as microfibrils and polymer matrices.

Sugarcane bagasse and straw recalcitrance is one of the main bottlenecks in the Brazilian E2G production; the low accessibility of native cellulose hinders its depolymerization for further processing. A deep knowledge of the chemical nature of the constituent fractions of biomass is needed to understand their reactivity towards chemicals and/or biochemical reagents.
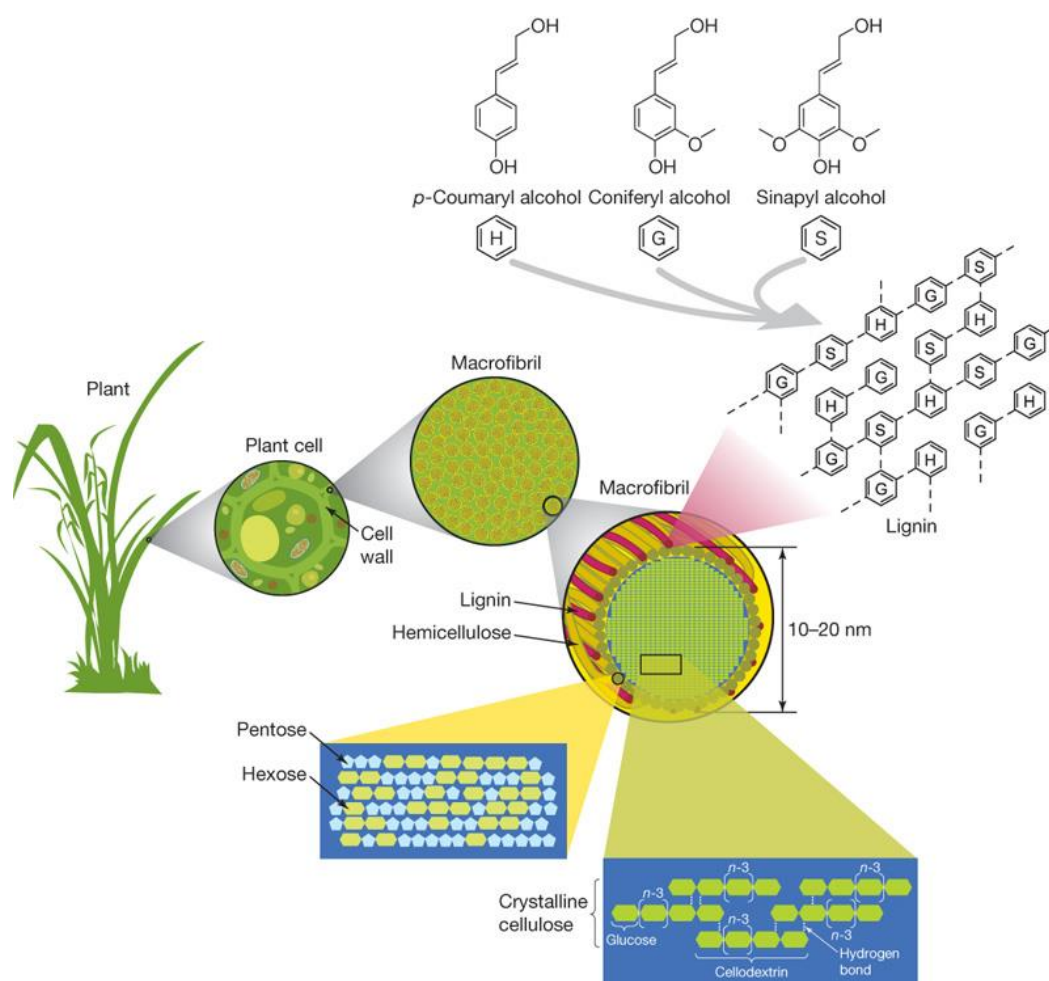
Fig. 2.4 — The complex interaction among hemicelluloses, cellulose and lignin is a consequence of the evolutionary adaptation of plants to protect themselves from exogenous threats, making lignocellulosic biomass naturally recalcitrant (RUBIN, 2008).

2.4. Composition of sugarcane bagasse

Sugarcane bagasse is formed by the complex interaction of three components: two carbohydrates — cellulose and hemicellulose — and one aromatic macromolecule — lignin; and, in minor amounts, structural proteins, lipids and ashes (RABELO, 2010). Cellulose is a homopolysaccharide with molecular formula $(C_6H_{10}O_5)_n$; its linear chains result from the linkage of several anhydroglucopyranose (β-D-glucopyranose) units linked by β $(1 \rightarrow 4)$ bonds. Cellobiose is defined as the minimum conformational unit of cellulose, whereas glucose represents the fundamental unit of the homopolymer chains (TÍMAR-BALÁZSY and EASTOP, 1998).

In cellulose, glucose chains are bound by London forces and hydrogen bonds in the crystalline structure, in approximately 40 glucan chains known as elementary fibrils

(BIDLACK *et al.*, 1992 *apud* RABELO, 2010). Union of these elementary fibrils, which essentially have a very long length and a width of approximately 250 Å, forms the microfibrils (FAN *et al.*, 1982 *apud* RABELO, 2010). High order regions within the microfibrils are called crystalline regions and, the less organized, amorphous regions. Both regions occur in characteristic proportions in different celluloses (O'SULLIVAN, 1997).

Also known as polyoses, hemicelluloses are branched heteropolysaccharides with shorter chains than cellulose. Sugar moieties in hemicelluloses may be subdivided into groups, such as pentoses, hexoses, hexouronic acids and deoxyhexoses. Hydroxyl groups from β-D-xylopyranosyl units may be partially substituted by acetyl groups at O-2 or O-3 (CARVALHO *et al.*, 2017). The degree of acetylation varies according to the type of biomass and the amount of acetyl groups is between 1-6 wt% of total biomass in a dry basis (PENG *et al.*, 2011).

Hemicelluloses are also a major fraction of sugarcane bagasse and account for about 25-35 wt% in a dry basis (SUN *et al.,* 2004). Their major component is xylan (above 90%), with minor amounts of glucose, arabinose and traces of mannose and galactose. According to a study by SOUZA *et al.* (2012), the main types of sugars present in hemicelluloses are xyloglucan and arabinoxylan which are closely associated with cellulose.

Lignin is a phenolic macromolecule synthesized in plants by oxidative coupling of three major C9 (phenylpropanic units) units: syringyl alcohol (S), guaiacyl alcohol (G) and p-coumaryl alcohol (H) (Fig. 2.4) that together form a random structure in a 3D arrangement in the cell wall. The main bond type between the units is aryl-aryl ether, i.e., linkages between phenolic units. After cellulose, lignin is the most abundant organic macromolecule in plants. It is mainly present in the middle lamella and the secondary wall and provides rigidity to the cell wall. It also plays an important role in the transport of water, nutrients and metabolites, being responsible for the mechanical resistance of plants and protecting tissues against microorganisms (FENGEL and WEGENER, 1989).

2.5. E2G production process

As already mentioned, E2G production involves basically three stages — pretreatment, enzymatic saccharification and alcoholic fermentation. The first two correspond to the deconstruction of the lignocellulosic architecture in order to provide monomeric sugars that will be bioconverted into ethanol in the third stage. Subsequent processing of the fermented

broth is done by distillation of the produced ethanol. In this work, the main focus will be on the pretreatment process, considered one of the main bottlenecks in E2G production.

2.5.1. Pretreatment

Due to the natural recalcitrance of the biomass, native cellulose is practically inaccessible to chemical or enzymatic attack. A pretreatment is necessary to render biomass materials more available to chemical reagents or enzymes for efficient product generation (ZHAO *et al.*, 2012). In Fig. 2.5, a generic illustration of the process of biomass ultrastructure deconstruction before (Fig. 2.5a) and after a pretreatment (Fig. 2.5b) is shown.

Pretreatment, therefore, is the process by which it is aimed to increase the production rate as well as the total yield of sugars released during the subsequent hydrolysis step (ROMANÍ *et al.*, 2010). Removal of hemicelluloses and lignin from microfibers is thought to expose microcrystalline cellulose, which can be hydrolyzed by cellulolytic enzymes. In addition, pretreatment breaks down the macroscopic rigidity of biomass and decreases the physical barriers imposed on mass transfer properties of the system (HIMMEL *et al.*, 2007).

An ideal pretreatment should meet the following requirements (MOSIER *et al.*, 2005; PETERSEN *et al.*, 2009; PIENKOS and ZHANG, 2009; YANG and WYMAN, 2008): (i) economically and operationally simple; (ii) minimum energy, chemicals and process water requirements; (iii) use whole, non-comminuted biomass (iii) cause minimal corrosion; (iv) alter the structure of lignocellulosic materials; (v) selectivity for loss of polysaccharides; (vi) fermentability of the hydrolysates after a detoxification step (if possible without detoxification); (vii) minimum formation of degradation products from lignin, hemicelluloses or cellulose; (viii) production of substrates with high cellulose content and accessibility for enzymatic hydrolysis; (ix) high quality lignin or lignin derived products.

Fig. 2.5 — Modification of the lignocellulosic architecture before (a) and after (b) of a pretreatment with ionic liquids. In green, cellulose microfibrils, in yellow, hemicelluloses chains and in brown, lignin particles (source: SCY-STYLE, 2011).

2.5.2. **Types of pretreatment**

There is still no consensus on the best pretreatment from a technical and economic point of view (ROMANÍ *et al.*, 2010). Table 2.1 provides a comparison amongst the main pretreatment types being effectively used by the largest commercial E2G plants in the world. At least four types of pretreatment can be highlighted: ammonia fiber expansion (DuPont), hydrothermal (Beta Renewables), steam explosion (POET-DSM and GranBio) and dilute acid (Abengoa and Raízen). Variability in biomass composition is one of the main culprits for the lack of a universal pretreatment for lignocellulosic biomass. From all the plants listed in Table 2.1, only POET-DSM's production is close to its nominal capacity (DOERING, 2016), which showcases a clear issue with E2G technology development. Comprehensive literature reviews on pretreatment can be found in works by YANG; WYMAN (2009), PIENKOS; ZHANG (2009), JøRGENSEN *et al.*, (2007), JÖNSSON; MARTÍN, (2016) and KUMARI; SINGH, (2018).

The pretreatments mentioned above were compared in Table 2.2 in terms of advantages and disadvantages. The mentioned items were short descriptions and showed the main effects of each pretreatment, as well as difficulties related to each process. Dilute acid pretreatment has been studied for at least twenty years (YANG and WYMAN, 2008) with a particular focus on fuel production. The National Renewable Energy Laboratory (NREL) — one of the world's leading E1G/E2G technology centers — recommends using this pretreatment primarily because it promotes a recovery of up to 90% of hemicelluloses. The basic mechanism consists on the breakage of glycosidic bonds, very sensitive to the presence of the hydronium ion (H_3O^+) in the medium. Although it presents several advantages, such process is quite severe due to the low pH and high temperatures and requires special steel alloys to withstand such conditions, alkaline reagents for pH adjustment, and it causes the formation of degradation products from carbohydrates and lignin that impact negatively on the following steps (MOSIER *et al.*, 2005; YANG and WYMAN, 2008, MOSIER, 2005).

Table 2.1 — Major commercial cellulosic ethanol plants in the world and their pretreatment technologies (NOVACANA.COM, 2015).

Company	Biomass	Pretreatment	Nominal capacity (millions of $m^3 \cdot year^{-1}$)	Operational?	Location
DuPont	Rice straw, wheat straw and *miscanthus*	Ammonia fibre expansion	113.4	Yes, with stops	Iowa, EUA
Abengoa	Corn stover, wheat, sorghum and grasses	Steam explosion with acid catalysis	95	No, but inaugurated in 2014.	Kansas, EUA
POET-DSM	Corn cobs, leaves and stems	Steam explosion	94	Yes	Iowa, EUA
GranBio	Sugarcane bagasse and straw	Steam explosion *	82	Yes, with stops	Alagoas, Brazil
Beta Renewables	Rice, wheat and cane straw	Hydrothermal with steam injection	75	No	Crescentino, Italy
Abengoa	Energy cane straw	Not disclosed	64	Yes	São Paulo, Brazil
Raizen	Sugarcane bagasse and straw	Steam explosion with acid catalysis *	40	Yes, with stops	São Paulo, Brazil

* Pretreatments prone to technology upgrade according to the companies.

Table 2.2 — Comparison between some types of pre-treatment of lignocellulosic biomass (JØRGENSEN, KRISTENSEN and FELBY, 2007; PIENKOS and ZHANG, 2009; YANG and WYMAN, 2008; JÖNSSON and MARTÍN, 2016).

Pretreatment	Main effect on lignocellulosic biomass	Chemicals	Advantages	Disadvantages
Dilute acid	Hydrolysis of hemicelluloses to monosaccharides. Partial lignin removal.	Brønsted acids like H_2SO_4, H_3PO_4, HNO_3 e SO_2.	Good digestibility of pretreated material, high solubilization of hemicelluloses in monomeric form, short reaction times	Abrasive/corrosive, generation of degradation products (furfural, HMF, phenols, etc.),
Hydrothermal	Hydrolysis of hemicelluloses to oligosaccharides. Partial lignin removal.	Water (liquid or in the vapor form)	Environmentally friendly (no reagents other than water), low sugar degradation	Downstream of hemicellulosic hydrolysate, conversions lower than dilute acid
Steam explosion	Hydrolysis of hemicelluloses to oligosaccharides. Partial lignin removal.	Water vapor, SO_2	Environmentally friendly, low sugar degradation	Downstream of hemicellulosic hydrolysate, conversions lower than dilute acid
Alkaline	Removal of lignin and part of hemicelluloses	Arrhenius bases like NaOH, $Ca(OH)_2$ e NH_3	High digestibility of pretreated material, low sugar degradation	Recycle/recovery of chemicals (NH_3), long reaction times, high energy input
APILs	Solubilization of lignin, hemicelluloses and/or cellulose	Wide combination of cations and anions, e.g. 1-ethyl-3-methyl imidazolium chloride	High digestibility of pretreated material, selective solubilization of lignin/hemicelluloses / lignin	Recovery and recycling of IL, recovery of dissolved sugars in IL, high cost of reagents
PILs	Solubilization of lignin, hemicelluloses and/or cellulose	Wide combination of cations and anions, eg bis (2-hydroxyethyl) ethanol ammonium acetate.	High digestibility of pretreated material, selective solubilization of lignin/hemicelluloses / lignin	Recovery and recycling of IL, recovery of dissolved sugars in IL

Hydrothermal pretreatment in its different forms — hot liquid water or steam injection — does not require the addition of acid catalysts and is a more environmentally friendly alternative. The high temperatures of the process promote the formation of H_3O^+ ions by autocatalytic processes (GARROTE, DOMÍNGUEZ and PARAJÓ, 1999); therefore, the pretreatment mechanism is also ruled by acid catalysis. However, there is less recovery of the solubilized hemicelluloses and greater solubilization of the lignin compared to the diluted acid, which makes the downstream of the hemicellulosic hydrolysate more complex, mainly because the hemicelluloses are in the oligomeric form in the hydrolysate, requiring a post-hydrolysis of these sugars (GARROTE *et al.*, 2001; ZHANG *et al.*, 2015; NAKASU *et al.*, 2016). Steam injection pretreatment consists on pressurization of the reactor with water vapor and rapid decompression for physical disruption of the fiber. The main goal of this pretreatment is to remove hemicelluloses, which are also solubilized into the liquid fraction in the oligomeric form. It is also common to add catalysts like SO_2 to increase the medium's acidity and promote higher solubilization of the hemicelluloses (HENDRIKS and ZEEMAN, 2009).

An alkaline medium also favors the occurrence of structural modifications at macro and microscopic levels in the biomass. By means of epimerization reactions and breakdown of the glycosidic bonds (which are more stable in alkaline medium), carbohydrates are depolymerized by reactions of primary — hydrolysis of the reducing terminals — and secondary peeling — hydrolysis of the inner bonds in the sugar chains. Ammonia fiber expansion pretreatment (AFEX) promotes up to 90% conversion of cellulose and hemicelluloses into sugars for a number of biomasses such as wheat straw, barley, sugarcane bagasse and corn stover. For most of these materials, considerable cellulose conversions (above 80%) have been achieved in the enzymatic saccharification (YANG; WYMAN, 2008). However, there are also a number of challenges in developing the process: there is a high energy demand for ammonia pressurization and system heating for extended periods; there is ammonia reaction (consumption) with the biomass and also a post-hydrolysis of the hemicellulosic hydrolysate rich in oligomers is necessary (MATHEW *et al.*, 2016; YANG e WYMAN, 2008).

IL pretreatment is a recent alternative that has been gaining attention for its potential to be environmentally friendly. ILs can act as catalysts and alter the structure of lignocellulosic biomass under certain conditions. Due to the vast possibility of IL structures, it is possible to select

appropriate properties for pretreatment as the advantages outlined in Table 3. However, since both kinetics and thermodynamics of the IL-pretreatment are not well understood, there is no way to predict the reaction behavior of ILs (EARLE and SEDDON, 2000). The main disadvantages of the process arise mainly from their price and the fact that their use in biomass fractionation is recent with a lack on scale up information . In fact, interest in biomass pretreatment with ILs has been increasing since the last decade (REDDY, 2015; GREAVES and DRUMMOND, 2008), but little is known about some downstream stages such as LI recovery after pretreatment (NEGI and PANDEY, 2014).

2.5.3. Challenges in the pretreatment for E2G production

Lignocellulosic biomass is a promising feedstock for the long-term production of biofuels due to its low price, large-scale production, and environmental benefits. However, biofuels from biomass processing are not yet produced at a competitive level due to their high processing cost with currently available technologies (LYND, 1996). In Brazil, the attention is drawn to sugarcane bagasse pretreatment technologies and the development of enzymatic cocktails (MILANEZ, 2015).

As indicated by some studies, technology availability will no longer be the greatest obstacle for the implementation of lignocellulosic biomass conversion technologies in the coming years, but the availability and cost of biomass (ECONOMIST, 2013; SEABRA, 2008; ROSILLO-CALLE, 2010). In this case, Brazil is a potential front runner, since sugarcane straw, surplus bagasse and planted forests already cost between US$ 0.8 and US$ 1.2/GJ, while most of the biomass in the Northern hemisphere cost of around US$ 3/GJ.

Biomass conversion technologies still have a strong impact on the final cost of ethanol, especially the pretreatment stage, which can reach up to 20% of the total cost of an E2G plant (YANG and WYMAN, 2008) and, as already mentioned, it is the primary stage of bagasse processing which impacts on the subsequent steps — enzymatic saccharification and alcoholic fermentation. In fact, the pretreatment stage can be attributed as the main technical problem faced in the largest E2G plants in Brazil — Raizen and GranBio — regarding the transfer of pretreatment technology from other biomasses such oats, barley and wheat straw (Iogen Corp., Canada), and

wheat, rice straw and miscanthus (Beta Renewables, Italy) (JORNAL-CANA, 2016a; JORNAL-CANA, 2016b).

The main challenges of the pretreatment process are related to the reactors cost due to the need for special alloys; to equipment design due to the complexity of the biomass input; and to energy efficiency and consumption of steam /water. Drawing a connection with the items mentioned in section 2.6, it is desirable that the pretreatment process: (1) can operate with the whole biomass; (2) can operate at high solid: liquid (RSL) ratios; (3) be integrated to utilize heat /steam from other subprocesses in the pretreatment. This implies using robust equipment that tolerate the high corrosion rates promoted by the biomass under high concentrations, pressures and temperatures.

2.6. Ionic liquids

ILs are organic salts that melt below 100°C (WU *et al.*, 2011). The first ionic liquid at room temperature, ethylammonium nitrate, was discovered in 1914 (BRANDT *et al.*, 2013). However, interest in such compounds increased in the early 1990s by the discovery of stable room temperature ILs (WILKES and ZAWOROTKO, 1992). In general, ILs consist of a salt in which one or both ions are bulky, and the cation has a low degree of symmetry. These factors tend to reduce the lattice energy of the salt's crystal structure, thus lower its melting point (EARLE and SEDDON, 2000). ILs have been the object of intense study since then, and in recent years there has been a considerable increase in understanding their role in the synthesis of chemicals, catalysis, biocatalysis, as engineering fluids, as well as catalysts for the transformation of biomass (BRANDT *et al.*, 2013).

Modern ILs are made up of organic cations, usually aliphatic or aromatic quaternary ammonium ions; alkylated phosphoniums and, occasionally, alkylated sulfonates are also used. A representative selection of the most common cations is shown in Fig. 2.6. Many popular anions are replaced with electron withdrawing fluorine atoms, such as trifluoromethanesulfonate or tetrafluoroborate, which increases delocalization of the negative charge, but ionic liquids with non-halogenated anions, such as acetate and hydrogen sulphate, have recently been developed due to their lower price and toxicity (BRANDT *et al.,* 2013).
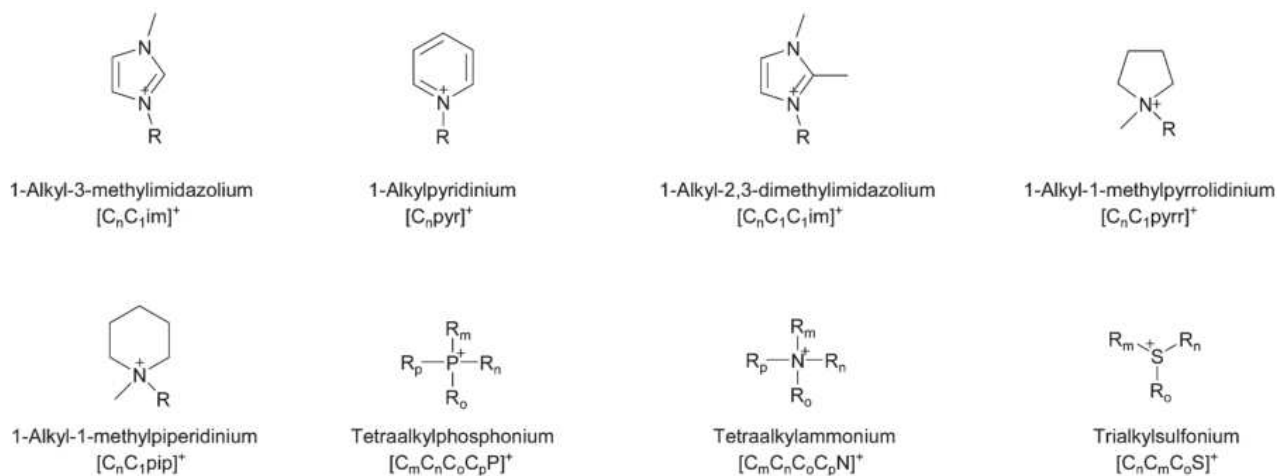
Fig. 2.6 — Most used cations in modern ionic liquids (BRANDT *et al.*, 2013).
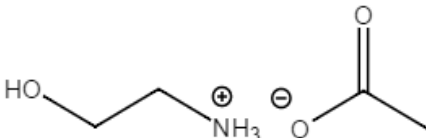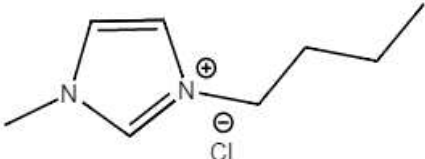
The physico-chemical characteristics of ILs heavily depend on the combination of cations and anions chosen. In general, ILs have negligible vapor pressure, in fact so low that, instead of boiling under high temperatures, they decompose. Such feature makes them non-flammable as well, unlike volatile organic solvents SOVs. ILs also tend to exhibit high density, thermal capacity/thermal stability, and high viscosity, which gives them interesting physical properties for various applications in science (GAMMONS, 2014; GREAVES and DRUMMOND, 2015).

2.6.1. IL categories and their synthesis

Two IL categories can be considered — protic ionic liquids (PILs) and aprotic ionic liquids (APILs). The main structural difference between PILs and APILs is the presence of an ionizable hydrogen in the PIL, that is, a hydrogen that can easily dissociate in aqueous medium and decrease the medium's pH. In comparison to APILs, PILs often have higher conductivity and lower viscosity, as well as lower melting points (GAMMONS, 2014).

PILs present simpler synthesis — via transfer of a proton (H^+) between an acid and a Brønsted base — and also cheaper (up to 40 times) when compared to APILs, widely studied in the literature for applications in biomasses (GEORGE *et al.*, 2014; MÄKI-ARVELA *et al.*, 2010). In Table 2.3 the main differences in the synthesis of two ionic liquids under an environmental perspective were summarized. It can be noted that PIL production tends to be more environmentally friendly due to reductions in by-product generation, solvent losses, energy use and carbon dioxide generation (SATHITSUKSANOH *et al.*, 2014). In the long term, one is expected to synthesize PILs from the lignocellulosic biomass itself in a strategy similar to SOCHA *et al.*, (2014). In this work, the focus will mainly be on PILs, their physico-chemical characteristics and applications in biomass fractionation. The aprotic counterparts will be mentioned as a comparison when necessary or when there isn't enough information on a certain PIL topic in the literature.

Table 2.3 — Comparison between the synthesis of two ionic liquids (BURRELL *et al.*, 2010; BRANDT *et al.*, 2012; WILKES *et al.*, 1982).

	PIL	APIL
Example	monoethanolammonium acetate	1-methyl-3-butyl-imidazolium chloride
Solvent requirement?	No	Yes
Energy demand	Low (exothermic reaction)	High (endothermic reaction)
Multistep?	No, single step synthesis	Multistep
Green chemicals?	Yes	No
Purification of product	Simple	Complex

2.6.2. Biomass pretreatment with PILs

Although there are advantages related mainly to cost, environmental footprint and structural modification of biomass, there are few studies in the literature regarding the use of

acetate PILs in biomass pretreatment. A literature search showed some recent work (REIS *et al.*, 2017; ROCHA *et al.*, 2017; SUN *et al.*, 2017), one of them from our research group (ROCHA *et al.*, 2017), which also resulted in a patent application.

The results obtained by ROCHA (2016) showed that the pretreatment with the PIL monoethanolammonium ammonium acetate led to promising results; conversion yields obtained in the enzymatic saccharification of bagasse were higher than hydrogen peroxide pretreatment, a highly effective pretreatment also studied in our research group (RABELO *et al.*, 2011), and whose patent application was also deposited (RABELO *et al*., 2008).

GEORGE *et al.*, (2014) studied the pretreatment of switchgrass (*Panicum virgatum*) with a combination of ammonium cations (Fig. 2.7a) and hydrogen sulphate anion (HSO_4^-). They compared the performances of these PILs with the APIL 1-ethyl-3-methylimidazolium acetate [EMIM][OAc]. The PILs showed lower enzymatic saccharification yields, however, there was no intention to optimize the pretreatment conditions for each PIL studied (GAMMONS, 2014; GEORGE *et al.*, 2014). Other studies worth mentioning were done by ACHINIVU *et al.* (2014), who studied the pretreatment of corn stover with PILs derived from pyrrolidinium, pyridinium and 1-methylimidazolium cations with the acetate anion (Fig. 2.7b). The choice of acetate as anion in PILs is generally due to its history on biomass dissolution with APILs. Chloride and acetate anions are the most used because of their high hydrogen bond basicities (SUN *et al.*, 2009).

GAMMONS (2014) performed a screening of PILs on the pretreatment of sugarcane bagasse, miscanthus, poplar, among other biomasses. Their strategy consisted on first selecting the best anion in terms of glucose conversion in the enzymatic hydrolysis; then, the best cation. The interpretation of the results, however, could be argued in terms of biomass screening planning, which was done first with miscanthus and then tested on other biomasses. Additionally, the enzymatic saccharification was performed in a high throughput system, which is subject to many errors.
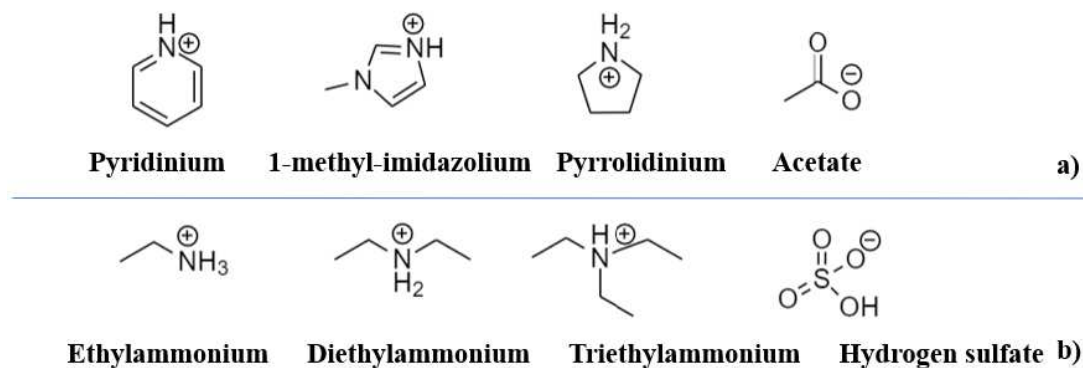
Fig. 2.7 — Some of the protic cations studied by (a) ACHINIVU *et al.*, (2014) and (b) GEORGE *et al.* (2014) in their study of lignocellulosic biomass deconstruction with PILs. The anions were (a) acetate (OAc^-) e (b) hydrogen sulfate (HSO_4^-).

The aforementioned works show that there is still a great horizon to be explored on biomass deconstruction with PILs. However, they have already provided indications that PILs act as delignifying agents and modify the ultra-structure of lignocellulosic biomass in general. A more comprehensive outlook of the pretreatment process is necessary so that bottlenecks can be identified. The process to be developed in this work is similar to the *IonoSolv* process developed by BRANDT *et al.* (2013) in terms of lignin dissolution during pretreatment.

Investigation on the pretreatment process with PILs can be divided into upstream, the process itself, and downstream. In the upstream, PIL design and synthesis are foremost. In the pretreatment process, some operational parameters such as temperature, reaction time, solid:liquid ratio, acid-base ratio (ABR) etc. require optimization, which then paves the way for validation on the downstream steps, enzymatic saccharification and alcoholic fermentation.

2.7. Bioconversion of sugars into ethanol

Bioconversion of lignocellulosic materials into ethanol involves the depolymerization of the carbohydrates in their constituent monomers and the subsequent fermentation of these sugars, it can be performed simultaneously in a single stage or sequentially in two stages (

Fig. 2.8). In the single-stage processes, hydrolysis and fermentation are performed in the same reactor. Direct conversion by the microorganism (DCM) is the process in which the same microorganism produces the enzymes and performs the fermentation. Simultaneous

saccharification and fermentation (SFF) involves the use of cellulase systems from a cellulolytic microorganism (usually a fungus from the genus Trichoderma), together with the presence of an ethanol producing microorganism (bacteria, yeasts, fungi, etc.) (ROSSELL, 2006 apud RABELO, 2010).

The main advantage of these processes is the reduction of final product inhibition that occurs in the two-step operation, since microorganisms together with the cellulolytic enzymes reduce sugar accumulation in the fermentor. Thus, higher hydrolysis rates and conversions can be achieved with lower enzyme loadings to increase ethanol yields (ROSSELL, 2006 *apud* RABELO, 2010).
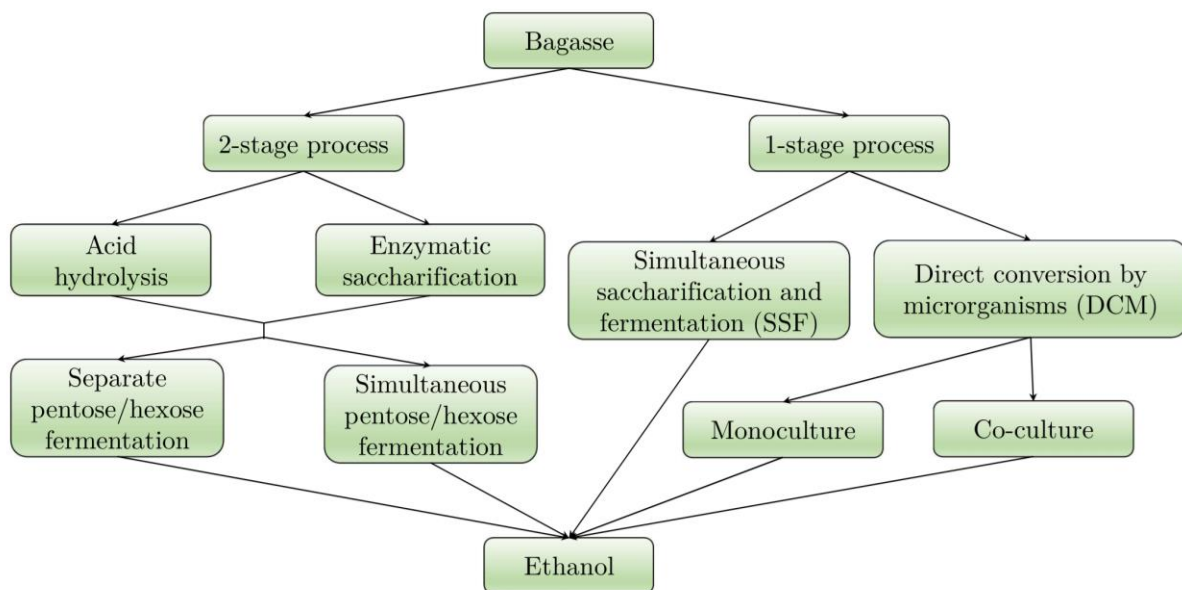
Fig. 2.8 — Fermentation and hydrolysis routes for ethanol production (OGIER *et al.*, 1999)**.**

One disadvantage of this process is related to the different optimum pH and temperature conditions in the hydrolysis and fermentation steps, which demand a compatible condition for both steps. The optimum temperature for enzymatic hydrolysis is close to 50°C and conventional ethanol producing yeasts operate at about 28-34°C, so thermo-tolerant microorganisms are more suitable for the single step process.

An approach that has shown greater flexibility to control operational conditions is the two-step process where saccharification (acid or enzymatic) and fermentation are performed separately. The advantage of this process is that, once performed separately, hydrolysis and fermentation may be carried out in their respective optimal conditions mentioned above. The main disadvantage of this process is the final product inhibition, as described above, decreasing the ethanol yields (RABELO, 2010; SZCZODRAK and FIEDUREK, 1996).

2.8. Enzymatic saccharification of biomass

The enzymatic processes employ cellulolytic complexes as biocatalysts in the hydrolysis, which require mild conditions — temperatures close to 50 ºC, pH in the range of 4.5 — 6.0 and operation at atmospheric pressure. Such features allow higher conversions than those obtained by chemical hydrolysis, lower sugar degradation and therefore less amount of fermentation inhibitors such as furfural and lignin derivatives (HAMELINCK *et al.*, 2005).

The enzyme system that hydrolyses cellulose consists of four main components: endo-1,4-β-D-glucanases (EC 3.2.1.4), exo-1,4-β-D-glucanases (EC 3.2.1.91), β-glucoside glucohydrolases (EC 3.2.1.21) and lytic polysaccharide mono-oxygenases (LPMO's). These components are generally referred to as endoglucanases, exoglucanases, β-D-glucosidases and mono-oxygenases, respectively (OGEDA and PETRI, 2010, LADISCH *et al.*, 1983).

Endoglycanases act randomly in the amorphous regions of cellulose and its derivatives, hydrolyzing β-(1,4) glycosidic bonds and producing glucose, cellobiose and cellotrioses. Exoglucanases act on the reducing ends of the cellulose chains releasing D-cellobiose. β-glycosidases catalyze the release of monomeric D-glucose units from cellobiose and soluble cellodextrins. The hydrolysis process does not occur in stages, but concomitantly, so that there is a synergism between the enzymes. Synergism refers to the higher activity of cellulase mixtures compared to the sum of the individual enzymes activities (WILSON and IRWIN, 2004). Individual cellulases alone will not degrade crystalline cellulose more than 5%, no matter how much enzyme is added to the reaction (OGEDA and PETRI, 2010).

Mono-oxygenases (PMOs), formerly called GH61s, had their function discovered recently. They do not act as hydrolases but as oxidative enzymes in crystalline cellulose generating

oxidized and non-oxidized terminals (DIMAROGONA *et al.*, 2012). They can be distinguished by the regioselectivity of cellulose oxidation sites: PMO1 – attack on C1, PMO2 – attack on C2. In this way, they increase the efficiency of the common cellulases by acting synergistically with them. However, they require an external reducing agent (electron donor). In the enzymatic cocktail, cellobiose dehydrogenase is a potential donor. In the case of sugarcane bagasse, it is believed that lignin exerts this function (DIMAROGONA *et al.*, 2012). The mechanism of action of the enzymes is summarized in Fig. 2.9.
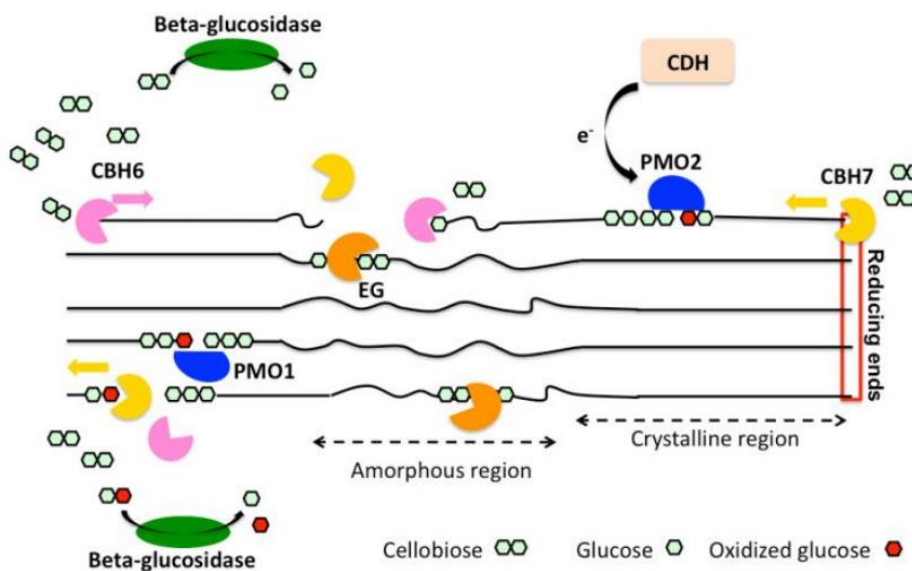
Fig. 2.9 — A simplified scheme of the current view on cellulose degradation involving cellobiohydrolases (CBH), Endoglucanases (EG) and PMO's (PMO1 and PMO2, respectively). (DIMAROGONA *et al.*, 2012).

2.8.1. Alcoholic fermentation

Commercial bioconversion of lignocellulosic biomass into ethanol requires the efficient fermentation of a sugar mixture (HINMANN *et al.*, 1992; HINMANN *et al.*, 1989). Lignocellulosic biomass generally contains five main sugars, and their abundance varies according to the raw material (PETTERSEN, 1984). They are hexoses — D-glucose, D-mannose and D-galactose — and pentoses — D-xylose and L-arabinose. Fructose and sucrose are not normally found in lignocellulose. In case of sugarcane bagasse, the component sugars are D-glucose from cellulose and hemicelluloses, and D-xylose and L-arabinose from the hemicelluloses.

Yeasts are the most suitable microorganisms to produce ethanol: they have drawn the attention for ethanol research since the early days of biorefinery and can grow in a variety of sugars with high tolerance to substrates and ethanol. However, they preferentially grow in six-carbon sugars, but some strains are also capable of using pentoses and converting them into ethanol (DIEN; JEFFRIES, 2003, HAHN-HAGERDAL *et al.*, 2007, PENG *et al.*, 2011).

D-glucose fermentation by the yeast *Saccharomyces cerevisiae* has been used for thousands of years and is well established. In contrast, the goal of producing ethanol from pentoses has emerged relatively recently, and despite many efforts in several research centers around the world, it remains a challenge (JEFFRIES and SHI, 1999). Among pentose-fermenting yeasts, microorganisms such as *C. shehatae*, *P. stipitis* and *Kluveromyces maxianus* were discussed in detail to produce ethanol (CHANDEL *et al.*, 2011). More recently, *S. passalidarum*, a yeast that also has a potential for D-xylose metabolism has been discovered (HOU, 2012a). Most yeasts are not able to ferment D-xylose directly. It has been observed that they use D-xylulose instead, an isomer of D-xylose, both by oxidation and fermentation. *S. stipitis* has also gained attention for its robustness and productivity in the bioconversion of pentoses to ethanol.

Chapter 3

3. PIL screening and design

In this chapter, the rationale behind PIL screening and design will be discussed. As already mentioned, there is a vast combination of cation and anion that could be form potential PILs as pretreatment agents. However, a thorough literature research may help filtering out and choosing suitable ions. Also, chemical knowledge on the reactivity of biomass towards acidic or basic ions is foremost for the design task.

The protic ionic liquid [MEA][OAc] or also monoethanolammonium acetate (usual name) was chosen as the first option due to preliminary studies carried out in our group showing that it can extract lignin from sugarcane bagasse and increase the glucan/hemicellulose yield on enzymatic saccharification (ROCHA, 2016). It was synthesized using equimolar amounts of acetic acid and monoethanolamine in jacketed reactor with a circulating cooling thermal fluid under constant mechanical stirring. Cooling is necessary since the acid-base neutralization reaction is exothermic (Fig. 3.1Fig. 3.1).
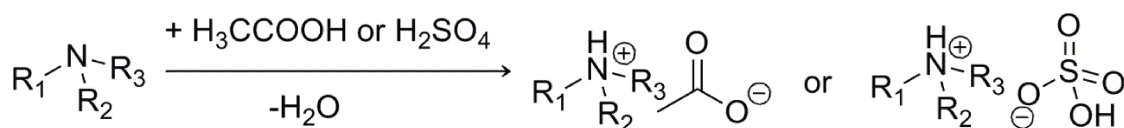
Fig. 3.1 — PIL synthesis from the screening via acid-base neutralization. The R substituent groups correspond to hydrogen, alkyl or hydroxyalkyl groups, anions are acetate and hydrogen sulfate.

The screening was performed with the ammonium cations shown in Table 3.1. The cations present three alkyl or hydroxyalkyl substituents (R_1 to R_3) plus a proton (H^+), which makes them protic. The anions were acetate (OAc^-) and hydrogen sulphate (HSO_4^-), which combined with the cations totalized twelve PILs. The choice of cations was made based on the results obtained by GEORGE *et al.* (2014), who studied the effect of alkyl and hydroxyalkyl substituents on ammonium cations in enzymatic saccharification conversions. The ammonium cations with only alkyl substituents — diethyl, triethyl and butyl — were chosen to study the carbon size/volume

effects and possible hydrophobic interactions with the biomass. Those with hydroxyalkyl substituents were chosen to study the possible effects of hydrogen bonds between the hydroxyl groups in the cations and the lignocellulosic biomass.

Table 3.1 — Ammonium cations with R substituents for the PIL screening with [OAc] and [HSO$_4$] as counter ions according to Fig. 3.1. The substituent R$_4$ corresponds to the H$^+$.

Ammonium cation	Formula	R$_1$	R$_2$	R$_3$
Diethyl	[NH$_2$Et$_2$]$^+$	–CH$_2$CH$_3$	–CH$_2$CH$_3$	–H
Triethyl	[NHEt$_3$]$^+$	–CH$_2$CH$_3$	–CH$_2$CH$_3$	–CH$_2$CH$_3$
Butyl	[NH$_3$Bu]$^+$	–(CH$_2$)$_3$CH$_3$	–H	–H
Monoethanol	[NH$_3$CH$_2$CH$_2$OH]$^+$	–CH$_2$CH$_2$OH	–H	–H
N-methyl-monoethanol	[NH$_2$Me(CH$_2$CH$_2$OH)]$^+$	–CH$_2$CH$_2$OH	–CH$_3$	–H
N-ethyl-monoethanol	[NH$_2$Et(CH$_2$CH$_2$OH)]$^+$	–CH$_2$CH$_2$OH	–CH$_2$CH$_3$	–H

The choice of anions, acetate and hydrogen sulphate, was based on their history in the literature (BRANDT *et al.*, 2013, 2015; GEORGE *et al.*, 2014; VERDÍA *et al.*, 2014). Acetate is well known for being part of APILs such as 1-ethyl-3-methyl-imidazolium acetate and, due to its hydrogen-bond basicity and small size, it can alter the biomass structure (BRANDT *et al.*, 2013). In contrast, the hydrogen sulfate anion is an acidic anion that has been used in the synthesis of biomass-deconstructing PILs (BRANDT *et al.*, 2015). That being said, it was intended to verify the effect of two anions with different acid-base behavior: an alkaline, acetate [OAc$^-$], and an acidic, hydrogen sulfate [HSO$_4$$^-$].

PIL synthesis — except that of [MEA][OAc] — was performed in collaboration with Prof. Silvana Mattedi from the Federal University of Bahia (UFBA). Once the screening involved synthesis and characterization of a considerable number of PILs, this stage was performed with the aid of a master student (PIN *et al.*, 2019). Once it was a screening, pretreatment conditions were not optimized for each PIL used. In fact, the choice of the pretreatment temperature for the PILs was made based on their degradation temperature obtained by TG (thermogravimetric) and DTG (thermogravimetric derivative) analyses. Interpretation of TG/DTG curves behavior was done according to studies by WANG *et al.*, (2014) and LV *et al.*, (2012). From such analyses, an

important parameter was obtained, the onset temperature (T_{onset}), the temperature in which the mass loss from PIL degradation starts, which corresponds to an extrapolated theoretical temperature value at the beginning of the mass loss.

In order to determine the pretreatment temperature for each PIL, it was decided to use a safety range of 10°C below T_{onset} to avoid their thermal degradation; this range was in fact applied for most acetate PILs (Table 5), except for [MEA][OAc], whose chosen temperature was about 35°C lower than T_{onset} because previous tests showed that glucan yields at 175°C were comparable to that at 150°C. Preliminary tests with the hydrogen sulfate PILs showed that temperatures above 120°C eventually degraded the biomass, even causing charring of the material. The reactor heating system — a glycerin bath — also had an upper limit of about 200°C, making it difficult to reach the temperatures indicated by the TG curves (above 280°C) of such PILs. Thus, the temperature of 120°C was chosen for the hydrogen sulfate PILs (Table 3.2). Pretreatment conditions were done according with PIN *et al.* (2019) with 10% solids loading and 5:1 IL:H2O ratio (w/w), the experiments were performed in triplicate.

We chose to use short reaction times — from 15 to 45 min — for PILs derived from hydrogen sulfate because it was known that due to their acidity, pretreatment could be more severe. Pretreatment time with acetate-derived PILs varied from 1 to 3 h, as literature reports usually employed such range (BRANDT *et al.*, 2013). PIL performance evaluation was done by the pulp yield, which measures the amount of biomass that remained in the solid fraction after pretreatment (Eq 3.1).

$$Y_{pulp} = \left(\frac{w_{biomass\ after\ PT}}{w_{biomass\ before\ PT}} \right) \times 100\% \qquad \text{(Eq. 3.1)}$$

In which Y_{pulp} stands for the pulp yield, $w_{biomass\ after\ PT}$ for the weight of dry biomass that remained after the pretreatment in the solid phase, $w_{biomass\ before\ PT}$ for the weight of dry biomass before pretreatment. Another form of evaluation was the glucan and hemicellulose yields obtained in the enzymatic saccharification of the pretreated materials which was performed according with PIN *et al.* (2019) at 50 °C, for 48 h at 10% (w/v) solids loading with Cellic Ctec2 (Novozymes) (15 FPU·g^{-1} dry bagasse) Calculation of glucan and hemicellulose yields was done according to Eq. 3.2:

$$Yield_{glucan/hemicellulose} = \left(\frac{w_{converted\ carbohydrate}}{w_{raw\ carbohydrate}}\right) \times 100\% \quad \text{(Eq.3. 2)}$$

Table 3.2 — Onset temperatures obtained by the TGA of the PILs and their chosen pretreatment temperatures.

Anion	Cation	T_{onset} (°C)	$T_{pretreatment}$ (°C)
[OAc]⁻	[NH$_3$CH$_2$CH$_2$OH]$^+$	185	150
	[NH$_2$Me(CH$_2$CH$_2$OH)]$^+$	170	160
	[NH$_2$Et(CH$_2$CH$_2$OH)]$^+$	155	145
	[NH$_2$Et$_2$]$^+$	130	120
	[NHEt$_3$]$^+$	140	130
	[NH$_3$Bu]$^+$	135	125
[HSO$_4$]⁻	[NH$_3$CH$_2$CH$_2$OH]$^+$	300	120
	[NH$_2$Me(CH$_2$CH$_2$OH)]$^+$	310	120
	[NH$_2$Et(CH$_2$CH$_2$OH)]$^+$	300	120
	[NH$_2$Et$_2$]$^+$	302	120
	[NHEt$_3$]$^+$	287	120
	[NH$_3$Bu]$^+$	300	120

Where $Y_{glucan/hemicellulose}$ stands for the glucan or hemicellulose yield in saccharification, $w_{converted\ carbohydrate}$ for weight of cellulose or hemicelluloses, which were respectively converted into glucose and xylose during the enzymatic hydrolysis, and $w_{raw\ carbohydrate}$ to the weight of cellulose or hemicelluloses originally in the raw bagasse.

3.1 Results and discussion

The results of the screening were summarized in Table 3.3 and Table 3.4, regarding the hydrogen sulfate and acetate anions, respectively. The pretreatments were evaluated according to their performance and their glucan and hemicellulose yields in the enzymatic saccharification, which gives an idea of how much cellulose and hemicelluloses initially present in the bagasse were in fact converted into sugar monomers.

In fact, a higher pretreatment severity was observed with hydrogen sulfate-derived PILs once with up to 45 min of reaction (Table 3.3) the same or even lower pulp yield values (lower yields indicate more degradation/solubilization) were obtained with the acetate analogs (Table Table 3.4). This is related to the higher acidity of the hydrogen sulfate PILs, since there is still an available proton (H^+) in the anion to be deprotonated. An acidic medium facilitates the hydrolysis of glycosidic bonds in the hemicelluloses and their consequent solubilization in the medium (VERDÍA *et al.*, 2014). Glucan and hemicellulose yields showed that the acetate PILs were more efficient in altering the lignocellulosic biomass structure, reaching up to 72% of glucan and 45% of hemicellulose with [$NH_2Me(CH_2CH_2OH)$][OAc]. Glucan and hemicellulose yields were drastically lower for the hydrogen sulfate derived PILs, the highest values were 32.87% of glucan and 14.91% of hemicellulose for the PIL [$NHEt_3$][HSO_4]. It can be inferred that there was clear a difference in the pretreatments mechanism of action. Acetate, a high basicity hydrogen bond anion ($\beta > 1.0$), played a key role in the modification of the lignocellulosic ultrastructure by permeating the biomass and selectively extracting the lignin from the bagasse (BRANDT *et al.* 2013). By following this idea, the pretreatment was delignifying and acted similarly to other alkaline pretreatments such as alkaline hydrogen peroxide pretreatment (RABELO *et al.*, 2011).

Table 3.3 — PIL screening with different cations and hydrogen sulfate as anion [HSO_4^-].

Cation	Temp. (°C)	Time (min)	Y_{pulp} (%)	Y_{Glucan} (%)	$Y_{Hemicellulose}$ (%)
[$NH_3CH_2CH_2OH$]$^+$	120	15	71.04 ± 0.35	17.29 ± 0.14	7.11 ± 0.13
		30	64.91 ± 0.15	16.99 ± 1.59	4.90 ± 0.01
		45	63.40 ± 2.16	15.57 ± 0.61	3.28 ± 0.51
[$NH_2Me(CH_2CH_2OH)$]$^+$	120	15	77.59 ± 2.03	17.33 ± 0.32	8.64 ± 0.03
		30	70.21 ± 0.22	18.73 ± 0.88	8.38 ± 0.38
		45	64.92 ± 2.78	19.33 ± 0.94	8.57 ± 1.16
[$NH_2Et(CH_2CH_2OH)$]$^+$	120	15	91.02 ± 1.01	17.03 ± 2.92	12.19 ± 0.06
		30	75.85 ± 0.65	21.65 ± 1.78	11.21 ± 0.82
		45	68.17 ± 1.30	22.52 ± 2.73	9.77 ± 2.42
[NH_2Et_2]$^+$	120	15	85.17 ± 1.53	18.48 ± 3.20	10.83 ± 1.50
		30	72.65 ± 1.19	26.47 ± 2.19	12.67 ± 1.41
		45	66.07 ± 2.51	29.26 ± 1.52	11.90 ± 1.38
[NH_3Bu]$^+$	120	15	60.54 ± 0.28	24.42 ± 0.26	8.60 ± 0.32
		30	55.96 ± 2.06	27.72 ± 0.14	3.86 ± 0.34
		45	50.44 ± 2.48	30.89 ± 0.92	5.96 ± 1.05
[$NHEt_3$]$^+$	120	15	91.38 ± 2.12	20.27 ± 2.49	11.06 ±1.29
		30	80.22 ± 1.08	23.48 ± 0.17	12.99 ±0.62
		45	73.18 ± 0.38	32.87 ± 0.00	14.91 ±0.49

Table 3.4 — PIL screening with different cations and acetate as anion, [OAc$^-$].

Cation	Temp. (°C)	Time (h)	Y_{pulp} (%)	Y_{Glucan} (%)	$Y_{Hemicellulose}$ (%)
[NH$_3$CH$_2$CH$_2$OH]$^{+*}$	150	2	64.30 ± 2.80	78.10 ± 2.78*	43.00 ± 2.05*
[NH$_2$Me(CH$_2$CH$_2$OH)]$^+$	160	1	67.43 ± 2.05	67.90 ± 2.15	47.54 ± 1.15
		2	65.93 ± 0.42	71.38 ± 0.05	47.05 ± 3.24
		3	64.79 ± 1.17	72.09 ± 1.17	45.90 ± 6.03
[NH$_2$Et(CH$_2$CH$_2$OH)]$^+$	145	1	79.83 ± 2.08	51.32 ± 0.38	37.70 ± 0.76
		2	73.45 ± 0.47	59.64 ± 1.71	40.48 ± 2.12
		3	70.91 ± 1.78	63.12 ± 5.11	45.21 ± 2.39
[NH$_2$Et$_2$]$^+$	120	1	88.28 ± 1.11	19.96 ± 1.60	11.40 ± 0.47
		2	85.99 ± 0.40	23.42 ± 0.05	14.13 ± 0.24
		3	85.76 ± 1.63	23.53 ± 2.15	15.33 ± 1.24
[NH$_3$Bu]$^+$	125	1	81.92 ± 4.31	31.97 ± 1.67	16.07 ± 2.52
		2	79.80 ± 4.51	50.22 ± 3.80	20.29 ± 0.37
		3	77.64 ± 2.23	56.97 ± 1.72	26.38 ± 4.26
[NHEt$_3$]$^+$	130	1	84.34 ± 0.03	32.10 ± 0.58	21.94 ± 0.33
		2	82.92 ± 0.69	37.35 ± 1.61	26.53 ± 0.68
		3	78.48 ± 0.67	43.73 ± 2.36	31.91 ± 1.47

* Results obtained in previous tests but added as a matter of comparison.

In contrast, pretreatment with hydrogen sulfate PILs acted similarly to an acid pretreatment and the conditions employed were not enough to efficiently deconstruct the biomass; the hypothesis that supports this idea is that acid pretreatments favor hemicelluloses solubilization into the liquid phase. In fact, hemicellulose yields were also very low, reaching as low as 3.28% with the PIL [NH$_3$CH$_2$CH$_2$OH][HSO$_4$], indicating that a considerable amount of hemicelluloses were solubilized during pretreatment.

To understand the role of the cation in pretreatment, the glucan (dark bars) and hemicellulose yields (light bars) for the acetate PILs are summarized in Fig. 3.2, which also groups the cations by the presence (in orange) or absence (in blue) of hydroxyl groups. It can be seen that, for the hydroxylated cations, the glucan and hemicellulose yields were generally higher than the non-hydroxylated cations. Acetate, due to its small size and high basicity, can permeate cellulose and interact with it by expanding the intra and intermolecular chains (RAJ *et al.*, 2016). Hydroxylated cations can somehow act in synergy with the acetate and assist in the role of chain expansion in cellulose. Non-hydroxylated cations, once they lack substituents that can interact with cellulose (other than the nitrogen proton), do not modify the cellulose structure as much as the hydroxylated ones. Higher hemicellulose yields can be explained by the ability of acetate anions to permeate lignin and break the phenyl glycoside and/or benzyl ether bonds between carbohydrates (cellulose and hemicelluloses) and lignin that allow cellulolytic enzymes to act more efficiently (BRANDT *et al.*, 2013).

In order to understand the role of the cations in the hydrogen sulfate PILs, glucan yields (dark bars) and hemicellulose yields (light bars) were shown in Fig. 3.3 and the cations were also categorized in hydroxylated (orange) and non-hydroxylated (in blue). Non-hydroxylated cations led to higher glucan yields than the hydroxylated ones, in a reverse trend to the acetate PILs. Hydrogen sulfate does not have the same permeation and interaction with cellulose as the acetate, since it presents a lower hydrogen bond basicity, $\beta = 0.67$ (BRANDT *et al.*, 2011), therefore the synergy between the hydroxylated cations and the anion can be ruled out. The most likely mechanism of interaction of hydrogen sulfate PILs with biomass is the interaction of cations with lignin in order to disrupt lignin-carbohydrate linkages. Thus, non-polar cations are more favored in this interaction, since lignin is predominantly a non-polar macromolecule. However, hydrogen sulfate's inefficiency to expand the cellulose chains does not allow considerable structural

modifications. Hemicelluloses were the most affected by the acidic medium provided by hydrogen sulfate and therefore hemicellulose yields were fairly low (below 30% and 15% of cellulose and hemicellulose yields)..
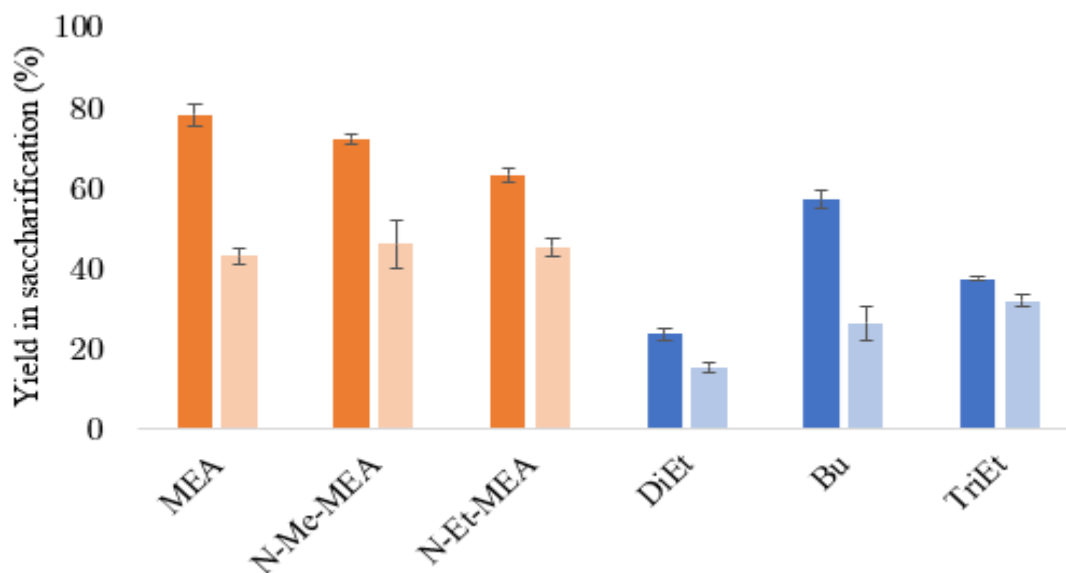
Fig. 3.2 — Glucan (dark bars) and hemicellulose yields (light bars) obtained in the screening of LIPs of acetate anion. The cations were divided into hydroxylated (in orange) and non-hydroxylated (in blue). Legend for the cations: MEA - $[NH_3CH_2CH_2OH]^+$, N-Me-MEA - $[NH_2Me(CH_2CH_2OH)]^+$, N-Et-MEA - $NH_2Et(CH_2CH_2OH)]^+$, DiEt - $[NH_2Et_2]^+$, Bu - $NH_3Bu]^+$, TriEt - $[NHEt_3]^+$ Deviations were calculated with duplicate of the samples. Pretreatment conditions time was 2h.

The highest glucan and hemicellulose yields from the screening were obtained with the PIL N-methyl-monoethanolammonium acetate, [N-Me-MEA][OAc], such values were comparable to those obtained in previous tests with [MEA][OAc] (Table 3.4). However, [MEA][OAc] synthesis is cheaper than the its N-methylated form and there is a comprehensive database concerning MEA utilization and know-how. Previous results with [MEA][OAc] have also confirmed that this PIL is efficient in deconstructing the lignocellulosic biomass structure.
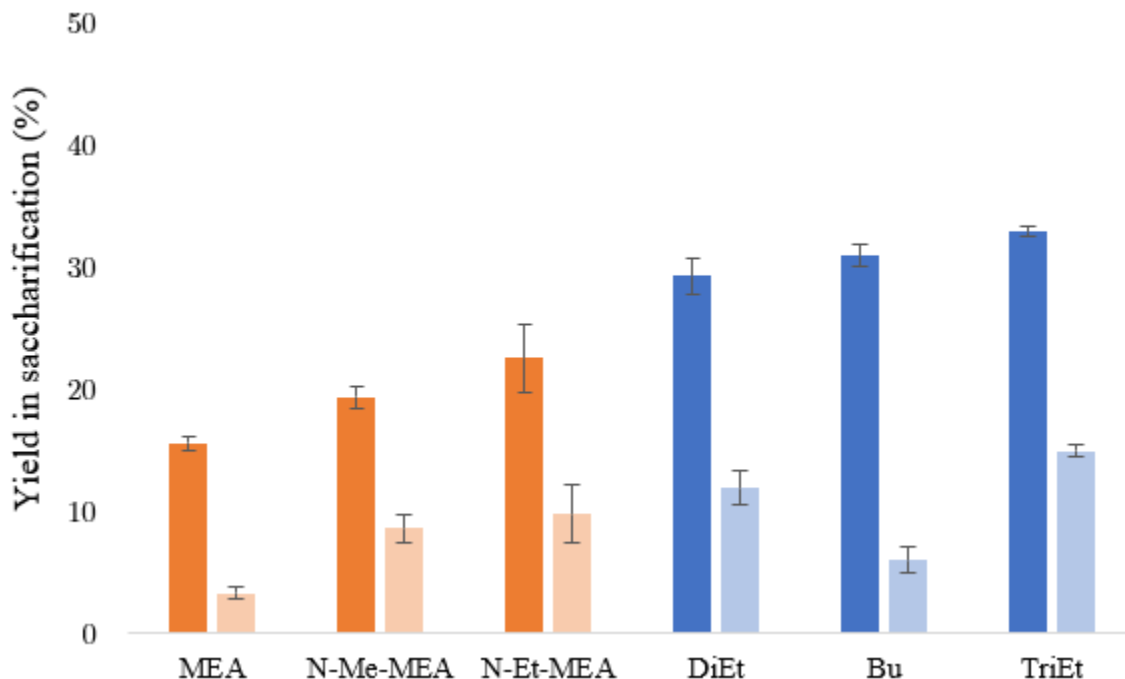
Fig. 3.3 — Glucan (dark bars) and hemicellulose yields (light bars) obtained in the screening of LIPs of hydrogen sulfate anion. The cations were divided into hydroxylated (in orange) and non-hydroxylated (in blue). Legend for the cations: MEA - $[NH_3CH_2CH_2OH]^+$, N-Me-MEA - $[NH_2Me(CH_2CH_2OH)]^+$, N-Et-MEA - $NH_2Et(CH_2CH_2OH)]^+$, DiEt - $[NH_2Et_2]^+$, Bu - $NH_3Bu]^+$, TriEt - $[NHEt_3]^+$ Deviations were calculated with duplicate of the samples. Pretreatment time was 45 min.

3.2 Conclusions

Acetate PILs outperformed hydrogen sulfate PILs in terms of selectivity and performance during enzymatic saccharification, which is due to a difference in the mechanism of action; acetate PILs behaved more like as an alkaline pretreatment whereas hydrogen sulfate PILs were similar to a dilute acid pretreatment. Amongst the acetate PILs, [MEA][OAc] and [N-Me-MEA][OAc] showed superior performance and we chose [MEA][OAc] for the pretreatment process due to its lower price and know-how of MEA use.

Chapter 4

4. PIL process evaluation

Protic ionic liquids (PILs) have been recently studied for biomass fractionation and have shown promising features, especially in terms of lignin solubilisation (ROCHA *et al.,* 2017; BRANDT *et al.*, 2013). PILs such as triethylammonium hydrogen sulphate, [TEA][HSO$_4$], are potential pretreatment agents to selectively solubilize lignin and hemicelluloses and generate cellulose-rich pulps (GEORGE *et al*., 2014). Most studies, however, were performed at a small scale in vials or glass tubes, suitable for introductory studies, but lacking information on following scale up. In this chapter, we aimed to evaluate the performance of [MEA][OAc], by testing several conditions in bench scale reactors (0.5 L) without milling or sieving of the raw biomass, in order to mimic a larger-scale process.

Pretreatment severity is a parameter mainly affected by temperature and residence time; higher severity usually implies higher biomass fractionation at the cost of lower selectivity (CHUM *et al.*, 1990). Pretreatment with PILs such as [MEA][OAc], however, may provide high delignification selectivity whilst effectively fractionating biomass components even under high severities (BRANDT *et al*., 2013). Pretreatment parameters that are directly linked to mass transfer properties, such as solids loading and water content, may also be considered in process optimization. The influence of water content is not as easily predictable. Early studies that evaluated the impact of water in ionic liquid pretreatment systems claimed ILs required a hygroscopic medium for a high performance (COSTA LOPES *et al.*, 2013), but this has been shown not to be true for PILs, which are water-compatible (BRANDT *et al.*, 2011).

An anti-solvent is added to the pretreatment mixture after the reaction to facilitate the separation of the pulp from the IL. Polarity and anti-solvent structure may affect lignin extraction from the pretreatment slurry and possibly increase enzyme accessibility and lignin recovery. Enzyme loading also plays an important role in the economics of cellulosic ethanol production and should thus be carefully optimized (KLEIN-MARCUSCHAMER *et al., 2010)*. However, there is a lack of such studies in the literature. To integrate and add value to sugarcane biorefinery, a structural characterization of the recovered lignins needs to be performed so that possible future

applications may be identified (GRAGLIA; KANNA; ESPOSITO, 2015). Therefore, in this study we also aimed to analyze the structure of the lignins obtained in the PIL pretreatment.

4.1. Materials and Methods

4.1.1. Feedstock

Sugarcane bagasse was provided by São João Mill (Araras-SP, Brazil). The material was collected in the 2012/13 crop (May/2012) by mechanical harvesting and resulted from the last milling before cane juice extraction. The material was air dried for chemical compositional analysis and pretreatment assays. Samples were not ground prior to PIL pretreatment. The chemical composition of raw sugarcane bagasse, as percentage of dry mass, was: cellulose, 41.95 ± 1.41%; hemicelluloses, 25.43 ± 0.69%; lignin, 23.79 ± 1.34%; extractives 2.13 ± 0.46%, acetyl groups 3.46 ± 0.07% and ash, 2.95 ± 0.80%.

4.1.2. Protic ionic liquid synthesis and characterization

Monoethanolammonium acetate, [MEA][OAc], was synthesized by adding equimolar amounts of acetic acid and monoethanolamine in a stirring jacketed glass reactor according to PIN *et al.* (2019). Physico-chemical properties of the synthesized [MEA][OAc], such as viscosity, refraction index, and density were also measured. NMR-H^1 and NMR-C^{13} spectra were recorded according to PIN *et al.* (2019) (data not shown).

4.1.3. Experimental design

Factorial designs were employed in this study in order to provide a better understanding of the factors' impact range and their interaction on glucan and hemicellulose saccharification yields, the main response variables evaluated in this work. To a lesser extent, the degree of delignification was also assessed and correlated with the carbohydrate conversions in saccharification. Some experiments were further validated by single-variable experiments (time-temperature and solids loading-water content) to ensure all parameters were appropriately optimized. Table 4.1 summarizes the experimental outlook of this work.

To study the influence of pretreatment's severity, a 3^2 full factorial design with center point triplicates was performed, with time and temperature as factors. The high temperature level, 150°C was chosen based on the onset degradation temperature of [MEA][OAc] as previously mentioned. Following this, pretreatment time was varied as a single factor to validate the assumptions from the time-temperature experiments. A 2^2 full factorial design with center point triplicates was performed to assess the impact of solids loading and water content — mass transfer parameters — on the PIL performance. Due to its importance, the water content was reevaluated in a single variable experiment. The impact of the anti-solvent was assessed by using protic solvents with different carbon numbers in their structure. Lastly, optimization of the enzyme loading was performed with a 2^2 full factorial design with 4 axial points and center point triplicates. Cellulases and hemicellulases loading were the considered factors.

4.1.4. Statistical analysis

All data collected from the optimization experiments was subjected to statistical tests. Levene's test was performed to guarantee the homoscedasticity of the data. ANOVA was performed on the factorial designs as well as linear regressions and, when necessary, Tukey's test was also performed for post-hoc analysis. The statistical tests were performed with the software STATISTICA (version 10.0, Statsoft) and R Studio (version 1.1.4.56, RStudio Inc.).

Table 4.1 — Experimental design employed in this study in chronological order.

Factors	Experimental design	Factors range/levels	Fixed pretreatment parameters
Time and Temperature	3^2 full factorial design with center point triplicates	30 -150 min; 120 -150 °C	Solids loading, 10 wt%; water content, 15 wt%; water as anti-solvent
Time	Single variable experiment	2 – 8 h	Temperature, 150ºC; water content, 15 wt%; water as anti-solvent
Solids loading and water content	2^2 full factorial design with center point triplicates	10 – 20 wt%; 10 – 30 wt%, respectively	Time, 2 h; temperature, 150ºC water as anti-solvent
Water content	Single variable experiment	10 – 70 wt%	Time, 2 h; temperature, 150ºC, water as anti-solvent
Anti-solvent	Single variable experiment	Ethanol, water, isopropyl alcohol, isoamyl alcohol	Time, 2 h; Temperature, 150ºC; solids loading, 20 wt%; water content, 20%
Cellulases and hemicellulases loading	2^2 full factorial design with 4 axial points and center point triplicates	5-15 FPU·$g_{biomass}^{-1}$; 1-5 wt% g·$g_{biomass}^{-1}$ respectively	Time, 2 h; Temperature, 150ºC; solids loading, 15 wt%; water content, 20 wt%; water as anti-solvent

4.1.5. Protic ionic liquid pretreatment

Pretreatment assays were performed in custom-built stainless-steel reactors of 0.5 L capacity. Unground, air dried sugarcane bagasse was added to the reactors together with a mixture of [MEA][OAc] and water. After mixing, the reactors were immersed in a glycerin bath (Marconi, MA 159/BB, Brazil) that was pre-heated to the pretreatment temperature. Pretreatment parameters were varied (or kept fixed) as detailed in Table 4.1. The heating ramps were based on the residence time calculations for the pretreatments according to SANTUCCI *et al.* (2015). Following the reaction, the reactors were cooled in an ice bath.

Pretreated samples were washed three times with 250 mL of water and filtered in cloth bags. The filtered solids were air dried for further enzymatic hydrolysis evaluation and the three liquid fractions were combined and evaporated by rotary evaporation (Ika, RV10 control VC, Germany) at 70ºC and 400 mbar to produce a mixture of PIL-water-lignin. The mixture was then centrifuged (Marconi, Brazil) at 7,500 RPM (6300 g) for 30 min to precipitate the lignin, which was then thoroughly washed with deionized water, dried in the oven for 24 h at 105ºC and stored in plastic bags for further analysis.

4.1.6. Enzymatic saccharification

Pretreated materials were subjected to enzymatic saccharification. For all the saccharification assays — except for the enzyme optimization experiments — cellulase cocktail Cellic Ctec2 (Novozymes) was employed with a loading of 15 FPU·g^{-1} dry biomass and 10 wt% solids loading. Enzyme optimization assays were also performed with a cocktail of hemicellulases Cellic Htec2 (Novozymes), the enzyme loading was varied according with Table 1 and solids loading was kept at 10% wt%. All saccharification assays were performed in flasks incubated in an orbital shaker (MA-832, Marconi, Brazil) at 150 rpm, 50ºC, for 72 h and held at pH 4.8 with a 0.05 mol·L^{-1} sodium citrate buffer.

Cellulases activity was determined as filter paper units per mL of enzyme, as recommended by IUPAC (ADNEY and BAKER, 2008). Xylanases activity was determined according to BAILEY *et al.* (1992), with reaction volumes adapted for micro reactions according to SQUINA *et al.* (2009). Total protein was determined by the Bradford method (BRADFORD,

1976). Measured enzyme activities were 154.17 FPU·mL^{-1} for the cellulases and 6783 IU·mL^{-1} for the hemicellulases. The total protein was 78.6 and 76.5 mg·mL^{-1} of protein for Cellic Ctec 2 and Htec2, respectively.

4.1.7. Compositional analysis of solid fractions

Pretreated bagasse samples obtained were air dried to less than 10 wt% of moisture content and milled prior to compositional analysis to less than 0.5 mm of particle size in a knife mill (Pulverisette 19, Fritsch GmbH, Idar – Oberstein, Germany). After ash quantification, samples were milled again in a shear and impact mill (Pulverisette 14, Fritsch GmbH, Idar – Oberstein, Germany) to obtain a particle size of less than 0.5 mm. Structural carbohydrates — glucan, xylan, arabinan — and acid-soluble and insoluble lignin were quantified according to SLUITER *et al.* (2016). Moisture content of the samples was determined using an automatic infrared moisture analyser MA35 (Sartorius Gmbh, Goettingen, Germany). This analysis was performed in CTBE/CNPEM.

4.1.8. Compositional analysis of liquid fractions

Monosaccharides and organic acids (formic and acetic acids) in the hydrolysates were analysed using an HPLC system 1260 Infinity (Agilent, Santa Clara, USA) equipped with a refractive index (RI) detector. Columns and mobile phase conditions were employed according to NAKASU *et al*. (2016b). This analysis was performed in CTBE/CNPEM.

4.1.9. Lignin analysis

4.1.9.1. Infrared

FTIR spectroscopy (Spectrum One FTIR system, PerkinElmer, Wellesley, MA) was performed on lignin samples with a universal attenuated total reflection (ATR) accessory. Samples were analyzed without prior pelletization. FTIR spectra were obtained by averaging 16-32 scans from wavelength of 600 to 4000 cm^{-1}. FTIR graphs were depicted in Appendix I of this thesis. This analysis was performed in Imperial College.

4.1.9.2.   2D-NMR – Heteronuclear single quantum coherence (HSQC)

HSQC analysis was performed on the precipitated lignin. 20 mg of lignin was dissolved in 0.25 mL of DMSO-d 6 and the solution was transferred to a Shigemi tube. HSQC NMR spectra were recorded on a Bruker 600 MHz spectrometer (BRANDT *et al.*, 2016). This analysis was performed in Imperial College.

4.1.9.3.   GPC

GPC analysis was performed using an Agilent 1260 Infinity instrument equipped with a Viscotek column set (AGuard, A6000M and A3000M) and RID detector was used for detection. DMSO containing LiBr (1 g·L^{-1}) was used as eluent at a flow rate of 0.4 mL·min^{-1} at 60°C. Samples and standards preparation was performed according with BRANDT *et al.* (2016). Standard deviations for the lignins were Mn ± 100, Mw ± 300 and PDI ± 0.3 or less. GPC graphs were depicted in Appendix I of this thesis. This analysis was performed in Imperial College.

4.1.10. Calculations

4.1.10.1.   Pulp yields

The pulp yields were calculated based on the mass ratios of bagasse before and after pretreatment in a dry weight basis, as described in Equation 4.1.

$$Pulp\ yield = \frac{Pretreated\ bagasse_{dry\ basis}}{Raw\ bagasse_{dry\ basis}} \times 100\% \qquad (Eq.4.1)$$

4.1.10.2.   Glucan and Hemicellulose yield in saccharification

Yields were calculated based on the mass ratios of glucan and hemicellulose (xylan and arabinan) released on enzymatic saccharification, normalized to the initial amount used in the pretreatment (Equation 4.2).

$$Glucan/hemicellulose\ yield = \frac{Glucan/Hemicellulose_{72\ h\ of\ saccharification}}{Glucan/Hemicellulose_{raw\ bagasse}} \times 100\% \text{ (Eq. 4.2)}$$

4.1.10.3.   Degree of delignification

The degree of delignification was calculated based on the mass difference in the lignin content before and after pretreatment relative to the lignin content in raw bagasse in a dry weight basis, as shown in Equation 4.3.

$$Delignification = \frac{Lignin_{raw\ bagasse} - Lignin_{pretreated\ bagasse}}{Lignin_{raw\ bagasse}} \times 100\% \qquad \text{(Eq.4.3)}$$

4.1.10.4.   Lignin recovery

The lignin recovery was calculated based on the amount of lignin recovered in the precipitation step relative to the lignin content in raw bagasse in a dry weight basis (Equation 4.4)

$$Lignin\ recovery = \frac{Lignin_{recovered\ from\ the\ PIL}}{Lignin_{raw\ bagasse}} \times 100\% \qquad \text{(Eq.4.4)}$$

4.2. Results and discussion

4.2.1.   Optimization of pretreatment parameters

Statistical analyses and overall optimization progress were summarized in Table 4.2Table 4.3. In order to avoid an exhaustive statistical description of each experiment, the

regression equations — with the significant factors — are shown in Table 4.2. All regressions passed the F test and reached significance levels of $p < 0.10$. Practical considerations were considered when selecting the optimized condition i.e. that parameters would improve overall process efficiency rather than just maximizing carbohydrate conversion. For instance, compromising between higher solids loading and water content in pretreatment, and a lower enzyme loading in saccharification.

Table 4.2 — Statistical tests together with regressions equations calculated for the optimization experiments. Only significant factors were shown in the equations. The interactions were shown with * signs.

Experiments/Factors	Glucan yield	Hemicelluloses yield
Time (X_1)-Temperature (X_2)	$Y = 56.91 + 20.72 \times X_1 + 25.92 \times X_2 - 6.77 \times X_1 * X_2$	$Y = 41.54 + 17.79 \times X_1 + 9.81 \times X_2 - 6.02 \times X_1 * X_2$
Time course (X_1)	$Y = 74.6 + 1.53 \times X_1$	-- [a]
Solids loading (X_3) -Water content (X_4)	$Y = 72.86 - 10.17 \times X_3 - 5.75 \times X_4$	$Y = 50.44 - 9.55 \times X_3 - 3.91 \times 4 - 2.64 \times X_3 * X_4$
Water content (X_4)	$Y = 85.22 - 0.49 \times X_4$	$Y = 59.94 - 0.42 \times X_4$
Cellulase (X_5)-Hemicellulase loading (X_6)	$Y = 80.29 + 7.22 \times X_5 + 6.03 \times X_6$	$Y = 48.9 + 16.56 \times X_5 - 4.7 \times X_5^2 + 11.5 \times X_6 + 3.56 \times 6^2 + 5.40 \times X_5 * X_6$

a. No significant effect estimates in the calculated model.

Table 4.3 — Summary of the pretreatment optimization progress throughout this work.

Experiment	Optimized condition	Glucan yield (%)	Pentosan yield (%)
Time-Temperature	150 min, 150 ºC	76.6 ± 0.71	51.1 ± 0.79
Time	120 min	75.3 ± 0.82	50.0 ± 2.48
Solids loading-Water content	15 wt% solids loading, 20 wt% water content	76.5 ± 1.94	52.3 ± 0.80
Water content	20 wt% water content	79.2 ± 4.15	50.28 ± 1.72
Anti-solvent	water as anti-solvent	77.7 ± 1.20	49.0 ± 1.70
Enzyme loading	15 FPU cellulase/g biomass	78.6 ± 0.92	49.0 ± 0.94

4.2.2. Time and temperature — the influence of severity

Residence time and temperature are fundamental parameters for a pretreatment, greatly impacting the severity of the process (CHUM *et al.*, 1990), and thus dictating the required robustness of the reactors and ease of downstream processing. In this work, it was decided not to combine time and temperature in a single parameter, i.e., the severity (R_0), in order to investigate their influence and possible interaction.

The statistical analysis shown in Table 4.2 indicated that both time and temperature were significant, and that their increase improved glucan and hemicellulose yields during saccharification. There was also a negative interaction between the two factors, as when they both increased there was a slight decrease in sugar yields, due to higher solubilization of cellulose and hemicelluloses in the pretreatment step. For the glucan yield, both time and temperature effects had similar orders of magnitude, despite temperature exerting a higher impact.

For the hemicellulose yield, however, time had almost twice the impact of temperature, indicating hemicelluloses are more time sensitive. Delignification also followed the same trend, with increased time and temperature both contributing to higher delignification rates. The graphs for the time-temperature experiments are summarized in Fig. 4.1. The best conditions based on this factorial design were 150 min and 150 ºC, which led to glucan and hemicellulose yields of 76.6% and 51.1%, respectively; and 63.7% delignification (Table 4.2). There is a clear trend found in the response surfaces (Fig. 4.1a): as temperature and time increased, the highest glucan and hemicellulose yields were obtained, as well the highest delignification.

It can be noted that glucan yield and delignification had higher slopes when compared with the hemicelluloses yield, which might indicate cellulose accessibility is more sensitive to delignification. It was possible to draw a correlation between delignification and glucan yield (Fig. 4.1b) with $R^2 = 0.92$. A similarly high correlation was also reported by ROCHA *et al.* (2017), who obtained an R^2 value of 0.94.

Lignin is well-known to act as a physical barrier to enzymes and hinder their access to cellulose (RAHIKAINEN *et al.*, 2013), and removal of this macropolymer from the biomass greatly improves enzyme performance in saccharification. Chambon *et al.* (2018) studied the pretreatment of sugarcane bagasse with the PIL triethyl ammonium hydrogen sulfate

[TEA][HSO$_4$] with several particle sizes. There was also a high correlation between delignification and glucan yields, especially for the whole bagasse samples, which is also the case in the present study. The hemicellulose yields, however, were low as [TEA][HSO$_4$] is an acidic PIL and promotes rapid hemicellulose degradation even at short pretreatment times.

Cellulose swelling rate accelerates as the temperature increases. Higher kinetic energy provided by high temperatures breaks down hydrogen bonds in the three-dimensional cellulose structure (LOPES *et al.*, 2013). ROCHA *et al.* (2017) also studied the impact of temperature on the pretreatment performance of sugarcane bagasse with several PILs (including [MEA][OAc]). They found that higher temperatures promoted higher glucan yields: by increasing the temperature from 75ºC to 150ºC, there was a 3-fold increase in glucan yield. SUN *et al.* (2017) evaluated the pretreatment performance of switchgrass with [MEA][OAc] and found that the glucan and hemicelluloses yield (reported as xylose yield only) increased by 20% and 18%, respectively, when the temperature was raised from 140ºC to 160ºC. In this study, from 120ºC to 150ºC with 150 min of pretreatment time, there was an increase of 30% and 15% in the glucan and hemicellulose yields, respectively.

Although aprotic ILs act differently on the biomass, the effect of temperature can also be compared. A study by KIMON *et al.*, (2011) with sugarcane bagasse pretreated with 1-butyl-3-methyl imidazolium chloride, [BMIM][Cl], at different temperatures (110-160°C) showed that partial cellulose dissolution occurred in all conditions. However, saccharification yields were significantly higher above 150°C. SILVA *et al.* (2011) studied the pretreatment of sugarcane bagasse with 1-ethyl-3-methyl imidazolium acetate, [EMIM][OAc] and observed that by increasing temperature from 60°C to 120°C there was a 2-fold increase glucose yield in the enzymatic saccharification of regenerated bagasse. The hemicellulose yield, however, decreased as temperature increased from 100ºC to 120°C, indicating hemicellulose degradation. This was not the case of the present study, proving [MEA][OAc] is more selective towards hemicelluloses fractionation.

(a)

(b)

(c)

$y = 0.89x + 5.18$
$R^2 = 0.92$
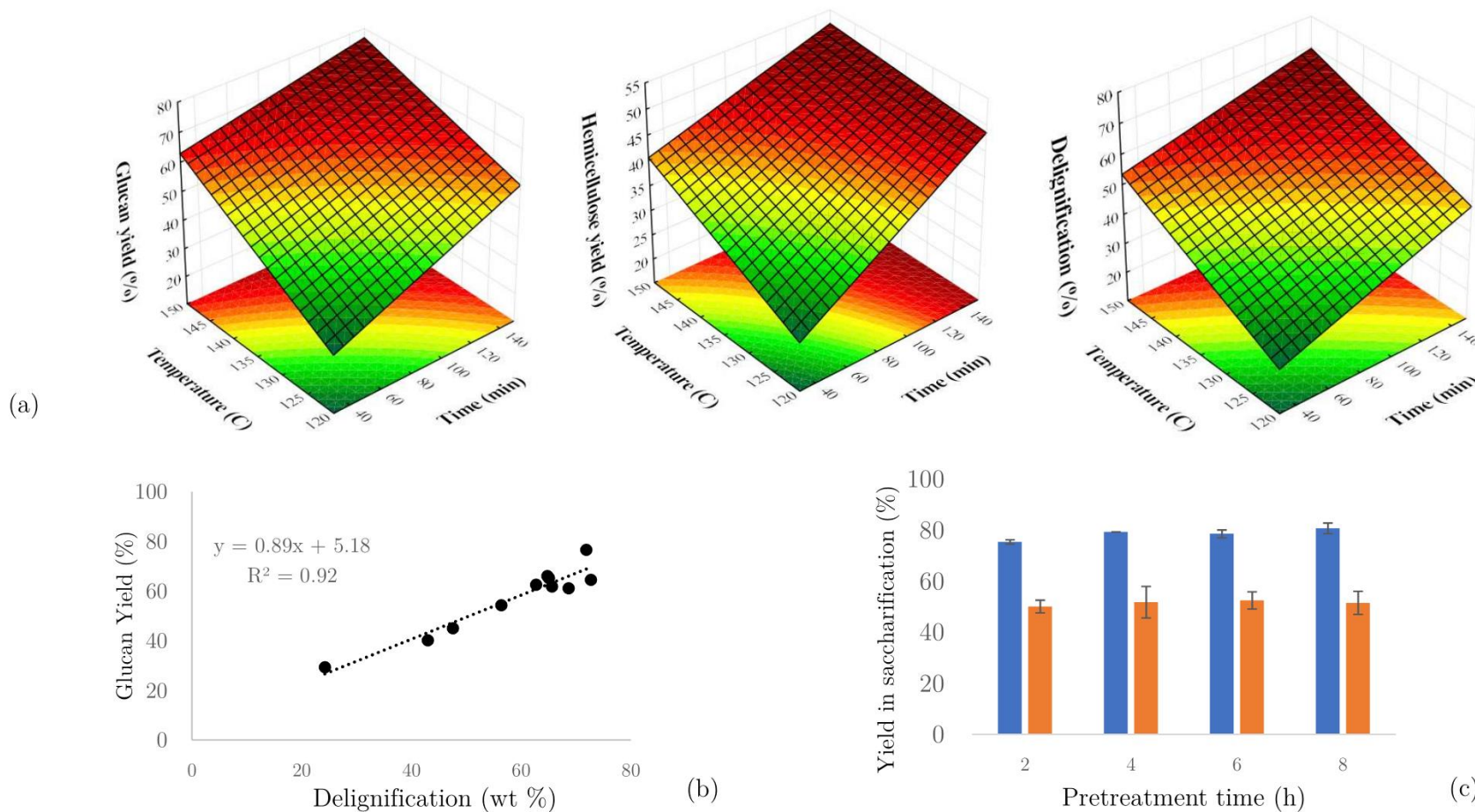
Fig. 4.1 — Response surfaces for the glucan yield, hemicellulose yield and delignification in the time-temperature experiments. (b) Correlation between delignification and glucan yield in the time-temperature experiments. (c) Glucan (blue bars) and hemicelluloses (orange bars) yield as a function of pretreatment time in the time-course experiment.

4.2.2.1. Time course experiment

Time-temperature factorial design showed that higher temperatures and longer residence times provided better PIL performance in terms of sugar yield and delignification. While the highest temperature and longest duration considered in this study were 150ºC and 8 hours respectively, it was possible that that longer pretreatment times and higher temperatures would further enhance the performance of the PIL. Prior tests (data not shown) with [MEA][OAc] showed that higher temperatures (up to 180ºC) did not significantly improve IL performance. Therefore, a time-course experiment at a fixed temperature (150ºC) was designed to investigate the isolated effect of residence time on the pretreatment performance of [MEA][OAc].

Statistical analysis of time-course data (Table 4.2) indicated that residence time did not impact substantially on glucan yield at 150ºC given its small effect, 1.53 and $R^2 = 0.62$. Analysis of variance revealed a significant difference amongst the different residence times, but the Tukey test (NAKASU, 2019, Mendeley Data) revealed that such difference only appears from 2 – 8 h. The hemicelluloses yields did not present any significant differences amongst the pretreatment times. Fig 4.1c. confirms the statistical analysis by showing a small difference for the different pretreatment times, both for glucan and hemicellulose yields. A 2 h pretreatment time was chosen as the optimized condition (Table 4.2) from the time-course experiment, since shorter pretreatment times allow higher productivity.

SUN *et al.* (2017) also investigated the effect of time on switchgrass pretreatment performance with [MEA][OAc] and reported a slight increase in glucan yield over time at high temperatures (160ºC). CHAMBON *et al.* (2018) varied pretreatment time with the PIL [TEA][HSO$_4$] from 1 to 24 h, and also observed satisfactory performance up to 8 h of pretreatment, however, due to the acidic PIL nature, there was a decrease in both glucan and xylose yield for longer pretreatment times. BRANDT *et al.* (2017) worked on the pretreatment of miscanthus with [TEA][HSO$_4$] and also reported good PIL performance up to 8 h of pretreatment and a drop in efficiency over time.

Aprotic ILs present a reverse trend compared to the aforementioned works with PILs. YOON *et al.* (2012), studied the effect of residence time on the pretreatment performance of sugarcane bagasse with [EMIM][OAc] and noticed that under low temperatures, longer

pretreatment times led to higher sugar yields, but at higher temperatures decreased the yields instead. Similar works with [EMIM][OAc] and red oak and kenaf powder also showed the same pattern. YOON *et al.* (2012) also found that longer pretreatment times at high temperatures led to the formation of coagulates that made it harder to regenerate the dissolved sugarcane bagasse.

4.2.3. Solids loading and water content — the impact on mass transfer

The solids loading and water content are important parameters related directly to the mass and heat transfer properties of the system. One of the most significant methods to decrease the cost of pretreatment is to increase biomass loading and reduce IL use (CRUZ *et al.* 2013; KLEIN-MARCHUSCHAMER *et al.*, 2011). Ideally, by employing high solids loading, higher ethanol titers could be obtained, increasing overall process productivity. High water contents allow less PIL to be used and therefore make the process less costly. Although in theory ILs are recyclable and recoverable, their recycle rates are never quantitative and there are thus losses over the recycles; a typical recycle rate obtained by BRANDT *et al.* (2017) with [TEA][HSO$_4$] varied between 98 and 99%. Hence, major PIL losses could be avoided by using less PIL. This would, however, come at the cost of losing catalytic efficiency if the PIL is too diluted. Eventually, a balance between high catalytic efficiency and highwater content must be reached.

Statistical analysis (Table 4.2) showed that both solids loading and water content impacted negatively on glucan and hemicellulose yields, as expected. However, solids loading had a larger impact on sugar yields: nearly twice that of the water content on average. This could be explained by higher biomass loadings heavily impacting the mass transfer properties (CRUZ *et al.* 2013). By increasing the solids loading, the overall viscosity of the system increases, whereas the opposite occurs by increasing the water content. By analyzing the graphs in Fig. 4.2a-b, it can be noted the center points present values closer to the point of highest glucan/xylan yield, i.e, 10 wt% solids and water, with statistical analysis indicating no significant difference between such yields. Therefore, the center point, corresponding to 15 wt% and 20 wt% of solids loading and water content respectively, was chosen as the optimized condition (Table 4.2) for such experiments.

SUN *et al.* (2017) studied the effect of biomass loading on the pretreatment performance of sugarcane bagasse with [MEA][OAc]. By increasing the solids loading from 5

wt% to 20 wt%, there was a drop in glucan yield of approximately 10%. In this study, for both water content levels (10 wt% and 30 wt%), there was also an average drop of 10% in the glucan yield as solids loading increased from 10 to 20 wt%. WEIGAND *et al.*, (2017) — in the pretreatment of willow with [TEA] [HSO$_4$] — and SEMERCI; GÜLER (2018) — in the pretreatment of cotton stalks with 1-butyl-imidazolium hydrogen sulfate [HBMIM][HSO$_4$] — also obtained satisfactory glucan yields by employing 15% solids loading and 20% water content, proving ammonium-based PILs are both water compatible and tolerate high biomass loadings.

APILs present different behavior, as they tolerate very high solids loadings, up to 50 wt%. By varying the solids loading from 5-50%, ZHANG *et al.* (2017), found an optimum load of 30% in the pretreatment of sugarcane bagasse with [EMIM][OAc]. CRUZ *et al.* (2013), in a similar study on the effect of solids loading on the pretreatment of switchgrass with [EMIM][OAc], observed that up to 50 wt% there were no decrease in overall glucan yields.

The major drawbacks of using APILs are their high price and incompatibility with water. Once their main goal is to solubilize cellulose, even small water impurities can be detrimental to cellulose solubility. For instance, a study by MAZZA *et al.* (2009) on the cellulose dissolution in APILs showed the onset of cellulose precipitation in [BMIM][Cl] occurred at about 0.15 wt% water and that it was essentially complete at 0.25 wt% water. While there is no consensus on the major reason behind APILs sensitivity to water, one possible explanation is the disruption of cellulose-IL interactions via hydrogen bonds (BRANDT *et al.*, 2013).
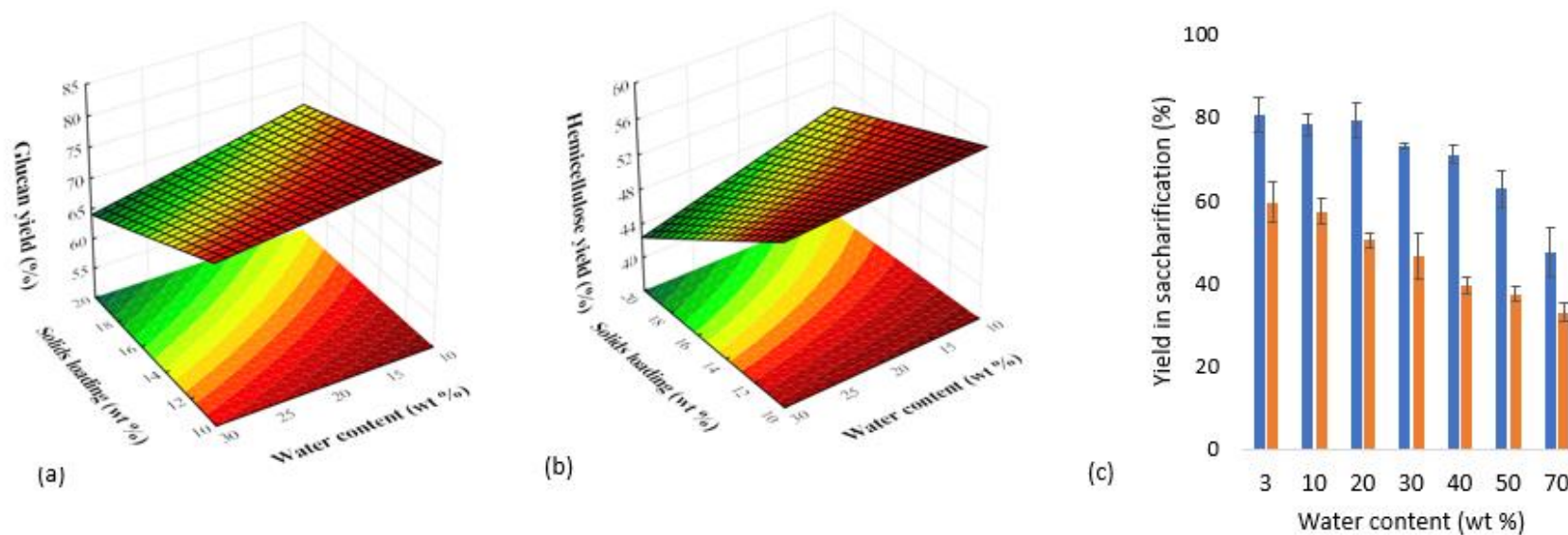
Fig. 4.2 — Response surfaces for the (a) glucan yield and (b) hemicellulose yield in the solids loading-water content experiments. (c) Glucan (blue bars) and hemicellulose (orange bars) yield as a function of the water content in the single variable experiment with the water content.

4.2.3.1. Water content experiment

The impact of water on IL performance in biomass deconstruction has been discussed in the literature (BRANDT *et al.*, 2011; ROGERS and MACFARLANE, 2012). As previously mentioned, aprotic ILs — that make up most of the studies — are quite sensitive towards low water concentrations. On the other hand, PILs, whose studies on biomass deconstruction are rapidly increasing, reveal a high water tolerance by altering cellulose structure rather solubilizing it in the IL (BRANDT *et al.*, 2011). The statistical analysis of the water content experiment (Table 4.2) showed that it impacted negatively on glucan/hemicellulose yields and delignification, although small coefficient values indicate a low slope. As mentioned before, higher water contents allow less PIL to be used, but consequently decrease its catalytic efficiency.

Fig. 4.2c appears to show that the glucan yield is only kept high up to 20 wt% water. However, Tukey tests on the glucan and hemicellulose yield showed there were no significant differences from 20 to 40 wt% water. Delignification also appeared to be negatively affected by higher water contents, but another Tukey test showed no significant differences amongst lower water contents of 3, 10 and 20 wt% (NAKASU, 2019, Mendeley Data). Hence, aiming to maintain high sugar yields but also avoiding a decrease in delignification, it was decided to keep 20 wt% water as the optimized condition (Table 4.2). This condition provided 79.2%, 50.3%, and 53.4% of glucan/hemicellulose yield and delignification, respectively.

BRANDT *et al.* (2011) in a study on the pretreatment of miscanthus with 1-butyl-3-methyl imidazolium methyl sulfate, [BMIM][MeSO$_4$], varied the water content from 1.1 to 80 vol% and observed that the highest glucan yields were obtained with 10-30 vol% water, which confirms the trend found in this work. Interestingly, the lowest water content in BRANDT's *et al.* work, 1.1 vol%, did not present the highest glucan content, whereas, in this work, the lowest possible water content 3 vol% did. Perhaps if a lower water content had been tested the same trend would have been found. PILs tend to exhibit a trend of water content converging to 20 wt% as seen from works by ROCHA *et al.* (2017), WEIGAND et al. (2017), BRANDT et al. (2013) and CHAMBON et al. (2018). The majority of aprotic ILs, as aforementioned, have a high sensitivity towards water. However, there are some exceptions. ABE *et al.* (2012) reported the dissolution of 15 wt% cellulose in aqueous solutions of tetrabutylphosphonium hydroxide, [(C$_4$)$_4$P][OH], and tetrabutylammonium hydroxide, [(C$_4$)$_4$N][OH], containing 40–50 wt% water at room temperature.

A study on the pretreatment of rice husk with 60 wt% $[(C_4)_4P][OH]$ showed incompatibility with a further enzymatic hydrolysis due to incorporation of phosphonium species in the regenerated biomass (LAU *et al.*, 2015). SHI *et al.* (2014) studied the pretreatment of switchgrass with [EMIM][OAc] with several water contents (20, 50 and 80 wt%). They showed that IL-water mixtures with up to 50 wt% water still provided high glucan yields after 72 h of saccharification. However, a closer look on more recent works on the biomass pretreatment with [EMIM][OAc] revealed that several authors prefer performing pretreatment under anhydrous conditions, which might still indicate such IL is not the best option for aqueous IL mixtures in the pretreatment (ÁVILA *et al.*, 2018, SAHA *et al.*, 2018, ODORICO *et al.*, 2018).

4.2.4. The effect of the anti-solvent

The anti-solvent plays a crucial role on the solid-liquid separation step after pretreatment. The main goal of the anti-solvent is to solubilize the PIL and the extracted lignin from the insoluble pretreated material. Three anti-solvents with different carbon numbers in their structure were tested: ethanol, isopropanol and isoamyl alcohol plus a control with water. Statistical tests on the glucan/hemicellulose yields showed there were no significant differences amongst the anti-solvents. However, the degree of delignification presented significant differences as can be observed from Fig. 4.3a. Alcohols with lower carbon number in the alkyl chain presented higher delignification of the pulps, the lowest value — from isoamyl alcohol — was comparable to the water control. Presumably a different mechanism of lignin extraction occurs with the alcohols. The short alkyl chains (2 or 3 carbons) contributed to more hydrophobic lignin-alcohol interactions. Water stands out by having a high polarity and small molecular size, the former lessening lignin-alcohol interactions and the latter enhancing them. Its high polarity might have impacted more on lignin solubility than its size. From the lignin balance in Fig. 4.3b, it can be seen that approximately half of the lignin amount, or 30-35 wt% of the total lignin, extracted from the biomass was recovered in the precipitation step.
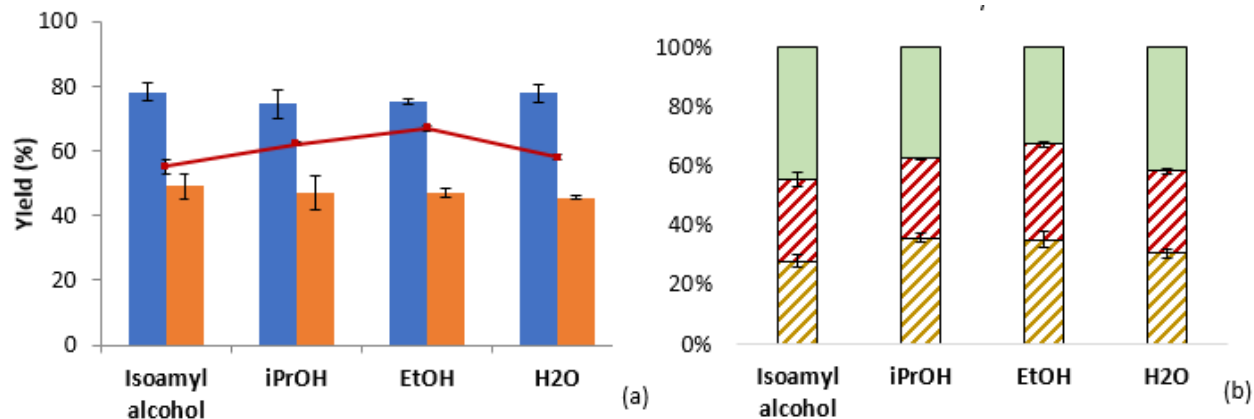
Fig. 4.3 — (a) Glucan yield (blue bars), hemicellulose (orange bars) yield and delignification (dark red line) as a function of the anti-solvent. (b) Mass balance for the lignin in the anti-solvent experiments: Patterned fill – degree of delignification, non-patterned green fill – lignin remaining in the pulp, patterned red fill – lignin soluble in the PIL, patterned light brown fill – lignin recovered from the PIL.

ROCHA *et al.* (2017) reported a higher delignification and lignin recovery of 68 and 41 wt%, probably due to the more severe pretreatment conditions, 150ºC and 3.5 h on the bagasse pretreatment with [MEA][OAc]. CHAMBON *et al.* (2018) reported even higher values of nearly 80 wt% for both delignification/lignin recovery using [TEA][HSO$_4$]. As previously mentioned, [TEA][HSO$_4$] is an acidic PIL and is therefore more "severe" towards biomass deconstruction, with high lignin and hemicellulose solubilization. Additionally, lignin precipitation is favored under low pHs.

SUN *et al.* (2017) reported high delignification rates of up to 75 wt% but did not recover the lignin from the PIL. There are no reports in the literature about the study of anti-solvents in PIL pretreatment. However, there are several studies upon the role of the anti-solvents in aprotic ILs pretreatment. SUN *et al.* (2011), when testing the solubility of commercial biomass fractions in [EMIM][OAc], showed that a mixture of 1:1 (v/v) water:acetone had a high solubility for Kraft lignin, whereas the solubility of xylan and microcrystalline cellulose (MCC) were negligible . LI *et al.* (2009) tested water, ethanol and methanol as anti-solvents for wheat straw regeneration from the IL mixture with 1-ethyl-3-methyl-imidazolium diethyl phosphate [EMIM][DEP] and did not find any significant differences in terms of sugar yield during saccharification.

WANG *et al.* (2011) observed that the addition of dimethyl sulfoxide (DMSO) to water as an anti-solvent increased the cellulose content in the regenerated biomass. However, DMSO recovery from the aqueous mixtures would demand high energy input. As for the acetone-water mixtures, prior pretreatment tests in our work showed that the fractionated lignin was insoluble, confirming that PILs present a different mechanism of action compared to their aprotic counterparts. Water was still chosen as the optimized anti-solvent (Table 4.2) due to its low cost and the lack of significant differences in sugar yields amongst the tested anti-solvents.

4.2.5. The impact of enzyme loading

The enzyme loading is an important process parameter as the enzyme price heavily impacts the ethanol price (KLEIN-MARCUSCHAMER *et al.* 2010). Although important, only a few studies with PILs evaluated the effect of the enzyme loading on sugar yields (SUN *et al.* 2017, ÁVILA *et al.*, 2018). The statistical analysis (Table 4.2) showed that both cellulases and hemicellulases had a strong positive impact on the glucan yield, with cellulases having a slightly higher effect (7.22 over 6.03). However, it is worth mentioning that the factors' ranges in terms of protein loading were substantially different: 2.55–7.65 mg cellulases$\cdot$g^{-1} biomass versus 10–50 mg hemicellulases $g_{biomass}^{-1}$. The recommended high hemicellulases dosage by Novozymes is 0.6 wt%, which is substantially lower than this study's upper level, 5 wt%. It was decided to choose such a high enzyme dosage for the upper level of hemicellulases loading due to the low hemicellulose yields obtained in past optimization experiments and prior tests with lower enzyme loadings. Glucan yields of up to 88% were obtained (Fig. 4.4a) with high enzyme loadings (17 FPU$\cdot$g$_{biomass}^{-1}$ and 5.83 wt%). The center point also provided considerable glucan yield 80.3%, still in the range of glucan yields obtained in previously optimized conditions (Table 4.2). The hemicellulose yield indeed was very sensitive towards both enzyme loadings as can be observed from Fig. 4.4b, which shows a steep response surface on the upper levels of both factors. Despite one negative quadratic estimate for cellulases loading (Table 4.2), all the remaining effect estimates impacted positively on the hemicelluloses yield with the linear effect of cellulases being the highest, 16.56, even employing higher hemicellulases loading. In fact, control experiments with only cellulases with 5, 10 and 15 FPU$\cdot$g$_{biomass}^{-1}$ provided 69.6, 77.1 and 78.6% of glucan yield in 72 h, while the hemicellulose yields were 38.3, 42.9 and 49% respectively.

Only the highest enzyme loadings provided yields higher than the control experiments, which would impact heavily on the process economics. Therefore, it was decided to keep 15 FPU $g_{biomass}^{-1}$ (7.65 mg·$g_{biomass}^{-1}$) without the addition of hemicellulases as the optimized condition (Table 4.2). The majority of works on PIL pretreatment (ÁVILA, FORTE and GOLDBECK, 2018; BRANDT *et al.*, 2017b; CHAMBON *et al.*, 2018; SUN *et al.*, 2017; WEIGAND *et al.*, 2017) employed 20 mg·$g_{biomass}^{-1}$ as recommended by the National Renewable Energy Laboratory (RESCH; BAKER; DECKER, 2015).
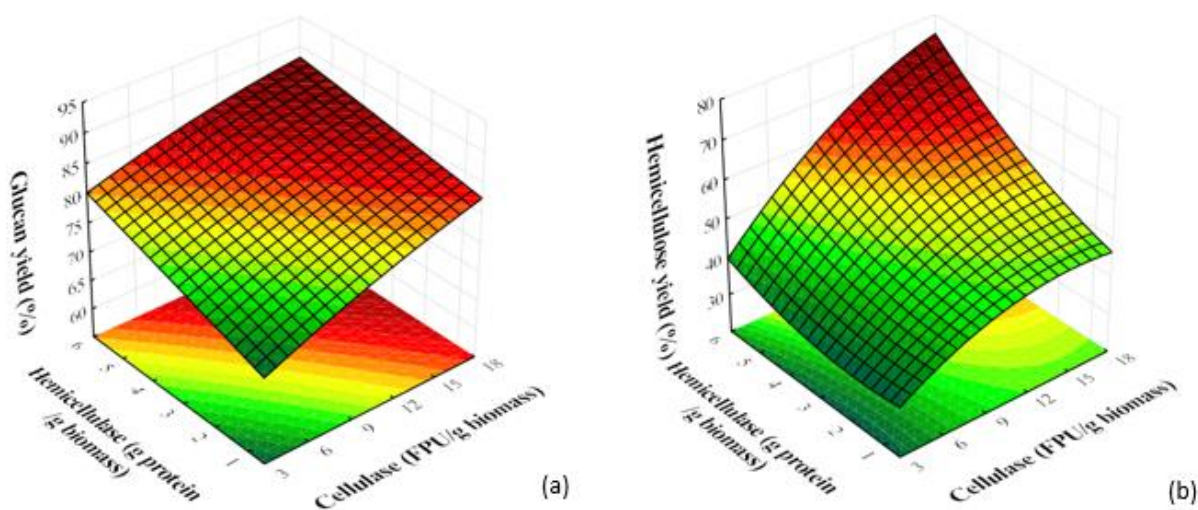
Fig. 4.4 — Response surfaces for the (a) glucan yield and (b) hemicellulose yield in the enzyme loading experiments.

ROCHA *et al.* (2017) also employed 15 FPU of celluclast per $g_{biomass}^{-1}$ but also added 20 IU·$g_{biomass}^{-1}$ of β-glucosidases as additional enzymes. In all saccharification samples subjected to HPLC analysis in this work, cellobiose was not detected, once the cellulase cocktail (Cellic Ctec 2) contained β-glucosidases. Hence, our work employed the lowest enzyme loading for PIL pretreated samples.

4.2.6. Mass balance for the optimized [MEA][OAc] pretreatment

A mass balance for the optimized conditions (last entry in Table 4.2) of [MEA][OAc] pretreatment is shown in **Fig 4.5.** One interesting feature is that the PIL pretreatment was highly selective towards delignification and carbohydrate preservation in the biomass. This is particularly noteworthy considering there are no reports in the literature on highly selective pretreatments. Enzymatic saccharification of the pulp yielded 33.65 g glucose·100 $g_{biomass}^{-1}$ and 13.94 g pentoses·100 $g_{biomass}^{-1}$. Rocha *et al.* (2017), on the pretreatment of sugarcane bagasse with [MEA][OAc], reported 35.5 g glucose·100 $g_{biomass}^{-1}$ and 15.0 g pentoses·100 $g_{biomass}^{-1}$, slightly higher values. However, they did not optimize pretreatment parameters. For instance, they employed lower solids loading (10 wt%), longer pretreatment times (3.5 h). Sugar yields obtained in this study were also higher than those of sugarcane PIL pretreatment works, such as BRANDT *et al.* (2017), CHAMBON *et al.* (2018) and SUN *et al.* (2017) or even aprotic ILs such as SAHA *et al.* (2017) and ÁVILA *et al.* (2018).

4.2.7. Lignin analysis

The lignins generated from the anti-solvents tested in the optimization process of [MEA][OAc] were analyzed for structural characterization. The pulps that resulted from such tests were subjected to enzymatic saccharification and there were no significant changes among the different pulps. By following the same trend, we would not expect significant changes across the lignins. This was confirmed by spectroscopic techniques and GPC. However, lignins from [MEA][OAc] pretreatment still present interesting structural features.
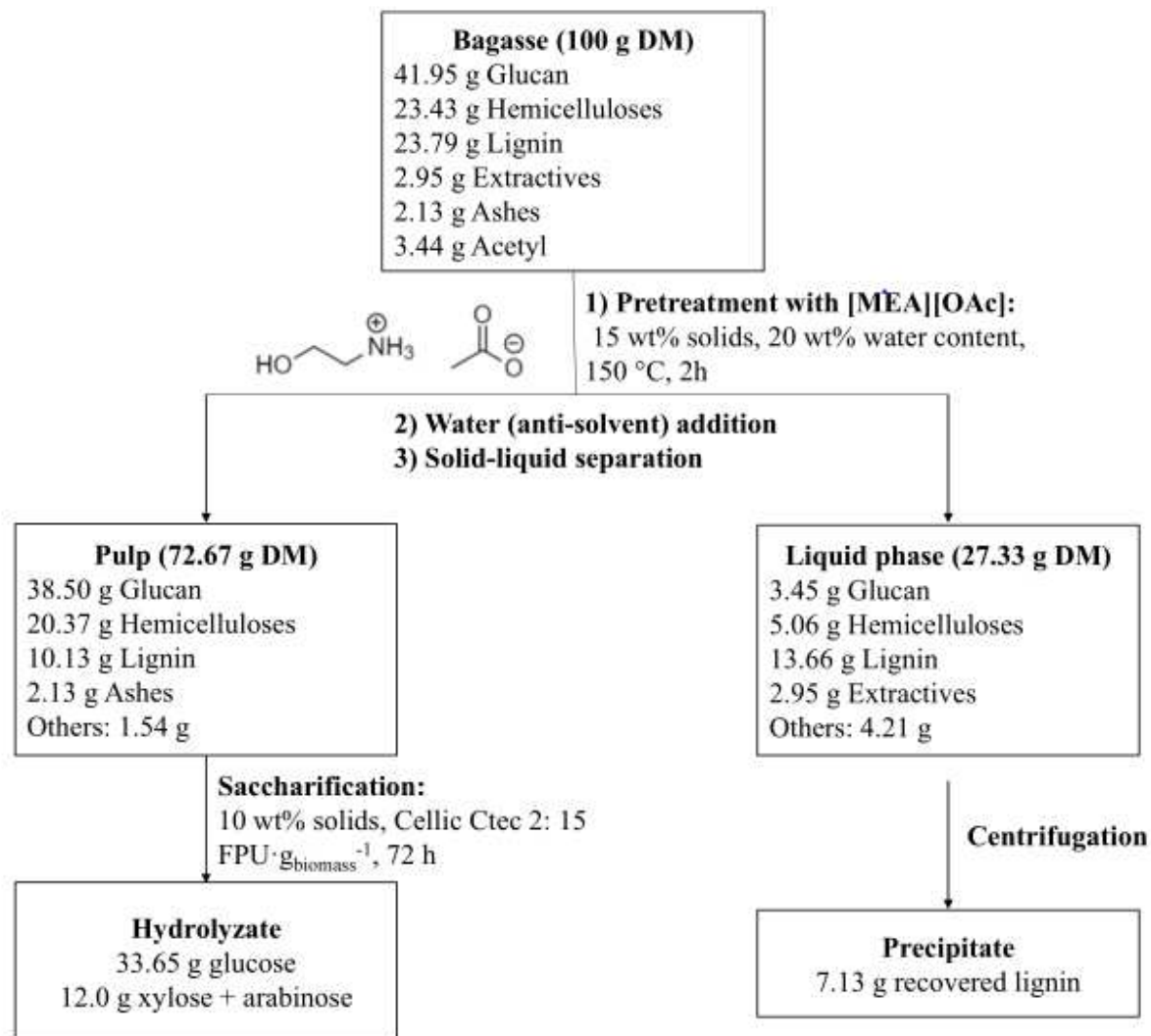
Fig. 4.5 — Mass balance for the optimized conditions of sugarcane bagasse pretreatment with [MEA][OAc].

4.2.7.1. FTIR

Lignin's FTIR spectrum (Fig. II-1 in Appendix I) presents three distinct regions, with the correspondent bands for each region described in Table 4.4. Region I contains the high frequency vibrations such as O–H stretching (3697 cm^{-1}) and C–H stretching (2917 and 2849 cm^{-1}). The large O–H stretching band indicates the lignin contains a lot of hydroxyl groups, whether phenolic or aliphatic, that interact through hydrogen bonds.

Region II contains mainly C=C (1630, 1557 and 1506 cm^{-1}) stretching vibrations that come from the aromatic rings. In the low frequency part of it, there are also some C—H (1455 cm^{-1}) and O—H bending vibrations (1420, 1375 and 1327 cm^{-1}) that come from aliphatic and aromatic hydroxyl groups. There was also an absence of strong carbonyl bands around 1715 and 1730 cm^{-1} that excluded the presence of aldehydes or ketones in the lignin samples. Region III contains O—H stretching from alkyl aryl ether and primary/secondary alcohols (1221, 1120 and 1031 cm^{-1}) and C=C bending vibrations (913 and 831 cm^{-1}). The strong O—H stretching band at 1031 cm^{-1} is a signature band for highly oxygenated materials such as lignocellulosic biomass.

Table 4.4 — Assignment of the absorption bands in the FTIR spectrum of lignin recovered from [MEA][OAc] pretreatment at 150°C, 2 h, 20 wt% water, 15 wt% solids and water as anti-solvent.

Absorption (cm^{-1})	Assignment	Region in the spectrum
3697	O—H streching in primary alcohols	
3280	O—H streching	
2917	C—H stretching	Region I
2849	C—H stretching	
1630	C=C stretching	
1557	C=C stretching	
1506	C=C stretching	
1455	C—H bending	Region II
1420	O—H bending	
1375	C—H bending	
1327	O—H bending in phenol	
1221	O—H streching alkyl aryl ether	
1120	C—O streching secondary alcohol	
1031	C—O streching in primary alcohol	Region III
913	C=C bending monosubstituted alkenes	
831	C=C bending trisubstituted alkenes	

4.2.7.2. HSQC

HSQC (Heteronuclear Single Quantum Coherence) NMR is one of the most powerful techniques to unveil lignin structures because it correlates carbon and proton signals and thus makes the assignment for specific molecular moieties easier. There are usually two main regions of an HSQC spectrum that can be analyzed — the aliphatic and aromatic. The aliphatic or side chain region lies between 2.0 and 6.0 ppm. As the name implies, signals corresponding to the functional groups attached to the side chain regions of lignin can be found. The HSQC spectrum of lignin and the moiety assignments are depicted in Fig. 4.6 and 4.7.
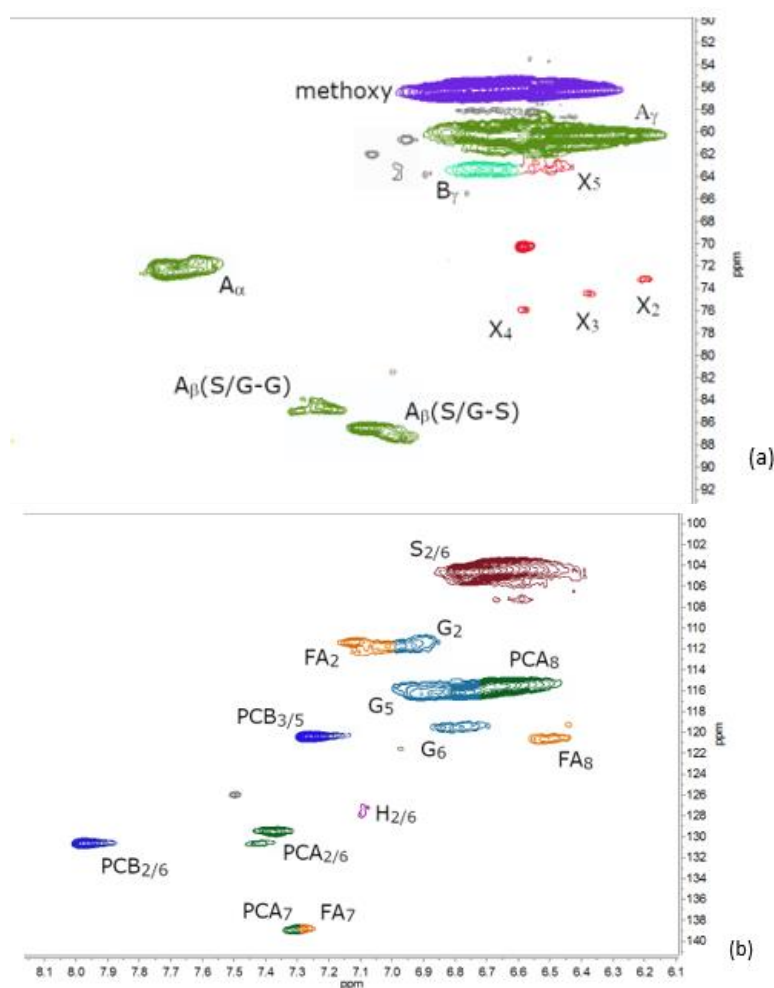
Fig. 4.6 — (a) Aliphatic and (b) aromatic parts from the HSQC spectrum of the lignin obtained from [MEA][OAc] pretreatment with water as anti-solvent. Pretreatment conditions with [MEA][OAc] were 150°C, 2 h, 15 wt% solids and 20 wt% water.
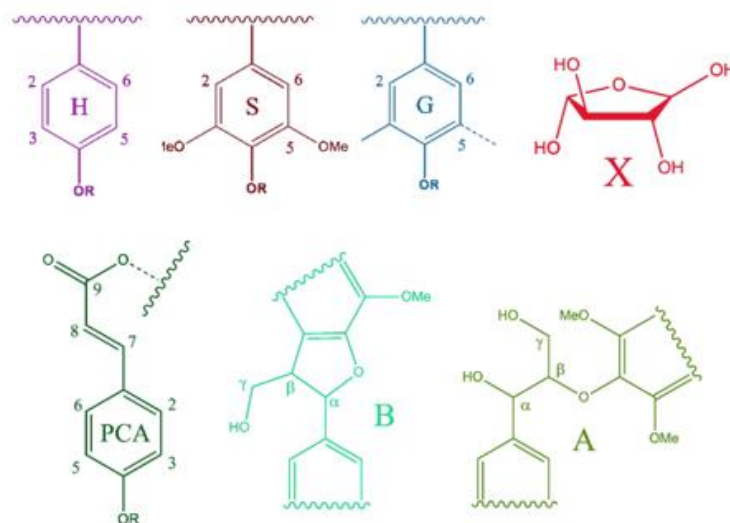
Fig. 4.7 - Some of the molecular moieties found in the HSQC spectrum of lignin.

From the side chain region (Fig. 4.6a), one moiety dominates the region, moiety A (Fig. 4.7) with two aliphatic hydroxyl groups and residual β-O-4 bonds that confirm the bands in region III from the FT-IR spectrum. A signal from the γ position in moiety B also appears (Fig. 4.6a). Some residual xylan was also visible (Fig. 4.6a), indicating that the PIL was not able to completely fractionate lignin from hemicelluloses. The strong signal from the methoxy groups is a signature signal in lignins due to the highly methoxylated aromatic moieties (BRANDT *et al.* 2017). The aromatic region of the HSQC usually lies between 6.0 and 8.0 ppm and contains the aromatic moieties that make up lignin architecture.

The basic building blocks of lignin are sinnapyl (S), guayacyl (G) and p-coumaryl (H) units (Fig. 4.7). Such units vary in their relative amount, say S:G:H ratio ,depending on the feedstock, harvest season and pretreatment conditions. However, as the H content is usually low in sugarcane's lignin, the S/G ratio is a more important parameter. The calculated S/G ratio for the lignin was 2.04, a slightly higher value compared to the lignin obtained from sugarcane's milled wood lignin, 1.6, indicating a decrease in G groups (DEL RÍO *et al.*, 2015). MENEZES *et al.* (2017), in the alkaline pretreatment of bagasse catalyzed by anthraquinone, obtained a similar S/G ratio of 2.2, which might confirm that pretreatment with [MEA][OAc] acts similarly to alkaline

pretreatments not only due to the high degree of delignification, but also to the decrease in G units content. The relatively low S/G ratio and presence of H groups in the lignin suggest these lignins are not condensed and are prone to chemical derivatization. Some other moieties such as p-coumaric acid (PCA), ferulic acid (FA) and p-benzoic acid (PBC) were also found. The abundance in aromatic moieties in the lignin recovered from [MEA][OAc] fosters future applications in further depolymerization and production of aromatic compounds (GRAGLIA; KANNA; ESPOSITO, 2015).

4.2.7.3.   GPC

Except for the lignin produced with isoamyl alcohol as anti-solvent, all the GPC peaks (Supplementary Information) present the exact same shape and retention time. This can also be confirmed by the molecular weights shown in Table 4.5. The polydispersity (PD) values varied between 3.74 (EtOH) to 8.88 (isoamyl alcohol); apart from isoamyl alcohol, such PD values are quite low and indicate that fractionation of lignin produced somehow more uniform lignin subunits. The M_w values varied between 4580 and 8141 g·mol^{-1}, which are quite low compared to the lignins obtained by Brandt *et al.* (2017) on the pretreatment of miscanthus with [TEA][HSO$_4$], whose average M_w varied between 5800 to 9000 g·mol^{-1}, showing that [MEA][OAc] deconstructed more the lignin structure. On the other hand, Saha *et al.* (2017) obtained a much lower M_w and PD values, 1769 g·mol^{-1} and 1.61, on the pretreatment of sugarcane bagasse with [EMIM][OAc], indicating that such IL was more efficient at lignin fractionation. Depending on the type of IL, it is possible to generate lignin fractions with different M_w/PD ranges that could be potentially tailored for future applications.

Table 4.5 — Molecular weights (Mw and Mn) and polidispersities (PD) of the lignins isolated from [MEA][OAc] pretreatment produced by different anti-solvents**.**

	Mn (g·mol^{-1})	Mw (g·mol^{-1})	PD
H$_2$O	1096	5099	4.65
EtOH	1223	4580	3.74
iPrOH	1045	5064	4.84
Isoamyl alcohol	917	8141	8.88

4.3. Conclusions

Process parameter optimization with the PIL [MEA][OAc] paved the way for several novel features: a highly selective pretreatment that delignifies sugarcane bagasse but also preserves the carbohydrates; high solids loading, compatibility with water and a low dosage of cellulases during enzymatic saccharification of the pulps. Structural characterization of the recovered lignin revealed a wide variety of functional groups and moieties that could potentially add value to the sugarcane biorefinery. The optimized conditions were found to be 150°C, 2h, 15 wt% solids loading, 20 wt% water content and water as anti-solvent.

Chapter 5

5. **The impact of acid-base ratio and recycling of a protic ionic liquid on the pretreatment performance of sugarcane bagasse**

The acid-base ratio (ABR) in PILs is an important parameter that affects the pretreatment (VERDÍA *et al.*, 2014). Sulfate-based PILs have been subject to studies on ABR modifications (BRANDT *et al.*, 2017a; VERDÍA *et al.*, 2014; WEIGAND *et al.*, 2017). One work has systematically changed the ABR of [TEA][HSO$_4$] on the pretreatment of miscanthus (VERDÍA *et al.*, 2014); a slight excess of acid promoted higher cellulose content in the pulp and sped up pretreatment, whereas a slight excess of base resulted in a higher hemicellulose recovery. Another study tested small ABR variations (0.98:1 to 1.02:1) of [TEA][HSO$_4$] on the pretreatment of willow (WEIGAND *et al.*, 2017). A slightly acidic ABR, 1.02:1 provided higher glucan yield in the enzymatic saccharification, which the authors assigned to the higher recalcitrance of hardwood, but longer pretreatment times led to lower yields due to the acidic medium. However, there are no reports in the literature about the impact of ABR during pretreatment with acetate-based PILs, which shed light on important questions such as:

- What is the impact of ABR changes on pretreatment efficiency?
- How is pretreatment selectivity affected by the ABR?
- Does the IL composition and the ABR change during recycle?

ABR values different than 1:1 may be classified as binary mixtures and as they get higher they behave more as the pure acid, conversely, lower ABRs behave more as the pure base. Low ABR values may selectively deconstruct the biomass and it is worth questioning whether pure MEA would be a better option than the binary mixtures. Some factors need to be considered: solvent's corrosivity and price. Pure MEA is quite reactive (FRONING and JONES, 1958; GUNASEKARAN, VEAWAB and AROONWILAS, 2013) and it requires resistant alloys in pipes and reactors and the addition of acetic acid decreases its corrosivity. Acetic acid is also cheaper than MEA, so higher ABRs decrease the overall solvent price. Additionally, the 1:1 ABR [MEA][OAc] is a supercooled PIL at ambient temperature; so it might crystallize at low moisture

contents and it could potentially clog pipes or equipments. Therefore, binary acid-base mixtures are good solvent alternatives to 1:1 PILs and pure amines.

In this study, the impact of the ABR and of recycling of [MEA][OAc] on sugarcane bagasse pretreatment performance was evaluated. Once such pretreatment primarily promotes delignification, analyses of the recovered lignins were also performed to better understand their relationship with ABR changes. This study was developed in Imperial College London under Dr. Jason Hallett and Dr. Agnieszka Brandt supervision.

5.1. Material and Methods

5.1.1. PIL and acid-base mixture synthesis

[MEA][OAc], was synthesized as described previously in Section 4.1.2. Acetic acid was added dropwise to cooled monoethanolamine in a round bottom flask under magnetic stirring. The moisture content was verified by Karl-Fischer titration (Mettler Toledo V20) in triplicate and was found to be less than 100 ppm.

For the ABR experiments, the same procedure was followed as aforementioned, but different amounts of acetic acid were added to monoethanolamine to generate 11 ABRs. Five ABRs corresponded to excess base: 0.1; 0.2; 0.5, 0.8 and 0.9, five to excess acid: 1.1; 1.25; 2.0; 5.0 and 10.0 plus the neutral PIL with 1.0 ABR. Two controls, pure monoethanolamine (MEA) and pure acetic acid were also used in the ABR assays. However, pretreatment with acetic acid resulted in charring of the biomass and its related data was not used in this study. Experiments were carried out in duplicate.

The ABRs were accurately confirmed via NMR-H[1] by measuring the ratio of the areas between the methyl protons in the acetate and the protons in the methylene closer to the amino group in monoethanolamine. NMR-H[1] spectra were recorded on a Bruker 400 MHz spectrometer. Chemical shifts (δ) are reported in ppm.

5.1.2. Biomass pretreatment

Pretreatment with [MEA][OAc] and its acid-base mixtures was carried out according to a standard protocol (GSCHWEND et al., 2016) with slight modifications. Around 10.67 g ± 0.05 g of ionic liquid (or mixture) and 2.67 g ± 0.05 water were weighed into a 100 ml glass pressure tube with a silicone front sealing ring (Ace Glass) and the exact weight recorded. Around 2 g of ground sugarcane bagasse were added, the vials capped, and the content mixed with a vortex shaker. The total water content in the system was 30% w/w. The samples were then placed into a preheated convection oven (OMH60 Heratherm Advanced Protocol Oven) at 150 ºC. After the pretreatment period (2 h), they were taken out and immediately cooled under running water. Experiments were carried out in triplicate.

After the pretreatment, 40 mL of water was added to the pretreatment mixture and the suspension transferred into a 50 mL centrifuge tube. The tube was shaken in a vortex for one minute and then centrifuged at 4000 rpm for 50 minutes. The supernatant was poured into a 250 mL round bottom flask. This washing step was repeated three more times. The decanted pulp was then transferred into a cellulose thimble and further washed by Soxhlet extraction with refluxing water (150 mL) for 15 h. The thimbles were then air dried overnight. The pulp yield was determined by weighing the recovered biomass from the cellulose thimbles. The water used for the Soxhlet extraction was combined with the previous washes and evaporated under reduced pressure at 40°C, leaving a concentrated mixture of water/PIL/lignin. The suspension was then transferred into a pre-weighed 50 mL falcon tube, shaken for one minute and then left at room temperature for at least 1 hour. The tube was centrifuged, and the supernatant collected in a round bottom flask. This washing step was repeated twice more. The falcon tube containing the lignin was then freeze-dried for 72 h. The lignins were stored in plastic containers and had their weight recorded.

5.1.3. Recycle of the PIL/acid-base mixtures

For the recycle experiments, the supernatants were concentrated under reduced pressure and had their water content measured by Karl-Fischer titration in triplicate to calculate the recycle rate. The concentrated PIL was then reused over 5 recycles without any additional neat

IL being added to it. The recycle experiments were performed in two sets, each set with 6 cycles in total with triplicates of the samples for each cycle.

5.1.4. Enzymatic saccharification

Enzymatic saccharification assays were carried out according to NREL protocol 'Enzymatic saccharification of lignocellulosic biomass' in triplicate. For all the saccharification assays cellulase cocktail Cellic Ctec2 (Novozymes) was employed with a loading of 15 FPU·g^{-1} dry biomass and 1 wt% solids loading. All saccharification assays were performed in 50 mL centrifuge tubes incubated in a Stuart Orbital Incubator (S1500) at 250 rpm, 50°C, for 72 h and held at pH 4.8 with a 0.05 mol·L^{-1} sodium citrate buffer. Samples were then filtered and the filtrate was analyzed by HPLC (Shimadzu, Aminex HPX-87P from Bio-Rad, 300 × 7.8 mm) for glucose, xylose, and arabinose. Cellulose and hemicelluloses yields were calculated as a percentage of the cellulose and hemicelluloses content of raw bagasse as determined by compositional analysis.

5.1.5. Feedstock and pulp characterization

5.1.5.1. Moisture content

The moisture content of raw bagasse, pretreated pulps, and hydrolysis residues was determined according to the NREL protocol 'Determination of Total Solids in Biomass and Total Dissolved Solids in Liquid Process Samples' as previously described in Section 4.1.7.

5.1.5.2. Compositional analysis

The composition of the raw bagasse and pretreated pulps was determined according to the NREL protocol 'Determination of Structural Carbohydrates and Lignin in Biomass' previously described in Section 4.1.7.

5.1.6. Lignin analysis

5.1.6.1. GPC

GPC analysis was performed using an Agilent 1260 Infinity instrument equipped with a Viscotek column set (AGuard, A6000M, and A3000M) and RID detector was used for detection. The method was previously described in Chapter 4.

5.1.6.2. Elemental analysis

CHNS/O analysis of the recovered lignins and pulps was determined using an Elementar VarioMICRO Cube equipped with a combustion column containing tungsten (IV) oxide operating at 1150°C, a reduction column containing reduced copper wires at 850°C and two adsorption columns operating at 850°C and from 40 to 210°C, respectively. The instrument is also equipped with a TCD detector operating at 60°C. Helium was used as carrier and flushing gas and the combustion was carried out by pulse injection of oxygen. Samples (~2 mg) were weighed and sealed in aluminium boats prior to analysis. Each sample was measured at least three times and the oxygen content was determined by subtraction (%O = 100 - %C - %H - %N - %S - %ash).

5.1.6.3. X-ray photoelectron spectroscopy (XPS)

XP spectra were recorded on a Thermo Fisher K-Alpha equipped with a 180° double focussing hemispherical analyser, 128-channel detector, and monochromated Al Kα microfocused x-ray source (hν = 1486.6 eV) operated at 6 mA emission current and 12 kV anode bias. Prior to XPS measurements, samples were degassed on a Schlenk line at <1 x 10^{-2} mbar for 24 h before mounting 5-10 mg on a welled copper plate. After degassing to < 3 x 10^{-7} mbar in the sample transfer chamber, samples were introduced to the analysis chamber, which operates with a base pressure of <2 x 10^{-9} mbar. A spot size of 400 µm and pass energies of 200 eV (survey) and 20 eV (high resolution) were used during analysis. Typically, 60 scans with a dwell time of 50 ms were used for HR scans; hence each HR scan equals ≈ 10 m of X-ray exposure. Samples were prevented from charging with a dual-beam flood source.

Survey scans were quantified in Avantage 5.951 using smart backgrounds and ALTHERMO1 RSFs. High resolution scans were converted to VAMAS files and processed in CasaXPS 2.3.19. Scans were charge referenced to the C 1s aliphatic signal (component 1) at 285.0 eV and each photoemission was fitted with the minimum number of GL (30) lineshapes (with spline-linear backgrounds) required to replicate the photoemission signals. C 1s components had FWHM constraints (1-1.3 eV), however, O 1s components were unconstrained. C 1s and O 1s B.E.s, FWHMs, and peak fittings were compared with existing literature reports (BAÑULS-CISCAR, ABEL and WATTS, 2016) to ensure samples were free from contamination and their spectra reflect that of lignin.

5.2. Results and Discussion

The summary scheme of this work is shown in Fig. 5.1. Two aspects of the pretreatment of sugarcane bagasse with [MEA][OAc] were investigated in this study. The first part of the study evaluated the impact of ABR on the pretreatment performance of freshly synthesised [MEA][OAc] at previously optimised pretreatment conditions (time, temperature, water content and solids loading). For the ABR, different amounts of acetic acid were added to monoethanolamine to generate 11 ABRs. Five ABRs corresponded to excess base: 0.1; 0.2; 0.5, 0.8 and 0.9, five to excess acid: 1.1; 1.25; 2.0; 5.0 and 10.0 plus the neutral PIL with 1.0 ABR. Two controls, pure monoethanolamine (MEA) and pure acetic acid were also used in the ABR assays. However, pretreatment with AA resulted in charring of the biomass and its related data was not used in this study. The partitioning of the main components in sugarcane bagasse was monitored by compositional analysis, including glucan, xylose and arabinose, extractives and lignin. The amount of lignin recovered after antisolvent precipitation and the amount of solvent recovered were also monitored, as was the release of sugars by cellulose hydrolysing enzymes from the solid fraction. Many acetate based PILs are not fully ionised (CHEN *et al.*, 2018), however, it has been shown that [MEA][OAc] has a high degree of ionicity in the 1:1 ABR (NUTHAKKI *et al.*, 2007). When excess acid or base is present, the molecular species become important, hence we will comment on the equilibrium in appropriate places.

The second part of the study investigated pretreatment performance during repeated use of [MEA][OAc] for two selected ABRs. Carbohydrate recovery and release of sugars by

cellulose hydrolysing enzymes were again monitored. Changes to the chemical properties of the isolated lignins were also evaluated.
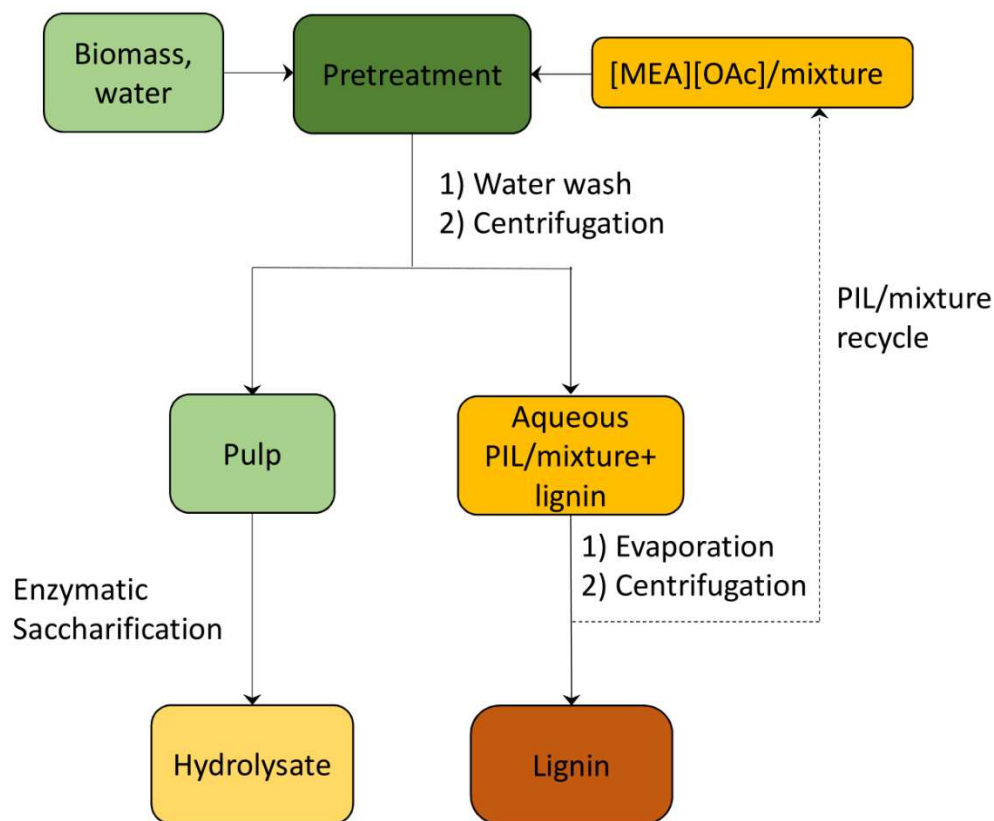
Fig. 5.1 — Summary scheme of this work. The solid lines correspond to the ABR experiments while the recycle experiments include the dotted line.

5.2.1. Effect of the ABR on pretreatment performance and solvent recovery

The chemical composition of raw sugarcane bagasse, as percentage of dry mass, is: cellulose, $41.95 \pm 1.41\%$; hemicelluloses, $25.43 \pm 0.69\%$; lignin, $23.79 \pm 1.34\%$; extractives $2.13 \pm 0.46\%$, acetyl groups $3.46 \pm 0.07\%$ and ash, $2.95 \pm 0.80\%$. The pulp yields (oven-dried weight) for the pretreatment of sugarcane bagasse with [MEA][OAc] with different ABRs are summarized in Fig. 5.2. For the lowest ABR values, 0.1 to 0.5 ABR, there were no major differences in terms of amount and nature of solubilized content.
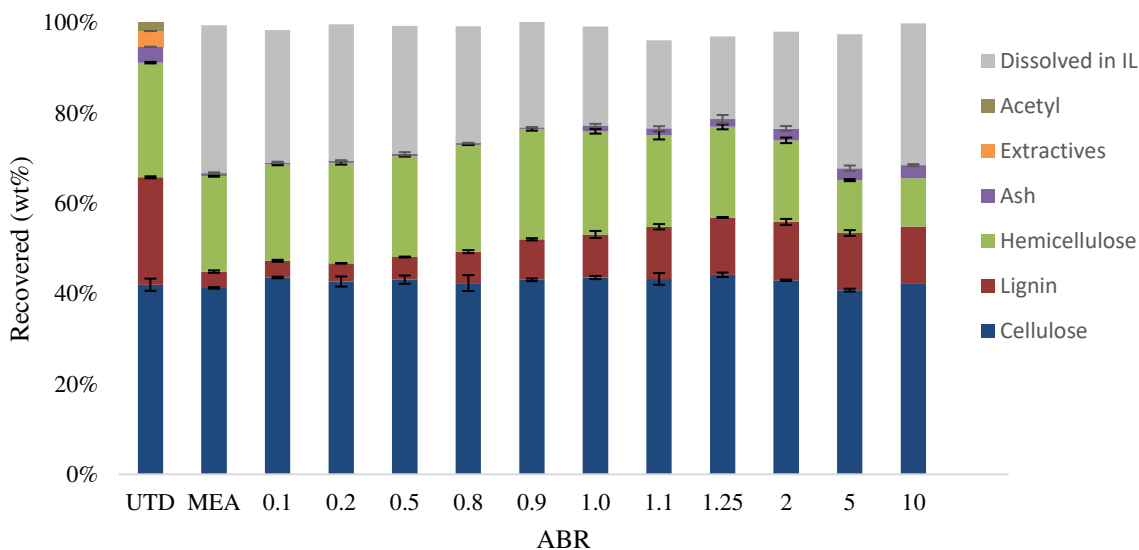
Fig. 5.2 — Pulp yields (non-grey fill) and pulps composition on the pretreatment of bagasse with [MEA][OAc] with different ABRs with 20 wt% water at 150°C for 2h and 15 wt% solids loading. Untreated (UTD) sugarcane bagasse was also displayed.

We note that there was very little cellulose solubilizations regardless of the ABR in the [MEA][OAc], while hemicelluloses solubilization increased under higher ABR values. This trend is also not surprising, as it is known that hemicelluloses hydrolyse easily at low pH. The glycosidic bonds between the pentose sugars are acetal bonds, a type of linkage easily accessible and hydrolyzed under acidic conditions (WYMAN *et al.*, 2005). Analysis of the liquid fractions by HPLC (Fig. II.1 in Appendix II) did not detect any cellulose degradation products i.e., glucose, HMF, formic and levulinic acid regardless of the ABR. As for hemicelluloses degradation products, only furfural was detected for the highest ABR values, 5 and 10, which confirms that PILs can be very selective towards isolating both cellulose and hemicelluloses.

There was ash solubilization under low ABR values, as indicated by the lower ash content remaining in the pulps. Extractives solubilization also followed the same trend, which probably is due to their reactivity towards alkali — tannins, lignans, fats and proteins are commonly found in extractives (SHESHMANI, 2013). It can be observed that lignin was the major component solubilized and that the delignification increased with increasing base content with up to 84 wt% of delignification for the lowest ABR value, 0.1. It is generally known that alkaline conditions favor lignin solubilization due to the hydrolysis of more susceptible linkages such as β-

O-4, which is the most common linkage in lignin, and solubilisation of lignin due to coordination and deprotonation of phenol groups. Alkaline pretreatments such as hydrogen peroxide (RABELO *et al.*, 2014), sodium hydroxide (NASCIMENTO *et al.*, 2016) and ammonia fiber explosion (AFEX) (BALS *et al.*, 2010), are known to remove a great portion of the lignin with up to 73.5, 90.7 and 80.9 wt% of delignification, quite similar to the value obtained in this work. However, carbohydrates can be also sensitive towards alkalis and they are also solubilized during such pretreatment with up to 4.4, 10, 2.7 wt% of cellulose and 26.7, 12, 71.4 wt% of hemicelluloses being solubilized in the AFEX, hydrogen peroxide and sodium hydroxide pretreatments of sugarcane bagasse, respectively. While only up to 2 wt% of hemicelluloses and practically no cellulose were solubilized under the low ABR values in this work, which shows that [MEA][OAc] has been proven to outperform other alkaline pretreatments. The compositional analysis results demonstrate that PILs cannot only be tailored by choosing different anion and cation configuration, but also by adjusting their molar ratio.

The compositional analysis results showed that PILs cannot only be tailored by choosing different anion and cation configurations, but also by adjusting their molar ratio. Fig. 5.3 illustrates the glucan and hemicellulose yields in saccharification. It can be noticed that both glucan and hemicellulose yields were higher for lower ABRs, i.e., excess base conditions. Hemicellulose yields were especially lower than glucan yields under excess acid conditions due to higher solubilization during pretreatment.

Interestingly, glucose release was also lower under excess acid conditions. This is likely due to the presence of larger amounts of lignin in the pulps obtained from higher ABR solutions. This lignin acts as a physical barrier to the enzyme access and may also reduce enzyme activity by adsorbing enzymes onto the lignins surface (RAHIKAINEN *et al.* 2013) The second conclusion is that changes in chemical composition of the pulps matter are not the only detrimental factor for enzyme accessibility. If we compare the glucose yields obtained for the excess base conditions, we can see that there was a decrease from pure MEA to 0.5 ABR, despite there being practically no differences in chemical composition as shown in Fig. 5.2. It can be inferred that the presence of acetic acid affected not only lignin removal but also affected morphological changes in the pretreated pulps, *i.e.* less creation of inter-chain spaces in the cellulose. However, additional

further analyses are required to prove this hypothesis, such as pore size distribution and surface area of the samples.

(a)

(b)
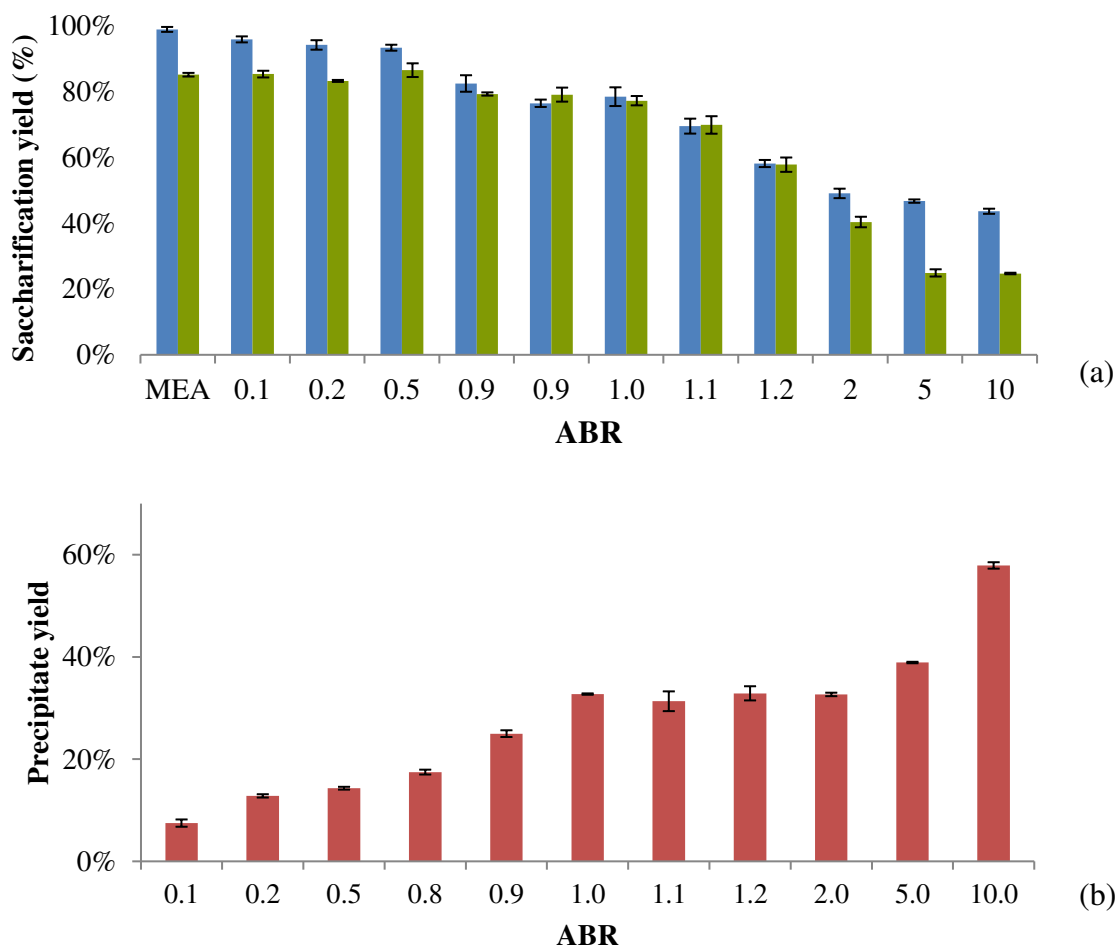
Fig. 5.3 — (a) Glucan (blue) and hemicellulose (green) yields in 72 h of enzymatic saccharification after pretreatment with [MEA][OAc] with different ABRs. (b) Lignin recovery from aqueous solutions of [MEA][OAc] with different acid-base ratios.

Hydrolysis residues were also weighed (Fig. II.3 in Appendix II) and compared with their estimated values based on the saccharification yields. Aside from the 1.1 ABR, there was a

high correspondence between calculated and experimental points, which shows saccharification yields may be roughly estimated by the amount of hydrolysis residues.

The precipitate (lignin) recovery for the ABR experiments is shown in Fig. 5.3b. For the lowest ABR values, from 0.1 to 0.9, the amount of recovered lignin decreased as the ABR decreased, which is likely due to increased lignin solubility in alkaline media. While for the highest ABRs, from 1.1:1 to 10:1, there was also an increase in lignin recovery. We note that for the 5:1 and 10:1 ABR, the lignin recovery exceeded the lignin extraction (Fig. 5.2), which indicates that there was pseudo-lignin formation from the hemicellulose fractions. Pseudo-lignin, also called humins, is a by-product of the decomposition of hemicellulose sugars in acidic media (HOANG, LEFFERTS and SESHAN, 2013). The extensive hemicellulose solubilization in the presence of acidic conditions promoted pseudo-lignin formation and can explain the high lignin recovery for high ABRs. The neutral PIL (ABR 1.0) provided 32.7 ± 1.9 wt% of recovered lignin (relative to total lignin in the raw bagasse), which is quite close to 27.8 wt% of biomass recovered as lignin for [MEA][OAc] pretreatment of sugarcane bagasse in a previous study (ROCHA *et al.*, 2017). In comparison, nearly 50 wt% of recovered lignin was obtained in the pretreatment of sugarcane bagasse with [TEA][HSO$_4$],(CHAMBON *et al.*, 2018) an acidic PIL; a lower amount, 20 wt%, was obtained in the pretreatment of willow with [TEA][HSO$_4$] (WEIGAND *et al.*, 2017), which indicates lignin recovery depends on biomass type and PIL used. It should be noted that the first pretreatment cycle does not necessarily reflect the lignin recovery that would be obtained at equilibrium in a process that uses recycled PIL.

We also examined PIL recovery rates (Fig. 5.4), which are key to commercial viability of such a solvent based process. The highest recovery, 97%, was found for [MEA][OAc] with 1:1 ABR. A recovery of around 97% is needed for a low-cost IL with a solvent price of USD 2.5/kg (KLEIN-MARCUSCHAMER, SIMMONS and BLANCH, 2011), which is the case for [MEA][OAc] whose estimated price is lower, USD 1.8/Kg (SUN *et al.*, 2017). Lower ABRs, i.e., excess MEA, generally resulted in higher solvent recovery. As the ABR decreased, the solvent system contained larger amounts of MEA, whose boiling point, 171°C, is higher than that of acetic acid, 118°C. since only one proton can be transferred between this acid and base, any mixture that does not have ABR = 1 may contain molecular species. The further away from ABR = 1 the more MEA or acetic acid was present. The recovery data suggest that most of the acetic acid evaporated

during solvent recovery, while most of the MEA did not. ACHINIVU *et al.* (2014) also recovered acetate PILs on the pretreatment of corn stover, but they employed partial vacuum distillation (0.1 mbar). They were able to recover up to 98% of the PIL pyridinium acetate, [Py][OAc], with 1:1 ABR. In this work, we employed weaker vacuum pressures — around 500 mbar — to evaporate water from aqueous solutions of [MEA][OAc].
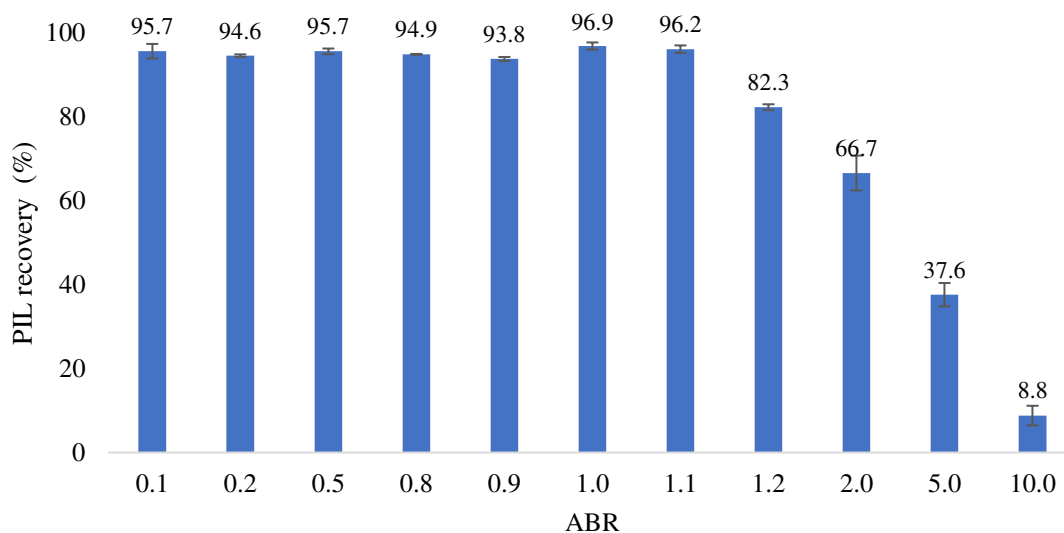
Fig. 5.4 - PIL recovery rates for the ABR experiments. The error bars were calculated based on duplicates.

Once recovery rates were not quantitative (~99 wt%) for low ABR values, we suspected there was PIL/MEA incorporation in the pulps or recovered lignins during pretreatment. Elemental analysis is a simple but elegant technique in which one can verify changes in composition. The results for the elemental analysis of pulps from the ABR experiments were summarized in 5.1. Raw sugarcane bagasse presents nearly 50 wt % of CHN and the rest is mainly oxygen plus some minor inorganic elements. There were slight variations on carbon content, the more extreme ABR values such as 0.1:1 and 10:1 had the lowest carbon contents, which might be related to an increase in oxygen/inorganic elements content. The overall nitrogen content of all pulps shows that practically no nitrogen incorporation in the pulps occurred. The most interesting fact, however, lies in the variation of nitrogen content, which decreases as ABR decreases. That is

to say, under low ABRs, even though there was a high probability of PIL incorporation in the pulps, resulting in higher nitrogen contents, it was, in fact, the opposite. Palm oil empty fruit bunch pretreatment with ammonia fiber expansion (ABDUL *et al.*, 2016) (AFEX) results in nitrogen incorporation in the pulp, which indicates [MEA][OAc] is less reactive than ammonia, probably due steric and electronic effects — a bulky and electro-withdrawing hydroxyalkyl group. Pretreatment of miscanthus with [TEA][HSO$_4$] (BRANDT *et al.*, 2017b) (from a tertiary amine) resulted in very low nitrogen content in the pulps, but there was sulfur incorporation, which may indicate the anion is interacting with cellulose in the pulps.

Table 5.1 — Elemental analysis of pulps obtained in the ABR experiments. Raw bagasse and monoetanolamine (MEA) pretreatment samples were also added as a matter of comparison. The error bars were calculated based on triplicates of samples.

Sample	C (%)	SD (%)	H (%)	SD (%)	N (%)	SD (%)
Raw bagasse	44.35	0.843	6.03	0.090	0.22	0.053
MEA	39.94	2.058	6.05	0.308	0.09	0.006
0.1:1	41.41	0.203	6.22	0.041	0.09	0.006
0.2:1	41.10	0.627	6.09	0.088	0.06	0.040
0.5:1	40.26	3.111	5.86	0.464	0.21	0.085
0.8:1	42.21	0.206	6.18	0.035	0.25	0.050
0.9:1	42.71	0.248	6.21	0.029	0.24	0.015
1.0:1	40.82	2.655	5.89	0.358	0.24	0.006
1.1:1	42.90	0.465	6.07	0.084	0.30	0.032
1.2:1	43.34	0.189	6.10	0.039	0.19	0.049
2.0:1	43.66	0.489	6.04	0.038	0.23	0.006
5.0:1	43.61	1.056	5.97	0.127	0.23	0.040
10:1	40.47	1.234	5.49	0.172	0.22	0.291

Results for the elemental analysis of lignins from the ABR experiments are shown in Table 5.2. The nitrogen content of all lignins is higher than the values found for the pulps in Table 5.1, showing the PIL is interacting with the lignin regardless of ABR and why recovery rates were not quantitative. Other studies have also reported nitrogen incorporation in the lignins from AFEX (ABDUL *et al.*, 2016, DA COSTA SOUSA *et al.*, 2016) and [TEA][HSO$_4$] (BRANDT *et al.*, 2017b) pretreatments, which seems to be a common feature of delignifying pretreatments. The most interesting trend, however, was the significant decrease in carbon content as the ABR decreased. CHN content in MEA lignin corresponds to less than 25 wt%; oxygen only wouldn't

account for the mass difference, suggesting there are also inorganic elements in the precipitated solids. This information, together with the fact that the "lignins" obtained from low ABRs presented lighter colour (Fig. II.4 in Appendix II) raised suspicion that they were not actually lignin. Either the lignins got derivatized during pretreatment or a different chemical/composite was recovered at low ABR values.

Table 5.2 — Elemental analysis of lignins obtained in the ABR experiments. The error bars were calculated based on triplicates of samples.

Sample	C (%)	SD (%)	H (%)	SD (%)	N (%)	SD (%)
MEA	15.90	0.029	3.59	0.029	3.08	0.050
0.1:1	21.80	0.330	4.00	0.330	2.79	0.050
0.2:1	25.28	0.133	4.29	0.133	3.15	0.029
0.5:1	50.95	0.109	6.14	0.109	3.04	0.045
0.8:1	54.37	0.037	6.41	0.037	3.63	0.023
0.9:1	57.51	0.015	6.62	0.015	2.83	0.021
1.0:1	58.56	0.151	6.56	0.151	3.63	0.053
1.1:1	60.74	0.036	6.43	0.036	2.33	0.032
1.2:1	61.20	0.092	6.43	0.092	2.37	0.124
2.0:1	62.10	0.017	6.24	0.017	2.59	0.083
5.0:1	62.35	0.140	6.07	0.140	2.86	0.071
10:1	62.64	0.037	5.93	0.037	2.74	0.046

XPS analysis is an elegant non-destructive technique that could fill in the gaps left from the elemental analysis. The survey scans of lignin isolated from [MEA][OAc] with 0.8:1, 1.1:1 and 2:1 ABRs, MEA, and [TEA][HSO$_4$] pretreatments were quantified and the atomic percentages are shown in Table 5.3. Lignin from [TEA][HSO$_4$] pretreatment was also analysed for comparison with a tertiary amine-derived PIL and also because it was one of the most common PILs used in the Hallett group, while [MEA][OAc] is synthesized from a primary one. [TEA][HSO$_4$] pretreatment conditions were similar to CHAMBON *et al.* (2018).

All lignin samples, including [TEA][HSO$_4$] pretreated lignin, showed N 1s signals in the survey spectra, confirming the nitrogen incorporation on the lignin samples found by elemental analysis. Except for MEA, all samples had higher carbon content than the elemental analysis values. One reason is related to the fact that XPS provides surface composition while elemental analysis does bulk and surface composition. Except for the MEA sample, lignin particles may have

aggregated in such a way during precipitation in water that the more hydrophobic aromatic moities would be in the surface.

As expected, an inorganic element was present in the [MEA][OAc] pretreated lignins, Si 2p signals were present in the survey scans. MEA pretreated lignin had the most silicon, which was present in 20.4 at.%, while all [MEA][OAc] samples showed small quantities of silicon (< 1 at.%); which indicates MEA eith reacted with the glass from the pressure tubes during pretreatment or with the ash already present in the biomass.

Table 5.3 — The atomic percentages of each lignin sample measured from survey spectra in Avantage using AL Thermo1 database.

	Atomic %					
	C	N	O	Si	S	Ca
RSF[a]	**1.00**	**1.68**	**2.89**	**0.90**	**1.89**	**5.97**
MEA	30.4	3.0	45.7	20.4		0.5
1:1	85.4	1.9	12.3	0.4		
1:0.8	78.6	2.8	17.7	0.9		
2:1	79.5	2.1	18.1	0.3		
[TEA][HSO$_4$]	74.6	0.0[b]	24.3		1.1	

[a] ALTHERMO1
[b] Rounds to 0.01%

The relative compositions of each Si chemical state are reported in Fig. 5.5. For MEA pretreated lignin, the Si 2p photoemissions show two chemical states in the HR spectrum (Fig. 5.5a). Component 1 has a B.E. of 102.6 eV, which is indicative of organo-silicon (e.g. siloxanes), whereas component 1 has a B.E. of 103.5 eV, which indicates the presence of inorganic silicon (e.g. SiO$_2$). Therefore, what was thought as lignin was, in fact, a SiO$_2$-lignin composite that stabilised from the reaction between MEA and the borosilicate in the pressure tubes and/or the ash in the biomass.

Fig. 5.5b shows the C 1s component (aliphatic carbon) percentage plotted against the O/C ratio. The correlation between these two indicators can be used to determine the amount of lignin or cellulose in a sample. The values are similar to those reported for other lignin samples (BAÑULS-CISCAR *et al.*, 2016), which also overestimate both the C 1s aliphatic and O/C ratios

of theoretical lignin values. The deviation of MEA pretreated "lignin" from the linear correlation is due to the high amount of silicon (20.4 at.%), which incurs a large drop in the carbon atomic percent. This is supported by the similarity of the carbon components (see Table 5.3).
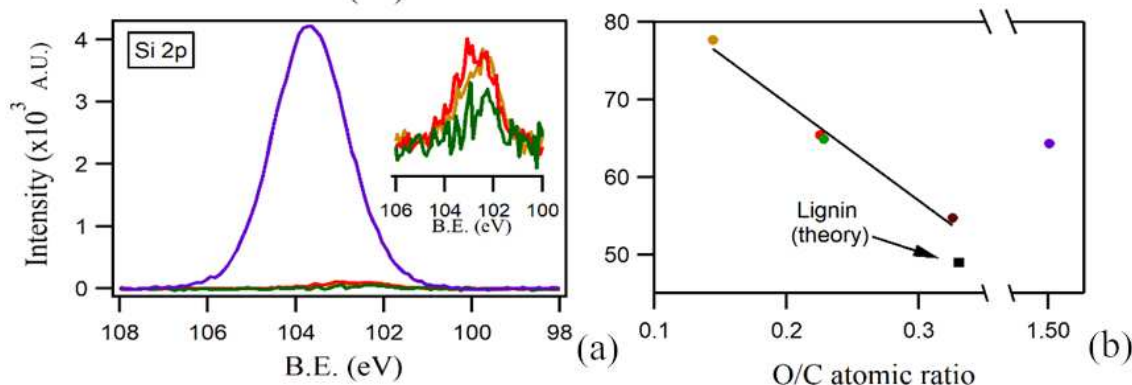
Fig. 5.5 - High resolution Si 2p scan (a) and plot of component 1 vs. O/C ratios.

To find out whether the silicon present in MEA lignin was originated from the pressure tubes or the ash in the biomass, we then analysed lignins obtained from pretreaments with MEA and 0.1 ABR in a stainless steel reactor. The results show that overall silicon content was lower than in the samples pretreated in glass tubes, 3.9 and 4.2 at.%, which confirms MEA reacted with the borosilicate in the pressure tubes, but also, to a small extent, MEA also reacted with the silicon present in the ash.

[TEA][HSO$_4$] pretreated lignin had less nitrogen in comparison to [MEA][OAc] pretreated lignins, however, sulfur was present (1.1 at.%) in the survey scans just like the lignin obtained from pretreatment of miscanthus (BRANDT *et al.*, 2017b). The presence of additional carbon chemical states at high B.E. (i.e. > 288 eV) and the small amount of nitrogen suggest that the hydrogen sulfate anion has chemically functionalised the lignin.

GPC analysis is an excellent technique to unfold structural changes in lignin such as recondensation and/or fragmentation. Dimethyl sulfoxide is one of the best solvents because it is highly polar and aprotic. The results from the ABR experiments were summarized in Table 5.4. The GPC profiles can be found in Fig. II-5 in Appendix II. The neutral PIL and high ABRs

presented Mn, Mw and PD values consistent with the ones obtained with [TEA][HSO₄] and [EMIM][OAc] pretreatments of miscanthus (BRANDT *et al.*, 2017b) and poplar (WEN *et al.*, 2014), respectively. Similar Mw values were also reported for the lignins obtained from lignin depolymerization experiments with diisopropylammonium acetate (TOLESA; GUPTA; LEE, 2017). It seems reasonable to assume the neutral PIL and excess acid ABRs generated "well-behaved" lignins. Under excess base conditions, however, as the ABR decreases, Mw and therefore PD (Mw/Mn) values increase, indicating the particles in solution are very heterogeneous. It is also noteworthy mentioning the poor solubility of the excess base "lignins" in all sorts of solvents, such as DMSO, alkaline water solutions, chloroform, and DMF, which supports the inorganic nature of these compounds.

Table 5.4 — Molecular weight parameters for the ABR experiments. Mn stands for average molecular weight, Mw, for number average weight and PD for polidispersity. The error bars were calculated based on triplicates of samples.

ABR	M_n	SD	M_w	SD	PD	SD
0.1	1530	47.6	29310	487.2	19.2	0.28
0.2	1384	248.2	26853	1536.7	18.4	0.65
0.5	1492	94.8	27043	1268.6	18.1	0.30
0.8	1460	90.5	16275	420.1	11.2	0.40
0.9	1240	138.6	9288	1294.7	7.6	1.89
1	1072	75.0	4742	75.7	4.4	0.24
1.1	1330	73.5	4410	113.8	3.3	0.10
1.2	1215	5.7	5199	306.2	4.3	0.23
2	1194	36.1	3705	43.8	3.1	0.06
5	1300	65.8	4576	118.1	3.5	0.27
10	1165	31.1	3905	31.1	3.4	0.12

The change in the ABR upon one reuse is summarized in Fig. 5.6. For the excess base conditions (Fig. 5.6a), there was a slight decrease in the ABR, which might be due to the loss of monoethanolamine and formation of an amide, whose formation was detected by ^{1}H-NMR and ^{13}C-NMR spectroscopy. For the excess acid conditions Fig. 5.6b), the drop in ABR was even more pronounced due to the evaporation of molecular acetic acid in the evaporation step.
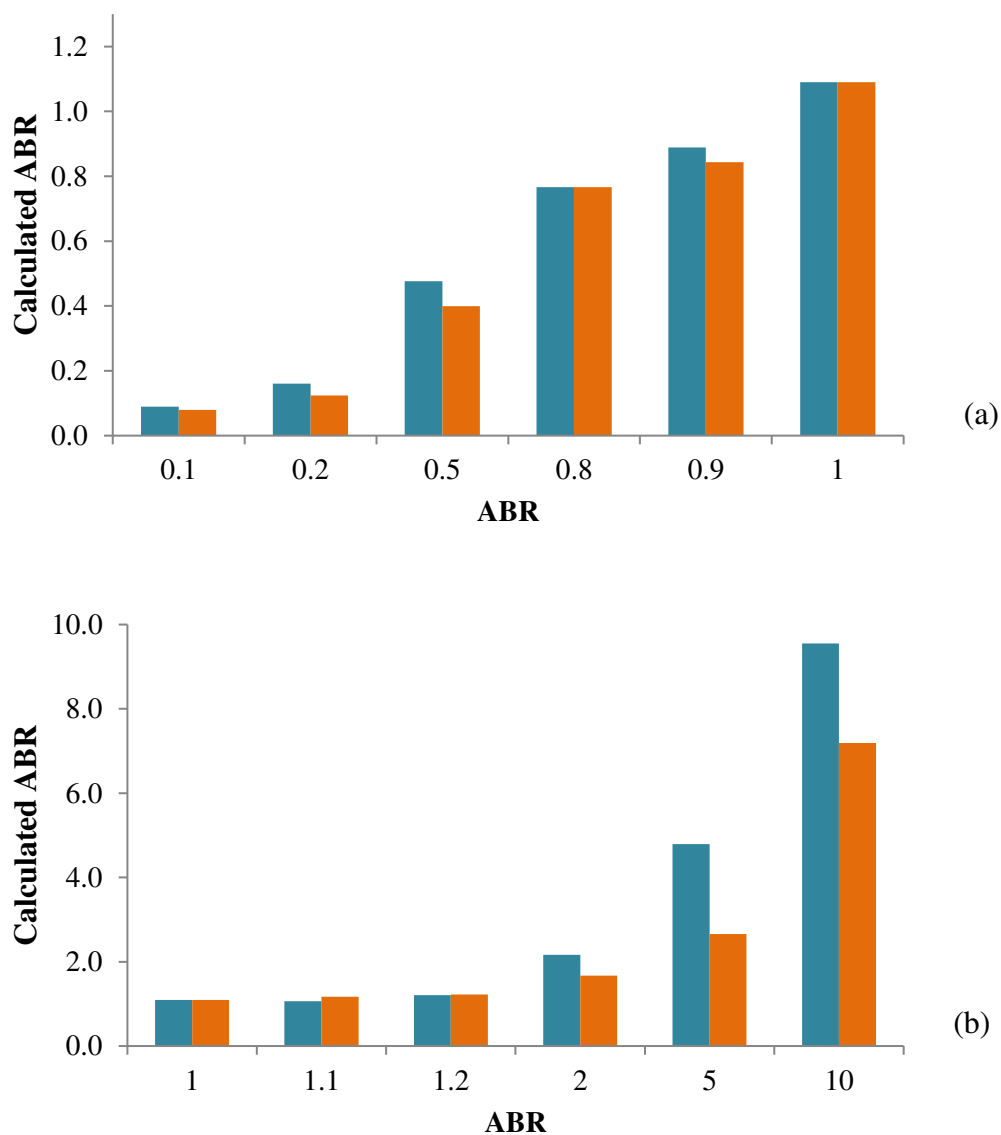
Fig. 5.6 — Calculated ABRs before (■) and after (■) pretreatment with [MEA][OAc] with excess base (a) and excess acid (b). The ABRs were calculated by NMR-H^1 spectroscopy based on the integral ratios of the protons in the acetate anion and 2-hydroxyethyl ammonium cation.

The mechanism for such conversion is shown in Fig. 5.7, with an equilibrium between PIL and the netral amine and base, which the latter pair being able to react in an amidation reaction to produce *N*-(2-hydroxyethyl)acetamide. Although the formation of amides is not kinetically favored between alkylamines and carboxylic acids — they usually require a catalyst at room temperature (PATTABIRAMAN and BODE, 2011), high pretreatment temperatures enable the

reaction into the thermodynamically more stable amide. Partial conversion of acetate based PILs into acetamides has been reported before for an IL comprising a secondary amine, pyrrolydinium acetate, [Pyrr][OAc] (ACHINIVU *et al.*, 2014) This suggests that primary and secondary acetate PILs are not inert at conditions used for lignocellulose pretreatment.
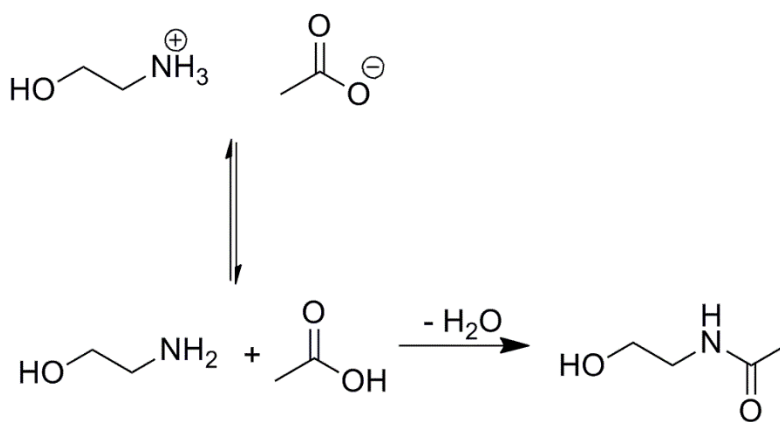
Fig. 5.7 — Mechanism for the PIL conversion into an acetamide.

The influence of ABR on the extent of amide formation can be seen in the NMR-H[1] spectra (Fig. II-6 in Appendix II). Under low ABR values (Fig. II-6a), the peaks for the acetamide (δ = 1.8, 3.05 and 3.35) decrease in intensity as the ABR decreases, suggesting that the amide formation was suppressed, especially for ABRs below 0.5:1. This is likely to the decrease of acetate concentration in the medium, which is deactivated for nucleophilic attack by the amine. Under high ABR values (Fig. II-6b), interestingly, the amide formation was also suppressed for ABRs higher than 2:1, which is likely associated with a decrease in the concentration of the nucleophile, monoethanolamine, due to its protonation.

There is also another report in the literature regarding changes in ABR in order to estimate the ionicity of PILs (CHEN *et al.*, 2018). ABR variations from 0.6:1 to 1.5:1 in PILs such as 1-methylimidazole acetate showed that acetate-based ammonium PILs are highly ionized even though the pKa difference between the acid and conjugate bases are not greater than 10 (NUTHAKKI *et al.*, 2007).

5.2.2. Recycle of [MEA][OAc] with 1:1 ABR

The saccharification yields were monitored for repeated use of the 1:1 ABR [MEA][OAc] and the results are shown in Fig. 5.8. A decrease in saccharification yield is noted for both glucose (Fig. 5.8a) and hemicelluloses (Fig. 5.8b) release, following the same trend found in studies with 1:1 ABR [MEA][OAc] pretreatment of sugarcane (ROCHA *et al.*, 2017) and apple cashew bagasse (REIS *et al.*, 2017). However, there were also some differences observed. In the previous work on [MEA][OAc] pretreatment of sugarcane bagasse, the glucan yield remained steady for the first 3 cycles at around 74.0% (ROCHA *et al.*, 2017). In this work, both the glucan and hemicellulose yields dropped to 50.0%. The main reason for the difference, is probablybecause in the previous work, fresh PIL was added before the new pretreatment cycles due to low PIL recovery rates, around $83.0 \pm 2.0\%$, which masked the yield decrease noted in this work.

The solvent recovery rates obtained in this work remained stable around 97.0% (Fig. II-7 in Appendix II) over the cycles, however, as previously mentioned, a great portion of the PIL was converted into acetamide, whose recovery rate was also high, as shown in Fig. II-7. The recovery rates, however, were not quantitative; as previosly confirmed in the ABR experiments, there was PIL/MEA incorporation in the biomass. We also found a characteristic methyl signal at $\delta_1 \approx 1.2$ ppm and $\delta_2 \approx 20$ ppm that indicates the presence of acetyl groups in the lignin (HANABUSA *et al.*, 2018) in the HSQC spectrum of the recovered lignin (Fig II-8 in Appendix II).

Recycling of [TEA][HSO$_4$] during the pretreatment of miscanthus (BRANDT *et al.*, 2017b) led to higher recovery rates of 99%, which is related to the low reactivity of tertiary amines, as they cannot form acetamides or react as nucleophiles.
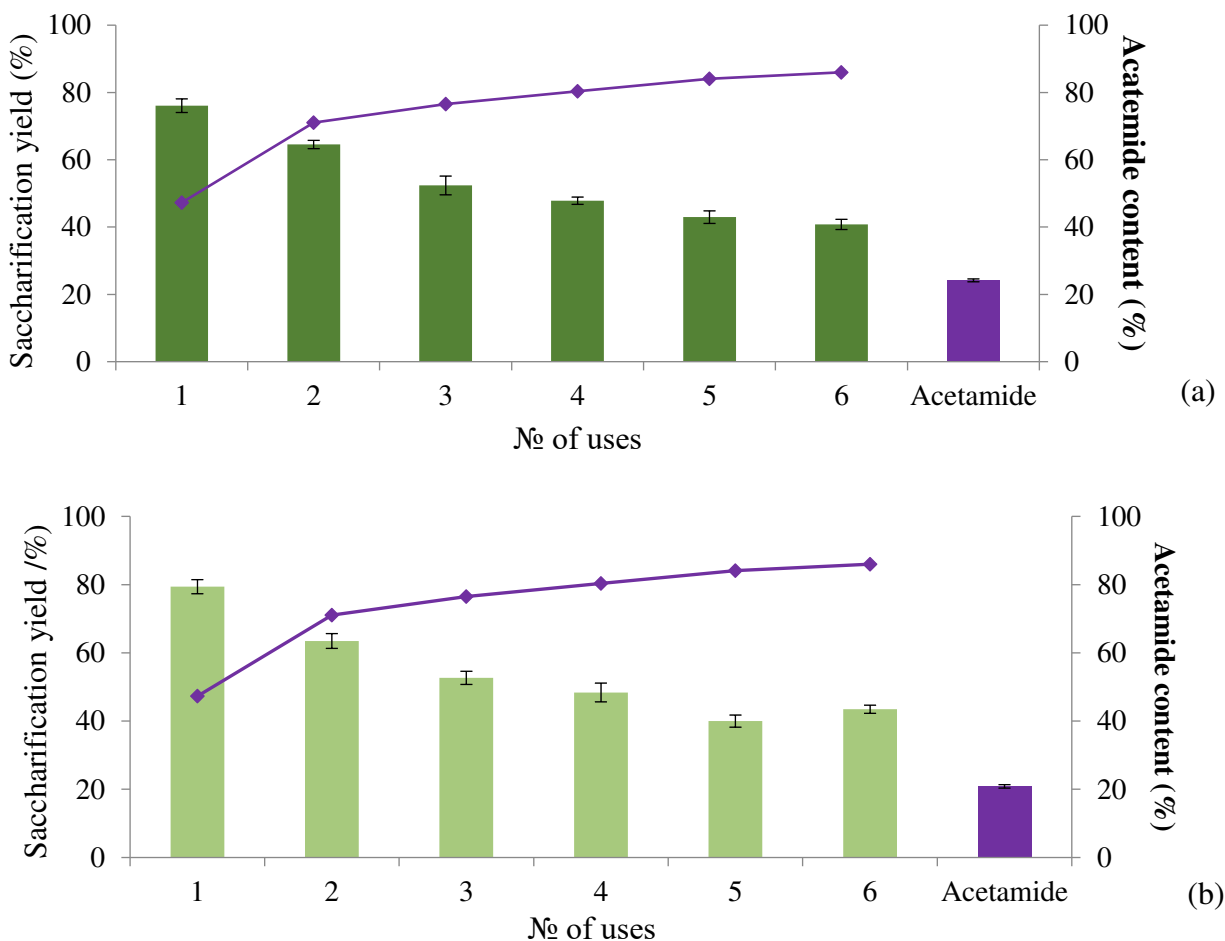
Fig. 5.8 — Glucan (a) and hemicellulose (b) yields in 72 h of enzymatic saccharification after pretreatment recycle with [MEA][OAc] with 1:1 ABR. A pretreatment control with pure acetamide (purple bar) was shown as a matter of comparison. Acetamide content in the mixtures was also plotted (purple curve).

Acetamide content in the mixtures was tracked along the cycles and shown in Fig. 5.8. A tendency towards a plateau by the end of the 6th cycle can also be noted and such yield (40% for glucan and hemicellulose yield) is still higher than using a pretreatment control with pure acetamide (violet bar). It appears that the PIL/acetamide mixture tend to reach a thermodynamic equilibrium after a number of recycles. The main reason behind the drop in PIL performance over the cycles is due to the PIL degradation into acetamide. A negative correlation between glucan yield in saccharification and acetamide content with data points from high ABRs and the neutral PIL was shown in Fig. 5.9, and an almost linear relationship ($R^2 = 0.96$) can be found, which

supports the need to avoid PIL degradation. A poor ($R^2 = 0.40$), slightly positive correlation was found with the high ABRs (Fig. 5.9), which may be due to evaporation of the solvent during its recovery. By analyzing the reaction scheme in Fig. 5.7 , one possible way to do that would be having water in the system, which is the case, 30 wt%. However, even though the tubes were sealed so that no water could evaporate and shift the equilibrium to the amide, the high temperatures employed in the pretreatment favored the formation of the more thermodynamically stable amide.
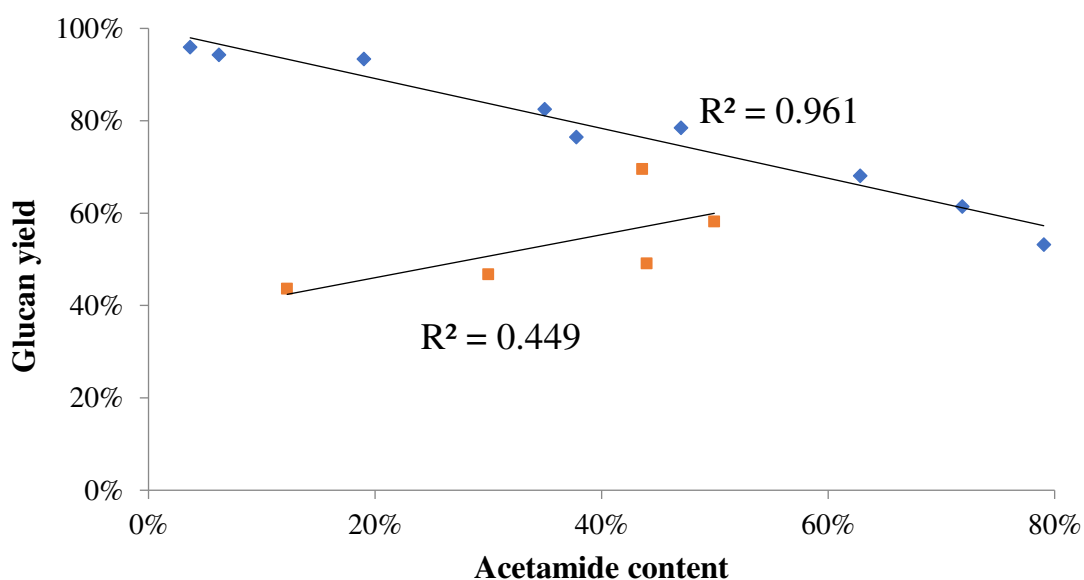
Fig. 5.9 — Correlation between glucose yield after 72 h of enzymatic saccharification and acetamide content in the recovered IL. Blue data points: low ABRs and recycle of [MEA][OAc] with 1.0 ABR. Orange data points: high ABR ratios.

Lignin recovery for the recycle experiments is shown in Fig. 5.10. A slight increase in lignin recovery can be observed as recycling progressed, with a tendency towards reaching a plateau by the 6th cycle. However, the delignification and also the cumulative lignin recovery (lignin recovery summed over all previous cycles) decreased. The cumulative lignin recovery was lower than the lignin extraction, which means that lignin is accumulating in the solvent. It is interesting to note that the recoveries were higher than the acetamide control, even though over

80% of the pretreatment mixture was acetamide in the last cycle, showing that even a small ionic component is important for pretreatment performance.
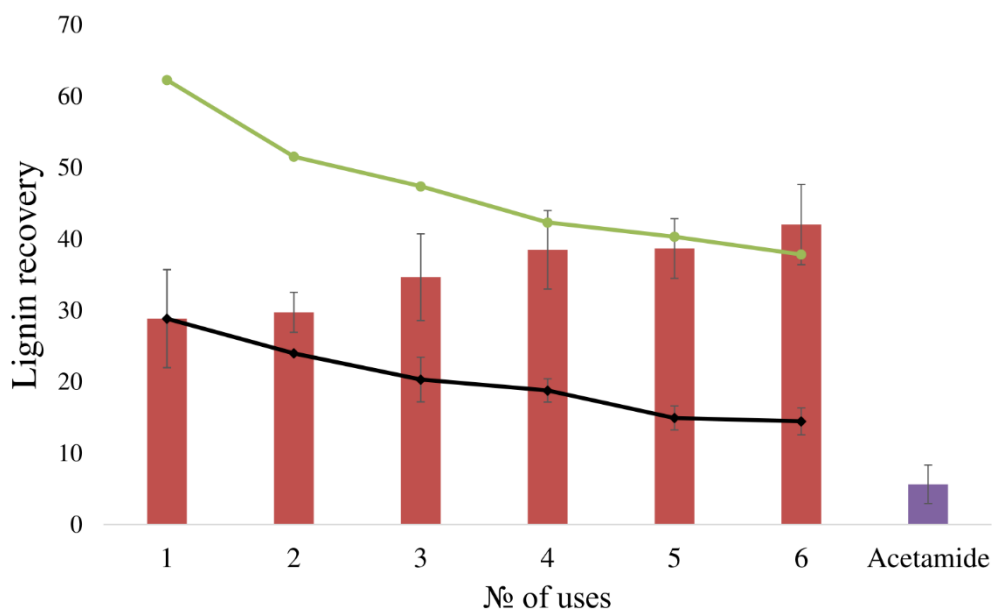
Fig. 5.10 — Lignin recovery (red bars), delignification (green line) and cumulative lignin recovery (black line) from aqueous solutions of [MEA][OAc] during solvent recycling. Lignin recovery from pretreatment with the pure -(2-hydroxyethyl)acetamide is also shown (purple bar) for comparison.

The compositional analysis of the pulps, shown in Fig. 5.11, supports the aforementioned hypothesis: even though the pulps had a very similar composition, there were significant differences in saccharification efficiency, which indicates that not only changes in the composition but morphological modifications in the biomass structure play an important role in deconstruction. A work on computational simulation (RAJ *et al.*, 2016) suggests that ILs may help to reorganize the cellulose structure by breaking and forming new intra and intermolecular hydrogen bonds. Such reorganization expands the inter-chain distances and increases cellulose accessibility.
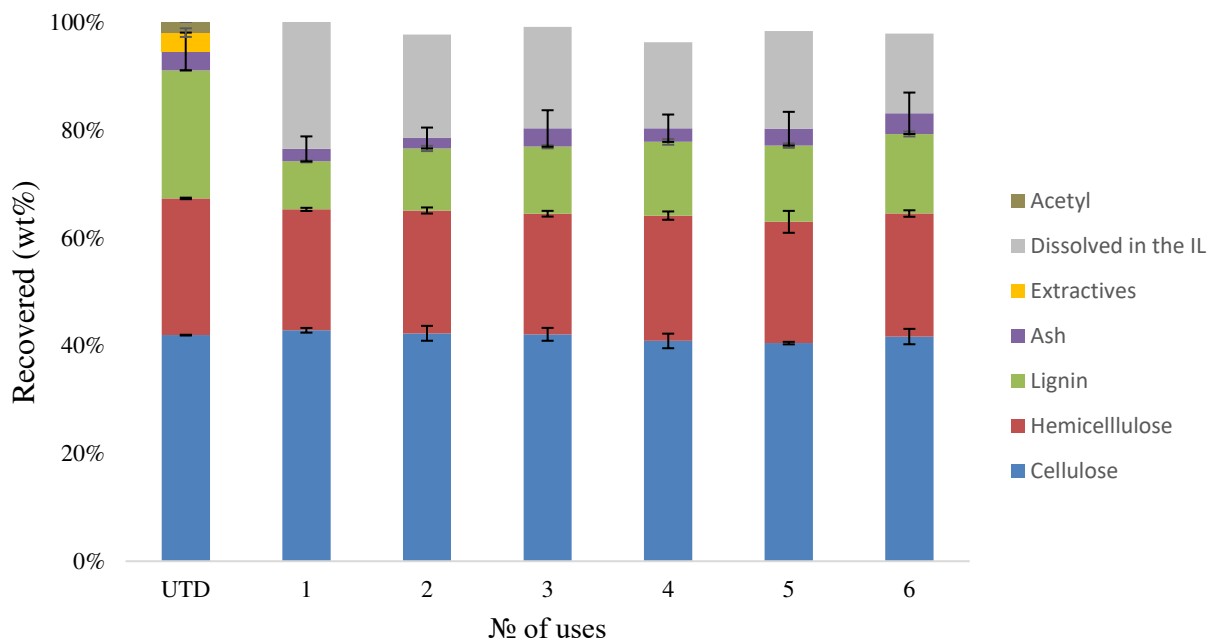
Fig. 5.11 —Pulp yields (solid blue fill), ash (purple) and components solubilized during pretreatment (patterned fill) — Lignin solubilisation (brown), hemicellulose solubilisation (green) and extractives (red) along the cycles for the PIL recycle.

The variation in ABR was also tracked in the recycle experiments (Fig. II.8 in Appendix II). As expected, the ABR hasn't changed much upon reuse. Formation of the amide consumes both acetic acid and monoethanolamine, so the reaction would not significantly change the ABR. In a study using the PILs pyrrolidinium acetate (ACHINIVU *et al.*, 2014), comprising a secondary amine, and pyridinium acetate, comprising a tertiary amine, the authors found that the ABR ratio remained practically unchanged after one pretreatment cycle.

5.2.3. Recycle of [MEA][OAc] with 0.5:1 ABR

In order to avoid PIL degradation into acetamide, it was decided to study the recycle of [MEA][OAc] with 0.5 ABR, a slightly basic condition that would not, in theory, favor the amide formation. The glucan and hemicellulose yields along 3 cycles were shown in Fig. 5.12. There was not a significant decrease in yield compared to the previous recycle experiments, which confirms the assumption that conversion into acetamide was behind the efficiency loss. Acetamide content

hasn't varied much, reaching up to 30% by the end of the 3rd cycle. Hemicelluloses also had very high yields, values were similar to the MEA control. Excess base PIL has proven to be more selective towards delignification and carbohydrates preservation and also increased carbohydrate digestibility.
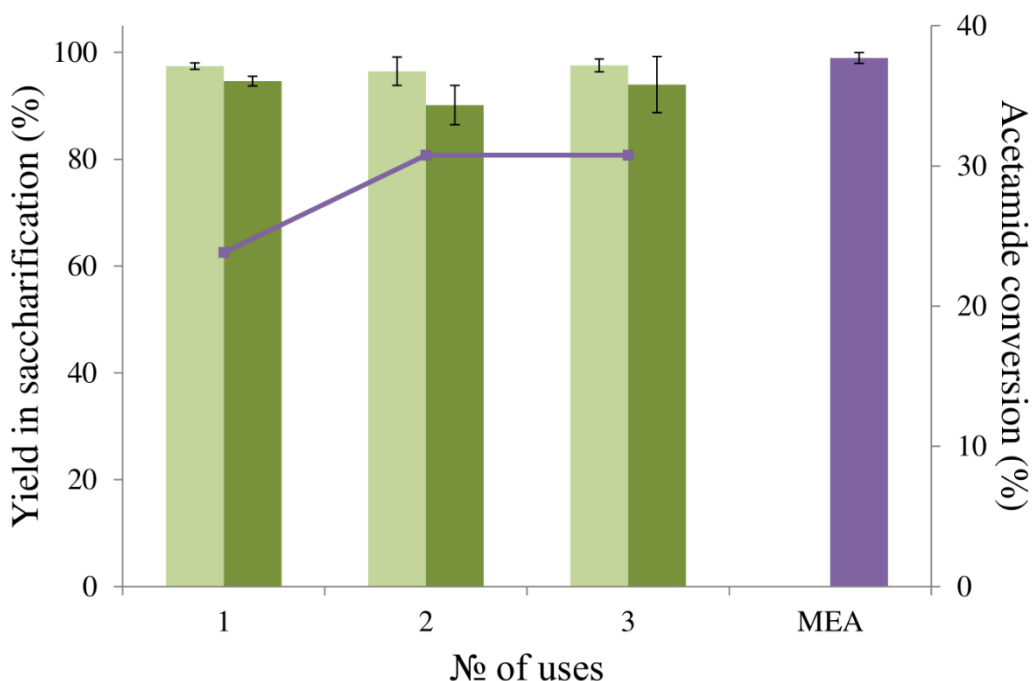
Fig. 5.12 — Glucan (light green) and hemicellulose (dark green) yields in 72 h of enzymatic saccharification along three pretreatment cycles with [MEA][OAc] with 0.5:1 ABR. A pretreatment control with pure MEA was shown as a matter of comparison. Acetamide content (purple line) was also plotted.

The ABR variation along the cycles was shown in Fig. 5.13. There is a small decrease after the 1st cycle in the same way it happened in the ABR ratio experiments, which might be linked to PIL conversion into acetamide. It is important to address that suppression of acetamide formation with [MEA][OAc] is essential to guarantee efficiency in the PIL recycle. Acetate-based PILs tend to form acetamides with cations of primary and secondary amines and by using tertiary amines there is a high chance that the PIL has a low ionicity/poor water solubility due to a limited number of hydrogen bonds with N-H bonds.
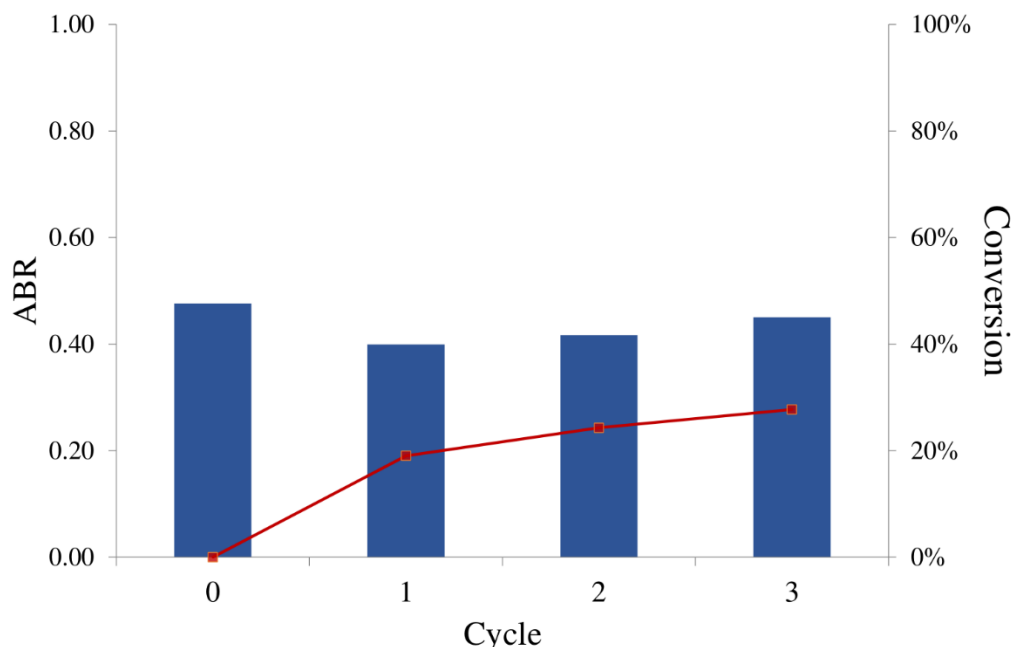
Fig. 5.13 — Calculated ABRs (blue bars) for the recycle of [MEA][OAc] with 0.5:1 ABR. The IL conversion into acetamide was also plotted (—■—). The ABRs were calculated via NMR-H[1] spectroscopy based on the integral ratios of the protons in the acetate anion and 2-hydroxyethyl ammonium cation.

Molecular weight parameters for the recycle experiments were shown in Table 5.5. Both Mw and Mn values decreased along the cycles. However, since the decrease in Mw values was more pronounced, PD also decreased. Usually, decreasing Mw values indicate harsher pretreatment conditions (WEN *et al.*, 2014), which was not the case once the pretreatment conditions were kept constant. As previously mentioned, there is a drop in delignification and cumulative lignin recovery along the cycles, lower Mn and Mw values may indicate a decrease in delignification efficiency with smaller lignin fragments being released to the PIL solution during pretreatment.   The rationale behind this is that PIL conversion into acetamide depletes the amine/ammonium cation in the medium — the main source of interaction between lignin/cellulose and the PIL/mixture— therefore decreasing the permeability of the catalyst; lignin deconstruction might then be limited to the primary peeling reactions (ZHAO, ZHANG and LIU, 2012). Even though using glass pressure tubes might not have been the best material's choice for the pretreatment vessels, it revealed how reactive/corrosive excess monoethanolamine solutions are during pretreatment. A balance between lignin recovery, efficiency in saccharification and PIL

mixture corrosivity must be found in order to make a pretreatment process fully operational and feasible.

Table 5.5 — Molecular weight parameters for the recycle experiments. Mn stands for average molecular weight, Mw, for number average weight and PD for polidispersity. Standard deviations (SD) were calculated based on triplicates of the samples

Cycle	Mn	SD	Mw	SD	PD	SD
1	1561.5	91.2	7161.5	400.9	4.6	0.0
2	1397.0	69.3	5073.5	173.2	3.6	0.3
3	1024.5	129.4	4065.5	638.5	4.0	1.1
4	978.0	12.7	3233.0	1.4	3.3	0.0
5	859.0	21.2	3141.5	126.6	3.7	0.2
6	737.0	48.1	2718.0	56.6	3.7	0.3

5.3. Conclusions

The study of ABR showed that it is possible to keep track of ABR variations — by NMR-H[1] — and excess base conditions provide excellent PIL performance, with nearly quantitative glucan/xylan yield in saccharification and up to 84% of the delignification with ABR 0.1:1. Even under excess base conditions there was not significant cellulose degradation, despite a considerable hemicellulose solubilization and possible humins formation for ABR 5.0:1 and 10.0:1. PIL recovery was high for the neutral PIL and excess base conditions, however, it decreased significantly with increasing ABR values due to loss of molecular acetic acid in the evaporation steps. For the same reason, ABR values after pretreatment decreased greatly under excess acid conditions.

Recycle experiments with neutral [MEA][OAc] confirmed a drop in PIL performance along cycles. However, we were able not only to qualitatively verify such information, but also quantitatively correlate it with the PIL conversion into an acetamide. The drop in PIL performance was overcome by recycling [MEA][OAc] with excess base, 0.5:1 ABR acetamide conversion was considerably lower and therefore the glucan/hemicellulose yields in saccharification were kept high up to the last recycle.

Investigation on the recovered lignins from the ABR experiments showed that under neutrality and excess acid conditions, there are "well-behaved" lignins in terms of properties such as molecular weight, polydispersity and elemental composition. However, excess base conditions (ABR < 1.0:1) generated inorganic compounds rich in silicon whose surface composition indicated the presence of organo-silicon functions. The molecular weight of lignins recovered from the recycle experiments decreased along the cycles, which indicates that under the same pretreatment severity, high molecular weight lignins are generated from a better PIL performance. Although excess base conditions provided higher yields in saccharification, a compromise between lignin recovery and PIL mixture corrosivity must also be found to ensure an economically feasible process.

Chapter 6

6. The impact of washing on enzymatic saccharification and fermentation

6.1. Introduction

Water consumption must be considered when it comes to designing a sustainable ethanol production process. The sugar-ethanol industry demands high quantities of water; for instance, an annexed mill that produces 50% ethanol and 50% sugar consumes 22 m^3 of water per ton of cane in average, and approximately 10% of this amount is used to wash the cane (NETO, 2013). In the second generation process there is an even higher consumption of water, since a post-washing step of the cellulose-rich pulp is required after most pretreatments in order to remove potential inhibitors of the enzymatic saccharification and/or alcoholic fermentation.

The enzymatic saccharification consists on the biochemical deconstruction of the lignocellulosic biomass. Cellulolytic cocktails have been engineered and upgraded to maximize sugar monomer production with increased robustness. However, there are some chemicals that may interfere on the enzyme's accessibility. Phenolic compounds from lignin degradation may non-productively adsorb the enzymes and decrease the amount of active enzyme species in the medium (XIMENES *et al.*, 2010). A careful understanding of the dynamics of the chemical transformations that occur during pretreatment is needed to avoid lignin/carbohydrate degradation into potential inhibitors (JÖNSSON and MARTÍN, 2016).

Alcoholic fermentation comprises the last step in the production of E2G and therefore it validates the efficiency of the enzymatic saccharification and pretreatment steps. In this stage, any chemicals such as furfural or phenolic compounds that might have been generated during pretreatment or released during enzymatic saccharification may impact negatively on the yeast metabolism (JÖNSSON and MARTÍN, 2016; LARSSON, REIMANN and NILVEBRANT, 1999). There are, however, several ways to overcome the presence of fermentation inhibitors, such as physico-chemical, chemical or biological detoxification methods (JÖNSSON and MARTÍN, 2016). Despite generating an inhibitor-free hydrolysate, detoxification means an additional step prior to fermentation that can ultimately impact on the final ethanol selling price.

The water consumption or water footprint (NETWORK, 2019) of a biofuel is an interesting parameter which examines the full life cycle, starting with the water required to grow the crop, including water from rainfall (HOLLY, 2012). Despite some studies on simulation of the water footprint of E2G (ARGO *et al.*, 2013; CHIU; WU, 2012) , there are only a few experimental studies on water consumption (or use) — especially in the pulp washing — in E2G production (LEE, ZHENG and VANDERGHEYNST, 2015; NAKASU; RABELO, 2012; SÖDERSTRÖM; GALBE and ZACCHI, 2004). Stablishing quantitative correlations between water consumption and the yields in saccharification and fermentation is not only important for more accurate input data in process simulations, but also for a deeper understanding on the importance of water in the overall process.

Pretreatment with [MEA][OAc] with 1:1 ABR or higher is similar to mild alkaline pretreatments and therefore produces practically no saccharification/fermentation inhibitors, as shown in Chapter 4. However, incomplete pulp washing results in the presence of residual PIL that might interfere on the subsequent steps in two ways: 1) by altering the ionic strength of the medium and decreasing the enzyme activity and/or yeast performance 2) by inhibiting the yeast growth due to the presence of acetate. This chapter aims to evaluate the fermentation of the hydrolysates obtained with [MEA][OAc] pretreatment; also, the impact of wash water will be investigated on both enzymatic hydrolysis and fermentation, once the enzymes and yeast are affected by the presence of PIL or degradation products.

6.2. Experimental

The experimental setup of this chapter was summarized in Fig. 6.1. Once we aim to calculate a material balance, all the steps in Fig. 6.1 were gravimetrically measured. This last part of this thesis entails all steps of E2G production, pretreatment, saccharification and fermentation.
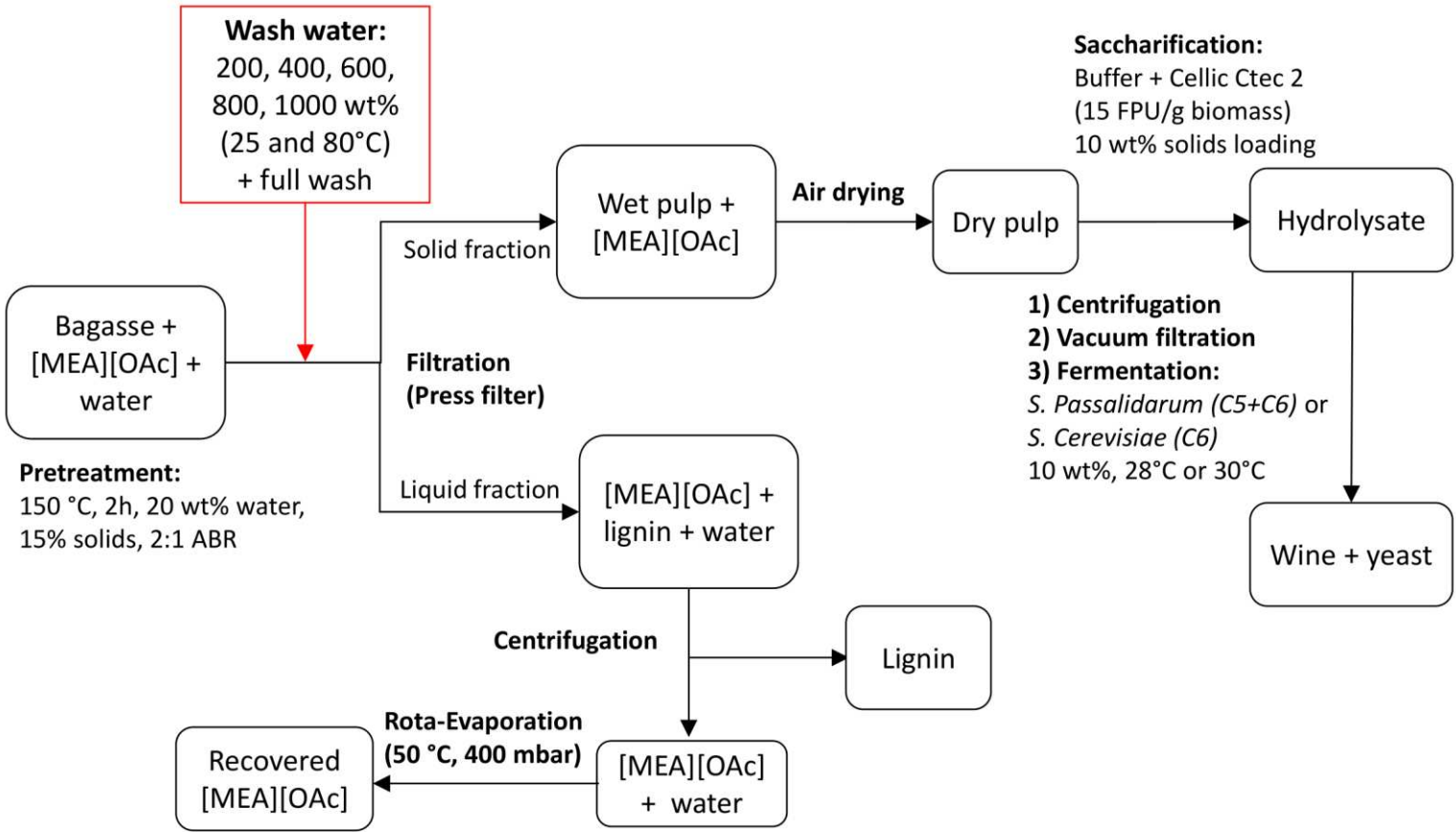
Fig. 6.1 — Scheme of the study of the impact of washing on enzymatic saccharification and alcoholic fermentation.

6.2.1. Pretreatment

Approximately 8.3 g of bagasse (7% moisture content), 34.6 g of [MEA][OAc] and 10.7 g of water were used, according to previously optimized conditions obtained in Chapter 3: 150 °C, 2h, 15% solids loading, 20 wt % water content. Differently from Chapter 3, the IL used - [MEA][OAc] – was produced with an acid-base ratio (ABR) of 2:1, as indicated by the results from Chapter 5.

6.2.2. Washing experiments

In order to investigate the effect of washing of the pulps on the subsequent steps, two temperatures — 25 and 80°C — and 5 different amounts of wash water were tested based on the total mass of the system PIL + water + bagasse: 200, 400, 600, 800 and 1000 wt%. For the pretreatment assays the total mass of [MEA][OAc] + water + bagasse corresponds to 53.6 g. Therefore, 100% of wash water would correspond to 53.6 g, 200%, 107.2 g of water, etc. The mixtures were then washed in water portions in glass beakers for 5 minutes and then filtered in a press filter. A full wash control was also generated by thoroughly washing the pulp in cloth bags. Washing experiments were performed in duplicates. Table 6.1 summarizes the total amount of wash water, portions and their equivalent in solvent:biomass ratio. For more information about the experimental setup, see Appendix IV.

Table 6.1 - Summary of water quantities in the washing experiments.

Samples	Total amount of wash water	Portions	Solvent:biomass ratio (g solvent/ g biomass)
200 %	107 g	2	13.4
400 %	213 g	3	23.6
600 %	320 g	4	40
800 %	426 g	5	53.2
1000 %	533 g	6	66
Full wash	5000 g	-	625

The liquid fractions were then centrifuged at 4000 RPM for 10 min to precipitate the lignin and the supernatant was evaporated by rotary evaporation to yield a concentrated recovered [MEA][OAc] which had its moisture content determined by Karl Fischer titration in triplicate.

6.2.3. Enzymatic saccharification

The solid fractions obtained from pretreatment were air dried and then subjected to enzymatic saccharification according with section 4.1.6 in Chapter 4. Saccharification conditions were 10 wt% solids loading, 15 FPU of Cellic Ctec2·g biomass^{-1}, 72 h in sodium citrate buffer. Saccharification samples also had their pH adjusted with H_2SO_4 6 mol·L^{-1} to the range between 4.5-5.0 to ensure maximum enzyme activity. The hydrolysates were centrifuged at 4000 RPM for 10 min to precipitate the cell mass and then filtered under vacuum through 0.45 μm cellulose membranes to 125 mL Erlenmeyers and subjected to the alcoholic fermentation.

6.2.4. Alcoholic fermentation

Alcoholic fermentation consisted on fermenting the hydrolysates with the microorganism *Spathaspora passalidarum*, capable of fermenting hexoses and pentoses. The inoculum suspension (10 wt%) was added to the hydrolysates together with KH_2PO_4, $(NH_4)_2HPO_4$, $MgSO_4.7H_2O$, yeast extract, malt extract and trace elements solution with the following concentrations: 4 g·L^{-1}, 2 g·L^{-1}, 0.5 g·L^{-1}, 3 g·L^{-1}, 3 g·L^{-1} and 1 mL·L^{-1} according with FARIAS, ANDRADE and MAUGERI-FILHO (2014). A fermentation control consisting of glucose (60 g·L^{-1}) and xylose (30 g·L^{-1}) was also used as a matter of comparison. The samples were agitated at 110 RPM in an orbital shaker at 28°C. The fermentation profiles were obtained by sampling 1.5 mL of each sample in the following intervals: 0, 6, 12, 24, 36, 48 and 72h. For the fermentation with higher cell loading, the time intervals were: 0, 6, 12, 18, 24, 36, 48 and 54 h. Yeast activation, propagation, pre-inoculum and inoculum preparation were done according with FARIAS, ANDRADE and MAUGERI-FILHO (2014).

One fermentation test was also performed with the yeast *Saccharomyces cerevisiae*, only capable of fermenting hexoses. The inoculum suspension (10 wt%) was added to the hydrolysate obtained by full washing the pulps together with KH_2PO_4, NH4Cl, $MgSO_4.7H_2O$, KCl,

yeast extract and trace elements solution with the following concentrations: 5 g·L^{-1}, 1.5 g·L^{-1}, 0.7 g·L^{-1}, 1.2 g·L^{-1}, 5 g·L^{-1} and 1 mL·L^{-1} according with ANDRADE *et al.*, (2013). Yeast activation, pre-inoculum and inoculum preparation were done according with ANDRADE *et al.*, (2013).

6.2.5. Analytical methods

Dry cell mass concentrations were determined gravimetrically after centrifuging the samples for 5 min at 4000 RPM, washing with DI water and oven-drying the cells at 50°C for 24 h.

The supernatants from the fermentation samples were used for determination of sugars (glucose, xylose and arabinose), polyols (glycerol and xylitol), acetic acid and ethanol by HPLC according with Section 4.1.8.

6.3. Results and discussion

6.3.1. Interplay of PIL and enzyme performance in saccharification

PIL recovery as a function of the amount of wash water is depicted in Fig. 6.2. Recovery of [MEA][OAc] increases with higher amounts of wash water, as expected, and the effect of temperature was not pronounced. A Tukey test done on the PIL recovery for the washing at 25°C (95% confidence, Appendix III) showed that there were no significant differences amongst samples with 600% wash water or higher. While for PIL recovery from washing at 80°C, the Tukey test detected significant differences amongst all samples, except between 800-1,000%. It is interesting to note that PIL recovery was high for 800 and 1,000% wash water for both temperatures studied. The full wash sample did not present quantitative recovery, as seen in Chapter 5, due to PIL incorporation into the biomass, so we would not expect much higher recovery values.
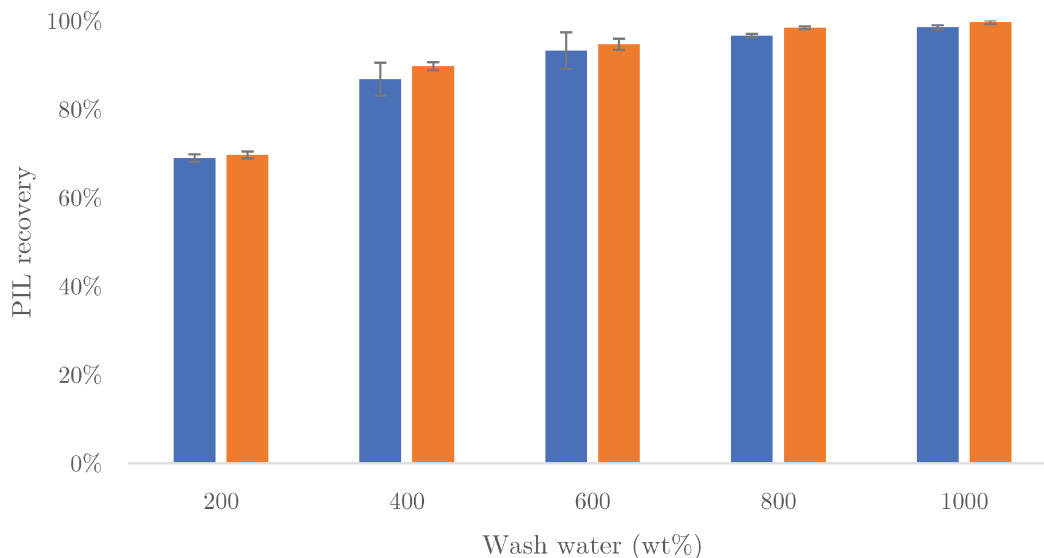
Fig. 6.2 - PIL recovery as a function of wash water at 25°C (blue bars) and 80°C (orange bars).

A study by NINOMIYA *et al.* (2015) on the washing of bagasse with cholinium acetate (a PIL), [Ch][OAc], and [EMIM][OAc] (an APIL) pretreatments showed that even after almost 4000 wt% of wash water there was still nearly 10% and 5% of residual [Ch][OAc] and [EMIM][OAc] in the pulps, showing that these ILs might interact by chemo-sorption or chemically bonding to the biomass, especially [EMIM][OAc], whose residual values were higher than [Ch][OAc].

Glucan and hemicellulose yields in saccharification for the washing experiments were shown in Fig. 6.3a-b. Hemicellulose yields were much more affected than glucan with only 20% of yield with 200% wash water, which indicates that enzyme inhibition by the PIL impacts more on the breakage of hemicellulose bonds. Between 200 and 400% there seems to be a sudden increase in enzyme activity, which might indicate there is an upper threshold that ensures cellulase activity. For the glucan yields (Fig. 6.3a), a Tukey test (95% confidence level, Appendix III) showed that from 400% to 1,000% of wash water there were no significant differences between the water quantities for both temperatures. For the hemicellulose (6.3b), besides the lowest value at 200%, the yields were significantly different every two levels apart, i.e., 400-800, 600-1,000, etc. What is also intriguing is that, despite almost all [MEA][OAc] being extracted from the pulps at 1,000% (Fig. 6.2), saccharification yields were still lower than the full wash sample. The

presence of unremoved low molecular weight lignin (LMW) particles in the biomass might have contributed to a lower enzyme performance. NINOMIYA *et al.* (2015) showed that the enzymes present higher tolerance to [Ch][OAc] than [EMIM][OAc], with the latter presenting almost twice the cEC_{50} value, i.e., a minium IL concentration (in wt%) to decrease the enzyme activity by 50%, which shows that the imidazolium cation interacts more strongly with the enzymes than cholinium.

(a)

(b)
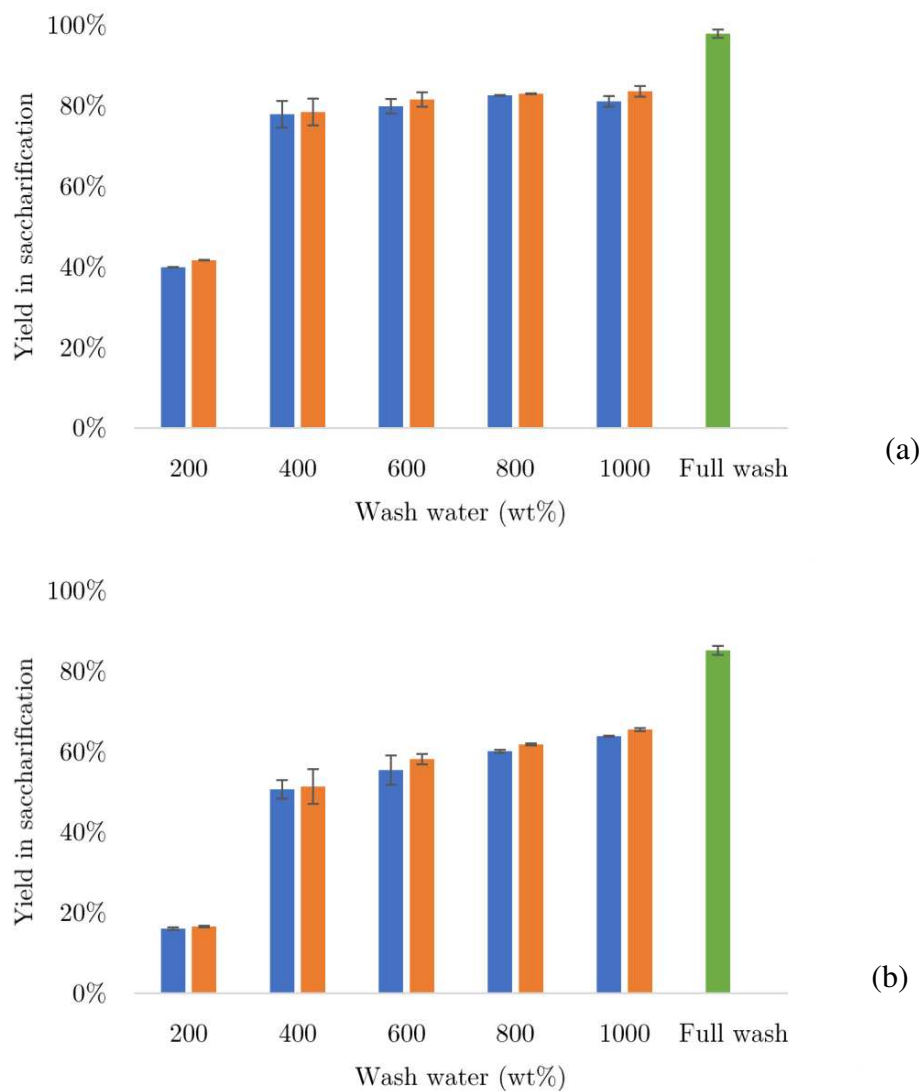
Fig. 6.3 — (a) Glucan and (b) hemicellulose yields in saccharification (xylose and arabinose) along different wash water contents at 25°C (blue bars) and 80°C (orange bars). A full wash control was also plotted as a matter of comparison.

PIL recovery values were used to estimate the amount of residual PIL in the hydrolysates, which were plotted against the yields in saccharification (Fig. 6.4). Strong negative correlations were found — with R^2 values ranging from 0.91 to 0.99 — showing that the presence of residual [MEA][OAc] is one of the causes of decrease of enzyme activity. By analyzing the graphs, it appears the aforementioned upper threshold is in between 10-15 wt% of the PIL.

(a)

(b)
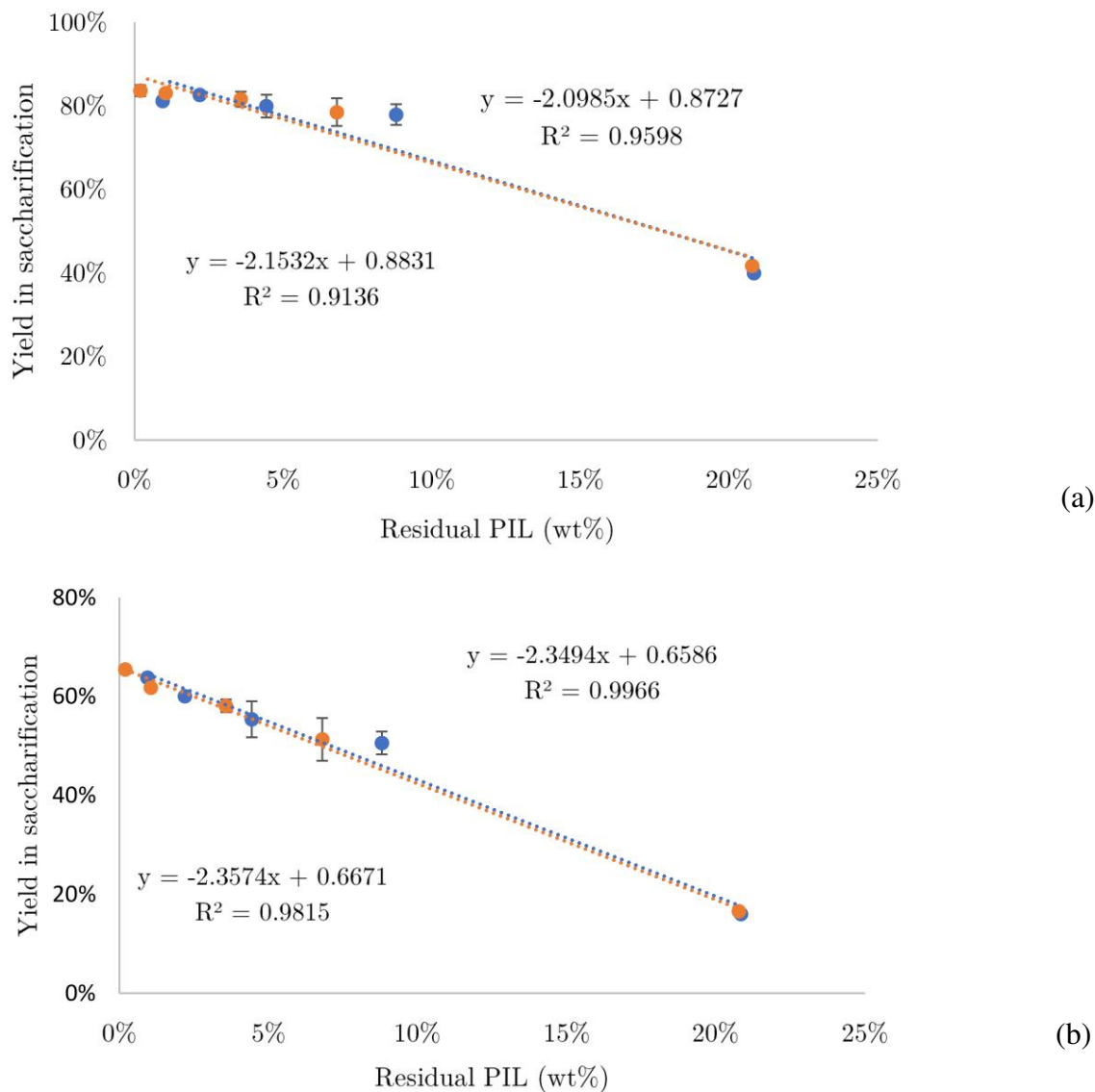
Fig. 6.4 — Linear regression between (a) glucan, (b) hemicellulose (xylose and arabinose) yields in saccharification (washing at 25°C in blue and 80°C in orange) and the amount of residual PIL in the medium.

NINOMIYA *et al.* (2015) also correlated the amount of residual [Ch][OAc] and [EMIM][OAc] with saccharification yields. However, they obtained much lower R^2 values (values were not calculated) which could be inferred by data points distribution in the graphs.

In a study by SUN *et al.*, (2017) on the effect of increasing loadings of [MEA][OAc] on saccharification yields of pretreated switchgrass, there was no yield drop between the fully washed pulp and the ones with 5, 10 and 20 wt% PIL. However, they employed a different methodology. After pretreatment, they added water to dilute the slurry to the desired PIL loading, that is to say, the solids loading of the saccharification was not 10 wt%. By diluting the medium, the mass transfer properties of the system change and the odds for enzyme inhibition by LMW lignin particles are lower. On the other side, the threshold between 10-15 wt% of PIL to ensure a reasonable enzyme activity also seemed to appear, a property that does not seem to depend on the solids loading of the system.

Cellulase inhibition by the presence of ILs have been subject of study in the literature (LATIFFAH and ZAHARI, 2019; TURNER *et al.*, 2003). Although the mechanism of enzyme denaturation is not fully understood, it is known that they become irreversibly denatured under high ionic strength media. A decrease of the enzyme activity may be due to a negatively induced conformational change within the enzyme upon refolding. The high ionic strength of the media forces protein aggregation during refolding (SUMMERS and FLOWERS II, 2000 apud TURNER *et al.*, 2003). These aggregates serve to "lock" proteins in inactive conformations and may be the culprit behind the drop of activity of the refolded cellulase in the [MEA][OAc] solutions (TURNER *et al.*, 2003). The development of IL biocompatible (and thermo-tolerant) cellulases (MADEIRA LAU *et al.*, 2004) is an interesting approach to overcome enzyme inhibition and may eventually allow enzyme recyclability, which would then ensure the economic feasibility of the process.

6.3.2. Interplay of PIL and alcoholic fermentation performance

Fermentation profiles of the hydrolysates obtained from the washing experiments were shown in Fig. 6.5. Washing temperature had a higher impact on the ethanol yields as can be noticed from 600% (Fig. 6.5 a and b), 800% (Fig. 6.5 c and d), and 1000% (Fig. 6.6 a and b). That's a different trend found with the saccharification yields, confirming that microorganisms are in fact more sensitive to the presence of harmful compounds.

Glucose depletion occurred between 72-96h for the 25°C wash samples, while it took between 48-72 h for the 80°C wash samples. Xylose intake started near glucose depletion around 48h and its depletion was reached with 96 h, showing the preference for hexose metabolization prior to pentose. There was no arabinose consumption (data not shown) by the yeast within the fermentation time, indicating the following preference order of sugar consumption for the yeast in a sugarcane hydrolysate: glucose > xylose > arabinose. RODRUSSAMEE, SATTAYAWAT and YAMADA, (2018) studied the intake profile of several monosaccharides — glucose, galactose, mannose, arabinose and xylose — and, amongst all sugar, arabinose showed the slowest intake rate.

It can also be noted a small decrease in acetic acid along the fermentation, especially for 600%-25°C (Fig. 6.5a), which started with nearly 4 g·L^{-1} of acetic acid and ended up with around 2 g·L^{-1}. Acetic acid is known to be a potent yeast inhibitor (FELIPE *et al.*, 1995; VAN ZYL, PRIOR and DU PREEZ, 1991). In its undissociated form, which is liposoluble, it can diffuse across the plasma membrane. In the cytosol, it dissociates due to the neutral intracellular pH, therefore decreasing the cytosolic pH. The cell then diverts its metabolism from growth and ethanol production in order to restore intracellular pH neutrality (PALMQVIST and HAHN HÄGERDAL, 2000).

The fact that the yeast assimilated acetic acid shows an interesting coping mechanism. SU; WILLIS; JEFFRIES (2015) studied the effect of aeration on growth, ethanol and polyol accumulation by *S. passalidarum* and found that there was acetic acid accumulation along the fermentation — a reverse trend found in the current study — and higher aeration rates increased such accumulation. One hypothesis is that the strain used in this study differs in the acetic acid metabolism from the one used by SU, WILLIS and JEFFRIES (2015).
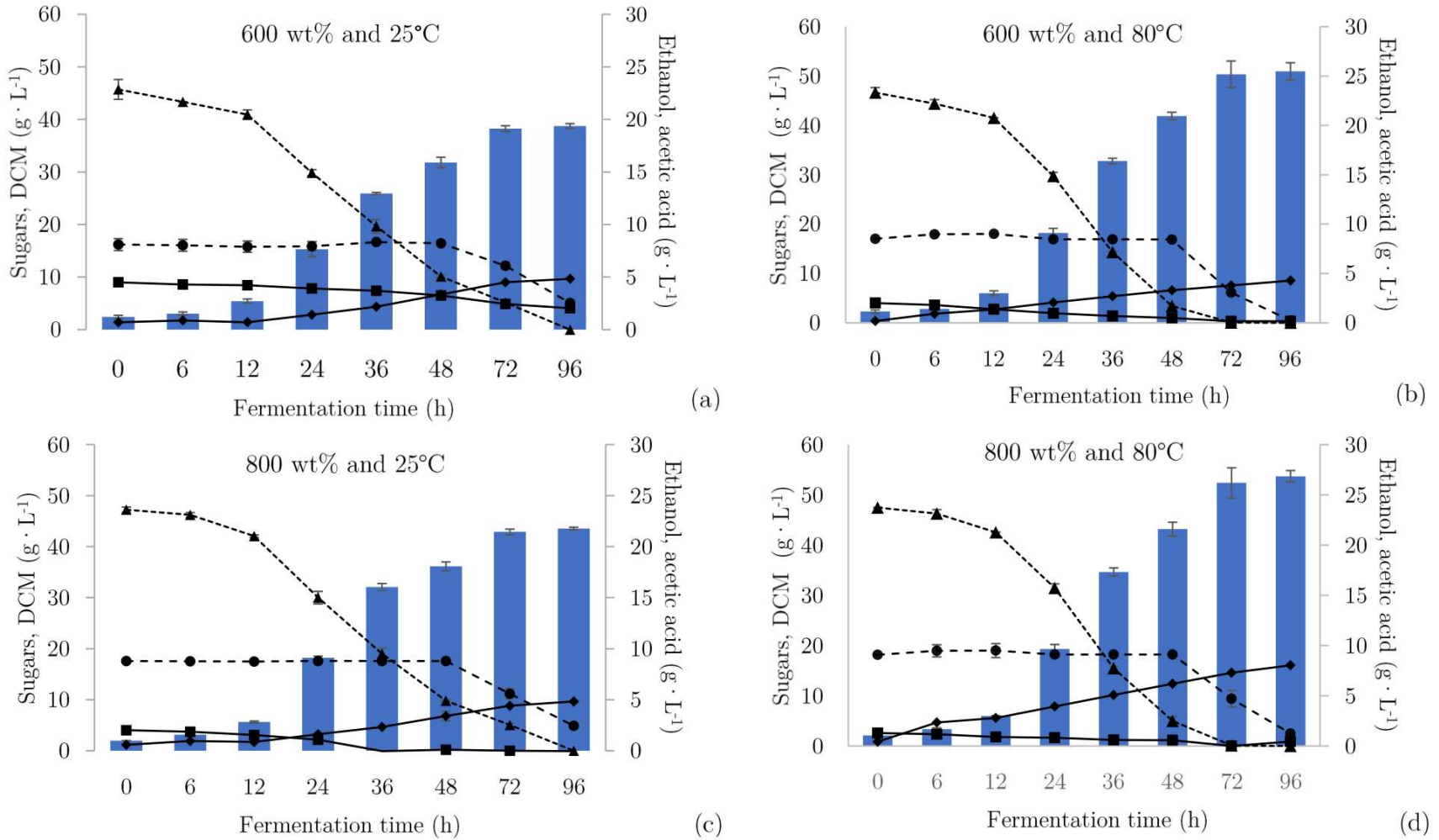
Fig. 6.5 - Fermentation profiles of the samples from the washing experiments. (a) 600 wt% at 25°C; (b) 600 wt% at 80°C; (a) 800 wt% at 25°C; (a) 800 wt% at 80°C. ▮ Ethanol, ---▲--- Glucose, --●-- Xylose, —♦— DCM, —■— acetic acid.
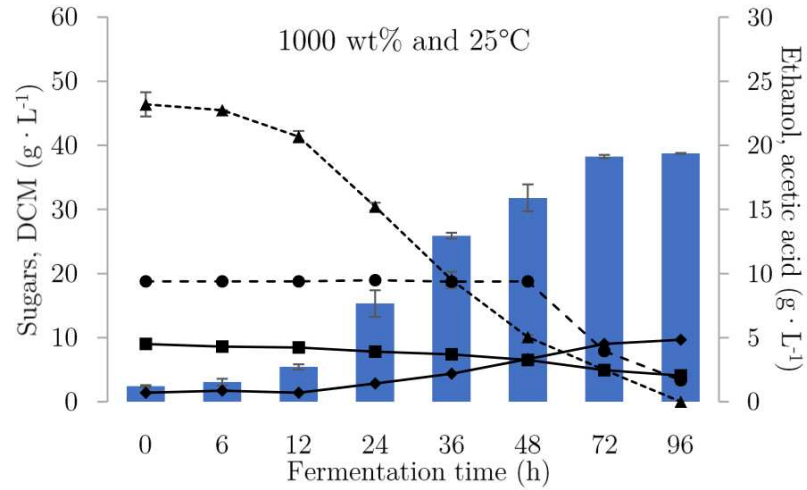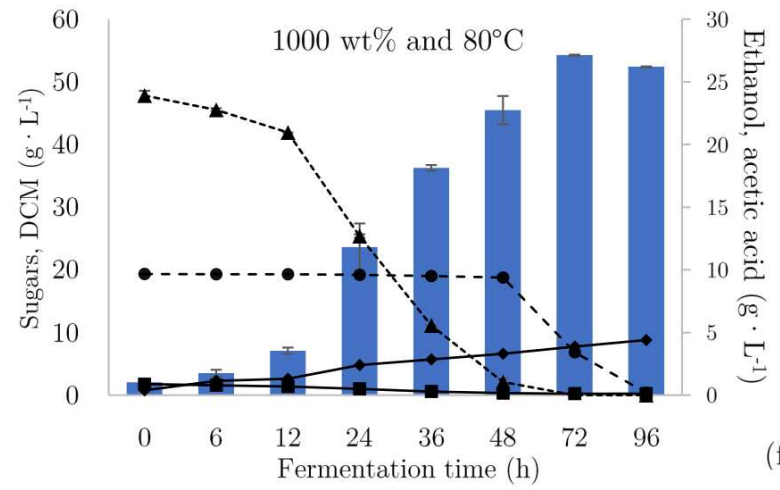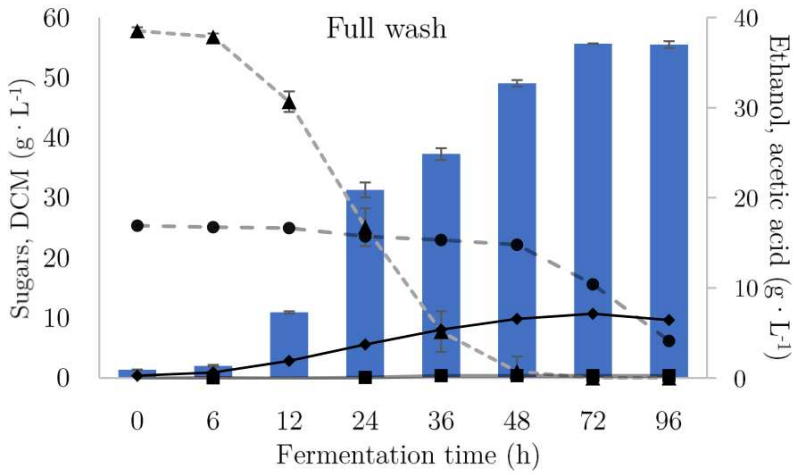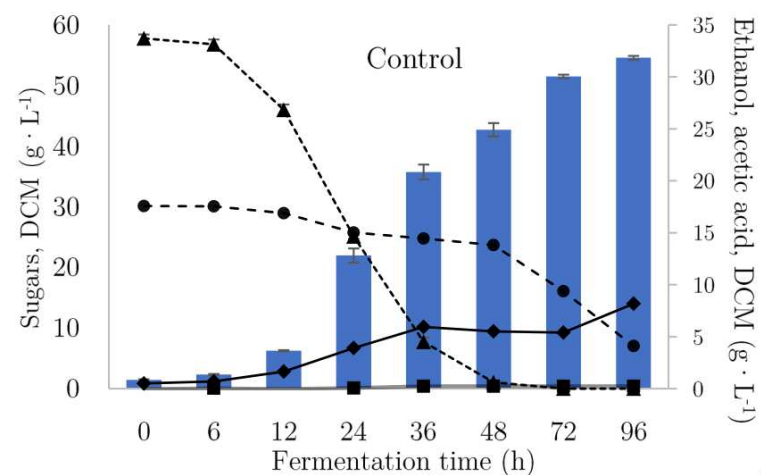
Fig. 6.6 - Fermentation profiles of the samples from the washing experiments. (a) 1000 wt% at 25°C; b) 1000 wt% at 80°C; (c) Full wash; (d) Fermentation control. ▬ Ethanol, ---▲--- Glucose, --●-- Xylose, ——◆—— DCM, ——■—— acetic acid.

Wash water contents of 200 and 400 wt% did not ferment due to the very high acetic acid concentrations from the residual PIL, which varied from around 20 $g \cdot L^{-1}$ for the 400 wt% and 40 $g \cdot L^{-1}$ for the 200 wt%. SOARES (2018) studied the effect of inhibitory compounds such as acetic acid, 5-HMF, furfural and vanillin, on the fermentation performance of *S. passalidarum*, and found an upper threshold of 2.5 $g \cdot L^{-1}$ of acetic acid to ensure satisfactory yeast performance, which might seem the case for this work, in which acetic acid assimilation from 600%-25°C sample decreased its concentration below the threshold.

The fermentation parameters were shown in Table 6.2. Ethanol production when the wash was at 80°C was superior and ranged between 25-27 $g \cdot L^{-1}$. The $Y_{P/S}$ values for the 25°C wash — ranging between 0.41-0.43 — however, were not substantially different from the 80°C wash — ranging between 0.42-0.43, which consequently reflected on similar theoretical yield ranges, 80-84% and 82-85%, respectively, which could drive us to think there was no overall difference between fermentation yields for both temperatures. However, by analyzing the productivity values, we can notice there were significant differences between the two temperatures, for the 25°C wash, they varied between 0.25 and 0.31 $g \cdot L^{-1} \cdot h^{-1}$, and for the 80°C wash, they varied between 0.33 and 0.36 $g \cdot L^{-1} \cdot h^{-1}$. The higher productivity obtained when washing was performed at the highest temperature was mainly due to the faster glucose consumption. NINOMIYA *et al.* (2015) obtained 60% and 24% of the theoretical ethanol yield for the fermentation of bagasse hydrolysates from [Ch][OAc] and [EMIM][OAc] pretreatment by using approximatelly 1,600 wt% of wash water. In the present work, higher yields (84%) were obtained by using half the amount of wash water with both temperatures.

Y_{XS} values for the 25°C wash samples — 0.19-0.16 $g \cdot L^{-1} \cdot h^{-1}$ — were higher than the 80°C wash —0.14-0.13 $g \cdot L^{-1} \cdot h^{-1}$, which may be related to the high acetic acid concentration in the lowest temperature. The yeast responds to the presence of inhibitors by trying to assimilate/metabolize them; by growing, chances to accomplish that are higher. Polyol accumulation in 72 h (Appendix IV) was proportional to the ethanol yields; 80°C wash samples had higher polyol levels — glycerol, 0.18-0.34 $g \cdot L^{-1}$ and xylitol 0.13-0.17 $g \cdot L^{-1}$ from 600 to 1000 wt% wash, respectively. Glycerol content was higher for the control, 0.41 $g \cdot L^{-1}$ against 0.32 $g \cdot L^{-1}$ for the full wash sample. On the other hand, the full wash sample had the highest xylitol content, 0.55 $g \cdot L^{-1}$, which was the same as the control. Xylitol accumulation, however, was lower than

NAKANISHI's *et al.* (2017) in a fed-batch fermentation of sugarcane bagasse hydrolysate from with alkaline pretreatment (NaOH with anthraquinone as additive); xylitol levels varied from 2.20 $g \cdot L^{-1}$ in the first batch to 0.67 $g \cdot L^{-1}$ in the fourth one. SU, WILLIS and JEFFRIES (2015) found even higher xylitol contents — 2.9-3.8 $g \cdot L^{-1}$ — on the fermentation of a synthetic media with 12 wt% xylose and 3 wt% glucose. Xylitol is the first intermediary in the xylose metabolism by the yeast, its accumulation implies the lack of NAD^+ or $NAD(P)^+$, two cofactors that are essential for xylitol oxidation into xylulose by xylitol dehydrogenase (AGBOGBO and COWARD KELLY, 2008 *apud* NAKANISHI *et al.*, 2017). The absence of NAD^+ or $NADP^+$ indicate a lack of oxidizing agents, i.e., molecular oxygen, with the microaerophily being the main cause behind it.

The full wash sample had a better overall performance than the samples washed with limited amount of water, showing a higher ethanol titer, 30 $g \cdot L^{-1}$, productivity, 0.41 $g \cdot L^{-1} \cdot h^{-1}$, and $Y_{P/S}$, 0.44; such values were quite comparable to the fermentation control, 30 $g \cdot L^{-1}$, 0.50 and 0.45, respectively, showing that, once inhibitors are removed by fully washing the pulp, pretreatment with [MEA][OAc] generates a highly digestible and fermentable mixture. Despite quite satisfactory, fermentation results led us to think of strategies to increase sugar intake and ethanol productivity whilst dealing with the presence of acetic acid in the medium.

Increasing initial cell density is one simple but elegant strategy. SOARES (2018) employed increasing *S. spathaspora* cell densities — 5, 15 and 30 $g \cdot L^{-1}$ — in a fermentation of a xylose/glucose synthetic media spiked with acetic acid (2.07 $g \cdot L^{-1}$), furfural (0.15 $g \cdot L^{-1}$), 5-HMF (0.06 $g \cdot L^{-1}$) and vanillin (0.42 $g \cdot L^{-1}$). She found that overall ethanol yields and productivity increased from 55.5% to 72.4% and 0.13 to 0.70 $g \cdot L^{-1} \cdot h^{-1}$. In the light of such facts, we decided to test higher initial cell densities for the conditions, 600 w% at 80°C, full wash plus the fermentation control (Fig. 6.7a-c); initial cell concentrations were 8.75 ± 0.64, 10.8 ± 0.42 and 10.0 ± 0.35 g/L. A much faster glucose intake can be observed with its depletion between 36 and 48 h. However, xylose consumption followed a different trend found with lower initial cell density; xylose consumption started from the beginning of fermentation but remained at a slow rate indicated by the flatter slopes. The slopes indicate xylose depletion might occur within 72 h of fermentation, which is in accordance with SOARES (2018), which had nearly 15 $g \cdot L^{-1}$ of initial cell concentration and whose xylose depletion also occurred in 72 h.

Table 6.2 - Fermentation parameters for the washing experiments with *S. passalidarum*.

Temperature	Sample	Initial Sugars $g \cdot L^{-1}$	Ethanol $g \cdot L^{-1}$	$Y_{P/S}$[a]	Yield %	Q_P $g_{EtOH} \cdot L^{-1} \cdot h^{-1}$	$Y_{X/S}$ $g_{DCM} \cdot g_{substrate}^{-1}$
	600	61.9 ± 3.03	19.1 ± 0.27	0.408 ± 0.017	79.9 ± 3.78	0.25 ± 0.001	0.19 ± 0.010
25°C	800	64.8 ± 0.62	21.4 ± 0.27	0.428 ± 0.000	83.9 ± 0.07	0.29 ± 0.088	0.17 ± 0.002
	1000	65.2 ± 0.29	23.3 ± 0.13	0.430 ± 0.006	84.4 ± 0.37	0.31 ± 0.137	0.16 ± 0.005
	600	63.7 ± 1.42	25.2 ± 1.35	0.418 ± 0.003	82.0 ± 4.33	0.33 ± 0.016	0.14 ± 0.015
80°C	800	65.6 ± 0.02	26.2 ± 1.51	0.429 ± 0.013	84.1 ± 2.60	0.35 ± 0.030	0.14 ± 0.031
	1000	67.1 ± 0.64	27.1 ± 0.05	0.433 ± 0.005	84.9 ± 0.37	0.36 ± 0.099	0.13 ± 0.014
	Full wash	81.4 ± 3.03	30.0 ± 0.03	0.445 ± 0.009	87.2 ± 1.69	0.41 ± 0.000	0.09 ± 0.001
	Control	87.9 ± 3.03	37.1 ± 0.17	0.448 ± 0.008	87.8 ± 1.50	0.50 ± 0.001	0.09 ± 0.021

Ethanol production was also faster than our previous experiment and we considered 48h of fermentation time for parameter calculations (Table 6.3), once the ethanol increment from 48 to 54h was small. The condition 600 wt%/ 80°C (Fig. 6.7b) also showed acid consumption along the fermentation. Acetic acid concentration decreased from 3.8 to 2.7 g·L^{-1}, not as substantial as the previous drop found with 600 wt%/ 25°C (Fig. 6.7a). But more interestingly, acetic acid accumulation could be seen for the fermentation control, despite the y-axis range did not allow us to verify this, acetic acid concentration reached up to 0.40 g·L^{-1} within 54 h of fermentation.
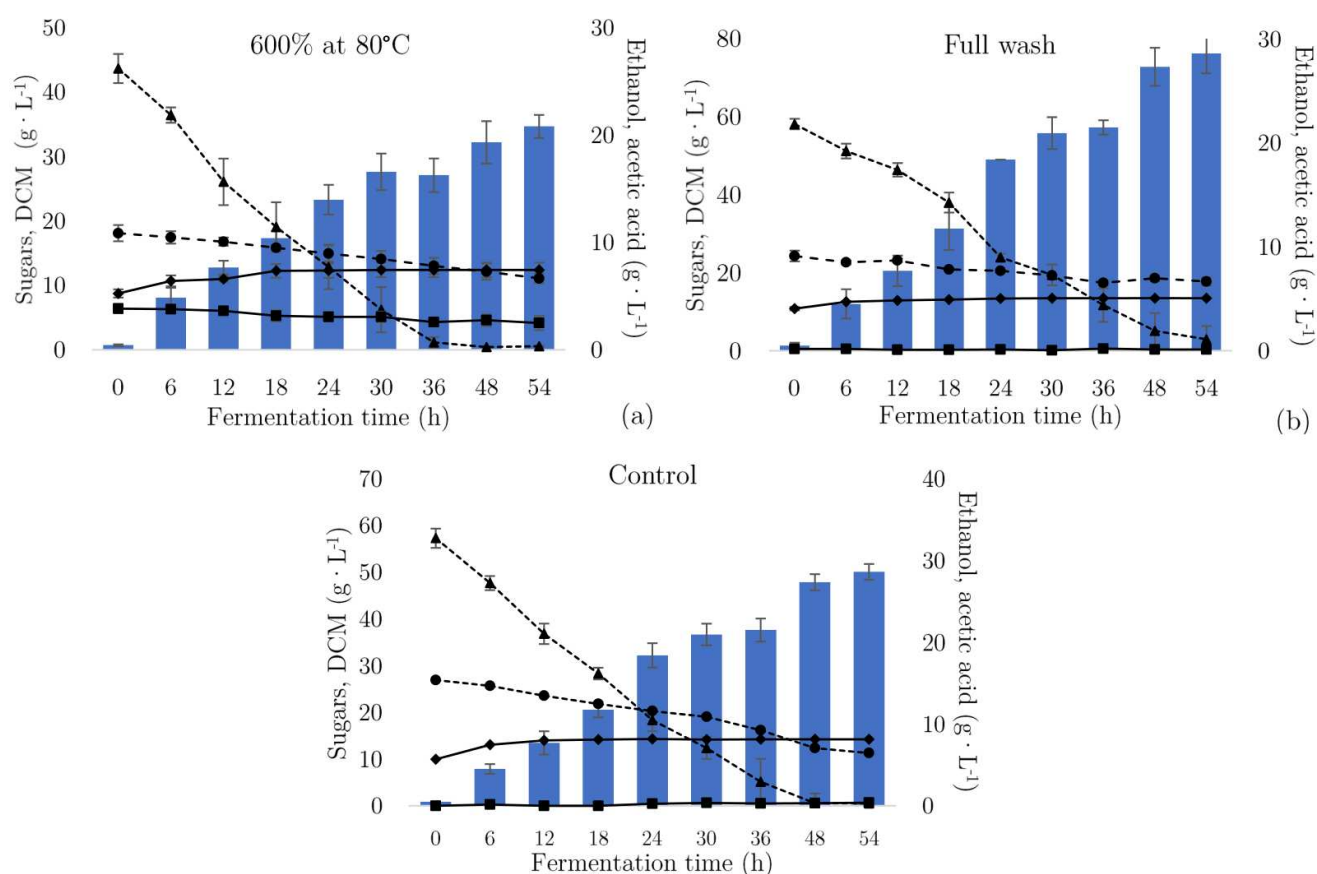
Fig. 6.7 — Fermentation profiles of the samples from the washing experiments with high initial cell density. (1) 600 wt% at 80°C (b) Full wash; (b) Fermentation control. ■ Ethanol, ---▲--- Glucose, - -●- - Xylose, ——◆—— DCM, ——■—— acetic acid.

Following the same trend, xylitol accumulation (Appendix IV) was also higher with 0.24, 0.57 and 0.80 g·L^{-1} for 600 wt%/80°C, full wash and fermentation control, respectively,

which is a bit contrasting since acetic acid accumulation is linked to limited $NAD(P)H+H^+$ concentration (through partial oxidation of acetaldehyde) in the medium and, as mentioned, xylitol accumulation is linked to the limited NADH or $NAD(P)^+$. For the 600 wt%/ 80°C the $Y_{P/S}$ practically remained the same, 0.41 against 0.42 from the previous experiment. However, full wash and the fermentation control had higher $Y_{P/S}$ values, showing higher cell densities favored inhibitor-free hydrolysates.

Table 6.3 — Fermentation parameters for the fermentation with higher initial cell density *with S. passalidarum.*

	Initial Sugars	Ethanol	$Y_{P/S}$	Yield	Q_P	$Y_{X/S}$
	$g \cdot L^{-1}$	$g \cdot L^{-1}$		%	$g_{EtOH} \cdot L^{-1} \cdot h^{-1}$	$g_{DCM} \cdot g_{substrate}^{-1}$
600 wt%; 80°C	61.8 ± 3.52	20.8 ± 1.98	0.406 ± 0.021	79.7 ± 4.19	0.39 ± 0.039	0.18 ± 0.013
Full wash	82.5 ± 0.04	28.6 ± 1.83	0.455 ± 0.015	89.3 ± 3.01	0.56 ± 0.032	0.10 ± 0.009
Control	84.2 ± 2.54	33.8 ± 1.00	0.457 ± 0.020	89.5 ± 3.83	0.69 ± 0.022	0.13 ± 0.001

Although initial cell densities were higher, there was still a considerable cell growth along the fermentation, as noticed from the higher $Y_{X/S}$ values, especially for the 600 wt%/ 80°C sample, which shows a need for aeration rate optimization. According to SU, WILLIS and JEFFRIES (2015), a liquid volume of 50 mL with an agitation rate of 110 RPM in a 125 mL erlenmeyer flask corresponds to 4.27 $mmolO_2 \cdot L^{-1} \cdot h^{-1}$, lower aeration rates would in theory increase the medium's microaerophile and favour ethanol production over cell growth.

Some fermentation studies with *S. passalidarum* and *S. cerevisiae* are summarized in Table 6.4. It can be noticed different initial xylose and glucose concentrations were used in each work, and most works were still done in flasks except for NAKANISHI's *et al.*, (2017), who employed a fed-batch system in a bioreactor and were able to obtain a high ethanol titer, 58 $g \cdot L^{-1}$, and BONAN (2018), who used a batch system. It is noteworthy mentioning that, amongst all works, we were able to obtain the highest $Y_{P/S}$ value, 0.46, with the full wash sample without a previous optimization of fermentation parameters, i.e. the yeast was able to efficiently consume monosaccharides and produce ethanol.

Table 6.4 — Comparison amongst different studies with *S. passalidarum* and *S. cerevisiae*. (Adapted from NAKANISHI *et al.*, 2017 and SU;,WILLIS and JEFFRIES, 2015).

Type[a]	Xylose (g·L^{-1})	Glucose (g·L^{-1})	Ethanol(g·L^{-1})	$Y_{P/S}$	Q_P (g$_{EtOH}$·L^{-1}.h^{-1})	Reference
F	24.3	58.2	28.6	0.46	0.56	This study[b,c]
Br +FB	14.9	42.9	58.3	0.32	0.65	NAKANISHI *et al.*, (2017)[c]
F	5.6	13	3.92	0.36	0.08	NINOMIYA *et al.* (2015)[d]
F	7	27	15	0.43	0.62	NINOMIYA *et al.*, (2018)[e]
F	65	35	36	0.37	0.60	LONG *et al.*, (2012)[c]
F	32	30	25	0.41	1.04	HOU, (2012)[f]
F	120	0	16	0.32	0.34	SOUZA, (2014)[g]
F	140	0	27-40	0.43	0.72	SU, WILLIS and JEFFRIES, (2015)[c]
Br	27	67	30	0.32	0.58	BONAN, (2018)[c]
F	27	67	32	0.35	0.58	SOARES, (2018)[c]

a. F – Flask, FB – fed batch, Br – bioreactor.

b. Obtained with the full wash of the pulp with higher initial cell density, 11 g·L^{-1}.

c. *S. passalidarum* Y-27907.

d. *S. cerevisiae* MT8-1.

e. *S. cerevisiae* YPH499XU.

f. *S. passalidarum* MYA-4345.

g. *S. passalidarum* HM 14.2.

However, the productivity obtained in this study still falls behind most studies, confirming the need for a more in-depth look into aeration rates, which is related to the headspace volume of the flask and the agitation rate. NINOMIYA *et al.*, (2018) obtained a considerable productivity on the fermentation of a bagasse hydrolysate from [Ch][OAc] pretreatment and by using a genetically modified *S. cerevisiae* strain able to ferment pentoses. Negative *Crabtree* yeasts divert their metabolic pathway in face of oxygen availability, favoring cell growth in the presence of higher dissolved oxygen content in the medium, consequently affecting ethanol production (DU PREEZ, 1994; AGBOGBO and COWARD KELLY, 2008; *apud* BONAN, 2018). For this group of microorganisms, ethanol production is favored under OD limiting conditions.

A fermentation test with *S. cerevisiae* was also performed (Fig. 6.8a-b). It is evident how such yeast — through evolutionary engineering along centuries — is superior in terms of glucose consumption and ethanol production. Glucose depletion occurred within 12-18h for both full wash and fermentation control, ethanol production also peaked in 18 h and slowly decreased, indicating consumption by the yeast. Once this strain was not genetically engineered for xylose metabolization, there was no xylose consumption. Additionally, no acetic acid accumulation was detected for both samples. NINOMIYA *et al.*, (2018) by using *S. cerevisiae* YPH499XU able to metabolize xylose, were able to deplete both glucose and xylose in 24 h; this strain co-expresses xylitol dehydrogenase and xylose reductase from *P. stipitis.* However, they provided no further information about acetic acid or polyol accumulation.
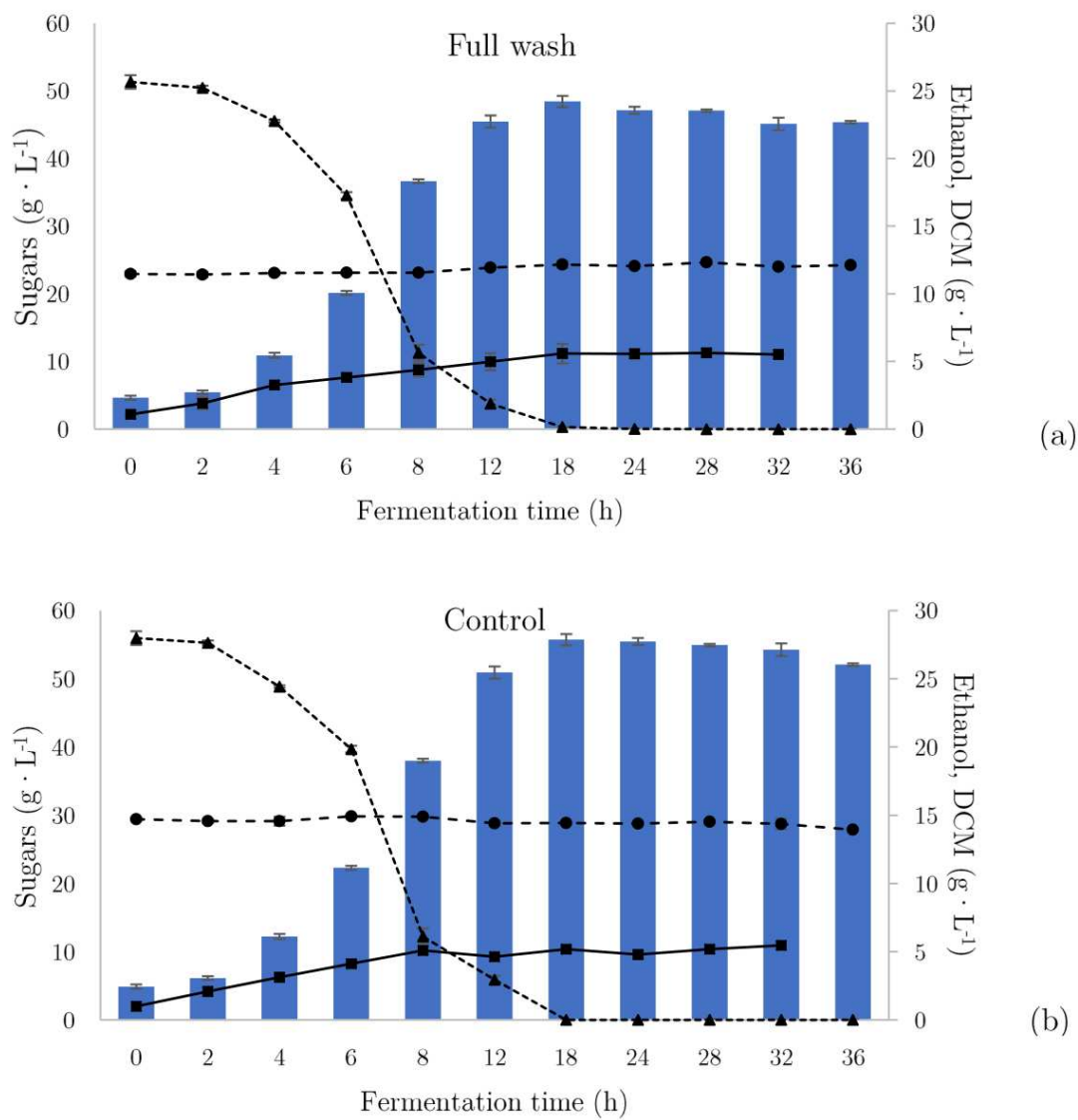
Fig. 6.8 — Fermentation profile of the samples from the washing experiments wish *S. cerevisiae* (a) Full wash; (b) Fermentation control. ▮ Ethanol, ---▲--- Glucose, --●-- Xylose, ——◆—— DCM, ——■—— acetic acid.

Fermentation parameters for the fermentation with *S. cerevisiae* are shown in Table 6.5. Ethanol titer and $Y_{P/S}$ values were quite comparable to the fermentation control, 24.2 $g \cdot L^{-1}$ and 0.438 against 27.9 $g \cdot L^{-1}$ and 0.442, which shows the yeast had a favorable fermentation media for glucose metabolization. Fermentation control, however, had a higher productivity, 1.41 $g \cdot L^{-1} \cdot h^{-1}$ against 1.22 $g \cdot L^{-1} \cdot h^{-1}$. $Y_{X/S}$ values for both control and full wash were 0.055, which were comparable to the values found by ANDRADE *et al.*, (2013), which found Yx/s =0.046, on the fermentation of a bagasse hydrolysate obtained with alkaline peroxide pretreatment and mixed with molasses. These authors also obtained an $Y_{P/S}$ value of 0.46. NINOMIYA *et al.*, (2018) obtained an $Y_{P/S}$ value of 0.43, which was quite high considering nearly 25 wt% of residual [Ch][OAc] was still present in the pulp as they did not wash the pulps after pretreatment once they employed a very low solids loading, 2 wt.

Table 6.5 — Fermentation parameters for the fermentation with *S. cerevisiae*.

	Initial Sugars	Ethanol	$Y_{P/S}$	Yield	Q_P	$Y_{X/S}$
	$g \cdot L^{-1}$	$g \cdot L^{-1}$		%	$g_{EtOH} \cdot L^{-1} \cdot h^{-1}$	$g_{DCM} \cdot g_{substrate}^{-1}$
Full wash	74.3 ± 1.34	24.2 ± 0.42	0.438 ± 0.011	85.8 ± 2.15	1.22 ± 0.031	0.055 ± 0.006
Control	85.4 ± 0.62	27.9 ± 0.04	0.442 ± 0.014	86.7 ± 0.76	1.41 ± 0.001	0.055 ± 0.003

SUN *et al.*, (2017), on a simultaneous saccharification and fermentation (SSF) of a switchgrass hydrolysate obtained with [MEA][OAc] pretreatment, obtained $Y_{P/S}$ value of 0.36, a quite lower value even though the hydrolysates presented 5 wt% of PIL. They also employed very low enzyme and yeast loadings, 2 wt% and 0.1 wt%, which ultimately impacts on equally low productivities. Additionally, an SSF strategy with such diluted media would require a considerable energetic input for water evaporation to yield feasible ethanol titers.

Despite presenting much higher productivity, fermentation with *S. cerevisiae* did not consume any xylose. As stated in the scope of this work in Chapter 1, process design for [MEA][OAc] envisioned a platform for both C5 and C6 utilization. Therefore, a genetically engineered strain of *S. cerevisiae* could be used, or a mixed culture with a C5-metabolizing yeast.

6.3.3. Mass balances for overall E2G production

Mass balances for the whole E2G process with [MEA][OAc] were depicted in Fig. 6.9 and 6.10 for 1,000 wt% wash and full wash of the pulp. For the 1,000 wt% wash, nearly 228 L of ethanol·ton^{-1} bagasse were obtained; while for the full wash approximately 300 L of ethanol·ton^{-1} bagasse were achieved, a difference of 72 L·ton^{-1} bagasse. However, water wash consumption was much higher for the full wash sample, 625 ton of wash water·ton^{-1} pulp against only 66.6 ton of wash water·ton^{-1} pulp. It is important to notice the PIL will be diluted with the wash water and eventually recovered by water evaporation, so the energetic demand for PIL recovery with the full wash sample is definitely higher. An in-depth techno-economic analysis is necessary in order to quantitatively estimate important E2G parameters such as the minimum ethanol selling price — MESP.

1000 wt% and 80°C wash water

Bagasse (1000 Kg DM)
419.5 Kg Glucan
254.3 Kg Hemicelluloses
237.9 Kg Lignin
29.5 Kg Extractives
21.3 g Ashes
34.4 Kg Acetyl

1) Pretreatment with [MEA][OAc]:
15 wt% solids, 20 wt% water content, 150 °C,
0.5:1 ABR, 2h

2) Water (anti-solvent) addition:
66.6 ton wash water/ton pulp in dry basis
3) Solid-liquid separation

Pulp (732.8 Kg DM)
419.1 Kg Glucan
250.5 Kg Hemicelluloses
51.2　Kg Lignin
5.3　　Kg Ashes
6.6　　Kg Others (acetyl,
extractives, etc)

Liquid stream (267.2 Kg DM)
0.4　　Kg Glucan
3.8　　Kg Hemicelluloses
186.7 Kg Lignin
76.3　Kg Others (acetyl,
extractives, etc)

Centrifugation

Precipitate
34.0 Kg recovered lignin

Saccharification:
10 wt% solids, Cellic Ctec 2:
15 FPU · $g_{biomass}^{-1}$, 72 h

Hydrolysis residue
137.3 Kg glucan
120.1 Kg Hemicelluloses
5.3 Kg Ashes

Hydrolysate
313.1 Kg glucose
133.0 Kg xylose
11.9 Kg arabinose

Fermentation:
S. Passalidarum NRRL Y27907,
10 wt% solids, 72 h

Wine
193.2 Kg etanol (228 L)

Fig. 6.9 — Mass balance for E2G production from [MEA][OAc] pretreatment of sugarcane bagasse with 1000 wt% wash water.

Full wash

Bagasse (1000 Kg DM)
419.5 Kg Glucan
254.3 Kg Hemicelluloses
237.9 Kg Lignin
29.5 Kg Extractives
21.3 g Ashes
34.4 Kg Acetyl

1) Pretreatment with [MEA][OAc]:
15 wt% solids, 20 wt% water content, 150 °C, 0.5:1 ABR, 2h

2) Water (anti-solvent) addition:
625 ton wash water/ton pulp in dry basis
3) Solid-liquid separation

Pulp (732.8 Kg DM)
419.1 Kg Glucan
250.5 Kg Hemicelluloses
51.2   Kg Lignin
5.3   Kg Ashes
6.6   Kg Others (acetyl, extractives, etc)

Liquid stream (267.2 Kg DM)
0.4   Kg Glucan
3.8   Kg Hemicelluloses
186.7 Kg Lignin
76.3   Kg Others (acetyl, extractives, etc)

Centrifugation

Precipitate
34.0 Kg recovered lignin

Saccharification:
10 wt% solids, Cellic Ctec 2:
15 FPU · $g_{biomass}^{-1}$, 72 h

Hydrolysis residue
73.7 Kg glucan
75.1 Kg Hemicelluloses
5.3 Kg Ashes

Hydrolysate
383.8 Kg glucose
178.2 Kg xylose
16.7 Kg arabinose

Fermentation:
S. Passalidarum NRRL Y27907,
10 wt% solids, 72 h

Wine
249.9 Kg etanol (300 L)

Fig. 6.10 — Mass balance for E2G production from [MEA][OAc] pretreatment of sugarcane bagasse with full wash.

A comparison amongst different pretreatment types and their overall ethanol yield is shown in Table 6.6. We were able to achieve the highest ethanol yields for almost both conditions, full wash of the pulp and 1000 wt%/80 °C with 300 and 228 L ton^{-1} bagasse. Only RABELO's *et al.* (2014) and NINOMIYA's *et al.* (2018) studies figure in between the two yields obtained in this work with 237L and 266 L of ethanol ton^{-1} bagasse. However, it is worth mentioning NINOMIYA's pretreatment time is longer than ours, 21 h compared to 2 h, and they also employ very low solids loading 2 wt%, which require great amounts of water for dilution. Also, they don't wash the pulps after pretreatment, which end up in PIL losses along cycles.

As mentioned in Chapter 4, we aimed to ensure pretreatment parameters would be feasible for a future scaleup. When comparing with other [MEA][OAc] pretreatments, a lower ABR and higher solids loading during pretreatment increased overall ethanol yields. Our lower ethanol yield with 1000 wt%/80°C was still superior to ROCHA's *et al.*, (2017) with similar pretreatment conditions, which estimated an ethanol yield of 95% of glucose and 50% of xylose.

SUN *et al.*, (2017) obtained nearly 148.2 of ethanol·ton^{-1} switchgrass with an SSF strategy and pretreatment with [MEA][OAc]. As already mentioned, they employed very low enzyme and yeast loadings which ultimately decreased overall ethanol productivity. Nevertheless, by analyzing Table 6.6 it is clear the superiority of using PILs when comparing to other conventional pretreatments such as alkaline, hydrothermal (NAKANISHI *et al.*, 2017) and dilute acid (SRITRAKUL, NITISINPRASERT and KEAWSOMPONG, 2017), even better than RABELO's *et al.*, (2014) yield, whose alkaline hydrogen peroxide pretreatment stands out against other pretreatments.

Table 6.6 — Comparison amongst different E2G pretreatment processes in terms of overall ethanol yield.

Pretreatment type	Conditions	Overall ethanol yield	Reference
PIL — [MEA][OAc]	150°C, 2h, 15 wt% solids, 20 wt% H_2O, 0.5:1 ABR	300.0 L·ton^{-1} bagasse	**This study[a]**
PIL — [MEA][OAc]	150°C, 2h, 15 wt% solids, 20 wt% H_2O, 0.5:1 ABR	228.0 L·ton^{-1} bagasse	**This study[b]**
PIL — [MEA][OAc]	150°C, 2h, 10 wt% solids, 20 wt% H_2O, 1:1 ABR	218.0 L·ton^{-1} bagasse	ROCHA *et al.* (2017)
PIL — [MEA][OAc]	160°C, 0.5 h, 10 wt% solids, 1:1 ABR	148.2 L·ton^{-1} switchgrass	SUN *et al.* (2017)
PIL — [Ch][OAc]	110°C, 21 h, 2 wt% solids, 1:1 ABR	266 L·ton^{-1} bagasse	NINOMIYA *et al.* (2018)
Sodium hydroxide-anthraquinone	130°C, 0.5 h, 10 wt% solids, 1.5 wt/v% NaOH	224.8 L·ton^{-1} bagasse	NAKANISHI *et al.* (2017)
Hydrothermal	190°C, 10 min, 9 wt% solids	222.7 L·ton^{-1} bagasse	NAKANISHI *et al.* (2017)
Alkaline H_2O_2	25°C, 1h, 4 wt% solids, 7.4% v/v H_2O_2	237.5 L·ton^{-1} bagasse	RABELO *et al.* (2014)
Dilute sulfuric acid	120°C, 0.5 h, 10 wt/v% solids, 1% w/w H_2SO_4	84.1 L·ton^{-1} bagasse	SRITRAKUL *et al.* (2017)

a. Full wash of the pulp after pretreatment.
b. 1000 wt% wash water at 80 °C after pretreatment.

6.4. Conclusions

A quantitative evaluation of water wash consumption in the pretreatment with [MEA][OAc] has shown that water contents between 600-1,000 wt% (for both temperatures, 25 and 80°C) decreased overall enzyme performance in saccharification compared to the full wash sample with up to 83.6% and 76.7% of glucose and xylose yields with the 1000 wt%/80 °C sample against 97.9 and 84.3% for the full wash. However, despite the full wash still presenting superior ethanol yield, 87.2%, the best water wash condition, 1000 wt%/80 °C, had a comparable ethanol yield of 84.9%. Fermentation of the full wash sample with *S. cerevisiae* showed higher ethanol productivity than *S. passalidarum*, nonetheless, no xylose metabolization occurred, which ultimately implies pentose sub utilization in the overall process. Mass balance calculations confirmed that optimized [MEA][OAc] pretreatment conditions provided the highest ethanol yield per ton of biomass amongst several types of pretreatments, including [MEA][OAc], for both 1000 wt%/80°C and full wash conditions. A techno-economic analysis, however, is necessary in order to better understand the balance between water consumption, ethanol yield and the energetic requirements for PIL recovery.

General conclusions and suggestions for future works

Amongst the PILs employed in the screening, [MEA][OAc] has shown great potential for biomass deconstruction. By means of an in-depth parameters optimization, pretreatment with [MEA][OAc] has proven to be selective towards lignin solubilization and carbohydrate preservation. Water has shown to be the best anti-solvent which facilitates the feasibility of the process. However, investigation of the ABR of [MEA][OAc] has shown the PIL degrades along the cycles into an acetamide. By using a mixture with 0.5 ABR, we were able to suppress the amide formation within 3 cycles of pretreatment and obtain high yields in saccharification. Fermentation of the hydrolysate obtained with the 0.5 ABR mixture with a pentose metabolizing yeast, *S. passalidarum*, has shown its high fermentability with nearly 87% of the theorical ethanol yield with the full wash sample. Productivity values, however, still require improvement, which can be obtained by using different fermentation strategies, such as fed-batch mode and cell recycle. Overall mass balances showed that nearly 245 and 317 L of ethanol ton^{-1} bagasse can be obtained by using 67 and 625 ton of wash water per ton of pulp respectively, showing that a compromise between water usage and ethanol yield need to be achieved. As suggestions for future works, we may cite:

1) A techno-economic assessment of the impact of ABR in [MEA][OAc] composition and its performance on saccharification.

2) A techno-economic assessment of the impact of wash water on overall ethanol production.

3) Fermentation of the hydrolysate from [MEA][OAc] pretreatment with a genetically modified *S. cerevisiae* strain.

4) Design new ammonium-based PILs whose structure would not allow its degradation along pretreatment cycles.

5) By means of simulations and by using model lignin-carbohydrate compounds, trying to establish the mechanism of action of the PIL.

References

ABDUL, P. M. et al. Effects of changes in chemical and structural characteristic of ammonia fibre expansion (AFEX) pretreated oil palm empty fruit bunch fibre on enzymatic saccharification and fermentability for biohydrogen. **Bioresource Technology**, v. 211, p. 200–208, 2016.

ABE, M.; FUKAYA, Y.; OHNO, H. Fast and facile dissolution of cellulose with tetrabutylphosphonium hydroxide containing 40 wt% water. **Chem. Commun.**, v. 48, n. 12, p. 1808–1810, 2012.

ACHINIVU, E. C. et al. Lignin extraction from biomass with protic ionic liquids. **Green Chemistry**, v. 0, n. 0, p. 1–6, 2014.

ADNEY, B.; BAKER, J. Measurement of Cellulase Activities. **Laboratory Analytical Procedure (LAP)**, n. January, 2008.

AGBOGBO, F. K.; COWARD KELLY, G. Cellulosic ethanol production using the naturally occurring xylose-fermenting yeast, Pichia stipitis. **Biotechnology letters**, v. 30, n. 9, p. 1515–24, set. 2008.

ANDRADE, R. R. et al. Evaluation of the alcoholic fermentation kinetics of enzymatic hydrolysates from sugarcane bagasse (Saccharum officinarum L.). **Journal of Chemical Technology & Biotechnology**, v. 88, n. 6, p. 1049–1057, 2013.

ARGO, A. M. et al. Investigation of biochemical biorefinery sizing and environmental sustainability impacts for conventional bale system and advanced uniform biomass logistics designs. **Biofuels, Bioproducts and Biorefining**, v. 7, n. 3, p. 282–302, 2013.

ÁVILA, P. F.; FORTE, M. B. S.; GOLDBECK, R. Evaluation of the chemical composition of a mixture of sugarcane bagasse and straw after different pretreatments and their effects on commercial enzyme combinations for the production of fermentable sugars. **Biomass and Bioenergy**, v. 116, p. 180–188, 2018.

BAILEY, M. J.; BIELY, P.; POUTANEN, K. Interlaboratory testing of methods for assay of xylanase activity. **Journal of Biotechnology**, v. 23, p. 257–270, 1992.

BALS, B. et al. Evaluation of ammonia fibre expansion (AFEX) pretreatment for enzymatic hydrolysis of switchgrass harvested in different seasons and locations. **Biotechnology for biofuels**, v. 3, n. 1, p. 1, 2010.

BAÑULS-CISCAR, J. et al. Surface characterisation of pine wood by XPS. **Surface and**

Interface Analysis, v. 48, n. 7, p. 589–592, 2016.

BAÑULS-CISCAR, J.; ABEL, M.-L.; WATTS, J. F. Characterisation of cellulose and hardwood organosolv lignin reference materials by XPS. **Surface Science Spectra**, v. 23, n. 1, p. 1–8, 2016.

BIDLACK, J.; MALONE, M.; BENSON, R. Molecular structure and component integration of secondary cell wall in plants. **Proc. Okla. Acad. Sci.**, n. 72, p. 51–56, 1992.

BONAN, C. I. D. G. **Avaliação da produção de bioetanol sob diferentes condições de transferência de oxigênio para a levedura Spathaspora passalidarum NRRL Y-27907**. [s.l.] State University of Campinas, 2018.

BONOMI, A. **Termo de referência do "III Workshop Tecnológico sobre hidrólise" - Projeto de Pesquisa em Políticas Públicas**. Etanol. **Anais**...2006

BRADFORD, M. A rapid and sensitive method for the quantification of microgram quantities of protein utilizing the principles of protein-dye binding. **Analytical Biochemistry**, v. 72, n. 1–2, p. 248–254, 1976.

BRANDT, A. et al. Ionic liquid pretreatment of lignocellulosic biomass with ionic liquid-water mixtures. p. 2489–2499, 2011.

BRANDT, A. et al. Soaking of pine wood chips with ionic liquids for reduced energy input during grinding. **Green Chemistry**, v. 14, n. 4, p. 1079, 2012.

BRANDT, A. et al. Deconstruction of lignocellulosic biomass with ionic liquids. **Green Chemistry**, v. 15, n. 3, p. 550–583, 2013.

BRANDT, A. et al. Structural changes in lignins isolated using an acidic ionic liquid water mixture. **Green Chem.**, v. 17, n. 11, p. 5019–5034, 2015.

BRANDT, A. et al. An economically viable ionic liquid for the fractionation of lignocellulosic biomass. **Green Chemistry**, v. 19, n. 13, p. 3078–3102, 2017a.

BRANDT, A. et al. An economically viable ionic liquid for the pretreatment of lignocellulosic biomass. p. 1–18, 2017b.

BURRELL, G. L. et al. Preparation of protic ionic liquids with minimal water content and (15)N NMR study of proton transfer. **Physical chemistry chemical physics : PCCP**, v. 12, n. 7, p. 1571–7, 2010.

CHAMBON, C. L. et al. Pretreatment of South African sugarcane bagasse using a low-cost protic ionic liquid: a comparison of whole, depithed, fibrous and pith bagasse fractions. **Biotechnology for Biofuels**, v. 11, n. 1, p. 247, 2018.

CHANDEL, A. K. et al. Detoxification of lignocellulosic hydrolysates for improved bioethanol production. **Biofuel production-Recent …**, 2011.

CHEN, K. et al. Equilibrium in Protic Ionic Liquids: The Degree of Proton Transfer and Thermodynamic Properties. **The Journal of Physical Chemistry B**, v. 122, n. 1, p. 309–315, 2018.

CHIU, Y.-W.; WU, M. Assessing County-Level Water Footprints of Different Cellulosic-Biofuel Feedstock Pathways. **Environmental Science & Technology**, v. 46, n. 16, p. 9155–9162, 21 ago. 2012.

CHUM, H. L. et al. Pretreatment catalysis effects and the combined severity parameter. **Ind.Eng. Chem. Res.**, v. 29(2), n. 1, p. 156-- 162., 1990.

CRUZ, A. G. et al. Impact of high biomass loading on ionic liquid pretreatment Impact of high biomass loading on ionic liquid pretreatment. 2013.

DA COSTA LOPES, A. M. et al. Ionic liquids as a tool for lignocellulosic biomass fractionation. **Sustainable Chemical Processes**, v. 1, n. 1, p. 3, 2013.

DA COSTA SOUSA, L. et al. Isolation and characterization of new lignin streams derived from extractive-ammonia (EA) pretreatment. **Green Chemistry**, v. 18, n. 15, p. 4205–4215, 2016.

DA SILVA, A. S. et al. Major improvement in the rate and yield of enzymatic saccharification of sugarcane bagasse via pretreatment with the ionic liquid 1-ethyl-3-methylimidazolium acetate ([Emim][Ac]). **Bioresource Technology**, v. 102, n. 22, p. 10505–10509, 2011.

DE MENEZES, F. F. et al. Alkaline Pretreatment Severity Leads to Different Lignin Applications in Sugar Cane Biorefineries. **ACS Sustainable Chemistry and Engineering**, v. 5, n. 7, p. 5702–5712, 2017.

DEL RÍO, J. C. et al. Differences in the chemical structure of the lignins from sugarcane bagasse and straw. **Biomass and Bioenergy**, v. 81, p. 322–338, 2015.

DIEN, B. S.; A., C. M.; JEFFRIES, T. W. Bacteria engineered for fuel ethanol production current status. **Appl. Microbiol. Biotechnol.**, v. 63, p. 258–266, 2003.

DIMAROGONA, M.; TOPAKAS, E.; CHRISTAKOPOULOS, P. Cellulose degradation by

oxidative enzymes. **Computational and structural biotechnology journal**, v. 2, n. September, p. e201209015, 2012.

DOERING, C. **Poet's Emmetsburg plant could be at full output in 2016**, 2016. Disponível em: <http://www.desmoinesregister.com/story/money/business/2016/04/04/poets-emmetsburg-plant-could-full-output-2016/82434182/>

DU PREEZ, J. C. Process parameters and environmental factos affecting D-xylose fermentation by yeasts. **Enzyme Microb Technol**, v. 16, p. 944–956, 1994.

EARLE, M. J.; SEDDON, K. R. Ionic liquids. Green solvents for the future. **Pure and Applied Chemistry**, v. 72, n. 7, p. 1391–1398, 2000.

ECONOMIST, T. H. E. **The fuel of the future**, 2013. Disponível em: <economist.com/news/business/21575771-environmental-lunacy-europe-fuel-future>

ESPINOZA-ACOSTA, J. L. et al. Ionic liquids and organic solvents for recovering lignin from lignocellulosic biomass. **BioResources**, v. 9, n. 2, p. 3660–3687, 2014.

FAN, L. T.; LEE, Y. H.; GHARPURAY, M. M. The nature of lignocellulosics and their pretreatments for enzymatic hydrolysis. **Adv. Biochem. Eng.**, v. 23, p. 157–187, 1982.

FARIAS, D.; ANDRADE, R. R.; MAUGERI-FILHO, F. Kinetic Modeling of Ethanol Production by Scheffersomyces stipitis from Xylose. **Appl Biochem Biotechnol**, v. 172, p. 361, 2014.

FELIPE, M. G. et al. Effect of acetic acid on xylose fermentation to xylitol by Candida guilliermondii. **Journal of basic microbiology**, v. 35, n. 3, p. 171–177, 1995.

FENGEL, D.; WEGENER, G. **Wood chemistry, ultrastructure, reactions**. Berlin: [s.n.].

FRONING, H. R.; JONES, J. H. Corrosion of Mild Steel in Aqueous Monoethanolamine. **Industrial & Engineering Chemistry**, v. 50, n. 12, p. 1737–1738, 1 dez. 1958.

GAMMONS, R. J. Optimising the Pre-treatment Effects of Protic Ionic Liquids on Lignocellulosic Materials. n. September, 2014.

GARROTE, G.; DOMÍNGUEZ, H.; PARAJÓ, J. C. Hydrothermal processing of lignocellulosic materials. **Journal of Wood and Wood Products**, v. 57, p. 191–202, 1999.

GARROTE, G.; DOMÍNGUEZ, H.; PARAJÓ, J. C. Generation of xylose solutions from Eucalyptus globulus wood by autohydrolysis-posthydrolysis processes: Posthydrolysis kinetics.

Bioresource Technology, v. 79, n. 2, p. 155–164, 2001.

GEORGE, A. et al. Design of low-cost ionic liquids for lignocellulosic biomass pretreatment. **Green Chem.**, n. 2, p. 1728–1734, 2014.

GLOBO. **Estados Unidos e China ratificam acordo do clima assinado em Paris**, 2016. Disponível em: <http://g1.globo.com/natureza/noticia/2016/09/estados-unidos-ratificam-acordo-do-clima-assinado-em-paris.html>

GOLDEMBERG, J. The Brazilian biofuels industry. **Biotechnology for biofuels**, v. 1, n. 1, p. 6, jan. 2008.

GRAGLIA, M.; KANNA, N.; ESPOSITO, D. Lignin Refinery: Towards the Preparation of Renewable Aromatic Building Blocks. **ChemBioEng Reviews**, v. 2, n. 6, p. 377–392, 2015.

GREAVES, T. L.; DRUMMOND, C. J. Protic ionic liquids: properties and applications. **Chemical reviews**, v. 108, p. 206–237, 2008.

GSCHWEND, F. J. V. et al. Pretreatment of Lignocellulosic Biomass with Low-cost Ionic Liquids. **Journal of Visualized Experiments**, n. 114, p. e54246–e54246, 2016.

GUNASEKARAN, P.; VEAWAB, A.; AROONWILAS, A. Corrosivity of Single and Blended Amines in CO2 Capture Process. **Energy Procedia**, v. 37, p. 2094–2099, 2013.

HAHN-HÄGERDAL, B. et al. Towards industrial pentose-fermenting yeast strains. **Appl. Microbiol. Biotechnol.**, v. 74, p. 937–953, 2007.

HAMELINCK, C. N. et al. Ethanol from lignocellulosic biomass: techno-economic performance in short-, middle- and long-term. **Biomass and Bioenergy**, v. 28, n. 4, p. 384–410, abr. 2005.

HANABUSA, H. et al. Cellulose-dissolving protic ionic liquids as low cost catalysts for direct transesterification reactions of cellulose. **Green Chem.**, v. 20, n. 6, p. 1412–1422, 2018.

HENDRIKS, A. T. W. M.; ZEEMAN, G. Pretreatments to enhance the digestibility of lignocellulosic biomass. **Bioresource technology**, v. 100, n. 1, p. 10–18, jan. 2009.

HIMMEL, M. E. et al. Biomass recalcitrance: engineering plants and enzymes for biofuels production. **Science (New York, N.Y.)**, v. 315, n. 5813, p. 804–7, 9 fev. 2007.

HINMANN, N. D. et al. Xylose fermentation. **Applied Biotehcmistry and Biotechnology**, v. 20--21, p. 391–401, 1989.

HINMANN, N. D. et al. Preliminary estimate of the cost of ethanol production for ssf technology. **Applied Biochemistry and Biotechnology**, v. 34/35, p. 639, 1992.

HOANG, T. M. C.; LEFFERTS, L.; SESHAN, K. Valorization of humin-based byproducts from biomass processing - A route to sustainable hydrogen. **ChemSusChem**, v. 6, n. 9, p. 1651–1658, 2013.

HOLLY, J. Dropping Water Use. **Ethanol Producer Magazine**, 2012.

HOU, X. Anaerobic xylose fermentation by Spathaspora passalidarum. **Applied Microbiology and Biotechnology**, v. 94, n. 1, p. 205–214, 2012a.

HOU, X. Anaerobic xylose fermentation by Spathaspora passalidarum. **Appl Microbiol Biotechnol**, v. 94, n. 1, p. 205, 2012b.

JEFFRIES, T. W.; SHI, N. Q. Genetic engineering for improved regulation of xylose fermetation by yeasts. **Adv Biochem Eng Biotechnology**, v. 65, p. 117–161, 1999.

JÖNSSON, L. J.; MARTÍN, C. Pretreatment of lignocellulose: Formation of inhibitory by-products and strategies for minimizing their effects. **Bioresource Technology**, v. 199, p. 103–112, 2016.

JØRGENSEN, H.; KRISTENSEN, J. B.; FELBY, C. Enzymatic conversion of lignocellulose into fermentable sugars: challenges and opportunities. **Biofuels, Bioproducts and Biorefining**, v. 1, n. 2, p. 119–134, 2007.

KAMM, B.; GRUBER, P.; KAMM, M. **Biorefineries–industrial processes and products**. [s.l.] WILEY-VCH Verlag GmbH & Co. KGaA, 2007.

KIMON, K. S.; ALAN, E. L.; SINCLAIR, D. W. O. Enhanced saccharification kinetics of sugarcane bagasse pretreated in 1-butyl-3-methylimidazolium chloride at high temperature and without complete dissolution. **Bioresource Technology**, v. 102, n. 19, p. 9325–9329, 2011.

KLEIN-MARCUSCHAMER, D. et al. Technoeconomic analysis of biofuels: a wiki-based platform for lignocellulosic biorefineries. **Biomass and Bioenergy**, v. 34, n. 12, p. 1914–1921, 2010.

KLEIN-MARCUSCHAMER, D.; SIMMONS, B. A.; BLANCH, H. W. Techno-economic analysis of a lignocellulosic ethanol biorefinery with ionic liquid pre-treatment. **Biofuels, Bioproducts and Biorefining**, v. 5, n. 5, p. 562–569, 2011.

KUMARI, D.; SINGH, R. Pretreatment of lignocellulosic wastes for biofuel production: A critical review. **Renewable and Sustainable Energy Reviews**, v. 90, p. 877–891, 2018.

LADISCH, M. R. et al. Process considerations in the enzymatic hydrolysis of biomass. **Enzyme and Microbial Technology**, v. 5, p. 82–102, 1983.

LARSSON, S.; REIMANN, A.; NILVEBRANT, N. Comparison of different methods for the detoxification of lignocellulose hydrolysates of spruce. **Appl. Biochem. Biotechnol.**, v. 77--79, p. 91–103, 1999.

LATIFFAH, K.; ZAHARI, S. M. S. N. S. Stability of cellulases in ionic liquids. **Malaysian Journal of Fundamental and Applied Sciences**, v. 15, n. 3, p. 432–435, 2019.

LAU, B. B. Y. et al. Facile, room-temperature pre-treatment of rice husks with tetrabutylphosphonium hydroxide: Enhanced enzymatic and acid hydrolysis yields. **Bioresource Technology**, v. 197, p. 252–259, 2015.

LEE, C.; ZHENG, Y.; VANDERGHEYNST, J. S. Effects of pretreatment conditions and post–pretreatment washing on ethanol production from dilute acid pretreated rice straw. **Biosystems Engineering**, v. 137, p. 36–42, 2015.

LI, Q. et al. Improving enzymatic hydrolysis of wheat straw using ionic liquid 1-ethyl-3-methyl imidazolium diethyl phosphate pretreatment. **Bioresource Technology**, v. 100, n. 14, p. 3570–3575, 2009.

LONG, T. M. et al. Cofermentation of Glucose, Xylose, and Cellobiose by the Beetle-Associated Yeast Spathaspora passalidarum. **Applied and Environmental Microbiology**, v. 78, n. 16, p. 5492–5500, 2012.

LU, B.; XU, A.; WANG, J. Cation does matter: how cationic structure affects the dissolution of cellulose in ionic liquids. **Green Chem.**, 2014.

LV, Y. et al. Infrared spectroscopic study on chemical and phase equilibrium in triethylammonium acetate. **Science China Chemistry**, v. 55, n. 8, p. 1688–1694, 2012.

MADEIRA LAU, R. et al. Dissolution of Candida antarctica lipase B in ionic liquids: effects on structure and activity. **Green Chem.**, v. 6, n. 9, p. 483–487, 2004.

MÄKI-ARVELA, P. et al. Dissolution of lignocellulosic materials and its constituents using ionic liquids-A review. **Industrial Crops and Products**, v. 32, n. 3, p. 175–201, 2010.

MATHEW, A. K. et al. An evaluation of dilute acid and ammonia fiber explosion pretreatment for cellulosic ethanol production. **Bioresource Technology**, v. 199, p. 13–20, 2016.

MAZZA, M. et al. Influence of water on the dissolution of cellulose in selected ionic liquids. **Cellulose**, v. 16, p. 207–215, 2009.

MILANEZ, A. Y. et al. De promessa a realidade: como o etanol celulósico pode revolucionar a indústria da cana-de-açúcar - uma avaliação do potencial competitivo e sugestões de política pública. v. 41, p. 237–294, 2015.

MORAIS DE CARVALHO, D. et al. Isolation and characterization of acetylated glucuronoarabinoxylan from sugarcane bagasse and straw. **Carbohydrate Polymers**, v. 156, p. 223–234, 2017.

MOSIER, N. et al. Features of promising technologies for pretreatment of lignocellulosic biomass. **Bioresource technology**, v. 96, n. 6, p. 673–686, abr. 2005.

NAKANISHI, S. C. et al. Fermentation strategy for second generation ethanol production from sugarcane bagasse hydrolyzate by Spathaspora passalidarum and Scheffersomyces stipitis. **Biotechnology and Bioengineering**, v. 114, n. 10, p. 2211–2221, 2017.

NAKASU, P. Statistical tests in R for protic ionic liquid pretreatment optimization. **Mendeley Data**, 2019.

NAKASU, P. Y. S. et al. Acid post-hydrolysis of xylooligosaccharides from hydrothermal pretreatment for pentose ethanol production. **Fuel**, 2016a.

NAKASU, P. Y. S.; RABELO, S. C. **Uso de água e recuperação de açúcares: estudo de caso para o pré-tratamento hidrotérmico**. Relatório de estágio supervisionado. 2012.

NAKASU, P. Y. S. Y. S. et al. Acid post-hydrolysis of xylooligosaccharides from hydrothermal pretreatment for pentose ethanol production. **Fuel**, v. 185, p. 73–84, 2016b.

NASCIMENTO, V. M. et al. Effect of anthraquinone on alkaline pretreatment and enzymatic kinetics of sugarcane bagasse saccharification: Laboratory and pilot scale approach. **ACS Sustainable Chemistry and Engineering**, v. 4, n. 7, p. 3609–3617, 2016.

NEGI, S.; PANDEY, A. K. Ionic Liquid Pretreatment. **Pretreatment of Biomass: Processes and Technologies**, p. 137–155, 2014.

NETO, E. **Gestão dos Recursos Hídricos na Indústria Canavieira**. [s.l: s.n.].

NETWORK, W. FOOTPRINT. **What is water footprint?** Disponível em: <https://waterfootprint.org/en/water-footprint/what-is-water-footprint/>. Acesso em: 19 ago. 2019.

NINOMIYA, K. et al. Saccharification and ethanol fermentation from cholinium ionic liquid-pretreated bagasse with a different number of post-pretreatment washings. **Bioresource Technology**, v. 189, p. 203–209, 2015.

NINOMIYA, K. et al. Pretreatment of bagasse with a minimum amount of cholinium ionic liquid for subsequent saccharification at high loading and co-fermentation for ethanol production. **Chemical Engineering Journal**, v. 334, p. 657–663, 2018.

NOVACANA.COM. **Raízen tem plano de expansão mais robusto para 2016**, [s.d.]. Disponível em: <https://www.jornalcana.com.br/raizen-tem-plano-de-expansao-mais-robusto-para-2016/>

NOVACANA.COM. **GranBio paralisa usina em Alagoas**, [s.d.]. Disponível em: <https://www.jornalcana.com.br/granbio-paralisa-usina-em-alagoas/>

NOVACANA.COM. **Mapa do etanol celulósico no mundo**, 2015. Disponível em: <https://www.novacana.com/n/etanol/2-geracao-celulose/mapa-etanol-celulosico-mundo-160315/>

NUTHAKKI, B. et al. Protic ionic liquids and ionicity. **Australian Journal of Chemistry**, v. 60, n. 1, p. 21–28, 2007.

O'SULLIVAN, A. Cellulose: the structure slowly unravels. **Cellulose**, p. 173–207, 1997.

ODORICO, F. H.; MORANDIM-GIANNETTI, A. A.; LUCARINI, A. C. Pretreatment of Guinea grass (Panicum maximum) with the ionic liquid 1-ethyl-3-methyl imidazolium acetate for efficient hydrolysis and bioethanol production. **Cellulose**, v. 25, p. 2997, 2018.

OGEDA, T. L.; PETRI, D. F. S. Hidrolise enzimática de biomassa. **Química Nova**, v. 33, n. 7, p. 1549–1558, 2010.

OGIER, J. C. et al. Production d'éthanol à partir de biomasse lignocellulosique. **Oil and Gas science and technology-Revue de l'IFP**, v. 54, p. 67–94, 1999.

PALMQVIST, E.; HAHN HÄGERDAL, B. Fermentation of lignocellulosic hydrolysates. II: inhibitors and mechanisms of inhibition. **Bioresource Technology**, v. 74, n. 1, p. 25–33, ago. 2000.

PATTABIRAMAN, V. R.; BODE, J. W. Rethinking amide bond synthesis. **Nature**, v. 480, p. 471, 21 dez. 2011.

PENG, F.; REN, J. L.; SUN, R. C. **Chemicals from hemicelluloses: a review, in Sustainable Production of Fuels, Chemicals, and Fibers from Forest Biomass**. Washington DC, USA: [s.n.].

PETERSEN, M. Ø.; LARSEN, J.; THOMSEN, M. H. Optimization of hydrothermal pretreatment of wheat straw for production of bioethanol at low water consumption without addition of chemicals. **Biomass and Bioenergy**, v. 33, p. 834–840, 2009.

PETTERSEN, R. C. **The chemical composition of woo**. (R. M. Rowell, Ed.)The chemistry of solid wood. **Anais**...1984

PIENKOS, P. T.; ZHANG, M. Role of pretreatment and conditioning processes on toxicity of lignocellulosic biomass hydrolysates. **Cellulose**, v. 16, n. 4, p. 743–762, 10 jun. 2009.

PIN, T. C. et al. Screening of protic ionic liquids for sugarcane bagasse pretreatment. **Fuel**, 2019a.

PIN, T. C. et al. Screening of protic ionic liquids for sugarcane bagasse pretreatment. **Fuel**, v. 235, n. July 2018, p. 1506–1514, 2019b.

PORTAL-NOVA-CANA. Consumo de etanol hidratado em 2019 supera recorde do ano anterior em 37%. 2019.

RABELO, S. C. **Avaliação e otimização de pré-tratamentos e hidrolise enzimática do bagaço de cana-de-açúcar para a produçao de etanol de segunda geraçao**. Tese de doutorado. Universidade Estadual de Campinas, 2010.

RABELO, S. C. et al. Ethanol production from enzymatic hydrolysis of sugarcane bagasse pretreated with lime and alkaline hydrogen peroxide. **Biomass and Bioenergy**, v. 35, n. 7, p. 2600–2607, 2011.

RABELO, S. C. et al. Alkaline hydrogen peroxide pretreatment, enzymatic hydrolysis and fermentation of sugarcane bagasse to ethanol. **Fuel**, 2014.

RABELO, S. C.; COSTA, A. C.; FILHO, R. M. **Processo de Pré-Tratamento e Hidrólise de Biomassa Vegetal Lignocelulósica e Produto para a Produção Industrial de Alcoóis**. Patente PI0802559-2. 2008.

RAHIKAINEN, J. L. et al. Inhibitory effect of lignin during cellulose bioconversion: The effect of lignin chemistry on non-productive enzyme adsorption. **Bioresource Technology**, v. 133, p. 270–278, 2013.

RAJ, T. et al. Ionic liquid pretreatment of biomass for sugars production: Driving factors with a plausible mechanism for higher enzymatic digestibility. **Carbohydrate Polymers**, v. 149, n. November,

p. 369–381, 2016.

REDDY, P. A critical review of ionic liquids for the pretreatment of lignocellulosic biomass. **South African Journal of Science**, v. 111, n. 11–12, p. 1–9, 2015.

REIS, C. L. B. et al. Pretreatment of cashew apple bagasse using protic ionic liquids: Enhanced enzymatic hydrolysis. **Bioresource Technology**, 2017.

RENEWABLE-FUELS-ASSOCIATION. **World Fuel Ethanol Production**. Disponível em: <https://ethanolrfa.org/statistics/annual-ethanol-production/>. Acesso em: 20 jul. 2017.

RESCH, M. G.; BAKER, J. O.; DECKER, S. R. Low Solids Enzymatic Saccharification of Lignocellulosic Biomass. **Laboratory Analytical Procedure (LAP)**, v. NREL/TP-51, 2015.

ROCHA, E. G. A. **Síntese, caracterização, uso e reciclo de líquidos iônicos próticos no pré-tratamento do bagaço de cana-de-açúcar visando a produção de etanol de segunda geração**. [s.l.] Faculdade de Engenharia Química, State University of Campinas, 2016.

ROCHA, E. G. A. et al. Evaluation of the use of protic ionic liquids on biomass fractionation. **Fuel**, v. 206, 2017.

RODRUSSAMEE, N.; SATTAYAWAT, P.; YAMADA, M. Highly efficient conversion of xylose to ethanol without glucose repression by newly isolated thermotolerant Spathaspora passalidarum CMUWF1–2. **BMC Microbiology**, v. 18, n. 1, p. 73, 2018.

ROGERS, R. D.; MACFARLANE, D. Ionic Liquid-water mixtures: from hostility to conciliation. **Chem. Commun.**, v. 48, p. 7119–7130, 2012.

ROSSELL, C. E. V. \TEXTITET AL. Saccharification of sugarcane bagasse for ethanol production using the Organosolv process. **Sugar Industry/zuckerindustrie**, v. 131, 2006.

RUBIN, E. M. Genomics of cellulosic biofuels. **Nature**, v. 454, n. 7206, p. 841–5, 2008.

SAHA, K.; DWIBEDI, P.; GHOSH, A. Extraction of lignin, structural characterization and bioconversion of sugarcane bagasse after ionic liquid assisted pretreatment. **3 Biotech**, v. 8, p. 374, 2018.

SANTUCCI, B. S. et al. Autohydrolysis of Hemicelluloses from Sugarcane Bagasse During Hydrothermal Pretreatment: a Kinetic Assessment. **BioEnergy Research**, v. 8, n. 4, p. 1778–1787, 2015.

SATHITSUKSANOH, N. et al. Lignin fate and characterization during ionic liquid biomass pretreatment for renewable chemicals and fuels production. **Green Chemistry**, v. 16, n. 3, p. 1236, 2014.

SCY-STYLE. **Lignocellulose change**, 2011. Disponível em: <http://portfolio.scistyle.com/Lignocellulose>

SEABRA, J. E. A. **Avaliaçãoo técnico-econômica de opções para o aproveitamento integral da biomassa de cana no Brasil**. [s.l.] Universidade Estadual de Campinas, Faculdade de Engenharia Química -- FEQ, 2008.

SEMERCI, I.; GÜLER, F. Protic ionic liquids as effective agents for pretreatment of cotton stalks at high biomass loading. **Industrial Crops & Products**, v. 125, n. September, p. 588–595, 2018.

SHESHMANI, S. Effects of extractives on some properties of bagasse/high density polypropylene composite. **Carbohydrate Polymers**, v. 94, n. 1, p. 416–419, 2013.

SHI, J. et al. Understanding the Role of Water during Ionic Liquid Pretreatment of Lignocellulose: Co-solvent or Anti-solvent? **Green Chemistry**, v. 16, n. 8, p. 3830–3840, 2014.

SLUITER, J. B. et al. Evaluation of Brazilian sugarcane bagasse characterization: An interlaboratory comparison study. **Journal of AOAC International**, v. 99, n. 3, p. 579–585, 2016.

SOARES, L. B. **O efeito de inibidores do hidrolisado hemicelulósico e seu impacto no desempenho da fermentação etanólica de Scheffersomyces stipitis NRRL Y-7124 e Spathaspora passalidarum NRRL Y-27907**. [s.l.] State University of Campinas, 2018.

SOCCOL, C. R. et al. Bioethanol from lignocelluloses: Status and perspectives in Brazil. **Bioresource technology**, v. 101, n. 13, p. 4820–4825, jul. 2010.

SOCHA, A. M. et al. Efficient biomass pretreatment using ionic liquids derived from lignin and hemicellulose. **Proceedings of the National Academy of Sciences of the United States of America**, v. 111, n. 35, p. E3587–E3595, 2014.

SÖDERSTRÖM, J.; GALBE, M.; ZACCHI, G. Effect of washing on yield in one- and two-step steam pretreatment of softwood for production of ethanol. **Biotechnology Progress**, v. 20, n. 3, p. 744–749, 2004.

SOUZA, A. P. et al. Composition and Structure of Sugarcane Cell Wall Polysaccharides: Implications for Second-Generation Bioethanol Production. **BioEnergy Research**, v. 6, n. 2, p. 564–579, 6 nov. 2012.

SOUZA, R. F. R. **Produção de etanol a partir de hidrolisado enzimático do bagaço de canade-açúcar por leveduras isoladas do bioma amazônico**. [s.l.] Federal University of Pernambuco,

2014.

SQUINA, F. M. et al. Xylan decomposition by Aspergillus clavatus endo-xylanase. **Protein Expression and Purification**, v. 68, p. 65–71, 2009.

SRITRAKUL, N.; NITISINPRASERT, S.; KEAWSOMPONG, S. Evaluation of dilute acid pretreatment for bioethanol fermentation from sugarcane bagasse pith. **Agriculture and Natural Resources**, v. 51, n. 6, p. 512–519, 2017.

SU, Y. K.; WILLIS, L. B.; JEFFRIES, T. W. Effects of aeration on growth, ethanol and polyol accumulation by Spathaspora passalidarum NRRL Y-27907 and Scheffersomyces stipitis NRRL Y-7124. **Biotechnology and Bioengineering**, v. 112, n. 3, p. 457–469, 2015.

SUMMERS, C. A.; FLOWERS II, R. A. Protein renaturation by the liquid organic salt ethylammonium nitrate. **Protein Science**, v. 9, n. 10, p. 2001–2008, 2000.

SUN, J. et al. One-pot integrated biofuel production using low-cost biocompatible protic ionic liquids. p. 3152–3163, 2017.

SUN, N. et al. Complete dissolution and partial delignification of wood in the ionic liquid 1-ethyl-3-methylimidazolium acetate. **Green Chemistry**, v. 11, n. 5, p. 646, 2009.

SUN, N. et al. Where are ionic liquid strategies most suited in the pursuit of chemicals and energy from lignocellulosic biomass? **Chemical communications (Cambridge, England)**, v. 47, n. 5, p. 1405–1421, 2011.

SUN, Y.; CHENG, J. Hydrolysis of lignocellulosic materials for ethanol production: a review. **Bioresource technology**, v. 83, n. 1, p. 1–11, maio 2002.

SZCZODRAK, J.; FIEDUREK, J. Technology for conversion of lignocellulosic biomass to ethanol. **Biomass and Bioenergy**, v. 10, n. 5/6, p. 367–375, 1996.

TANAKA, N. Technology Roadmap Biofuels for Transport. **Renewable Energy**, p. 56, 2011.

TÍMAR-BALÁZSY, A.; EASTOP, D. .**Chemical Principles of Textile Conservation**. [s.l.] Butterworth Heinemann, 1998.

TOLESA, L. D.; GUPTA, B. S.; LEE, M.-J. The chemistry of ammonium-based ionic liquids in depolymerization process of lignin. **Journal of Molecular Liquids**, v. 248, p. 227–234, 2017.

TURNER, M. B. et al. Ionic liquid salt-induced inactivation and unfolding of cellulase from

Trichoderma reesei. **Green Chem.**, v. 5, n. 4, p. 443–447, 2003.

UNICA. **Moagem de cana-de-açúcar e produção de etanol e açúcar**, 2015. Disponível em: <http://www.unica.com.br/unicadata>

VAN ZYL, C.; PRIOR, B. A.; DU PREEZ, J. C. Acetic acid inhibition of d-xylose fermentation by Pichia stipitis. **Enzyme and Microbial Technology**, v. 13, p. 82–86, 1991.

VERDÍA, P. et al. Fractionation of lignocellulosic biomass with the ionic liquid 1-butylimidazolium hydrogen sulfate. **Green Chemistry**, v. 16, n. 3, p. 1617, 2014.

VOHRA, M. et al. **Bioethanol production: Feedstock and current technologiesJournal of Environmental Chemical Engineering**, 2014.

WANG, X. et al. Cellulose extraction from wood chip in an ionic liquid 1-allyl-3-methylimidazolium chloride (AmimCl). **Bioresour Technol.**, v. 102, p. 7959–7965, 2011.

WEIGAND, L. et al. Effect of pretreatment severity on the cellulose and lignin isolated from: Salix using ionoSolv pretreatment. **Faraday Discussions**, v. 202, p. 331–349, 2017.

WEN, J.-L. et al. Understanding the chemical transformations of lignin during ionic liquid pretreatment. **Green Chemistry**, v. 16, n. 1, p. 181–190, 2014.

WILKES, J. S. et al. Dialkylimidazolium chloroaluminate melts A new class of room-temperature ionic liquids for electrochemisry, spectroscopy, and synthesis. v. 237, n. 1980, p. 1263–1264, 1982.

WILKES, J. S.; ZAWOROTKO, M. J. Air and water stable 1-ethyl-3-methylimidazolium based ionic liquids. **J. Chem. Soc.{,} Chem. Commun.**, n. 13, p. 965–967, 1992.

WILSON, D. B.; IRWIN, D. C. **Genetics and properties of cellulases**. Berlin: Springer, 2004. v. 65

WU, H. et al. Facile pretreatment of lignocellulosic biomass at high loadings in room temperature ionic liquids. **Biotechnology and Bioengineering**, v. 108, n. 12, p. 2865–2875, 2011.

WYMAN, C. E. et al. Hydrolysis of Cellulose and Hemicellulose. In: DUMITRIU, S. (Ed.). . **Polysaccharides Structural Diversity and Functional Versatility, Second Edition**. [s.l.] CRC Press, 2005.

XIMENES, E. et al. Inhibition of cellulases by phenols. **Enzyme and Microbial Technology**,

v. 46, n. 3–4, p. 170–176, mar. 2010.

YANG, B.; WYMAN, C. E. Pretreatment: the key to unlocking low-cost cellulosic ethanol. **Biofuels, Bioproducts and Biorefining**, v. 2, n. 1, p. 26–40, 2008.

YOON, L. W. et al. Regression analysis on ionic liquid pretreatment of sugarcane bagasse and assessment of structural changes. **Biomass and Bioenergy**, v. 36, p. 160–169, 2012.

ZAFALON, M. **Exportação recorde e preços do açúcar elevam tonelada de cana para R$ 100**, 2016. Disponível em: <http://www1.folha.uol.com.br/colunas/vaivem/2016/11/1830613-exportacao-recorde-e-precos-do-acucar-elevam-tonelada-de-cana-para-r-100.shtml>

ZHANG, Q.; HU, J.; LEE, D. J. Pretreatment of biomass using ionic liquids: Research updates. **Renewable Energy**, v. 111, 2017.

ZHANG, T. et al. Xylose yields and relationship to combined severity for dilute acid post-hydrolysis of xylooligomers from hydrothermal pretreatment of corn stover. **Green Chem.**, v. 17, n. 1, p. 394–403, 2015.

ZHAO, X.; ZHANG, L.; LIU, D. Biomass recalcitrance. Part II : Fundamentals of different pre-treatments to increase the enzymatic digestibility of lignocellulose. **Biofuels, Bioproducts & Biorefining**, v. 6, p. 561–579, 2012.

ZUURBIER, P.; VAN DE VOOREN, J. **Contributions to climate change mitigation and Sugarcane ethanol**. [s.l.] Wageningen Academic Publishers, 2008.

Appendix I – Optimization of pretreatment parameters
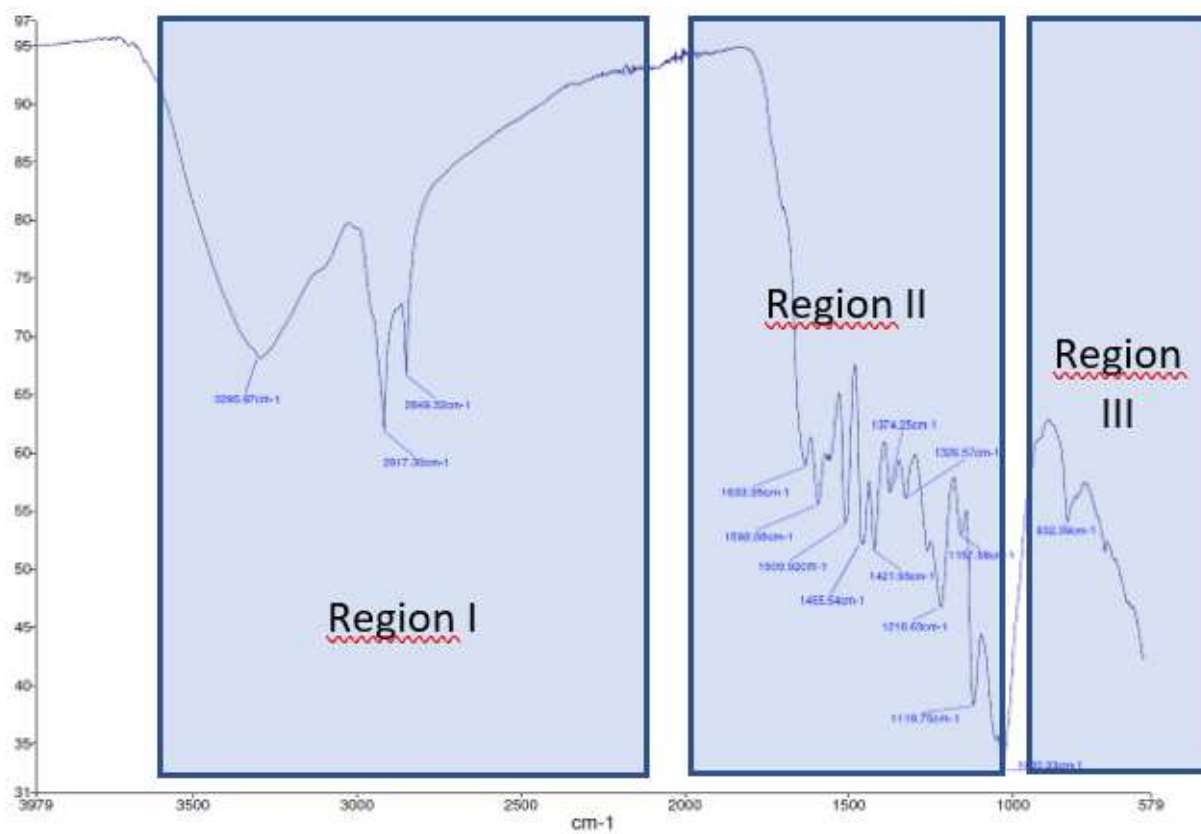
Fig. I-1. FT-IR spectrum of the lignin obtained from [MEA][OAc] pretreatment with water as anti-solvent. Pretreatment conditions with [MEA][OAc] were 150°C, 2 h, 15 wt% solids and 20 wt% water.

2. GPC profiles
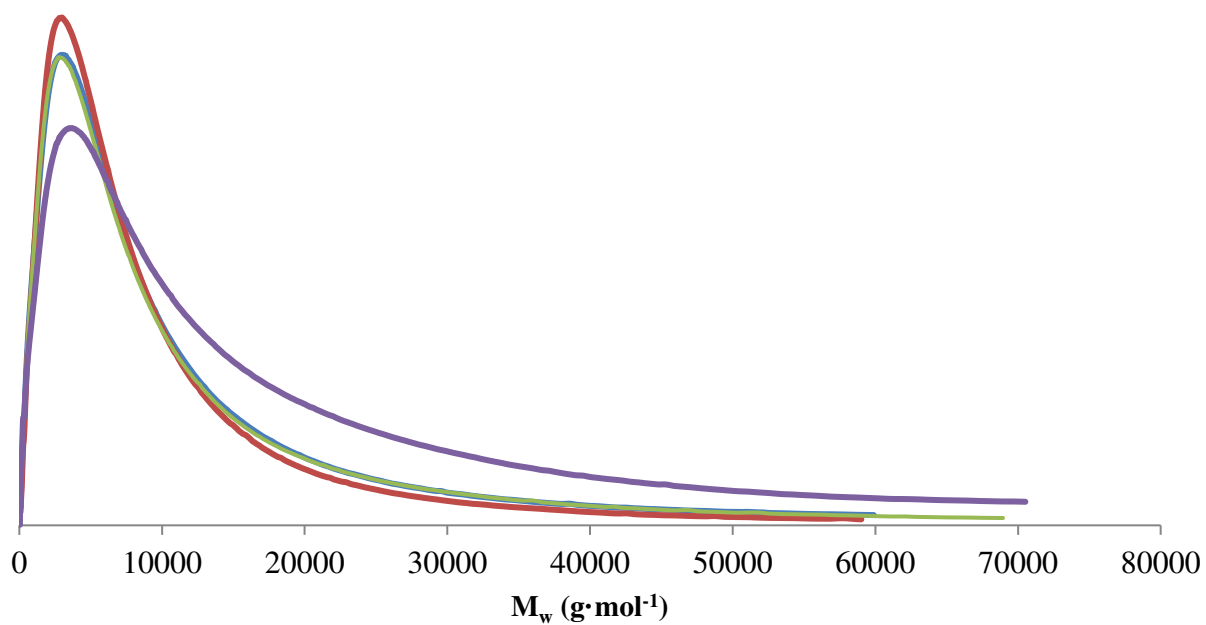
Fig. I-2 Representative GPC profiles of sugarcane bagasse lignin isolated from [MEA][OAc] pretreatment 150°C, 2 h, 15 wt% solids and 20 wt% water and (——) water, (——) ethanol, (——) isopropanol and (——) isoamyl alcohol as anti-solvents.

# Appendix II – Impact of acid-base ratio on ionic liquid performance
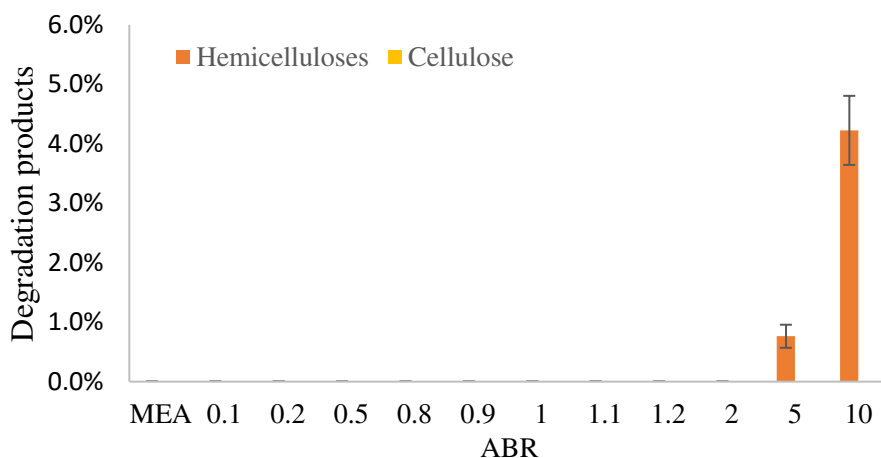
Fig.II-1. *Degradation products in the liquid fractions obtained in the ABR experiments expressed as percentage of hemicelluloses (orange) — in the form of furfural — and cellulose (yellow) — in the form of 2-hydroxymethylfurfural (HMF), formic and levulinic acids.*
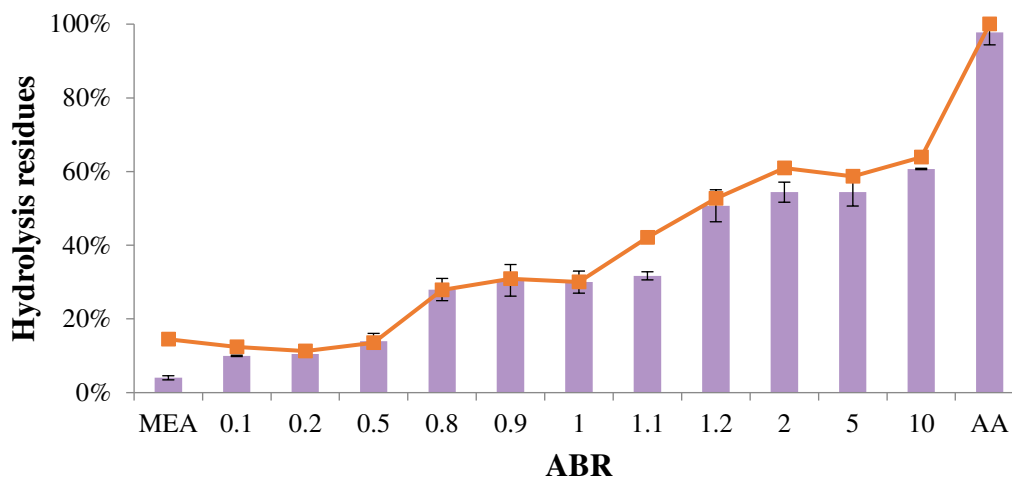
Fig. II-2. *Hydrolysis residues (purple bars) in oven dry basis obtained after 72 h of enzymatic saccharification and estimated hydrolysis residues (orange line) based on glucan and hemicellulose conversions in saccharification. The error bars were calculated based on duplicatesf the experiments. Pretreatment conditions with [MEA][OAc] were 150°C, 30% water content, 15% solids loading and 2h of reaction time.*
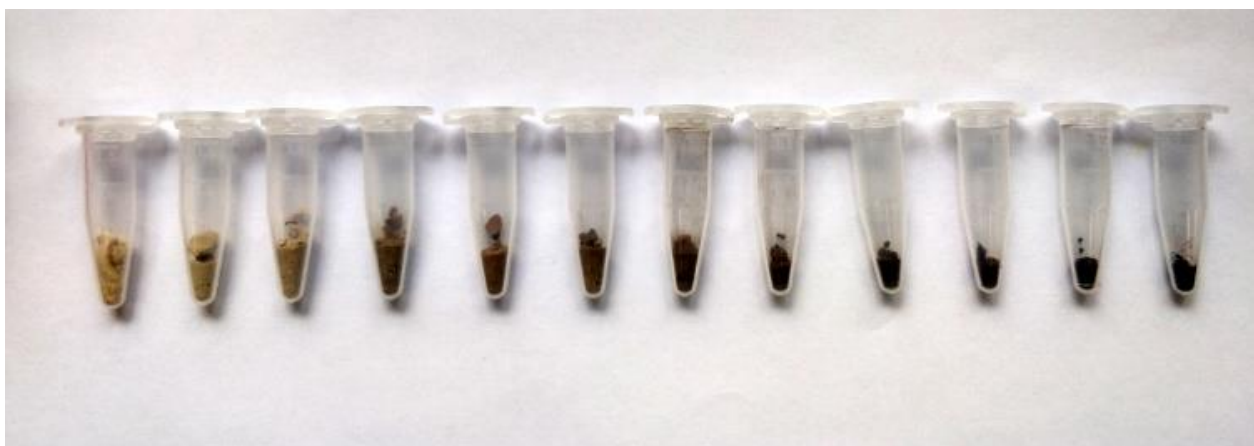
Fig. II-3. *From left to right: lignins obtained from MEA, 0.1, 0.2, 0.5, 0.8, 0.9, 1.0, 1.1, 1.2, 2, 5 and 10 ABR pretreatments.*
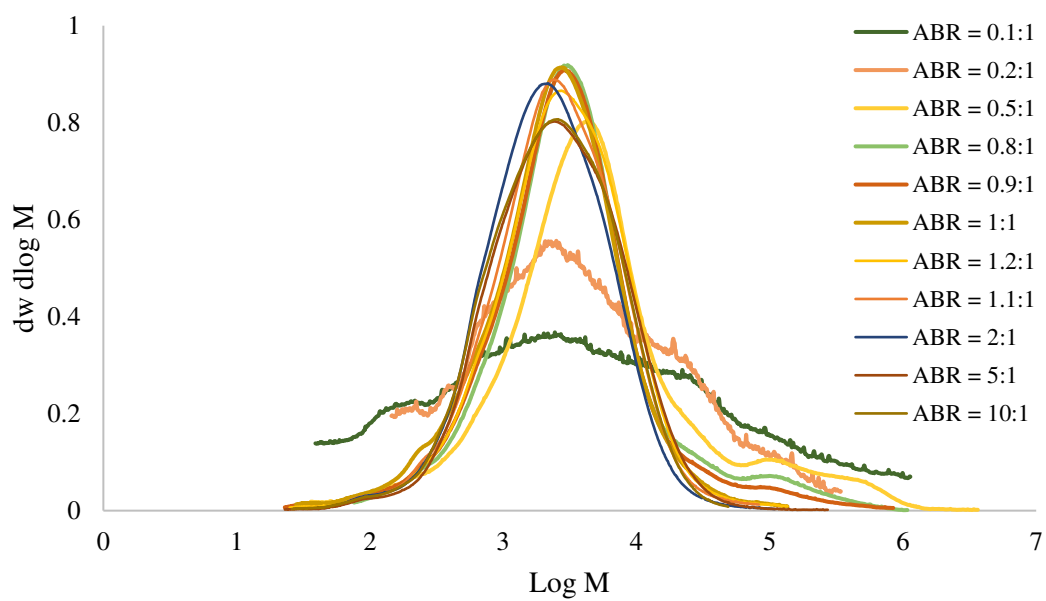

Fig. II-4. *GPC profiles of the recovered lignins from the ABR experiments.*

Table II-1. *Binding energies (eV) for the photoemissions of each lignin sample. All high-resolution XP spectra are charge corrected to the aliphatic component 1 (285.0 eV) and the most intense signals (i.e. 2p 3/2) are reported for doubly degenerate photoemissions.*

| | Binding Energy (eV) | | | | | | | | | | | |
	C 1s				N 1s		O 1s		Si 2p		S 2p	Ca 2p
Component	1	2	3	4	1[a]	2[a]	1	2	1	2	2	
MEA	285.0	286.2	287.1	288.5	400.2	402.2	531.2	533.0	102.6	103.5		347.6
1:1	285.0	286.3	287.0	288.3	400.0	401.7	530.7	532.8	102.4			
1:0.8	285.0	286.3	286.9	288.2	400.0	401.9	531.2	533.0	102.5			
2:1	285.0	286.3	286.8	288.3	400.2	402	531.5	533.1				
[TEA][HSO$_4$]	285.0	286.3	286.8	288.1		402.1		533.2			168.9	

[a] Components identified as neutral (1) and cationic (2) nitrogen.
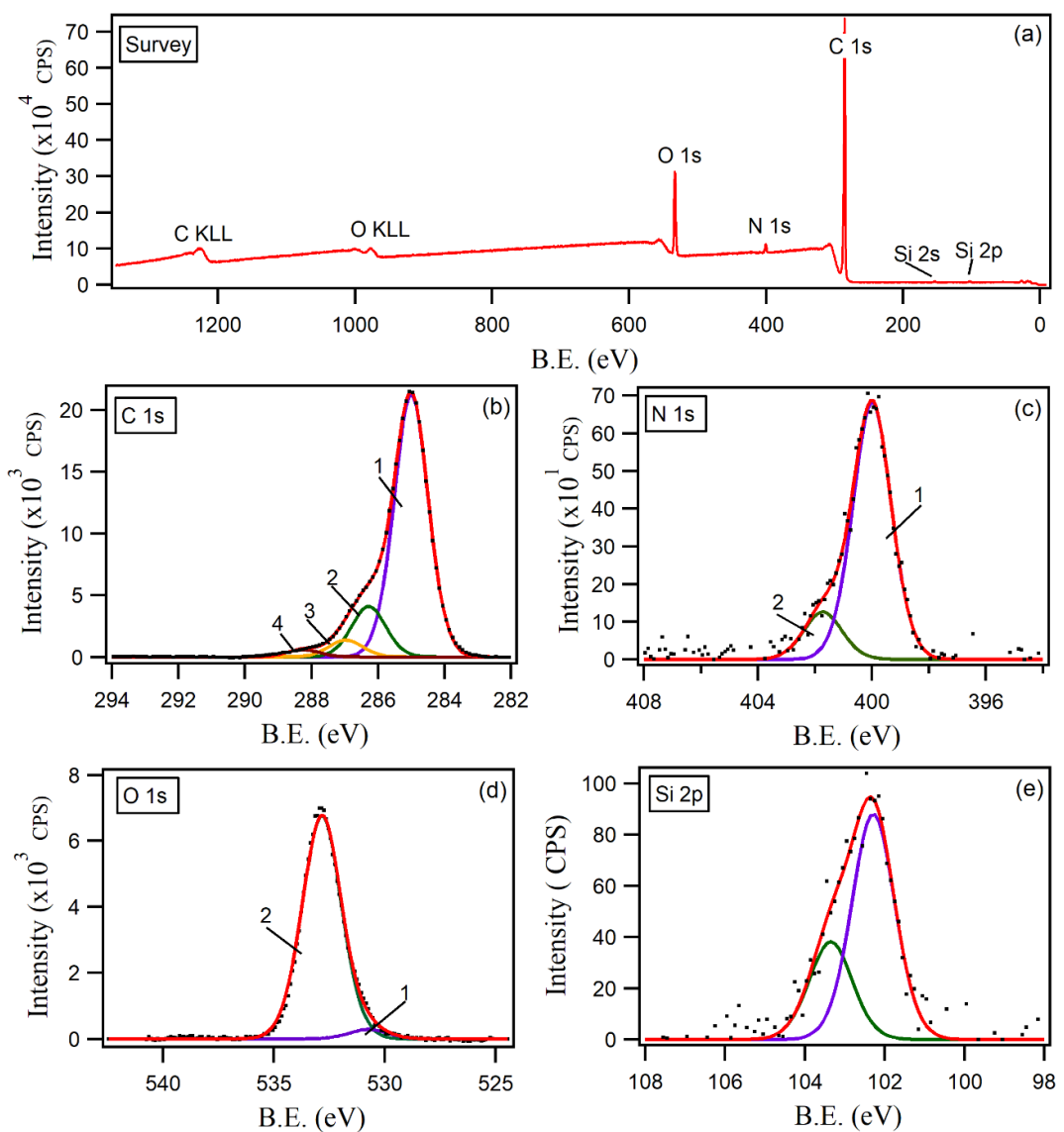
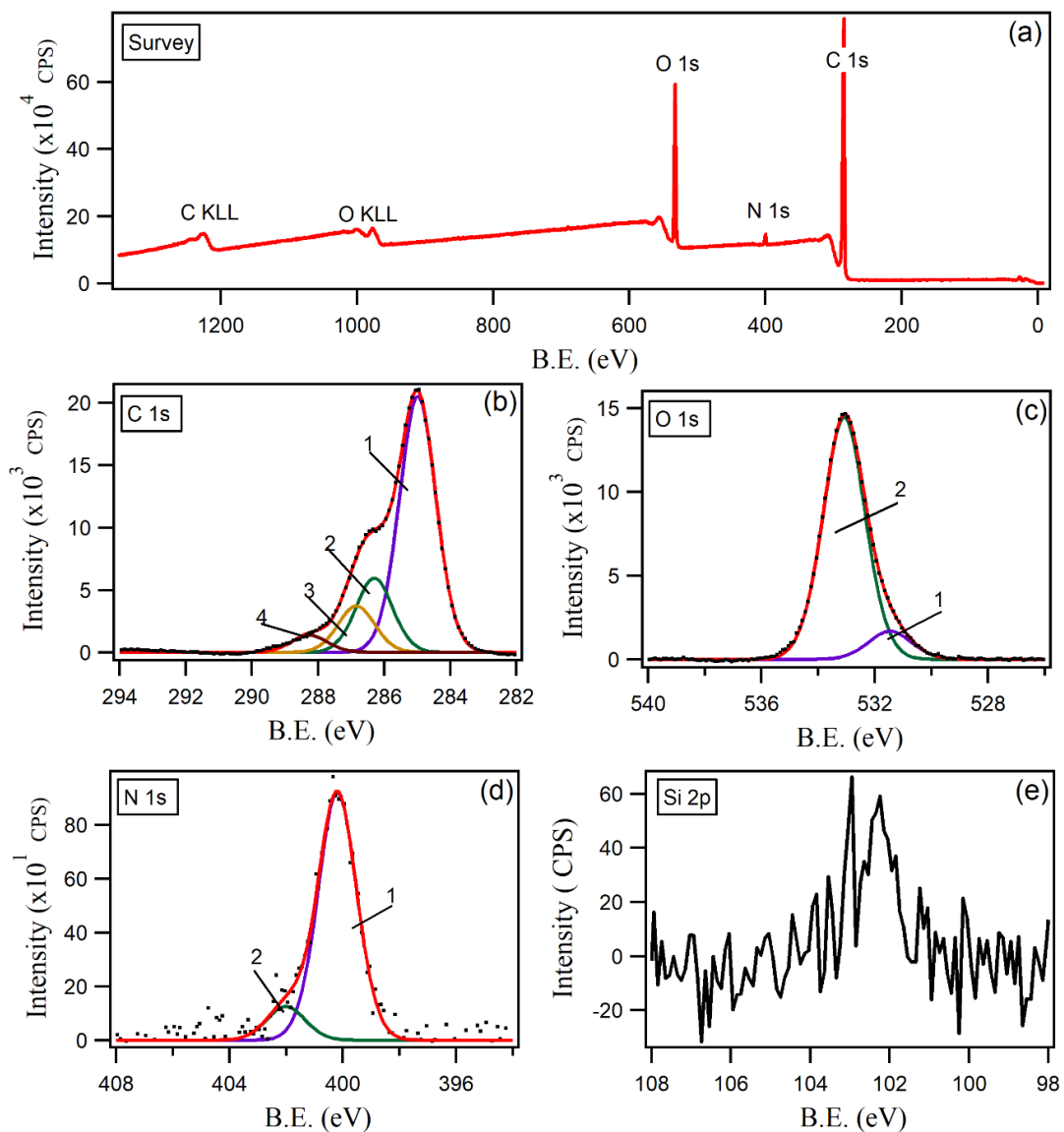**Fig. II-5.** *[MEA][OAc] 1:1 ABR lignin survey (a) and high resolution (b-f) photoemission spectra.*
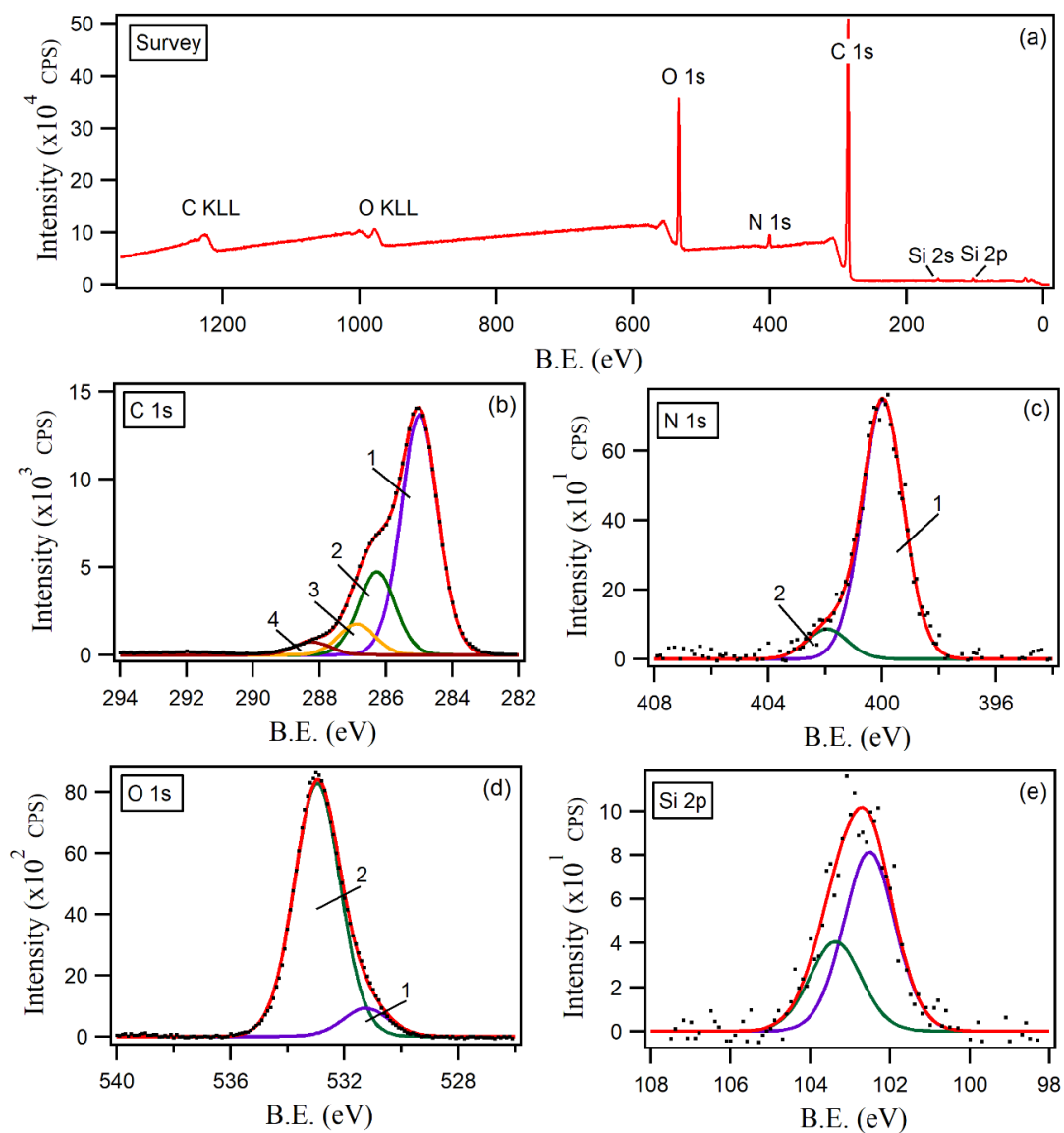
Fig. II-6. *[MEA][OAc] 0.8:1 ABR lignin survey (a) and high resolution (b-f) photoemission spectra.*

Fig. II-7. *[MEA][OAc] ABR lignin survey (a) and high resolution (b-f) photoemission spectra.*
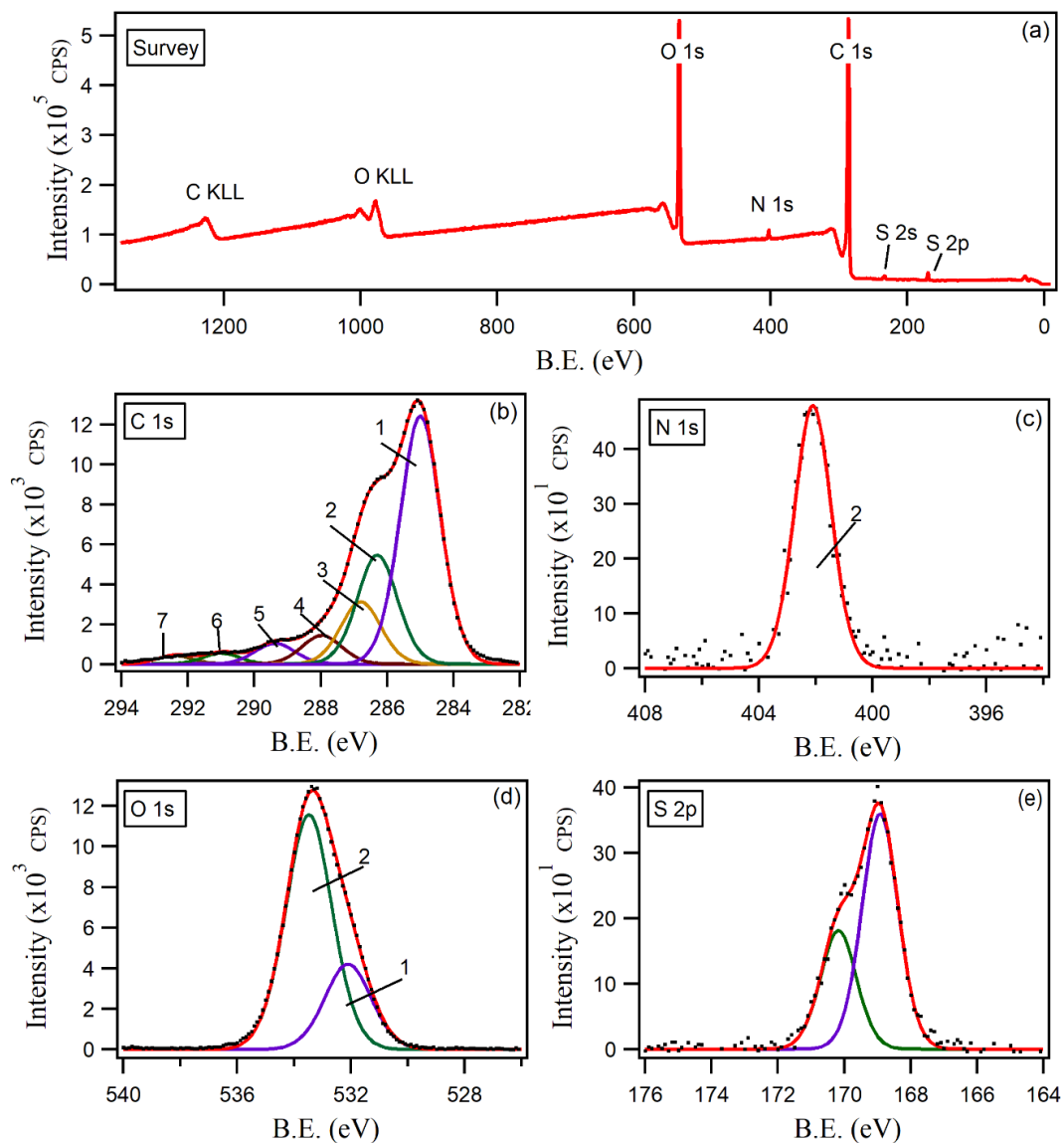
Fig. II-8. *[TEA][HSO4] lignin survey (a) and high resolution (b-f) photoemission spectra.*
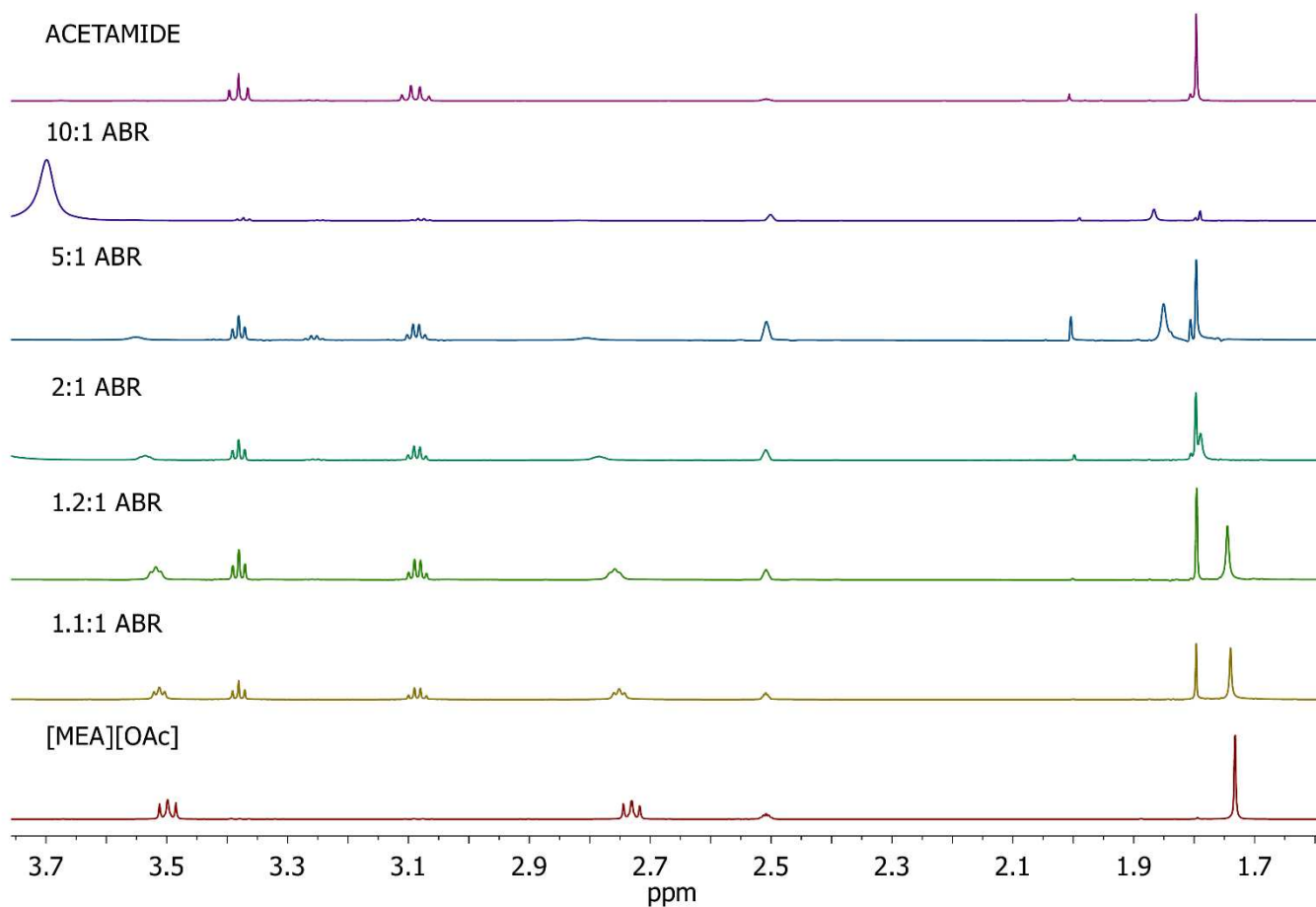
Fig. II-9. *¹H-NMR spectra of acid-base mixtures with ABR from 1.1:1 to 10:1. Acetamide and [MEA][OAc] spectra were also shown as a matter of comparison.*
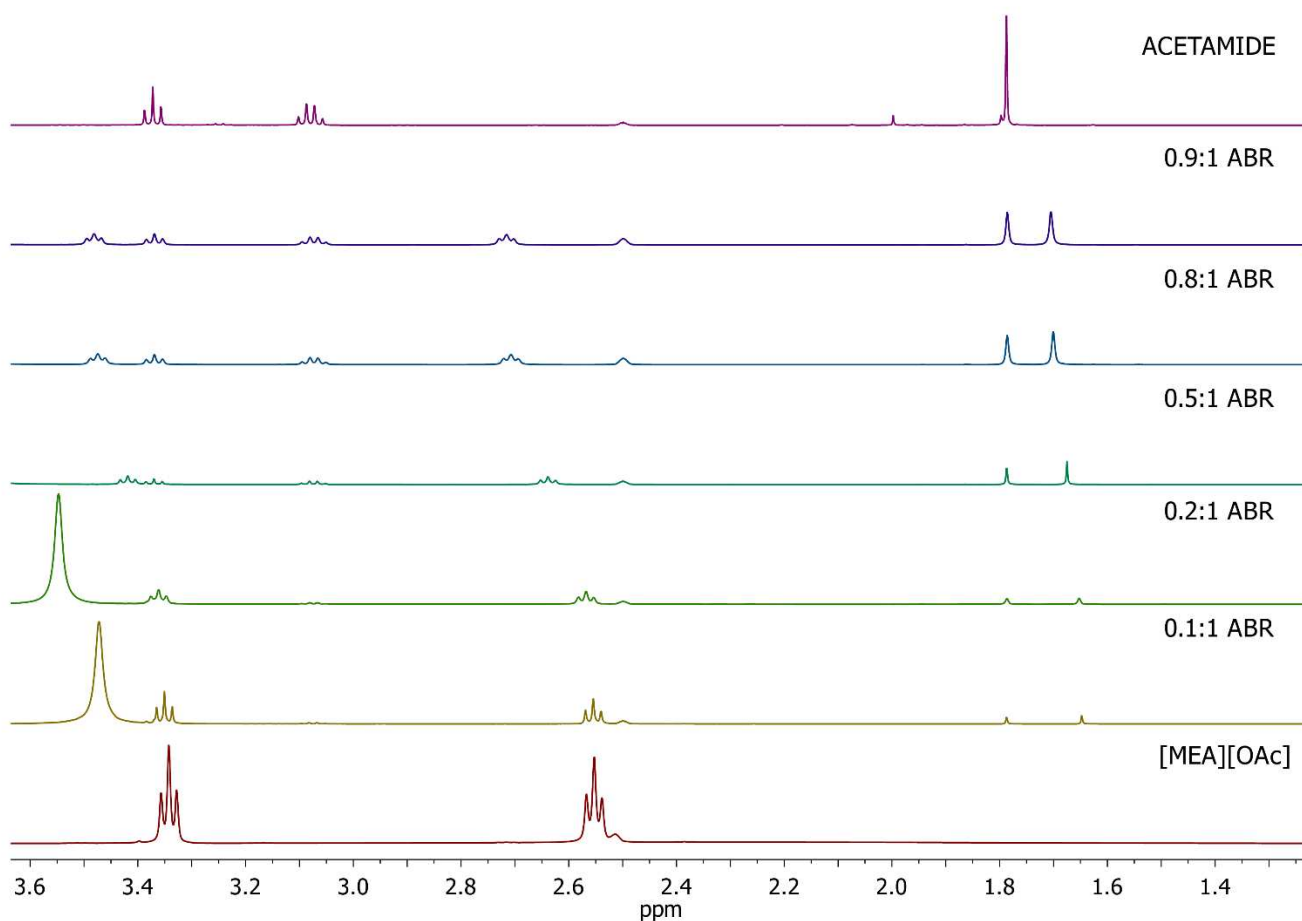
Fig. II-10. *^{1}H-NMR spectra of acid-base mixtures with ABR from 0.1:1 to 0.9:1. Acetamide and [MEA][OAc] spectra were also shown as a matter of comparison.*
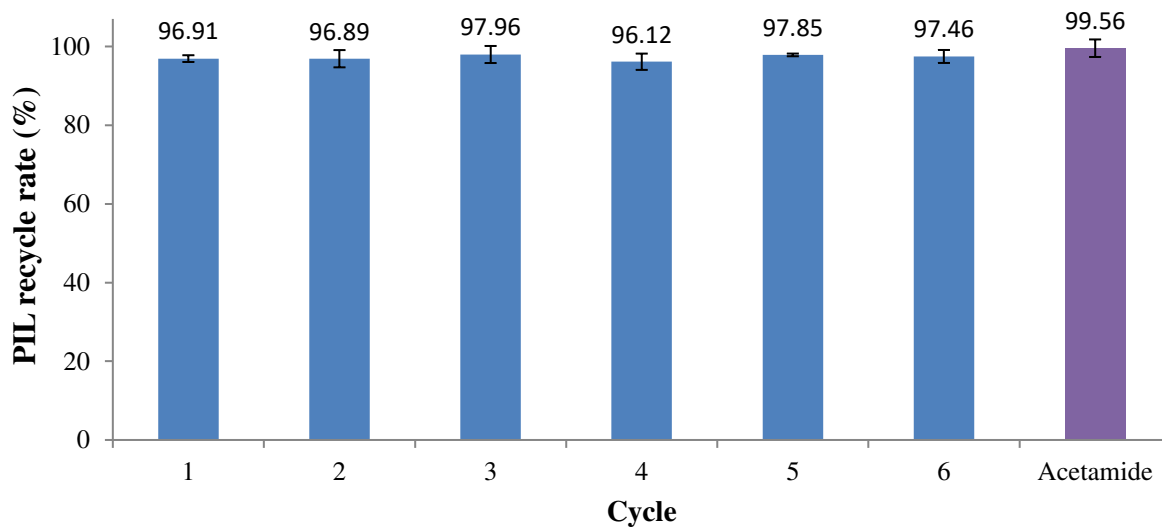
Fig. II-11. *Recovery rates obtained for [MEA][OAc] recycle with 1:1 ABR. The error bars were calculated based on triplicates of the experiment. A pretreatment control with pure acetamide (purple bar) was shown as a matter of comparison. Pretreatment conditions with [MEA][OAc] were 150°C, 30% water content, 15% solids loading and 2 h of reaction time.*
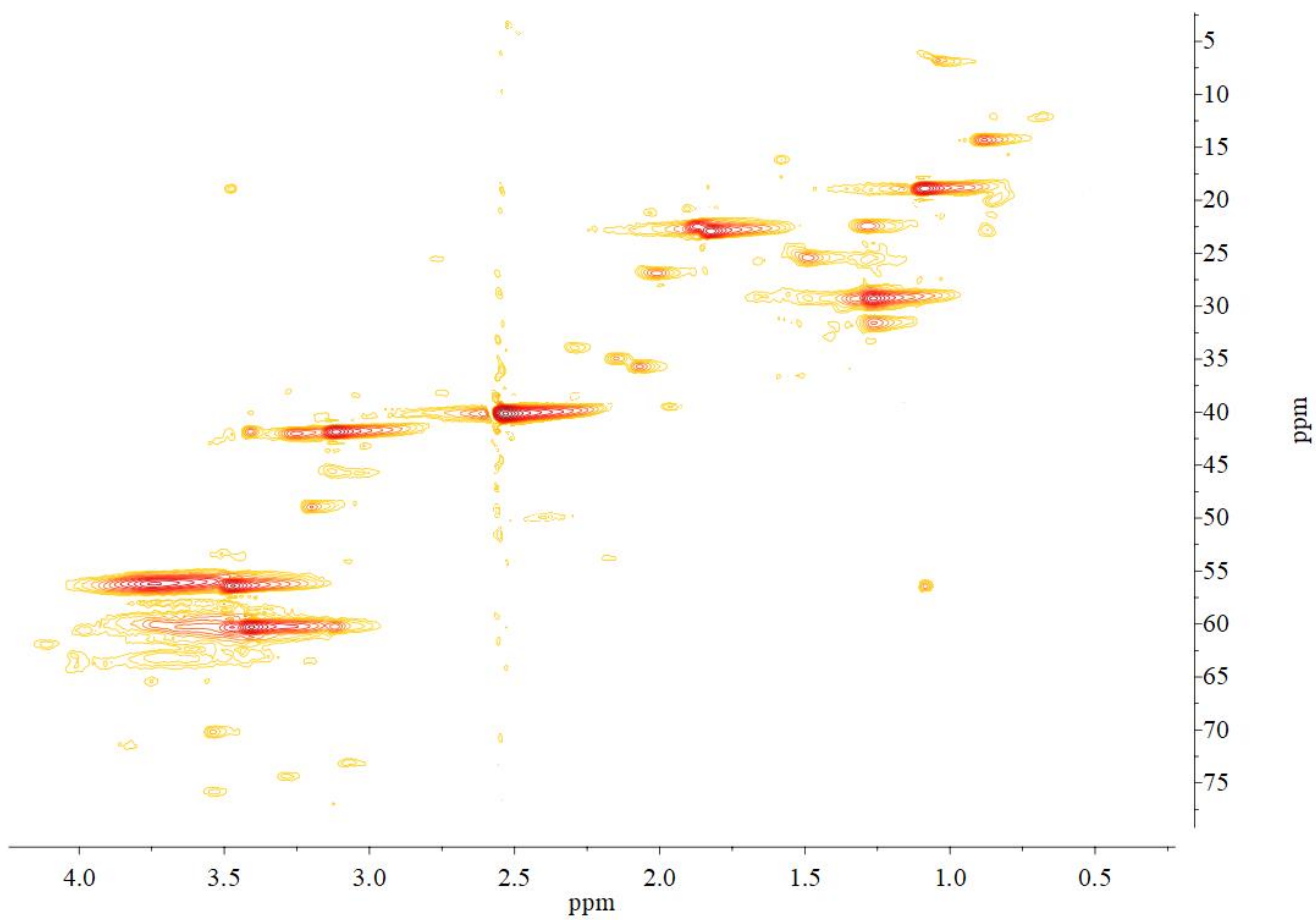
Fig. II-12. *Aliphatic region of the HSQC spectrum of [MEA][OAc] lignin. Pretreatment conditions with [MEA][OAc] were 150°C, 30% water content, 15% solids loading and 2 h of reaction time.*
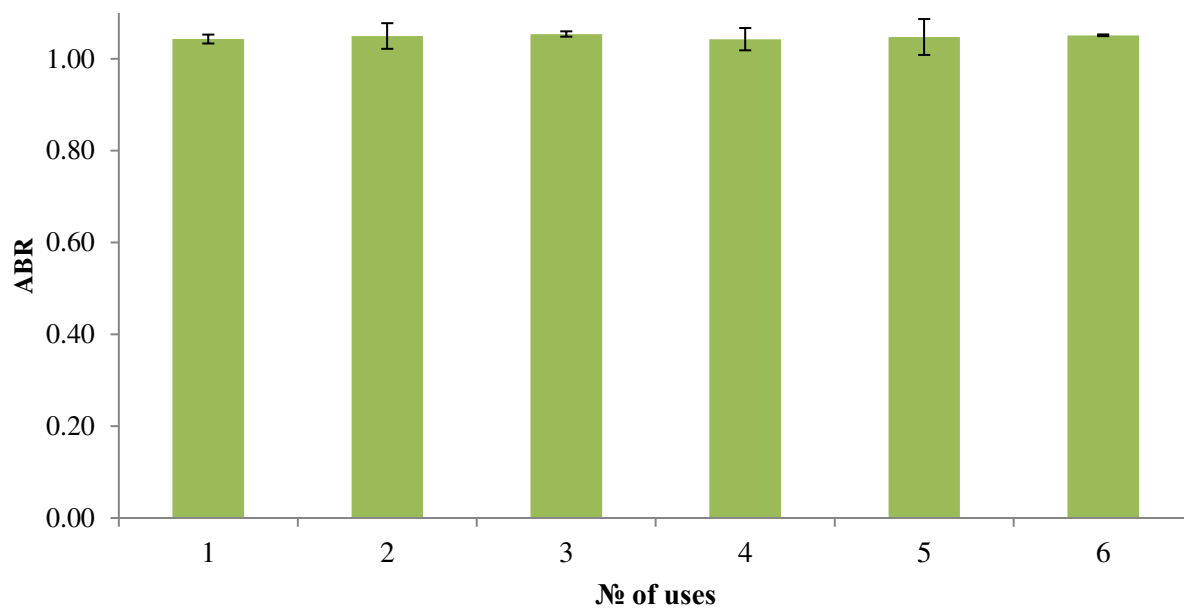
Fig. II-13. *ABRs (green bars) after use of [MEA][OAc] with 1:1 ABR for pretreatment of sugarcane bagasse.*
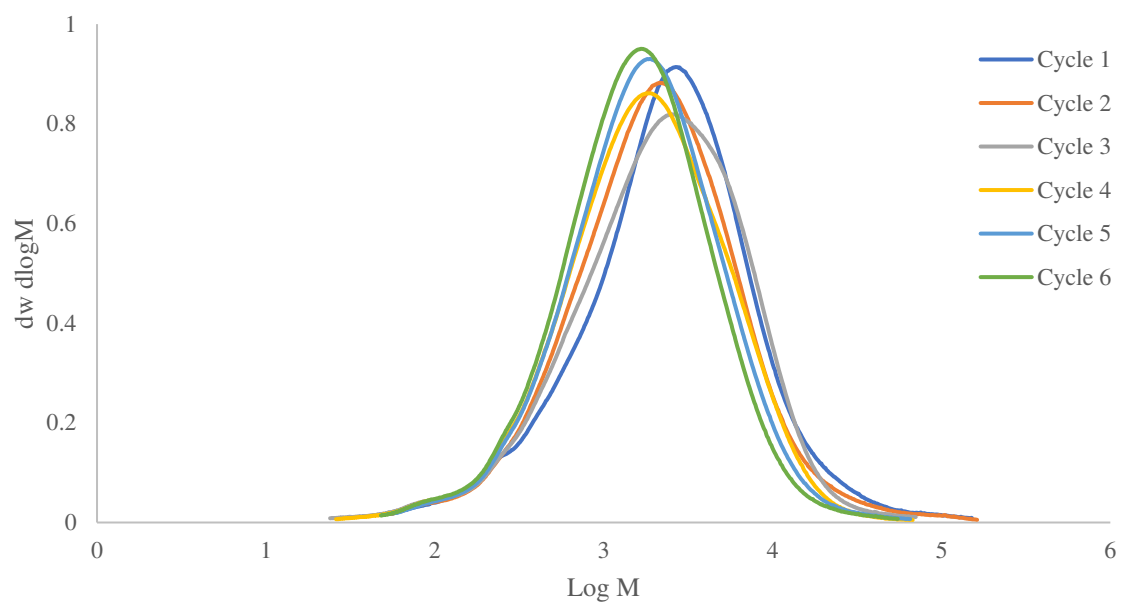
Fig. II-14. *GPC profiles of the recovered lignins from the ABR experiments.*

Fig. II-15. *NMR-H^1 spectrum of monoethanolammonium acetate in DMSO-d^6.*
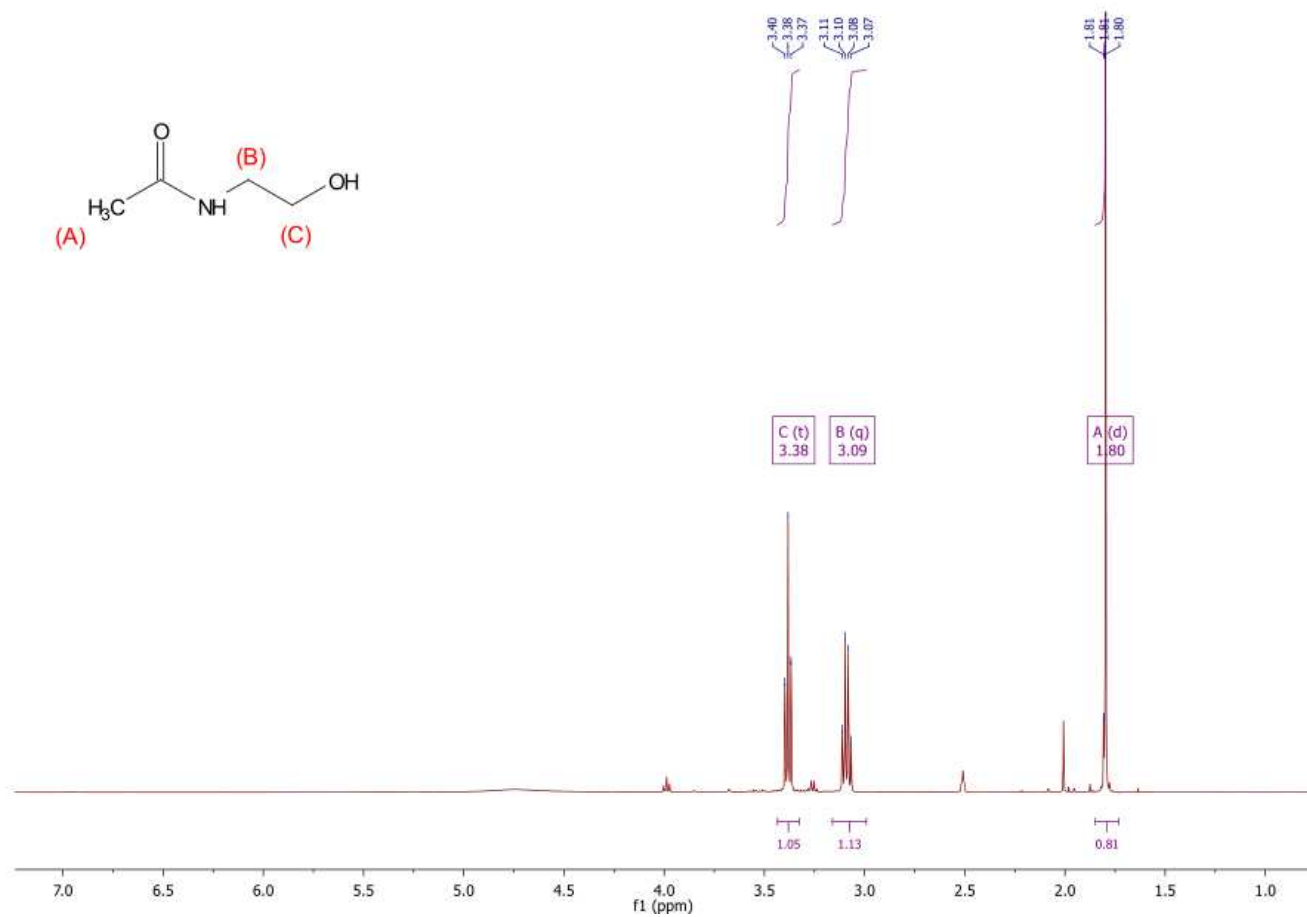
Fig. II-16. *NMR-H¹ spectrum of N-hydroxyethyl-acetamide acetate in DMSO-d⁶.*

Appendix III – Statistical tests in R for the washing experiments

5.1.1 ANOVA with global glucan yields with washing at 25°C

> aov_glu_25 <- aov(wash_exp$glu_25 ~ wash_exp$wash_levels)

> summary(aov_glu_25)

```
                  Df  Sum Sq Mean Sq F value   Pr(>F)
wash_exp$wash_levels  4 0.26414 0.06604   130.2 3.06e-05 ***
Residuals           5 0.00254 0.00051
---
```

Signif. codes: 0 '***' 0.001 '**' 0.01 '*' 0.05 '.' 0.1 ' ' 1

> TukeyHSD(aov_glu_25)

  Tukey multiple comparisons of means

   95% family-wise confidence level

Fit: aov(formula = wash_exp$glu_25 ~ wash_exp$wash_levels)

$`wash_exp$wash_levels`

```
          diff       lwr       upr    p adj
400-200   0.37965  0.28931843 0.46998157 0.0000694
600-200   0.39985  0.30951843 0.49018157 0.0000533
800-200   0.42665  0.33631843 0.51698157 0.0000391
1000-200  0.41180  0.32146843 0.50213157 0.0000461
600-400   0.02020 -0.07013157 0.11053157 0.8868407
800-400   0.04700 -0.04333157 0.13733157 0.3482655
1000-400  0.03215 -0.05818157 0.12248157 0.6388847
800-600   0.02680 -0.06353157 0.11713157 0.7582229
1000-600  0.01195 -0.07838157 0.10228157 0.9799258
1000-800 -0.01485 -0.10518157 0.07548157 0.9573094
```
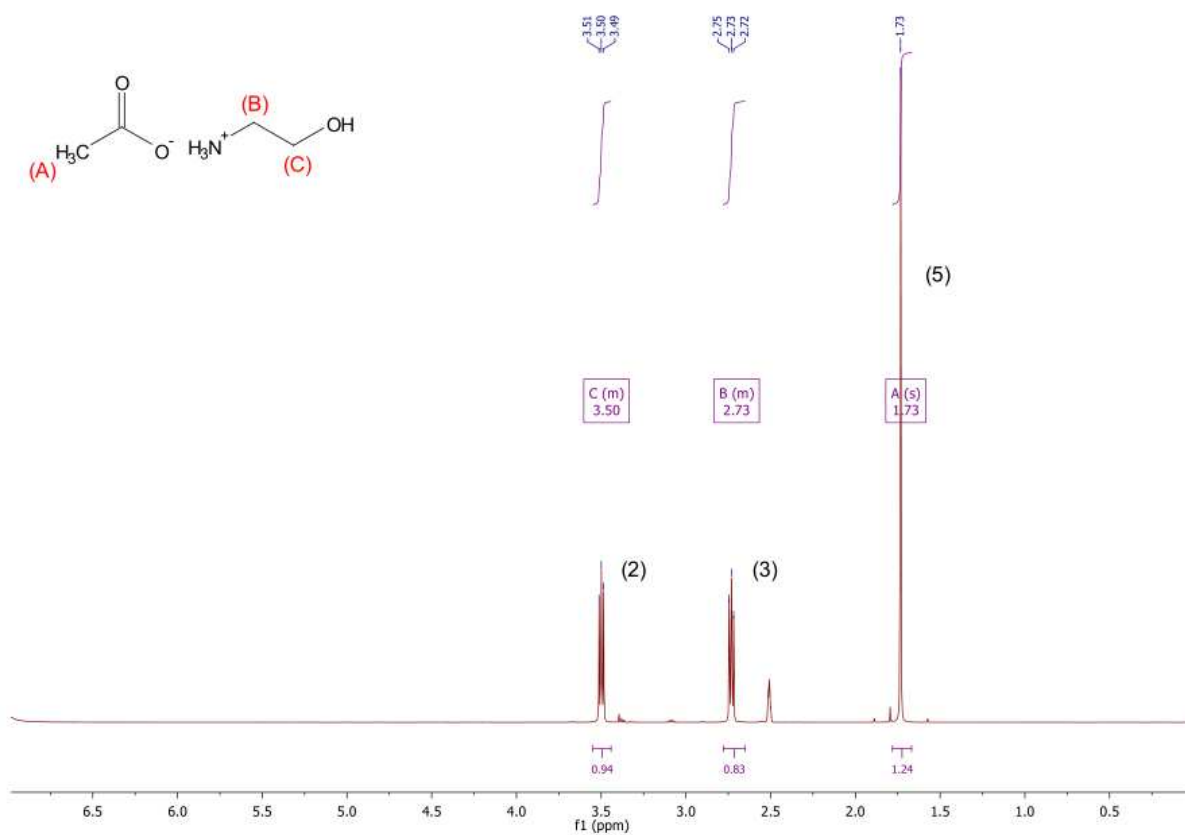
5.1.2 ANOVA with global glucan yields with washing at 80°C

> aov_glu_80 <- aov(wash_exp$glu_80 ~ wash_exp$wash_levels)

> summary(aov_glu_80)

```
                  Df  Sum Sq Mean Sq F value   Pr(>F)
wash_exp$wash_levels  4 0.25866 0.06467   202.8 1.02e-05 ***
```

Residuals   5 0.00159 0.00032

Signif. codes: 0 '***' 0.001 '**' 0.01 '*' 0.05 '.' 0.1 ' ' 1

> TukeyHSD(aov_glu_80)

 Tukey multiple comparisons of means

  95% family-wise confidence level

Fit: aov(formula = wash_exp$glu_80 ~ wash_exp$wash_levels)

$`wash_exp$wash_levels`

         diff   lwr   upr   p adj
400-200 0.36780 0.29617088 0.43942912 0.0000276
600-200 0.39860 0.32697088 0.47022912 0.0000209
800-200 0.41305 0.34142088 0.48467912 0.0000187
1000-200 0.41905 0.34742088 0.49067912 0.0000179
600-400 0.03080 -0.04082912 0.10242912 0.4947701
800-400 0.04525 -0.02637912 0.11687912 0.2197496
1000-400 0.05125 -0.02037912 0.12287912 0.1548776
800-600 0.01445 -0.05717912 0.08607912 0.9171340
1000-600 0.02045 -0.05117912 0.09207912 0.7799131
1000-800 0.00600 -0.06562912 0.07762912 0.9963154

5.1.3 ANOVA with global hemicellulose yields with washing at 25°C

> aov_hemi_25 <- aov(wash_exp$hemi_25 ~ wash_exp$wash_levels)
> summary(aov_hemi_25)
              Df Sum Sq Mean Sq F value   Pr(>F)
wash_exp$wash_levels 4 0.29472 0.07368   195.4 1.12e-05 ***
Residuals   5 0.00189 0.00038

Signif. codes: 0 '***' 0.001 '**' 0.01 '*' 0.05 '.' 0.1 ' ' 1

> TukeyHSD(aov_hemi_25)

 Tukey multiple comparisons of means

  95% family-wise confidence level

Fit: aov(formula = wash_exp$hemi_25 ~ wash_exp$wash_levels)

$`wash_exp$wash_levels`

	diff	lwr	upr	p adj
400-200	0.34600	0.268095585	0.4239044	0.0000524
600-200	0.39385	0.315945585	0.4717544	0.0000293
800-200	0.44070	0.362795585	0.5186044	0.0000198
1000-200	0.47795	0.400045585	0.5558544	0.0000155
600-400	0.04785	-0.030054415	0.1257544	0.2364356
800-400	0.09470	0.016795585	0.1726044	0.0232571
1000-400	0.13195	0.054045585	0.2098544	0.0055809
800-600	0.04685	-0.031054415	0.1247544	0.2494420
1000-600	0.08410	0.006195585	0.1620044	0.0373375
1000-800	0.03725	-0.040654415	0.1151544	0.4118896

5.1.4 ANOVA with global hemicellulose yields with washing at 80°C

> aov_hemi_80 <- aov(wash_exp$hemi_80 ~ wash_exp$wash_levels)
> summary(aov_hemi_80)

	Df	Sum Sq	Mean Sq	F value	Pr(>F)
wash_exp$wash_levels	4	0.31217	0.07804	190.1	1.2e-05 ***
Residuals	5	0.00205	0.00041		

Signif. codes: 0 '***' 0.001 '**' 0.01 '*' 0.05 '.' 0.1 ' ' 1
> TukeyHSD(aov_hemi_80)
  Tukey multiple comparisons of means
    95% family-wise confidence level

Fit: aov(formula = wash_exp$hemi_80 ~ wash_exp$wash_levels)

$`wash_exp$wash_levels`

	diff	lwr	upr	p adj
400-200	0.3475	0.266229645	0.4287704	0.0000635
600-200	0.4155	0.334229645	0.4967704	0.0000281
800-200	0.4522	0.370929645	0.5334704	0.0000209
1000-200	0.4888	0.407529645	0.5700704	0.0000164
600-400	0.0680	-0.013270355	0.1492704	0.0942809
800-400	0.1047	0.023429645	0.1859704	0.0182993

1000-400 0.1413 0.060029645 0.2225704 0.0049611

800-600 0.0367 -0.044570355 0.1179704 0.4563370

1000-600 0.0733 -0.007970355 0.1545704 0.0727922

1000-800 0.0366 -0.044670355 0.1178704 0.4584735

5.1.5 ANOVA with PIL recovery with washing at 80°C

> aov_il_recov_80 <- aov(wash_exp$il_recov_80 ~ wash_exp$wash_levels)

> summary(aov_il_recov_80)

```
            Df  Sum Sq  Mean Sq F value   Pr(>F)
wash_exp$wash_levels  4 0.11991 0.029976   453.8 1.38e-06 ***
Residuals          5 0.00033 0.000066
---
Signif. codes:  0 '***' 0.001 '**' 0.01 '*' 0.05 '.' 0.1 ' ' 1
```

> TukeyHSD(aov_il_recov_80)

  Tukey multiple comparisons of means

    95% family-wise confidence level

Fit: aov(formula = wash_exp$il_recov_80 ~ wash_exp$wash_levels)

$`wash_exp$wash_levels`

```
        diff       lwr      upr     p adj
400-200  0.20085  0.168246311 0.23345369 0.0000153
600-200  0.25045  0.217846311 0.28305369 0.0000068
800-200  0.28765  0.255046311 0.32025369 0.0000034
1000-200 0.30015  0.267546311 0.33275369 0.0000027
600-400  0.04960  0.016996311 0.08220369 0.0089850
800-400  0.08680  0.054196311 0.11940369 0.0006808
1000-400 0.09930  0.066696311 0.13190369 0.0003562
800-600  0.03720  0.004596311 0.06980369 0.0300286
1000-600 0.04970  0.017096311 0.08230369 0.0089061
1000-800 0.01250 -0.020103689 0.04510369 0.5837369
```

5.1.5 ANOVA with PIL recovery with washing at 25°C

> aov_il_recov_25 <- aov(wash_exp$il_recov_25 ~ wash_exp$wash_levels)

> summary(aov_il_recov_80)

```
            Df  Sum Sq  Mean Sq F value   Pr(>F)
wash_exp$wash_levels  4 0.11991 0.029976   453.8 1.38e-06 ***
Residuals          5 0.00033 0.000066
---
Signif. codes:  0 '***' 0.001 '**' 0.01 '*' 0.05 '.' 0.1 ' ' 1
```

> TukeyHSD(aov_il_recov_25)

  Tukey multiple comparisons of means

    95% family-wise confidence level

Fit: aov(formula = wash_exp$il_recov_25 ~ wash_exp$wash_levels)

$`wash_exp$wash_levels`

```
          diff        lwr        upr      p adj
400-200  0.17855  0.077099527 0.2800005 0.0046952
600-200  0.24295  0.141499527 0.3444005 0.0011262
800-200  0.27710  0.175649527 0.3785505 0.0006023
1000-200 0.29560  0.194149527 0.3970505 0.0004415
600-400  0.06440 -0.037050473 0.1658505 0.2169495
800-400  0.09855 -0.002900473 0.2000005 0.0556886
1000-400 0.11705  0.015599527 0.2185005 0.0287218
800-600  0.03415 -0.067300473 0.1356005 0.6780874
1000-600 0.05265 -0.048800473 0.1541005 0.3501459
1000-800 0.01850 -0.082950473 0.1199505 0.9398608
```

Appendix IV – Washing experiments

IV.1 Experimental setup

(a)   (b)

Fig. IV.1. (a) Wash water from the washing experiments (b) French press employed for solid:liquid separation of the pulp from the wash water.
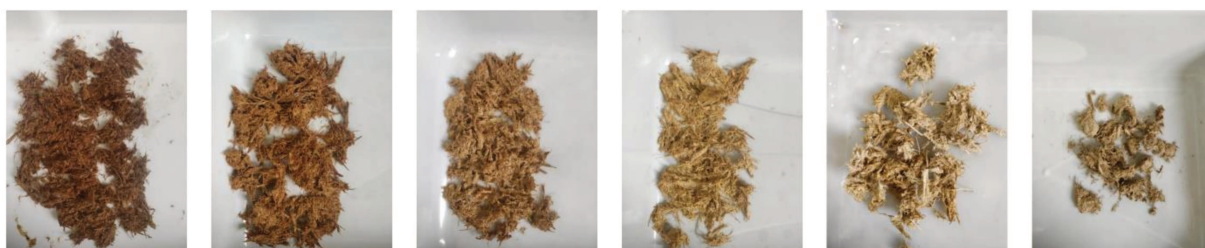
Fig. IV.2. From left to right: 200, 400, 600, 800, 1000 wt% wash water and full wash pulps from the washing experiments (25°C).
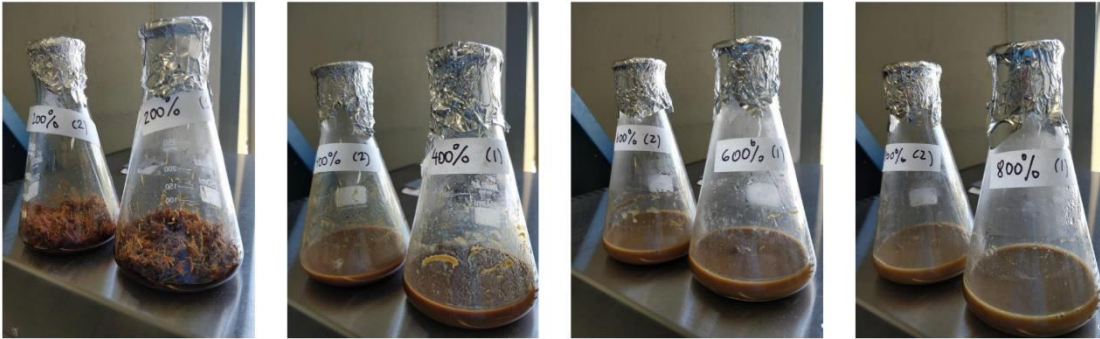
Fig. IV.3. From left to right: 200, 400, 600, 800 wt% wash water saccharification samples (wash at 25°C).

Fig. IV.4. From left to right: full wash, 800, 600, 400 and 200 wt% hydrolysates before yeast inoculation (wash at 25°C).

IV.2 Polyol accumulation during fermentation

Table IV.1 Xylitol accumulation for the fermentation samples obtained with washing at 25°C, the full wash (FW) and control were also shown as a matter of comparison. Deviations were calculated based on duplicate of the samples.

Xylitol accumulation (g·L^{-1}) - 25°C										
Time	600	DV	800	DV	1000	DV	FW	DV	Control	DV
0	0.04	0.00	0.07	0.01	0.03	0.00	0.02	0.01	0.03	0.01
6	0.05	0.00	0.07	0.00	0.05	0.01	0.09	0.00	0.08	0.01
12	0.05	0.00	0.08	0.01	0.07	0.00	0.14	0.01	0.10	0.01
24	0.05	0.01	0.09	0.01	0.08	0.00	0.21	0.00	0.20	0.09
36	0.06	0.01	0.12	0.03	0.16	0.04	0.11	0.21	0.23	0.02
48	0.06	0.00	0.18	0.04	0.24	0.04	0.33	0.09	0.31	0.06
72	0.12	0.08	0.26	0.01	0.29	0.04	0.55	0.09	0.55	0.09
96	0.08	0.01	0.35	0.04	0.38	0.09	0.61	0.09	0.58	0.14

Table IV.2 Xylitol accumulation for the fermentation samples obtained with washing at 80°C, the full wash (FW) and control were also shown as a matter of comparison. Deviations were calculated based on duplicate of the samples.

Xylitol accumulation (g·L^{-1}) - 80°C										
Time	600	DV	800	DV	1000	DV	FW	DV	Control	DV
0	0.05	0.00	0.08	0.01	0.04	0.00	0.02	0.01	0.03	0.01
6	0.06	0.00	0.09	0.00	0.06	0.01	0.09	0.00	0.08	0.01
12	0.06	0.00	0.10	0.01	0.08	0.00	0.14	0.01	0.10	0.01
24	0.07	0.01	0.10	0.01	0.09	0.00	0.21	0.00	0.20	0.09
36	0.07	0.01	0.15	0.03	0.19	0.04	0.11	0.21	0.23	0.02
48	0.07	0.00	0.22	0.04	0.27	0.04	0.33	0.09	0.31	0.06
72	0.15	0.09	0.30	0.00	0.33	0.05	0.55	0.09	0.55	0.09
96	0.10	0.01	0.42	0.05	0.43	0.11	0.61	0.09	0.58	0.14

Table IV.3 Glycerol accumulation for the fermentation samples obtained with washing at 25°C, the full wash (FW) and control were also shown as a matter of comparison. Deviations were calculated based on duplicate of the samples.

Glycerol accumulation (g·L⁻¹) - 80°C										
Time	**600**	**DV**	**800**	**DV**	**1000**	**DV**	**FW**	**DV**	**Control**	**DV**
0	0.03	0.02	0.03	0.01	0.05	0.08	0.05	0.00	0.03	0.02
6	0.04	0.03	0.05	0.00	0.13	0.00	0.09	0.01	0.12	0.01
12	0.06	0.04	0.08	0.01	0.16	0.01	0.17	0.02	0.21	0.01
24	0.09	0.06	0.09	0.01	0.19	0.03	0.23	0.00	0.31	0.01
36	0.10	0.04	0.18	0.03	0.29	0.05	0.29	0.06	0.40	0.00
48	0.12	0.07	0.20	0.03	0.39	0.07	0.29	0.06	0.29	0.06
72	0.16	0.09	0.25	0.06	0.20	0.25	0.32	0.02	0.42	0.16
96	0.18	0.03	0.28	0.07	0.34	0.07	0.27	0.01	0.39	0.19

Table IV.4 Glycerol accumulation for the fermentation samples obtained with washing at 80°C, the full wash (FW) and control were also shown as a matter of comparison. Deviations were calculated based on duplicate of the samples.

Glycerol accumulation (g·L⁻¹) - 25°C										
Time	**600**	**DV**	**800**	**DV**	**1000**	**DV**	**FW**	**DV**	**Control**	**DV**
0	0.02	0.02	0.03	0.01	0.05	0.07	0.05	0.00	0.03	0.02
6	0.03	0.02	0.04	0.00	0.11	0.00	0.09	0.01	0.12	0.01
12	0.05	0.03	0.07	0.01	0.14	0.01	0.17	0.02	0.21	0.01
24	0.07	0.05	0.08	0.01	0.16	0.03	0.23	0.00	0.31	0.01
36	0.08	0.03	0.15	0.02	0.26	0.04	0.29	0.06	0.40	0.00
48	0.10	0.05	0.17	0.03	0.34	0.06	0.29	0.06	0.29	0.06
72	0.13	0.07	0.21	0.05	0.17	0.22	0.32	0.02	0.42	0.16
96	0.14	0.02	0.24	0.06	0.30	0.06	0.27	0.01	0.39	0.19

Table IV.5 Xylitol accumulation for the fermentation samples obtained with high initial cell density. Deviations were calculated based on duplicate of the samples.

Xylitol accumulation (g·L⁻¹) – high initial cell density						
Time	**600**	**DV**	**FW**	**DV**	**Control**	**DV**
0	0.00	0.00	0.00	0.00	0.00	0.01
6	0.01	0.02	0.01	0.01	0.10	0.02
12	0.01	0.01	0.08	0.04	0.23	0.08
18	0.04	0.01	0.16	0.05	0.36	0.09
24	0.31	0.34	0.31	0.00	0.49	0.10
30	0.13	0.03	0.37	0.04	0.59	0.05
36	0.16	0.06	0.42	0.02	0.61	0.08
48	0.24	0.00	0.57	0.04	0.80	0.11
54	0.26	0.01	0.64	0.05	0.83	0.11

Table IV.6 Glycerol accumulation for the fermentation samples obtained with high initial cell density. Deviations were calculated based on duplicate of the samples.

Glycerol accumulation (g·L⁻¹) – high initial cell density						
Time	**600**	**DV**	**FW**	**DV**	**Control**	**DV**
0	0.10	0.01	0.05	0.00	0.02	0.02
6	0.19	0.10	0.10	0.02	0.14	0.02
12	0.29	0.04	0.19	0.04	0.22	0.03
18	0.32	0.01	0.24	0.07	0.27	0.02
24	0.35	0.04	0.28	0.00	0.31	0.02
30	0.42	0.01	0.29	0.04	0.33	0.02
36	0.39	0.06	0.29	0.03	0.30	0.01
48	0.50	0.07	0.34	0.04	0.34	0.00
54	0.46	0.01	0.37	0.02	0.33	0.01